A Study on Joint Optimization of Traffic and Energy Management in Wireless Mesh Networks Powered by Renewable Energy

A Study on Joint Optimization of Traffic and Energy Management in Wireless Mesh Networks Powered by Renewable Energy

再生可能エネルギー駆動型無線メッシュネットワークにおける通信と電力効率の最適化に関する研究

A dissertation presented
by

Meng Li

submitted to
Tohoku University
in partial fulfillment of the requirements
for the degree of

Doctor of Philosophy

Supervisor: Professor Nei Kato

Department of Applied Information Sciences
Graduate School of Information Sciences
Tohoku University

January, 2016

To my family and my dear friends

Abstract

The recently happened natural disasters on a world scale tell us the importance of a well-considered emergency plan in the post-disaster treatment. The accommodation of network service is one important part, since a well-designed network provision will not only convey the rescue information to the outside, but also guarantee the communication demands of the people inside the disaster area. Nevertheless, a major obstacle to meet the communication demands in the post-disaster case is the unavailability of the crucial infrastructures (i.e., power transmission cables, Internet cables). The emergence of the Renewable Energy-enabled Base Station (REBS)-based mesh network is an emerging technique, which gives us a possible solution to deal with this issue. The REBS still has intermittent renewable energy supplies when the power from power plant is cut off, then with the help of vehicle-borne network gateway, such kind of network will keep operating after disaster.

The REBS-based mesh network is the network composed of interconnecting REBSs and Microgrids. All the REBSs and Microgrids have the energy harvesting facilities, which can get renewable energy from surrounding environment. The Microgrid can distribute the energy from its battery to the connected REBSs'. In the post-disaster case, the REBSs in the network run entirely on renewable energy sources and such energy could be the energy from local harvesting facilities or from the remote Microgrids'. Besides the energy aspect, REBSs will use the pre-equipped network facilities to connect their neighbors, send the data hop-by-hop, and finally rely on the vehicle-borne network gateway to transfer data to the Internet. However, in the post-disaster case, both of the energy and network bandwidth are limited. Therefore, such limited resources need to be arranged efficiently before the network get recovered.

This dissertation addresses the issue of designing the algorithms to accommodate the network service with the limited bandwidth and energy resource in the post-disaster case. Because the network has to deal with a large amount of data transfer demand, and need to fulfill such demand as much as possible, toward such a target, in this thesis, we study the joint energy and traffic management for throughput maximization in the post disaster scenario.

At first, we consider an off-line throughput-maximization scheme when we have the exact traffic and energy profile in the finite time horizon. To formulate the problem, we analyze and investigate the data and energy profile as well as network structure, and develop an optimization framework that considers limited input energy and link capacity in the considered time span. Then we formulate the considered scheme as a Mixed Integer Linear Programming (MILP) problem. The simulation results show that our proposal can achieve high total system throughput compared with the naive idea.

Secondly, we propose an energy efficient scheme based on the maximal throughput value. The energy efficiency is to minimize the weighted energy consumption, which equals the ratio of the consumed energy to the harvested energy. Such optimization framework is also the MILP problem. Through the extensive simulation results, we validate that our scheme could significantly improve network performance in energy efficiency, comparing with the naive scheme and throughput-maximization scheme.

Thirdly, we extend the off-line energy efficient throughput-maximization scheme into the on-line case. We consider the possible imprecise estimation of the data traffic demands, and analyze the effects of such imprecision on the performance. After that, an on-line dynamic adjusting scheme is proposed, in the proposed on-line scheme, REBSs will adjust the previous strategy according to the latest traffic information at the beginning of each time slot. The numerical results demonstrate that the proposed on-line scheme outperforms the off-line scheme and the naive one with regard to estimation error, energy efficiency and system throughput.

Acknowledgments

First and foremost, I would like to express my deepest gratitude to my advisor, Prof. Nei Kato, for his insightful guidance, continuous supportance and proving an excellent research atmosphere throughout my study in Tohoku University. I cannot have imagined having a better advisor and mentor for my study.

It is also my great honor to thank Prof. Suganuma, and Prof. Omachi for being my dissertation committee members and giving me constructive comments to this dissertation in its final form.

I would like to express my appreciation to Prof. Hiroki Nishiyama for his insightful guidance in my study. His high standards of the research have inspired me to keep challenging myself, and I have learned a lot from the discussions and comments from him. This dissertation cannot be finished without his help.

I would like to acknowledge the China Scholarship Council (CSC) Foundation, for offering the financial supportance during my study in Tohoku University, one of the most prestigious universities in Asia. I would also like to thank Ms. Motoko Shiraishi and Ms. Takako Kase for helping me with the enrollment process, and providing me with all the necessary administrative documents.

I am grateful to the unreserved helps from my friends during my stay in Japan in both of the academic and the daily life, especially Dr. Jiajia Liu, Dr. Chao Wei, Dr. Wei Zhao, Ngo Duc Thuan, Fomo Desmond, Ko Togashi, Kei Saito and Panu Avakul.

In addition, I would like to give my sincere thanks to members of the Kato-Nishiyama Laboratory for the joyful and unforgettable life in Japan: Prof. Zubair Md. Fadlullah, Prof. Mostafa Fouda, Mr. Kaoru Chiba, Ms. Kimi Nishimura, Dr. Wei Liu, Dr. Kaoru Ota, Dr. Zanjie Huang, Dr. Ahmed E.A.A. Abdulla, Yuichi Kawamoto, Katsuya Suto, Shucong Jia, Daisuke Takaishi, Kazuma Kanako, Monder Rehamnia, Bomin Mao, Fengxiao Tang, Kenta Suzuki, Takahiro Nozue, Atsushi Toshinari, Timonen Henri Lauri, Kazuma Yoshida, Asato Takahashi, Shintaro Arai, Masaya Ito, Kazuhiro Matsumoto, Kenta Ito, Shoki Oiyama, Shin Koseki, Yu Saito, Keisuke Sato ,Tota Nakajo, Keisuke Miyanabe, Rodrigo Bernardino Barros, Takanobu Endo, Takayuki Nakazawa, Masanori Horiuchi, Naoki Miyashita, Daiki Murayama, Naoto Yamada, Yunseong Lee, Tiago Gama Rodrigues, Ken Sasaki, Yuya Kasahara, Hideki Kuribayashi, Yoshiki Shino, Hiroaki Takagi, Shikhar, Michael R. Zielewski, Julian A. Rick, and Weiming Liao.

Finally, and most importantly, I would like to acknowledge the immeasurable and unwaving support given by my parents (Song Wang and Xianjun Li) and my girlfriend

(Li Qiang) during the years I have been working on this thesis. Words cannot describe my gratitude toward them.

My apologies if I have inadvertently omitted anyone to whom acknowledge is due.

Contents

Abstract **i**

Acknowledgments **iii**

1 Introduction **1**

1.1 Background 1
1.2 Challenging Issues with REBS-based Mesh Networks 6
1.3 Research Objectives 7
1.4 Thesis Outline 9
1.5 Contributions 10

2 Overview of REBS-based Mesh Networks and Its Associating Settings in Disaster Area **12**

2.1 Introduction to the REBS-based Mesh Networks 12
2.1.1 Energy Flows inside REBS 12
2.1.2 Traffic Flows in Network 14
2.2 Spatial and Temporal Diversities of the Traffic and Energy 15
2.3 Related Work 16
2.4 Our Research Target 19
2.5 The Advantage of Joint Optimization 21
2.6 Summary 22

3 The Off-line Scheduling and Load Distribution for REBS Mesh Networks **24**

3.1 Introduction 24
3.2 Preliminaries 25
3.2.1 The Way of Energy Cooperation 25
3.2.2 The Energy and Traffic Input Profiles 26
3.3 System Model 27
3.3.1 Network Model 27
3.3.2 Energy Related Model 28

3.3.3 Traffic Related Model . . . 31
3.4 Research Objective . . . 35
3.5 Problem Formulation . . . 36
3.5.1 The Equivalent Transformation of Constraints . . . 36
3.5.2 Discussion on the Computation Cost . . . 38
3.6 Performance Evaluation . . . 39
3.6.1 Settings of the Simulation . . . 39
3.6.2 Impact of the Energy Input on Total System Throughput . . . 43
3.6.3 Impact of the Traffic Input on Total System Throughput . . . 45
3.7 Summary . . . 45

4 The Off-line Energy Efficient Scheduling and Load Distribution for REBS Mesh Networks 47
4.1 Introduction . . . 47
4.2 System Model and Optimization Objective . . . 48
4.2.1 System Model . . . 48
4.2.2 Optimization Objective . . . 50
4.3 Proposed Two-stage Energy Efficiency Scheme . . . 52
4.4 Performance Evaluation . . . 54
4.4.1 Settings of the Simulation . . . 54
4.4.2 Effect of Energy Input on Energy Efficiency . . . 55
4.4.3 Effect of Traffic Input on Energy Efficiency . . . 59
4.5 Summary . . . 59

5 On the On-line Energy-Efficient of Throughput-Based Scheme for REBS Mesh Networks 61
5.1 Introduction . . . 61
5.2 System Model . . . 62
5.3 Analysis on the Off-line Scheme . . . 63
5.4 Envisioned On-line Dynamic Adjusting Scheme . . . 67
5.5 Performance Evaluation . . . 71
5.5.1 Effect of Estimation Deviation of Data Traffic Demands on System Throughput and Energy Consumption . . . 75
5.5.2 Effect of Total Available Energy on Total System Throughput and Energy Efficiency . . . 80
5.5.3 Effect of Data Traffic Demands on Total System Throughput and Energy Efficiency . . . 84
5.6 Summary . . . 87

6 Conclusion **88**
6.1 Summary and Discussions 88
6.2 Future Directions 90

Bibliography **92**

Publications **100**

Appendix **101**

List of Figures

1.1 The traditional power supply for base stations. 1
1.2 New power supply for cellular network with energy harvesting facilities and Microgrids. 3
1.3 The power supply for REBS in disaster. 4
1.4 The traffic transmission for REBS in disaster. 5

2.1 The energy and the traffic flows in the considered REBS-based mesh networks. ©2014 IEEE. 14
2.2 The cooperation of the data traffic transmission among the REBSs. 20
2.3 The system topology of the example, and the associating solutions of the Naive scheme and joint-optimization scheme, respectively. 23

3.1 Traffic flow between REBSs, and energy flow inside REBSs and Microgrids. ©2015 IEEE. 34
3.2 System topology used in the part of performance evaluation. ©2014 IEEE. 41
3.3 The effect of average input renewable energy on system throughput of the proposed scheme and naive scheme. ©2014 IEEE. 42
3.4 The effect of average input traffic per base station on total system throughput of the proposed scheme and naive scheme. ©2014 IEEE. 44

4.1 System topology used in the part of performance evaluation. ©2014 IEEE. 56
4.2 The effect of average input renewable energy on consumed power per megabit of the proposed scheme, naive scheme and throughput maximization scheme. ©2014 IEEE. 57
4.3 The effect of average input traffic per base station on consumed power per megabit of the proposed scheme, naive scheme and throughput maximization scheme. ©2014 IEEE. 58

5.1 The topology used for the computer-based simulation. ©2015 IEEE. . . . 74
5.2 The effect of ϵ on system throughput of the off-line with expected information, off-line combined with on-line, and Naive scheme. ©2015 IEEE. . . . 76

5.3 The effect of ϵ on energy efficiency of the off-line with expected information and off-line combined with on-line scheme. ©2015 IEEE. 79
5.4 The effect of average input renewable energy on system throughput of the four schemes. ©2015 IEEE. 81
5.5 The effect of average input renewable energy on consumed power per megabit of the four schemes. ©2015 IEEE. 83
5.6 The effect of average input traffic per REBS on total system throughput of the four schemes. ©2015 IEEE. 85
5.7 The effect of average input traffic per REBS on consumed power per megabit of the four schemes. ©2015 IEEE. 86

List of Tables

3.1 Experimental Parameters ©2014 IEEE. 40

4.1 Variable Summarization 49
4.2 Experimental Parameters ©2014 IEEE. 55

5.1 Variable Summarization 64
5.2 Experimental Parameters ©2015 IEEE. 73

List of Acronyms

BS Base Station
CAPEX CAPital EXpenditure
COW Cell On Wheel
MILP Mixed Integer and Linear Programming
OPEX OPerating EXpense
PVT Poisson-Voronoi Tessellation
REBS Renewable Energy-enabled Base Station
SMS Short Message Service
SPOF Single Point Of Failure
VOIP Voice Over Internet Protocol
WSAN Wireless Sensor and Actuator Networks

Chapter 1

Introduction

1.1 Background

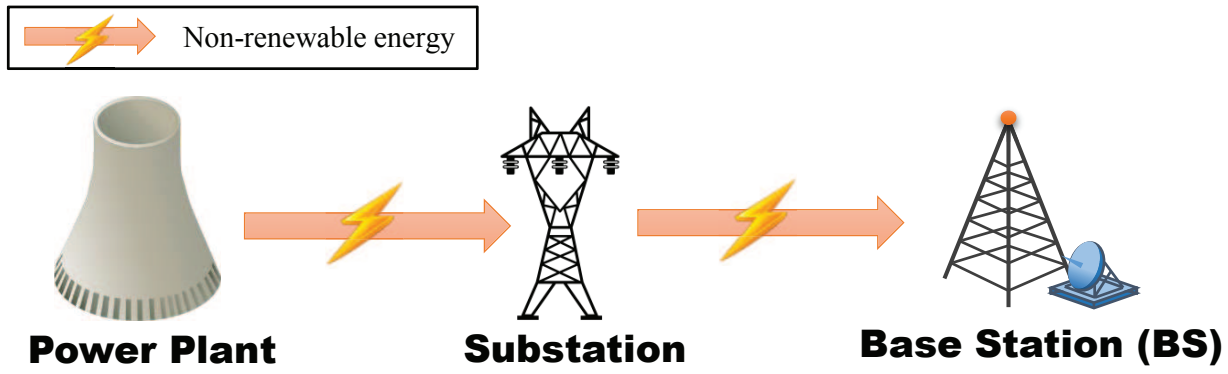

Figure 1.1: The traditional power supply for base stations.

The time of electricity usage of the human beings can be date back to hundreds of years ago. Thanks to the widespread usage of electricity and the fast development of the communication technology in recent years, the related energy supply and communication techniques have been drawing much attention. The traditional power supply for cellular networks is the non-renewable energy from power plant, its voltage will be transformed from high to low by electricity substation, and then the Base Station (BS) is powered by such low-voltage non-renewable energy (Fig. 1.1). However, this energy source and transmission approach have several shortcomings as follows:

- The traditional power plants use non-renewable energy resources (i.e., fossil fuels and nuclear fuel) to generate electricity. Such kind of energy resources aggravate environmental pollution (i.e, green house gases, radioactive waste).
- The CAPital EXpenditure (CAPEX) and OPerating EXpense (OPEX) of the plants are high. In other words, not all the places can afford to establish the power plant or connect to the power grid. Therefore, people outside the power plant's coverage area cannot use the electricity.
- There is a Single Point Of Failure (SPOF) problem for such architecture. The Base Stations (BSs) solely use the energy from power plants. Therefore, if the energy supply is cut off, or the power transmission cable is damaged, the BSs cannot operate due to the lack of energy.

The appearance of the Microgrids and Renewable Energy-enabled Base Station (REBS) offers a solution to deal with the above-mentioned shortcomings. These new type of power grids and cellular BSs can harvest the renewable energy (i.e., solar energy, wind energy) from ambient environments via energy harvesting facilities (i.e., solar panel, wind turbine) (Fig. 1.2).

Therefore, on a daily basis, the REBS will have extra cost-free energy input besides the expensive non-renewable energy supply, by using energy harvesting facilities. The introduced renewable energy input can effectively reduce the consumption of non-renewable energy. The non-renewable energy from power plant will be firstly transmitted to the Microgrid's place, then the Microgrid will deliver such non-renewable energy as well as its harvested renewable energy to the connected REBSs. For the REBS, it will combine such energy input with the energy from its local energy harvesting facilities as its operating energy sources. Additionally, because the REBS itself still has energy supply even the energy from power plant is cut off, such feature enables us to explore its availability in the case of zero grid energy input, such as the post-disaster communication case (Fig. 1.3).

The REBS - based mesh network is a mesh network composed by Microgrids and associating REBSs, which is designed for the provision of network service in disaster area.

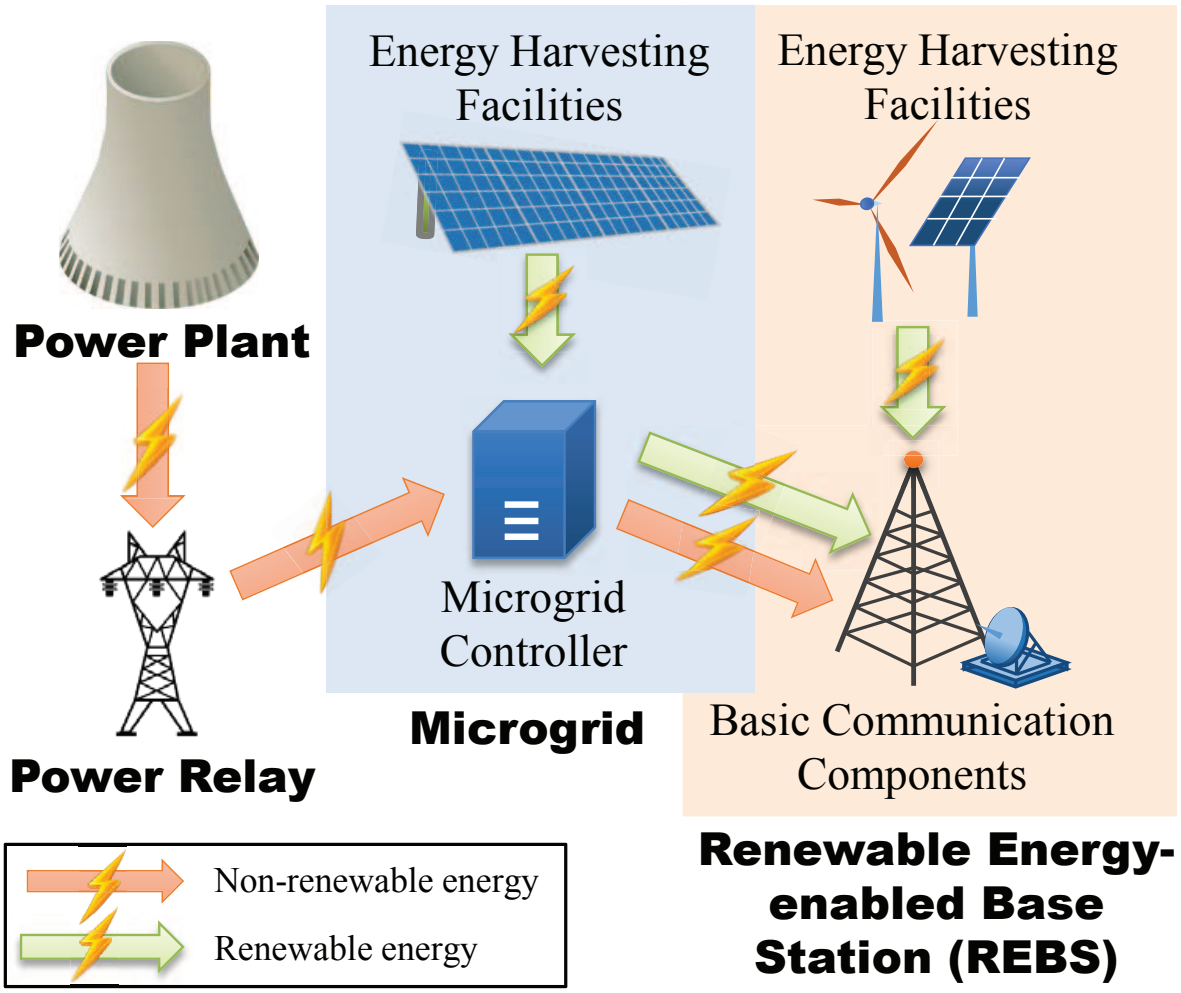

Figure 1.2: New power supply for cellular network with energy harvesting facilities and Microgrids.

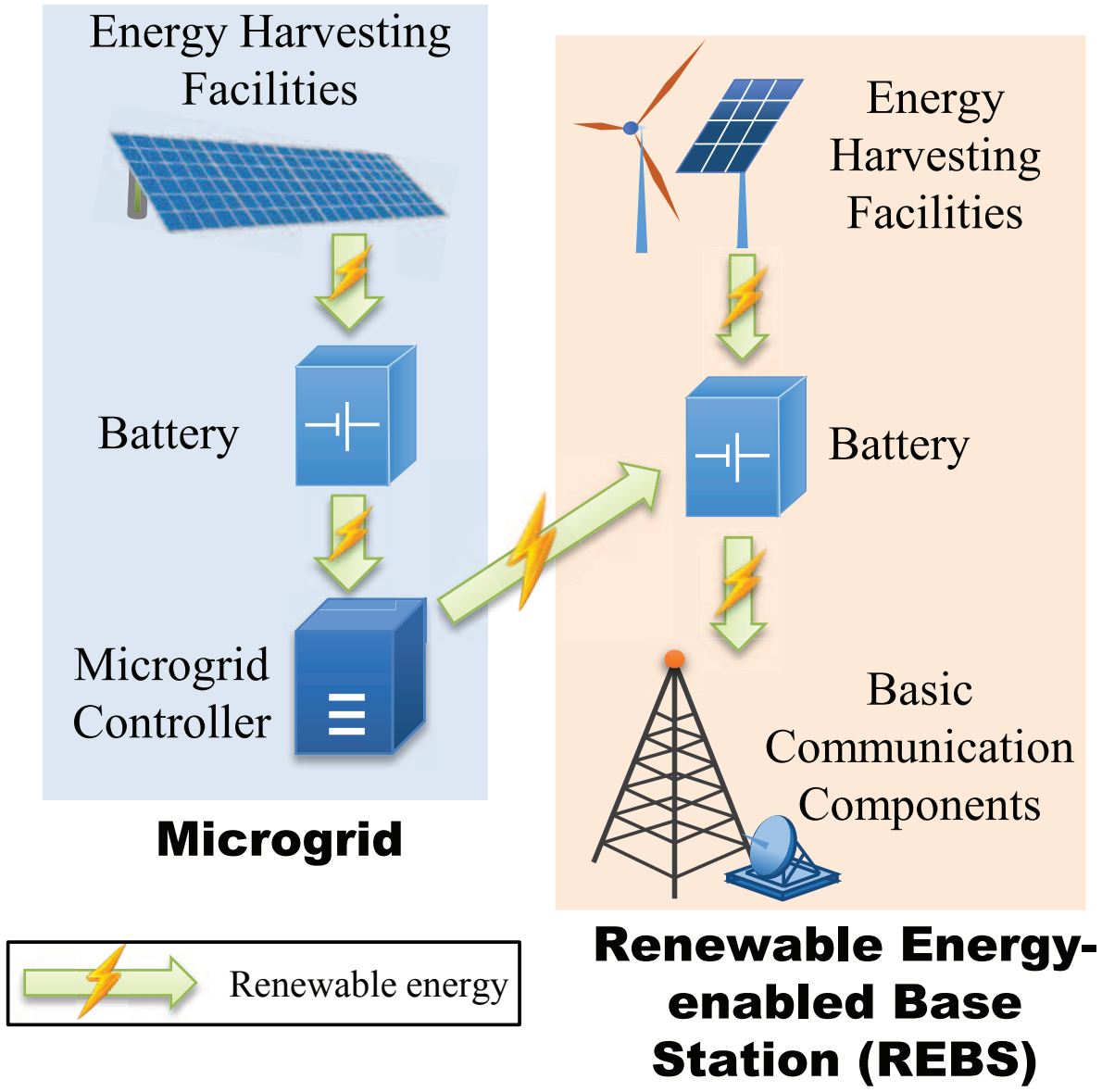

Figure 1.3: The power supply for REBS in disaster.

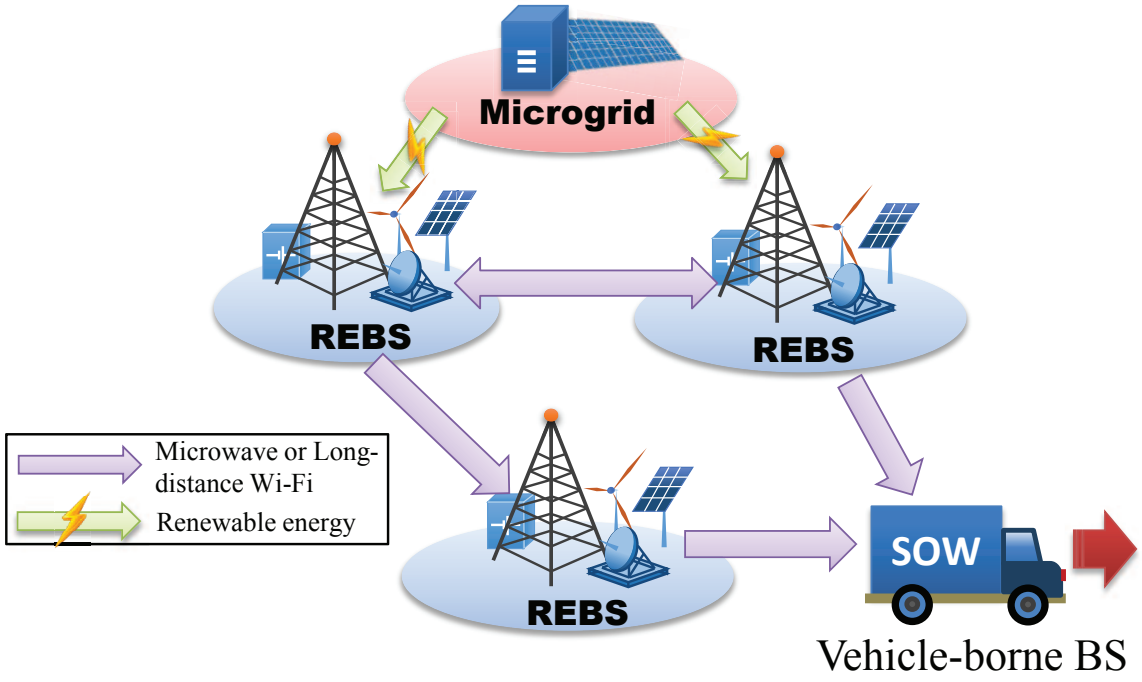

Figure 1.4: The traffic transmission for REBS in disaster.

It has one or multiple network gateway, which can provide network access to the outside Internet. The REBSs are interconnected by microwave plate or long-distance Wi-Fi. The data of the users inside the area is firstly collected by the local REBS, and such data will be transferred to the gateway hop-by-hop (Fig. 1.4). The network gateways are in charge of collecting the data traffic demands and transferring to the outside area. In the post-disaster case, the gateway should be easy-deployed and can accommodate network services in a rapid manner. Therefore, the vehicle-borne cellular is a relative reasonable choice, such as Movable and Deployable Resource Unit (MDRU) [1], or Cell On Wheel (COW).

A large number of research efforts have been devoted motivated by the above advantages of REBS - based mesh network. The utmost concern for such kind of network structure is the shortage of energy and network bandwidth. For the energy resources, because of the destruction of the disaster, the REBSs of the network are solely relying on the renewable energy. However, the input renewable energy may not always meet the operating demands. For example, the solar panel cannot harvest energy at night hence

input energy for REBS will be zero then. On the other hand, for the communication resources, the network connection may also be affected by the disaster. Although the vehicle-borne BSs (i.e., Switch On Wheel, SOW) resolve the concern of providing the network gateway in the emergency case, the destruction to the original network connections calls for a consideration toward the scarce network bandwidth. Furthermore, the rebuild effort for the affected area may last several days or even weeks. Therefore, an algorithm need to be proposed so as to effectively utilize the limited energy and communication resources. Additionally, the algorithm should deal with the finite time horizon and fulfill the data transmission demand as much as possible, because the applications such as Voice Over Internet Protocol (VOIP) or Short Message Service (SMS) will increase sharply after disaster, and then network throughput will be the major concern.

1.2 Challenging Issues with REBS-based Mesh Networks

In the last section, we discuss various features of the REBS-based mesh networks. Although the above-mentioned network components and structures satisfy the preconditions of accommodating network services in the post-disaster case, there are still several challenging issues yet to be solved. In order to design the scheme for the algorithm in post-disaster scenario, the following issues should be addressed accordingly.

Firstly, the energy inputs of the REBSs and Microgrids are instable and unbalanced. This is due to the different weather conditions and deployment places, respectively. As a result, for a certain energy harvesting facility, the input energy changes with time, and different energy harvesting facilities may have different energy inputs at the same time. Therefore, the algorithm will consider the spatial and temporal diversities of the renewable energy input.

Secondly, the data traffic demands of the users inside the affected area are also changing

with time and different from place to place. For example, the population densities for different REBS coverage areas are not the same, and for a certain REBS, the activities of the people inside the area are changing as time elapsed. Hence such features of the data traffic demand should also be considered.

Thirdly, as mentioned in the last section, the data traffic for a certain REBS will be relayed by the neighbor REBSs, and finally transferred to the network gateway in a hop-by-hop manner, therefore it is a multi-hop transmission. Moreover, there could be more than one transmission path for the data traffic demands of REBS, because the data traffic can be delivered to the network gateway by different neighbor REBSs.

Last but not least, the algorithm should aim at serving the data traffic demand as much as possible, and such provision should cover the finite time horizon and be energy-efficient. The reasons are threefold. The first reason is the sharp increase of data traffic demands after disaster. Therefore, the amount of data traffic transmission becomes the major concern. Secondly, because the REBSs operate solely on the renewable energy, the algorithm should address energy efficiency. For the rebuilt effort, it cannot be done at once, and the long-term optimization should be taken into consideration as well.

1.3 Research Objectives

The provision of network services is one important requirement for the post-disaster scenario. Because an efficient scheme can not only help the emergency relief by delivering the usable information to rescuers, but also satisfy the requirement for communication of the people in the affected place. The energy for the network is insufficient, and the REBSs in the disaster area cannot operate when the renewable energy is not enough. Therefore, the operation period of the REBSs in the network is limited. At the same time, the REBS will neither serve the users nor relay the data traffic demand of the other REBSs' if it is switched off. Therefore, the usage and transmission of the energy of REBSs and

Microgrids, and the transmission of the traffic among the REBSs should be considered jointly.

In this dissertation, we mainly focus on the occasions for the operating status of the REBSs (i.e., switch on, switch off), and the associating data traffic transmission policies for each REBSs. We will propose the optimization frameworks and algorithms for achieving different objectives. In addition, we validate our new proposals via theoretical analyses. Moreover, we will compare our proposals with other existing methodologies in terms of total system throughput and energy efficiency.

At first, we would like to propose a joint energy and traffic throughput-maximization algorithm for the REBS-based mesh network in the post-disaster scenario. The proposed scheme will determine the the energy distribution policy of the Microgrid, the time for switching on the REBSs, the number of collected data traffic demands for REBSs, and the data transmission policies including the local collected data traffic demands as well as the relayed ones.

Secondly, we will extend the previous model, and address the energy efficiency issue. Besides achieving maximized system throughput, the new model considers the total weighted renewable energy consumption of the REBSs as well. The result will have a less weighted energy consumption than the other strategies that have the maximal system throughput.

It is noticed that the previous proposed schemes are designed only for the idealized off-line case in which the energy and traffic estimation profiles are just the real ones. However, the solution for such assumption may not work when the data traffic demand is not estimated precisely. Therefore, we assume the traffic profile is inexact, and then we propose a dynamically adjusting scheme, in order to deal with the imprecise traffic estimation. Such scheme will be executed in each time slot to revise the old strategy. Compared with the off-line scheme, the on-line scheme can achieve higher performances even without precise traffic estimation profile.

1.4 Thesis Outline

The remainder of this thesis is outlined as follows:

Chapter 2 Overview of REBS-based Mesh Network and Its Associating Settings in Disaster Area. We introduce the REBS-based mesh networks in this chapter. At first, we analyze the factors cause energy alternation, as well as the way of traffic transmission inside this network. Then we analyze the reasons of the spatial and temporal diversities of the energy and traffic profiles. In addition, we analyze the availabilities of the traffic and energy profile estimation. After that, we retrospect the recently representative literatures. At last, we use an example to demonstrate the importance of the joint optimization of the energy and traffic.

Chapter 3: The Off-line Scheduling and Load Distribution for REBS Mesh Networks. In this chapter, an algorithm is proposed for maximizing the total system throughput for the considered scenario demonstrated in Chapter 2. Firstly, we model the operating behaviors of REBS, and the associating energy distribution between Microgrid and traffic transmission among REBSs, respectively. Secondly, we demonstrate the related work and discuss the problems that we would like to consider. Thirdly, we formulate the throughput-maximization problem for the joint optimization of energy and traffic. Fourthly, we demonstrate that the problem is a Mixed Integer Linear Programming (MILP). At the end of the chapter, we demonstrate that the optimized scheme has better performance than the existed methodology.

Chapter 4: The Off-line Energy Efficient Scheduling and Load Distribution for REBS Mesh Networks. In this chapter, we extend our consideration. Based on the maximized throughput, we proposed an energy efficient scheme. The energy efficiency is defined as the ratio of the consumed energy to the harvested energy. We define the energy efficiency as the optimization objective in the model, and the maximized throughput is regarded as the constraint. Because the harvested energy is the constant value (i.e., the profile of energy input is known), therefore such added constraints will not affect the

MILP feature of the considered problem. After that, we propose a two-stage algorithm in which the weighted energy consumption as well as the total system throughput are addressed. At last, we validate the energy efficiencies of the considered algorithms via numerical simulations.

Chapter 5. On the On-line Energy-Efficient of Throughput-Based Scheme for REBS Mesh Networks. In this chapter, we extend the previous research. The proposed models in Chapter 3 and 4 consider the energy and traffic profiles in a certain time span, which can be regarded as the expectations for such profiles. In previous consideration, we assume the expectations are always the real ones (i.e., the variance is zero). However, the result for such off-line assumption may not get the best result when facing the imprecise profile estimation. Therefore, an on-line dynamically adjusting scheme is proposed in this chapter. Firstly, we prove the performance bound of the off-line scheme in the previous chapter, and then an on-line energy-efficient of throughput-based scheme for REBS-based networks is introduced. This scheme is based on the result of the off-line scheme, and in each execution time, the on-line scheme will adjust the old plan based on the current-available information. The adjustment will not affect the future optimization strategy of the old plan, therefore it will have a better performance than the off-line one. We demonstrate that the proposed on-line scheme outperforms than the off-line one and naive scheme in term of the system throughput.

The summaries of thesis and the related discussions of the future works are demonstrated in the last chapter.

1.5 Contributions

In this dissertation, we studies the joint optimization of traffic and energy management in wireless mesh networks powered by renewable energy. The main contributions of the dissertation are summarized as follows:

1. We combine the energy and traffic management, and formulate a joint-optimization framework. After that, we propose a throughput-maximization algorithm in order to assist the distribution of the traffic and energy consumption of the REBSs in the network. In addition, we check the optimality of the proposal with regard to the total system throughput.

2. On the basis of our first throughput-maximization proposal, we develop an energy-efficient algorithm in order to reduce the energy consumption. Therefore, the new scheme has better sustainability in contrast with our first proposal. At last, we demonstrate that our proposal has better energy efficiency compare with the previous proposal as well as the naive idea.

3. We propose an on-line dynamically adjusting scheme handling the imprecise estimation traffic profile. We prove the performance bound of the off-line scheme, which is determined by the precision of the traffic estimation. Then an on-line scheme is proposed, which will adjust the old strategy without affecting the future plan. We finally conduct various simulations in order to justify the efficiency of our on-line proposal in relation to total system throughput and energy efficiency.

Chapter 2

Overview of REBS-based Mesh Networks and Its Associating Settings in Disaster Area

2.1 Introduction to the REBS-based Mesh Networks

In the disaster situation, both of the energy and network resources are limited. Therefore the distribution of the energy and traffic becomes our major concern. This chapter begins with the introduction of the network components, and we categorize such components by demonstrating the energy flows and traffic flows.

2.1.1 Energy Flows inside REBS

As we discussed in the last chapter, after disaster, it is assumed that the REBSs in the disaster area will solely rely on the renewable energy. The input energy for each REBS can be divided into two categories. The first one is from the connected Microgrids, which is the green energy harvested by the energy harvesting facilities of the Microgrids'. The

second one is from the REBS's local energy harvesting facilities. In the residual part of this dissertation, these two kinds of energies will be denoted by remote energy input and local energy input, respectively. Both of these two kinds of energy inputs will be then directed to the battery of the REBS.

The Battery of the REBS is used to store the input energy, and such kind of energy might be used at once, or stored in the battery for future use. For the energy usage of each REBS, there are mainly two factors. The first factor is the static energy consumption, which is the certain amount of energy consumed so long as the REBS is activated. Such static energy consumption is induced by air conditioning consumption, the AC/DC converter waste, and so on. The exact energy consumption depends on the scale of the base station: the larger the size, the more the energy consumption it will cause. For example, the static energy consumption of the macro base station is 712W per hour (from the EARTH project in [2]), while for the LTE micro base station with one sector and one power amplifier, the hourly cost will be about 120W [3]. The other factor is the dynamic energy consumption. which is proportional to the number of activated subcarriers. Each subcarrier will cause a fixed amount of energy consumption, and will carry a certain amount of data traffic demands from the users'. Therefore on one hand, the number of activated subcarrier determines the upper bound of the collected uplink traffic, and on the other hand, it is also proportional to the dynamic consumed energy. Besides these two factors, there are also other energy consumptions, such as the energy used by the point-to-point data traffic transmission between two REBSs. However, such kind of energy usage is not significant, for instance, the point-to-point data traffic transmission is about 50W, which is far less than the static consumption 712.2W of the macro base station. Therefore, in the rest of this dissertation, such kind of consumption is neglected. The details of the energy flows inside an REBS is as the left part of Figure 2.1 shows. It is noted that the energy consumption only happens when the REBS is active (i.e., is switched on), otherwise, there will be no energy output.

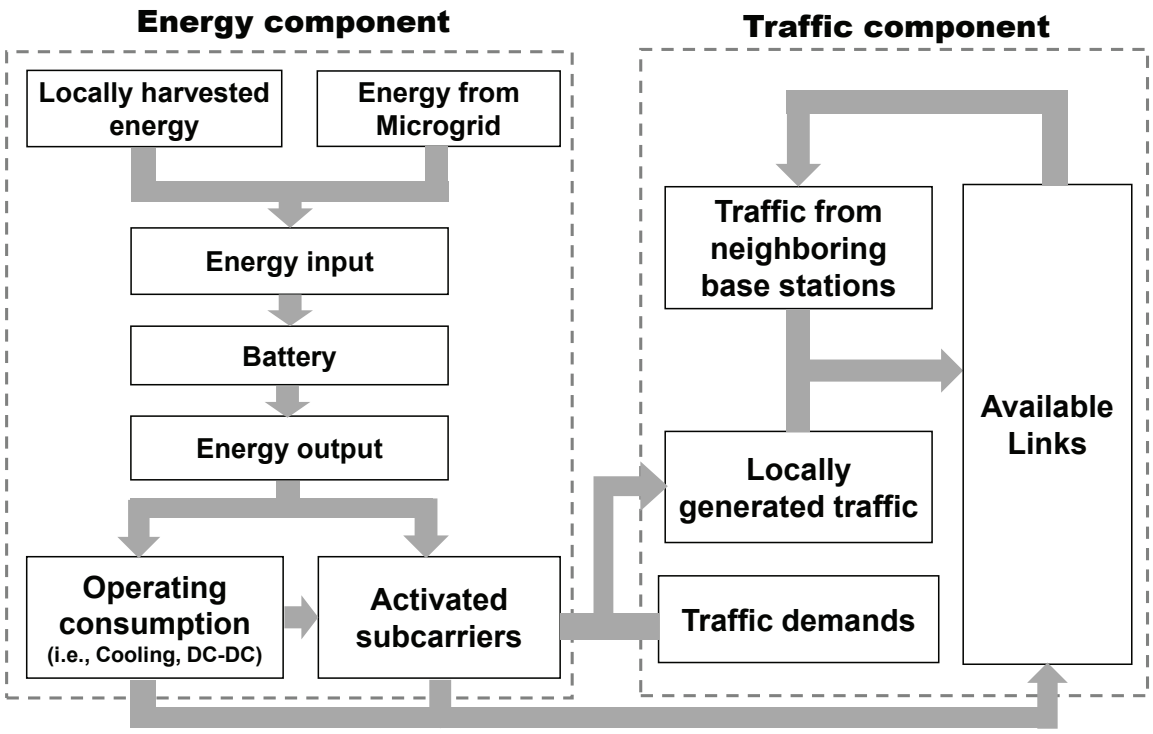

Figure 2.1: The energy and the traffic flows in the considered REBS-based mesh networks. ©2014 IEEE.

2.1.2 Traffic Flows in Network

As mentioned in the last chapter, the damages caused by the disaster will make the original network infrastructure (such as the connections to the MTSO, PSTN or others) unavailable. Therefore the REBS-based mesh network becomes our major concern. Because of the mesh feature, for each REBS, it has to not only deal with the local data traffic demand, but also help the neighbors' traffic reach the network gateway.

For a certain REBS, we denote the local data traffic demand as the one generated by the users in its coverage area. However, due to the limitation of the energy budget and bandwidth, such demands might not be fulfilled all the time. When the REBS is switched on, it can serve the local data traffic demand, and the amount of served data is limited by the number of activated subcarriers. We denote the amount of such to-be-served local

data traffic demand as local data traffic input. On the other hand, the REBS may receive the data traffic demand from activated neighbor REBSs, and that is the remote data traffic input.

Each REBS needs to deal with both of the local and remote data traffic input. There are two possible exits for the traffic: the first exit is the connected active REBSs, the connected active REBSs can act as a relay to transfer the traffic. If the REBS has a direct connection to the gateway, then it can directly send the traffic to the gateway. It is noted that the amount of the transferred traffic of each point-to-point link should be less than the bandwidth. For example, the Microwave panel such as MDR-8000 can afford about 300Mbps, while the typical bandwidth of the current long-distance WiFi such as NanoBridge can provide 80Mbps [4]. The traffic flows in the network is as the right part of Figure 2.1 shows.

According to the experimental result in [1], the state-of-the-art vehicle-borne cellular gateway has sufficient capabilities to transfer the traffics inside the network to the outside, therefore we assume that all the traffic sent to the network gateway can be dealt by the network gateways.

2.2 Spatial and Temporal Diversities of the Traffic and Energy

Due to the zero-grid energy input feature of the post-disaster case, the green energy generated from the energy harvesting facility is the only energy source. However, the energy input of such facility are not constant as the elapse of time. For example, the input energy of solar panel depends on the illumination intensity, and it is not hard to derive that the energy input at night would be zero, since there is no available sunlight in the evening. Similarly, the wind power also changes with time, therefore the wind turbine cannot have a stable energy input. For the REBSs in different places, the energy input

are not the same as well. Therefore the energy input of REBSs are different from time to time and from place to place.

On the other hand, the REBSs in the network also experience the spatial and temporal diversities of the data traffic demands. People inside the post-disaster area are likely to assemble in big shelters such as the stadium or auditorium. According to [5], one can estimate the data traffic demand by summarizing the details of the population in the coverage area as well as the ratio of active users. For each REBSs, the number of active users inside the coverage area causes the spatial diversity of the data traffic demand, while the changes of people's behaviors give the evidence in support for the temporal diversity of the data traffic demand.

2.3 Related Work

For the importance of the the considered structures and the associating schemes, a large number of research efforts have been devoted.

In [6] [7] [8], it is shown that in the post-disaster case, the Microgrid could play an important role in the energy distribution. Before disaster, the Microgrid is the energy distributer: it is used for handing off the energy received from power plant, to the connected BSs. When the disaster cause the disconnection of power plant to Microgrid, the Microgrid will then act in "Island Mode", which means the Microgrid will be apart from power grid, and it will use the solar panel or wind turbine to harvest the energy from ambient environment, such energy can be either stored in the local battery or sent to the connected REBSs. In [9], the control strategies of the Microgrid are studied, and in [10] [11] the energy management strategies are explored in order to reduce the non-renewable energy consumption from power grid with considering battery capacities, energy losses and so on. By inducing the Microgrid, it is demonstrated in [12] that the energy consumption cost can be significantly reduced by designing the schedule over a finite time

horizon. The similar Microgrid-assisted energy-efficient researches can be found in [13] [14] [15] [16] [17] and [18].

Besides the research on the assistance of the Microgrids in the post-disaster case, several studies are conducted so as to better utilize the energy of the REBSs. [3] [5] [19] deal with the non-renewable powered cellular systems. As the extensions, [20] [21] [22] [23] consider the hybrid energy input for the base stations, which includes the renewable energy from energy harvesting facilities, as well as the non-renewable energy from power plant.

Because the energy is sufficient in the above cases, these references are mainly address the issue of reducing the non-renewable energy consumption (or cost). The first aspect is to reduce the non-renewable energy consumption while fulfilling the users' requests. For the importance of the REBSs in reducing the OPEX, the second aspect is to reduce the associating costs for the non-renewable energy consumption. It is noted that these two kinds of objective are both for the energy efficiencies of the networks. [5] [3] [24] [25] and [26] investigate the energy consumptions of the base stations in the cellular network. The different energy-efficiency strategies for various scenarios are reviewed in [27].

As the only energy supply in the post-disaster case, the input renewable energy are analyzed in several literatures. According to the conclusion of [28] [29] [30] [31] and [32], one can get the expectation of the energy input profile by combining the information of the history input profile, the energy harvesting facilities (i.e., the size of solar panel, the type of wind turbine), the climate of the local area (i.e., the sunlight intensity and wind power). In [33] [34] [35] [36] [37] and [38], switching off the REBSs in the off-peak time of data traffic demand is demonstrated to be an efficient solution for saving the energy. When the base station is deactivated, the associating energy consumption would be zero, and the energy input would be zero at that time.

As another important aspect in the post-disaster case, in [39] and [40], the large-scale dataset of data traffic in cellular networks is studied. In [41], it is exhibited the high

fluctuation of data traffic demand of cellular network in both of time and space.

The flow control and load distribution schemes without considering the consumed energy are extensively studied. For example, for the transmission paths, [42] put the efforts on the trade off between the multiple one-hop paths and multiple hops in cellular networks. For the last-hop to the network gateway, [43] studies the load-balancing schemes for the gateway side, the proposed method can transfer some of the connections to the congested gateways, to the other light traffic gateways. However, in the post-disaster case, the bottleneck of the network performance caused by the limited energy has to be considered. Although the above-mentioned works cannot be directly employed, they shed lights on the latter studies on the joint optimization. Because of the diversities in spatial and temporal for both of the energy and traffic, the joint optimization scheme should be considered in the post-disaster case. Based on the assumptions, the existing studies for such studies can be categorized into three aspects. The first aspect is the optimization for a snapshot of the traffic and energy status. For example, in [44], the combination of routing, rate control as well as energy allocation are taken into consideration. In [45], the spectrum and energy efficiencies are addressed, the k-shortest path are employed to transfer the data traffic. Although both of the energy and traffic are covered in the solutions, the battery issues are not included, which may result in suboptimal result in the long run, in the condition of that energy or/and traffic profile are varying as the time elapse. [46] considers the spatial diversity of the traffic and energy consumption for Poisson-Voronoi tessellation (PVT) cellular networks, and explores the proposed energy-efficiency model. The second kind of studies assumes that the link capacities between two connected neighbor REBSs are always ample. For example, in [47], the energy input is supposed to follow G/G/1 process while the data input follows Poisson process respectively, and the way of transmitting the collected data traffic to the destinations is not in the scope of the consideration. Similarly, [48] considers various fairness routing strategies for the energy harvesting network with limited battery capacity, on the other hand, the routing are only supposed to be unsplittable routing or routing tree. In [49], the cooperations between the

neighboring REBSs in terms of spectrum and energy are explored, while the study is not based on the disaster case therefore the way of transmitting the data traffic is beyond the scope of this study. The study of [50] aims at extending the batteries' lives by carefully controlling the charging and discharging time. Thirdly, several works are conducted under the assumption that the energy is enough for sensor or BSs. In [51], a throughput maximization scheme is proposed, which can improve the network throughput and reduce the energy consumption.

It is noted that almost all of the above-mentioned solutions are solely relying on the local renewable energy supplies, and at our best knowledge, we are the pioneers that employing the remote energy input from the Microgrid in the REBS-based mesh networks, with considering the temporal-spatial diversities of energy input as well as the data traffic demands [52] [53].

2.4 Our Research Target

The target of this dissertation is to design the optimization frameworks, which aims at supporting the users' data traffic transmission demands as many as possible, and it also gives the best effort to reduce the energy consumption.

To realize such goal, the battery plays a crucial role, because the limited energy input should be used in the best time. Therefore, for the REBSs, the occasion for switching on or off, and the number of activated subcarriers when is switching on should be the controlled variables in order to save the current available energy for the future use. As a result, the topology of the REBS-based mesh network changes periodically because of the on and off status of the REBSs. It is noted that the operating status may not only affect the local supported data traffic, but also have the impact on the neighbors'. For example, as Figure 2.2 shows, in a certain time, REBS a wants to transfer its local supported data traffic. Because a does not have direct connection to the gateway, therefore, it has

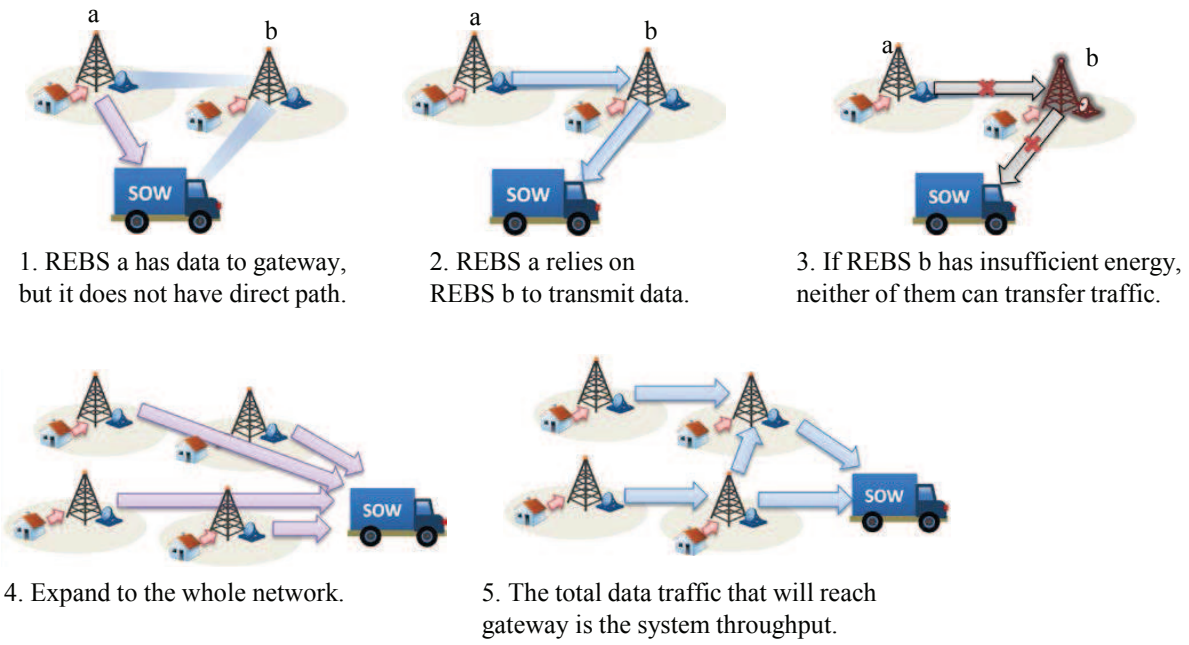

Figure 2.2: The cooperation of the data traffic transmission among the REBSs.

to rely on REBS b to relay the data. However, if b is switched off, then REBS a cannot transfer its data, because there is no available path to the gateway. For a certain time, the activated REBSs will carry the collected data traffic demand to the network gateway, and the collected data traffic demands is based on the temporally and spatially varying data traffic demands. The amount of collected traffic and the traffic delivering strategy are also the controlled variables. By combining the traffic and energy scheduling strategies, the scheme for improving the amount of supported data traffic demands of the users' within a certain time span can be derived. In the previous example, if we expand the single time slot condition to the whole network, then it will be the simplest case of our considered problem, and the total data traffic that reaches the network gateway is the total system throughput, which will be one of our goals in the thesis. In addition, in this thesis, we will also deal with the energy efficiencies, as well as the imprecise of the traffic profile.

2.5 The Advantage of Joint Optimization

As we mentioned, this dissertation will consider the joint optimization of the energy and traffic for the considered scenario. In order to address the necessity of the joint optimization, an example is introduced in this section. In the example, the Naive idea is used as the control algorithm: the major policy behind the Naive idea is to switch on the REBS so long it has enough energy.

The considered topology contains 7 REBSs and 1 network gateway. For simplicity, each REBS has 3.0 units of data traffic demand. The operating consumption equals 3.3 unit, and REBS 1, 2, 3, 4, 6 have initial energy of 6.6 unit while REBS 5 and 7 have 5.0 unit energy, in other words, these two categories of REBSs can operate for 2 and 1 time slot, respectively. The wireless connections and the capacity of each link are shown in Fig. 2.3. We consider the optimization for two time units, and the total system throughput is the sum of the system throughput within the considered time span. The topology and associating strategies of the two schemes are shown in Figure 2.3.

It can be seen that the energy and traffic strategies of the Naive scheme are not jointly considered (i.e., to get the maximum system throughput in current time, not the long-term optimization), and in the first time unit, all the REBSs can operate because of the sufficient energy, and the system throughput is 21.0 unit. In the second time, REBS 5 and 7 cannot be switched on due to lack of energy, and the system throughput is 8.0 then. The total system throughput is 29.0.

The strategy when considering the joint optimization is somehow different: REBS 5 is turned off in the first time unit even though it has enough energy, and the system throughput is 17.0, which is less than the one of Naive scheme. However, in the second time unit, REBS 5 has enough energy to operate, and is switched on. The system throughput is 17.0 then and the total system throughput is 34.0.

It can be seen that with the joint optimization scheme, the performance can be im-

proved.

2.6 Summary

In this chapter, we introduce the features of the REBS-based mesh network in disaster condition. Firstly, the rough graphs of the energy evolution and traffic transmission are demonstrated. After that, in the post-disaster scenario, the energy and traffic are various, and such varieties embody in space and time. We clarify the reasons that cause the diversities. In addition, the literature review is given by categories. Aiming at the drawbacks of the existed studies, we set the research goals in this dissertation, and the importance of joint optimization is addressed via an example.

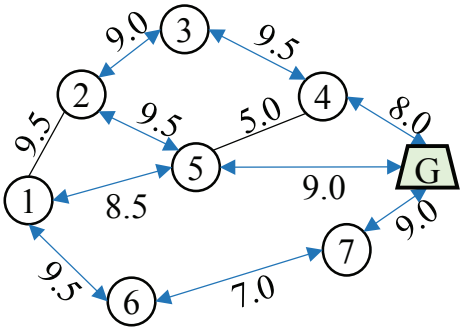

1. Network topology

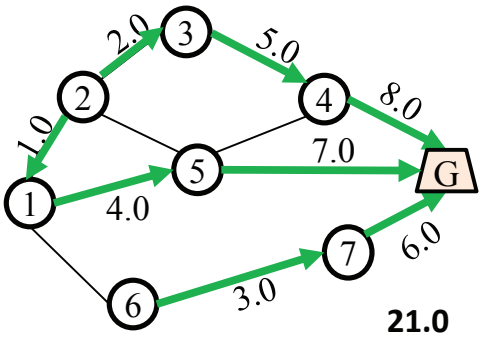

2. The system throughput in the first time unit is 21.0

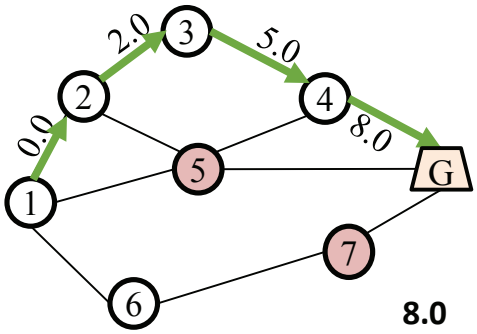

3. The system throughput in the second time unit is 8.0

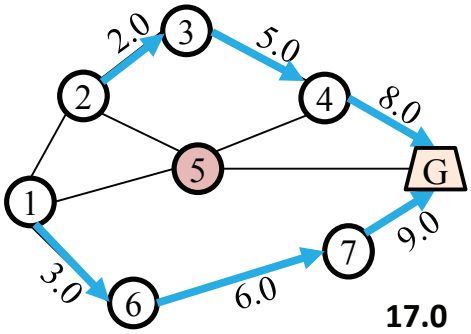

4. The system throughput in the first time unit is 17.0

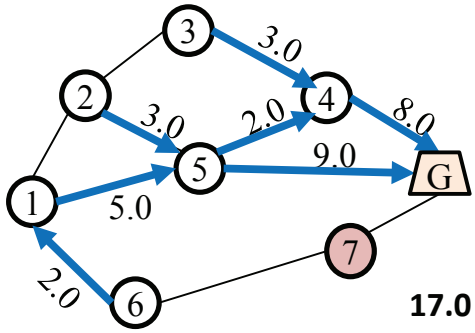

5. The system throughput in the second time unit is 17.0

Figure 2.3: The system topology of the example, and the associating solutions of the Naive scheme and joint-optimization scheme, respectively.

Chapter 3

The Off-line Scheduling and Load Distribution for REBS Mesh Networks

3.1 Introduction

In recent decades, the disasters happened all over the world demonstrate the importance of post-disaster treatment for the disaster area. The REBS-based mesh network is regarded as an effective solution for accommodating network services for such scenario, and we will subject the study to this network. However, as mentioned in the example in last chapter, the energy allocation strategy should be designed with the traffic distribution strategy in order to achieve good performance. In this chapter, we focus on maximizing the total system throughput, in other words, the users' data traffic demands are tried to be satisfied as mush as possible. To this end, we first investigate the characteristics in the post-disaster case. After that, we formulate the problem and propose the optimization framework. At the end of this chapter, we demonstrate the computer-based simulations. From the results, it can be seen that the proposed throughput optimization framework

can provide much higher total system throughput than the Naive idea.

The contributions of this chapter are summarized as follows:

- We analyze the scenario for the post-disaster case, and then give the reasonable assumptions for such scenario.
- We formulate the problem of maximizing the total system throughput with the assumption that the full-knowledge of the energy input profile as well as the traffic demand profile are available.
- Based on the formulated problem, we demonstrate its MILP-problem feature, and then an optimization framework is established for achieving the maximized total system throughput.
- We numerically demonstrate that the joint-optimization framework will yield performance improvement compared with the Naive solution in term of the total system throughput under various conditions.

3.2 Preliminaries

3.2.1 The Way of Energy Cooperation

As mentioned in previous chapter, the mission of the Microgrid in island mode is to deliver its local harvested energy to the connected REBSs. Therefore, the input energy for each REBS is the combination of the local energy harvesting facility, as well as the remote Microgrid. Due to such infrastructure limitations, the local energy input of REBS can only be used locally.

3.2.2 The Energy and Traffic Input Profiles

In order to design a long-term strategy, the knowledge of the energy input as well as the traffic demand of each REBS during this period is needed.

As analyzed in Chapter 2, the diversities of the energy input embody in time and space dimension. Therefore, for a certain REBS, the energy input changes with time. According to the analyses in [29][30][31], the energy input prediction can be derived by summarizing the information of weather condition (i.e., the wind strength is proportional to the energy input of wind turbine) and the historical energy provisions (i.e., the energy input changes periodically). Since the hourly energy input prediction can be achieved relative precisely with the modern techniques, we assume energy harvesting profiles of REBSs and Microgrids are the available information in the dissertation. It is noted that such technique is often used with the collaborative control with Wireless Sensor and Actuator Networks (WSANs) [54], in order to improve the harvesting efficiencies.

On the other hand, in the post-disaster area, the damages to the residential places will force the people to be gathered in the temporary shelters, such as the gymnasium and parks covered by the REBSs. Although in the causal case, it is relative hard to predict the data traffic demand due to the unpredictable people's activities, the data traffic demand after the disaster is much more simple, because the people inside the shelters will not move frequently. As a result, based on the previous researches such as [5], the data traffic demands can be estimated more precisely by the combination of the population, the ratio of active users as time elapse, the trend of the data traffic demand, and the previous profiles.

3.3 System Model

In this section, the system model is presented. As Fig. 1.3 and Fig. 1.4 shows, the energy flows and traffic flows are simultaneously existed in the considered network structure. Therefore, in the following subsections, we will respectively describe these two kinds of models. In addition, as the junction of the energy and traffic, the model that representing the network topology will be shown at first.

3.3.1 Network Model

The network topology can be denoted as an undirected graph $G = (\mathcal{N}, \mathcal{C})$, where $\mathcal{N}$ and $\mathcal{C}$ denote the set of REBSs in the disaster area and the connected links between two neighbor REBSs, respectively. Let n_i denote the ith REBS and therefore $\mathcal{N}$ equals $\{n_1, n_2, \ldots, n_N\}$, and N is the cardinal number of $\mathcal{N}$. For the two neighbor REBSs n_j and n_k, if there is a wired or wireless connection (n_j, n_k), then $(n_j, n_k) \in \mathcal{C}$, and the weight of (n_j, n_k), $c_{n_j}^{n_k}$, denotes its capacity.

When the input energy is sufficient, all the REBSs can be switched on and the aforementioned G can be used to denote the network topology during the considered time. However, in the post-disaster case, the REBSs may not be switched on all the time, since the energy input is not enough. When the REBS is inactive, the associated connections cannot be utilized, therefore the network topology will change with time due to the on-off status of the REBSs. Let $c_{(n_j,n_k)}(t_i)$ and $\rho_{n_j}(t_i)$ be the link capacity of (n_j, n_k) and the operating status of n_j in t_i, respectively, then $c_{(n_j,n_k)}(t_i)$ can be defined according to the following equations:

$$0 \leq c_{(n_j,n_k)}(t_i) \leq c_{n_j}^{n_k} \cdot \rho_{n_j}(t_i), \tag{3.1}$$

$$0 \leq c_{(n_j,n_k)}(t_i) \leq c_{n_j}^{n_k} \cdot \rho_{n_k}(t_i), \tag{3.2}$$

where $\rho_{n_j}(t_i)$ is a boolean variable and it can be given by

$$\rho_{n_j}(t_i) = \begin{cases} 1 & \text{if } n_j \text{ is active in } t_i, \\ 0 & \text{otherwise.} \end{cases} \tag{3.3}$$

From Eq.3.1 and 3.2, it can be seen that the operating status of a certain REBS determines the availabilities of the links: the link can be used if and only if the REBSs at the both ends are switched on.

We consider multiple network gateways in the scenario. We denote $\mathcal{G} = \{g_1, g_2, \ldots, g_F\}$ as the set of gateways. The cardinal number of $\mathcal{G}$ is F, and $\mathcal{G} \subset \mathcal{N}$. For the Microgrids, let $\mathcal{M}(\mathcal{M} = \{m_1, m_2, \ldots, m_M\})$ be the set of Microgrids, and $|\mathcal{M}| = M$. After disaster, several connections between Microgrids and REBSs are still available, we denote the set of the associating REBSs of m_k by $M^{(m_k)} = \{n_1^{m_k}, n_2^{m_k}, \ldots\}(n_i^{m_k} \in \mathcal{N})$. For some REBSs, because of the destruction to the connections, it will not have any energy input from Microgrids, therefore the union of $M^{(m_k)}$ $(m_k \in \mathcal{M})$ may not be equal to $\mathcal{N}$ for all instances.

3.3.2 Energy Related Model

As mentioned in Fig.2.1, the input energy of each REBS generally falls into two categories: the one is the local input energy from its own energy harvesting facilities, and the other one is the energy from Microgrid.

For the local energy input, it can only be used in the local place, this is due to the single energy transmission direction of the link between Microgrid and the REBSs. Let $l_{n_j}(t_i)$ be the local energy input of n_j in t_i. For a certain REBS, if it has the connection to the Microgrids, then the remote energy input is available. Suppose for Microgrid m_k, the amount of green energy it can receive in time t_i is $h^{m_k}(t_i)$, and the amount of energy that is sent to n_j is $h_{n_j}^{m_k}(t_i)$. It is noted that $h_{n_j}^{m_k}(t_i)$ also depends on the existence of the connection, and $h_{n_j}^{m_k}(t_i)$ is equal to 0 if there is no connection. The relationship between

$h_{n_j}^{m_k}(t_i)$ and $h^{m_k}(t_i)$ is given by the following equation:

$$0 \leq \sum_{n_j \in \mathcal{M}^{(m_k)}} h_{n_j}^{m_k}(t_i) \leq h^{m_k}(t_i) + B_{m_k}(t_i), \tag{3.4}$$

where $B_{m_k}(t_i)$ denotes the left energy of Microgrid m_k at the beginning of time t_i, the related formulation of the batteries will be demonstrated later. Eq.3.4 defines the constraint that the total amount of transferred energy in t_i should be less than the total available green energy of m_k.

Therefore, the total energy input of the REBS n_j in t_i can be defined according to the following equations:

$$H_{n_j}(t_i) = l_{n_j}(t_i) + \sum_{m_k \in \mathcal{M}} h_{n_j}^{m_k}(t_i). \tag{3.5}$$

It is noted that not all the REBSs have the remote energy input, this is because the damages of the disaster may cause the disconnection of the energy transmission links between the certain REBSs and Microgrids. Hence these REBSs will only have the local energy input.

So far the energy input of the REBSs is defined. The energy consumption aspect will be defined in the residual part of this section. After disaster, the REBSs will solely depend on the green energy to accommodate the network services. The total energy consumption of n_j in t_i is denoted by $P_{n_j}(t_i)$. As described in Fig. 2.1, $P_{n_j}(t_i)$ is the sum of the operating energy consumption and the subcarrier energy consumption. The subcarrier energy consumption is proportional to the number of active subcarriers [5], and let $s_{n_j}(t_i)$ ($s_{n_j}(t_i) \in \mathbb{Z}^+$) denote the number of active subcarriers of n_j in t_i, and we use e_s to represent the amount of consumed energy per active subcarrier. Moreover, we use e_0 to represent the static operating energy consumption. Therefore, for REBS n_j, the

energy consumption in t_i can be calculated by the following equations:

$$P_{n_j}(t_i) = [(s_{n_j}(t_i) \cdot e_s) + e_0] \cdot \rho_{n_j}(t_i), \tag{3.6}$$

From Eq.3.6, it can be seen that $P_{n_j}(t_i)$ is not zero only if $\rho_{n_j}(t_i)$ is 1. When $\rho_{n_j}(t_i) = 1$, the subcarrier can be activated, and the maximal number of active subcarriers is limited by S. Such relationship can be defined by the following equations:

$$0 \leq s_{n_j}(t_i) \leq S, \tag{3.7}$$

and

$$s_{n_j}(t_i) \leq S \cdot \rho_{n_j}(t_i). \tag{3.8}$$

It is noted that in the energy consumption model, the data transmission energy consumption is not taken into consideration, since such amount is not significant compared with these two major factors based on our analysis in Chapter 2.

The battery with finite capacity is equipped for each REBS and Microgrid, so as to stock the local or remote green energy input. The battery is with finite capacity, and let $B_{n_j}(t_i)$ denote the volume of residual energy in the battery of n_j at the beginning of t_i. Therefore, the energy evolution of the battery can be denoted as follows:

$$B_{n_j}(t_{i+1}) = B_{n_j}(t_i) + H_{n_j}(t_i) - P_{n_j}(t_i). \tag{3.9}$$

From Eq.3.9, the residual energy volume of a certain battery is determined by the original energy level $B_{n_j}(t_i)$, the total energy input $H_{n_j}(t_i)$, as well as the energy consumption during the current time $P_{n_j}(t_i)$. Moreover, the energy level of REBS n_j in t_i should be limited by its battery capacity $B^0_{n_j}$. Therefore, $B_{n_j}(t_i)$ can be denoted as the following constraint:

$$0 \leq B_{n_j}(t_i) \leq B^0_{n_j}. \tag{3.10}$$

As shown in Fig.1.3, the battery of the Microgrid also plays a crucial role in the disaster. The evolution of the battery of the Microgrid is similar to the REBS's. Denote $B^0_{m_k}$ as the battery capacity of the Microgrid, then the battery level of m_k in t_i should firstly satisfy the capacity constraint:

$$0 \leq B_{m_k}(t_i) \leq B^0_{m_k}, \tag{3.11}$$

Different from REBS, there will be no remote energy input for the Microgrids. For m_k, the energy output will be the energy transmitted to the connected REBSs. Then the energy evolution of m_k in t_i should then satisfy the evolution constraint:

$$B_{m_k}(t_{i+1}) = B_{m_k}(t_i) + h^{m_k}(t_i) - \sum_{n_j \in \mathcal{M}^{(m_k)}} h^{m_k}_{n_j}(t_i), \tag{3.12}$$

where $h^{m_k}(t_i)$ is the energy input of m_k in t_i, and $\sum_{n_j \in \mathcal{M}^{(m_k)}} h^{m_k}_{n_j}(t_i)$ represents the amount of energy that transmitted to the connected REBSs. The $B_{m_k}(t_i)$ is the residual energy level of m_k at the beginning of t_i.

3.3.3 Traffic Related Model

As demonstrated in 2.1, there might be two kinds of traffic inputs for a certain REBS. The first one is the locally generated traffic, and the second one is the traffic from neighboring REBSs.

The locally generated traffic is the traffic collected from the users in the coverage area of the REBS, and we use the data traffic demand to denote the such traffic. Denote $d_{n_j}(t_i)$ as the amount data traffic demand of n_j in t_i. In the post-disaster case, the input energy is insufficient, which will cause that the data traffic demand can be only partially satisfied. Let $f_{n_j}(t_i)$ be the real supported data traffic demand of n_j in t_i, therefore the

actual supported data traffic demand is limited by the data traffic demand:

$$0 \leq f_{n_j}(t_i) \leq d_{n_j}(t_i). \tag{3.13}$$

In t_i, the data traffic demand can be satisfied if and only if n_j is active. In other words, $f_{n_j}(t_i)$ is larger than 0 only if $\rho_{n_j}(t_i)$ is 1. On the other hand, the number of active subcarrier is also proportional to the actual supported traffic demand $f_{n_j}(t_i)$:

$$f_{n_j}(t_i) \leq \rho_{n_j}(t_i) \cdot s_{n_j}(t_i) \cdot r_0, \tag{3.14}$$

where $s_{n_j}(t_i)$ is the number of active subcarrier in t_i, and r_0 is the rate can be provided by an active subcarrier. It can be seen from Eq. 3.1, 3.2, 3.6 and 3.14 that there are the junctions between the energy and traffic scheduling strategy: when the REBSs as well as associating subcarriers are active, there might be more energy that will be consumed, but at the same time, the more traffic can be collected and transmitted.

Besides the local data traffic demand, the REBSs in the network also assume the responsibilities for relaying the neighbors' to the network gateways. The traffic sent from neighbors is denoted as the remote data traffic demands. We will present the traffic transmission from the point of view of flow: let $f_{n_l}^{(n_j,n_k)}(t_i)$ be the amount of actual supported data traffic demand of REBS n_l, and sent from n_j to n_k in t_i. Moreover, denote $f^{(n_j,n_k)}(t_i)$ as the total traffic that sent from n_j to n_k in t_i, then $f^{(n_j,n_k)}(t_i)$ and $f_{n_l}^{(n_j,n_k)}(t_i)$ have the following relationship:

$$f^{(n_j,n_k)}(t_i) = \sum_{n_l \in \mathcal{N}} f_{n_l}^{(n_j,n_k)}(t_i) \leq c_{(n_j,n_k)}(t_i). \tag{3.15}$$

It is noted that in Eq. 3.15, n_l and n_j can be the same REBS. Because the REBS n_j has

to deal with the local actual supported traffic demand $f_{n_j}(t_i)$, therefore

$$f_{n_j}(t_i) = \sum_{u \in \mathcal{N} \setminus \{n_j\}} f_{n_j}^{(n_j,u)}(t_i), \forall n_j \in \mathcal{N}. \tag{3.16}$$

The non-gateway REBSs are acting as relays when transferring the neighbors' traffic. As a result, for the non-gateway REBS n_j, it aims at sending the local traffic demand as well as the remote traffic demand to the network gateways. Therefore, the REBSs should follow the constraints below:

$$f_{n_j}^{(u,v)}(t_i) = -f_{n_j}^{(v,u)}(t_i), \forall u, v, n_j \in \mathcal{N}, \tag{3.17}$$

$$\sum_{v \in \mathcal{N}} f_{n_j}^{(u,v)}(t_i) = 0, \forall u \in \mathcal{N} \setminus (\{n_j\} \cup \mathcal{G}), n_j \in \mathcal{N}, \tag{3.18}$$

where the sign in Eq.3.17 represents the direction of the flow. The zero in Eq. 3.18 denotes that as the relay, n_j need to send all the relayed traffic.

We use an example to particularize the aforementioned models. Fig. 3.1 demonstrate the snapshot of network structure and the Microgrid connections of the example, and the time label is ignored. As shown in this figure, there are 5 REBSs, in which g_1 is the network gateway. In this figure, n_2 is inactive, and it can neither collect the local data traffic demand (i.e., Eq. 3.14) nor transfer the local and remote traffic input (i.e., Eq. 3.1, 3.2). On the other hand, n_4 connects to g_1, n_1 and n_3 and n_4 is active, therefore n_4 can collect and send the traffic. Because all the neighbors of n_4 are active, the amount of traffic sent to each REBS can be denoted as $f^{(n_4,n_1)}$, $f^{(n_4,n_3)}$ and $f^{(n_4,g_1)}$, respectively, and the sum of them is equal to f_{n_4} according to Eq. 3.16 and 3.18. In addition, the links in Fig. 3.1 are bi-directional hence the REBSs at the both side of the link can mutually transfer the data to each other.

In the energy layer, there are 2 Microgrids, hence $|M| = 2$. Since there is no connection

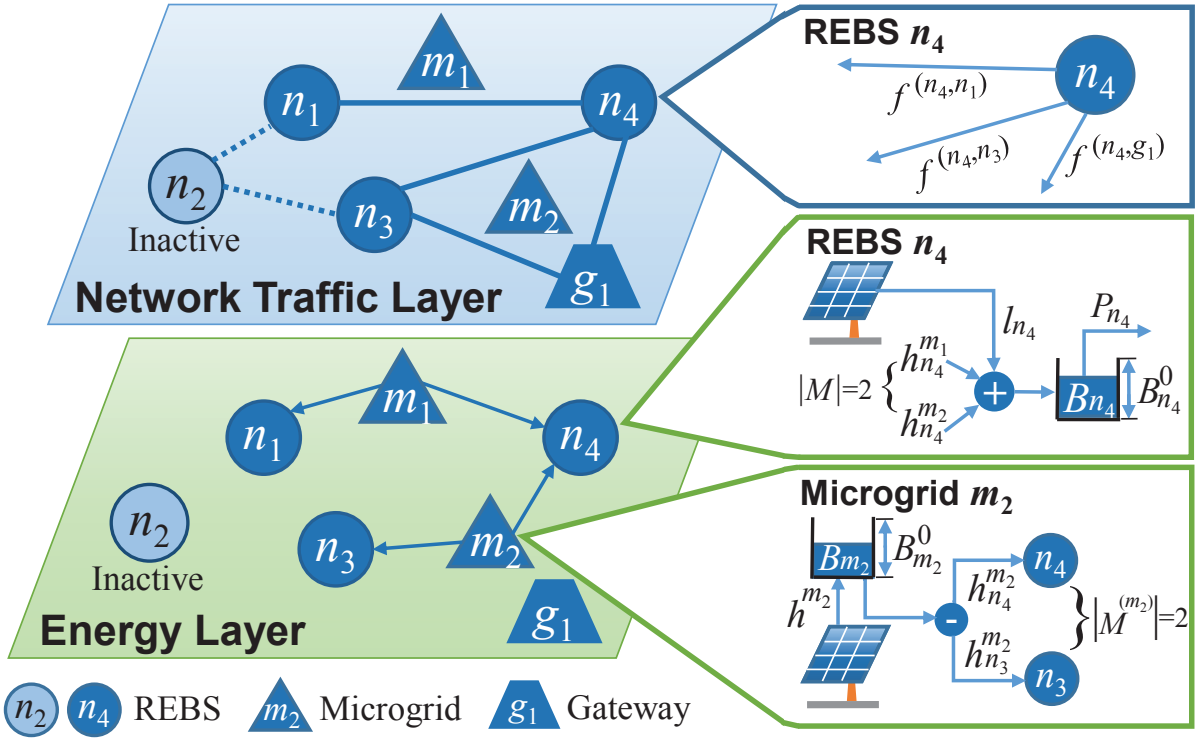

Figure 3.1: Traffic flow between REBSs, and energy flow inside REBSs and Microgrids. ©2015 IEEE.

to the Microgrids, n_2 does not have remote energy input. On the other hand, n_4 and n_1 have connection to Microgrid m_1 therefore they can receive the energy from m_1. In addition, n_4 can also get the remote energy from m_2, and according to Eq. 3.5, the amount of received remote energy is $h_{n_4}^{m_1} + h_{n_4}^{m_2}$, while the local energy input is l_{n_4}, and the total energy input of n_4 is $H_{n_4} = h_{n_4}^{m_1} + h_{n_4}^{m_2} + l_{n_4}$. The energy input will first reach the place of the battery as Fig. 1.3 shows, and then be used to activate the REBS and associating subcarriers (i.e., Eq.3.9 and Eq.3.6). From the viewpoint of the Microgrid, it will harvest the green energy and deliver to the connected REBSs. Take m_2 for the example, it will receive the h^{m_2} unit of local energy input, and send $h_{n_4}^{m_2}$ and $h_{n_3}^{m_2}$ to REBS n_4 and n_3, respectively. Note that the energy will also be sent to the battery of m_2 at first.

3.4 Research Objective

Let $[0, T_0)$ denote the considering time span, in which T_0 is used to denote the time that the network will be reconstructed. The time-slotted system is used in our consideration, which means that interval $[0, T_0)$ will be divided into equal samples. If T is the number of time slots, and the length of each sample is denoted by t_0, then $[0, T_0)$ can be denoted as the set $\mathcal{T} = \{t_1, t_2, ..., t_T\}$, where t_i $(0 \leq i \leq T)$ is the index of time slot i. We assume that the energy input and data traffic demand of each REBS and Microgrid will not change within each time sample.

The optimization objective in this chapter is to maximize the total system throughput. The total system throughput is the sum of system throughput in the considering time span:

$$U = \sum_{t_i \in \mathcal{T}} U(t_i), \tag{3.19}$$

where U and $U(t_i)$ denote the total system throughput and system throughput in t_i, respectively.

The system throughput in t_i, $U(t_i)$, is the sum of the data traffic sent to the network gateways:

$$U(t_i) = \sum_{g_k \in \mathcal{G}} \sum_{n_j \in \mathcal{N}} f^{(n_j, g_k)}(t_i). \tag{3.20}$$

According to Eq. 3.16, Eq. 3.17 and Eq. 3.18, the amount of data traffic which is sent to the network gateway is equal to the sum of the actual supported traffic demand of the REBSs. Therefore, the system throughput in t_i can be given by the following equation:

$$U(t_i) = \sum_{n_j \in \mathcal{N}} f_{n_j}(t_i), \tag{3.21}$$

and

$$U = \sum_{t_i \in \mathcal{T}} \sum_{n_j \in \mathcal{N}} f_{n_j}(t_i). \tag{3.22}$$

Our objective in this chapter is to maximize the total system throughput for the considered time span:

$$\text{P1: } \mathbf{max}\ U = \mathbf{max} \sum_{t_i \in \mathcal{T}} \sum_{n_j \in \mathcal{N}} f_{n_j}(t_i). \tag{3.23}$$

According the equations from Eq. 3.1 to Eq. 3.22, the variables that will affect the result of U are fourfold: the operating status of the REBS in each time slot (i.e., $\rho_{n_j}(t_i)$), the amount of energy distribution of each Microgrid in each time slot (i.e., $h_{n_j}^{m_k}(t_i)$), the amount of flow sent to each neighbor for each REBS in each time slot (i.e., $f_{n_l}^{(n_j,n_k)}(t_i)$), and the number of active subcarriers of each REBS in each time slot (i.e., $s_{n_j}(t_i)$). We use a quadruple $\mathcal{U}(\vec{\rho}, \vec{h}, \vec{f}, \vec{s})$ to represent the designed strategy, where $\vec{\rho}$, $\vec{h}$, $\vec{f}$ and $\vec{s}$ denote the strategy of the above-mentioned operating status, energy distribution, flow distribution, and number of active subcarrier, respectively.

3.5 Problem Formulation

3.5.1 The Equivalent Transformation of Constraints

Based on the aforementioned analysis, the maximized total system throughput can be calculated by a decent choice of the quadruple $\mathcal{U}$.

Eq. 3.6 can be transferred as the following equations:

$$P_{n_j}(t_i) = s_{n_j}(t_i) \cdot e_s \cdot \rho_{n_j}(t_i) + e_0 \cdot \rho_{n_j}(t_i), \tag{3.24}$$

and it can be seen that such constraint includes the non-linear variable combinations (Eq.3.14 is non-linear as well), therefore the optimization problem defined in Eq.3.23 is non-linear. However, the problem has special structure, and the non-linear constraint can

be transformed by the following procedures. Let us introduce a new extra variable $\delta_{n_j}(t_i)$, which is equal to:

$$\delta_{n_j}(t_i) = e_s \cdot \rho_{n_j}(t_i). \tag{3.25}$$

Moreover, we have the following relationship:

$$\delta_{n_j}(t_i) = e_s \cdot \rho_{n_j}(t_i) \leq S \cdot (\rho_{n_j}(t_i))^2 = S \cdot \rho_{n_j}(t_i). \tag{3.26}$$

Therefore Eq.3.23 and Eq.3.14 can be given as follows:

$$P_{n_j}(t_i) = s_{n_j}(t_i) \cdot \delta_{n_j}(t_i) + e_0 \cdot \rho_{n_j}(t_i), \tag{3.27}$$

and

$$f_{n_j}(t_i) \leq \delta_{n_j}(t_i) \cdot r_0. \tag{3.28}$$

It can be seen that the objective funtion in Eq.3.23 (P1) is the linear combination of $\mathcal{U}$. On the other hand, the equations that contain $\vec{s}$ and $\vec{\rho}$ are the linear combinations of integer variables, since $\rho_{n_j}(t_i)$ can only be 1 or 0, and the number of active subcarriers can only be the integers from 0 to S. Moreover, the residual equalities and inequalities from Eq.3.1 to Eq. 3.18 are linear. Therefore the problem with the combination of linear and integer constraint of the variable can be described as the MILP problem.

The MILP problem can be efficiently attacked by many of existing approaches such as branch and bound or cutting plane, In Algorithm 1, we demonstrate the algorithm of the branch and bound, and the detail steps of the procedure of branch and bound is in the appendix of [53].

Algorithm 1: Off-line Total System Throughput Maximization Scheme

Input: Network topology information: $\mathcal{N}, \mathcal{G}, \mathcal{M}, \mathcal{C}$.
Energy related information: e_s, e_0, $h_{n_j}^{m_k}(t_i)$, $h^{m_k}(t_i)$, $l_{n_k}(t_i)$.
Traffic related information: $d_{n_j}(t_i)$ r_0.
Output: $(\vec{\rho}, \vec{h}, \vec{f}, \vec{s})$ for problem P1.

Relax the integer constraints of $\vec{\rho}$ and $\vec{s}$ into linear ones, then the problem P1 is transformed into P1';
Solve the linear programming problem P1';
Let $\overline{O}$ record the result and $\boldsymbol{u}' = (\vec{\rho}', \vec{h}', \vec{f}', \vec{s}')$ is the associated variables;
if $\boldsymbol{u}'$ *satisfies integer constraints of P1* **then**
    $\underline{O}^* = \overline{O}$;
else
    $\underline{O} = 0$;
    $Cons$ = the constraints of P1;
    Choose one relaxed constraint x that does not follow the constraints of P1. Let χ denote the value of x;
    $(\underline{O}^*, \overline{O})$= BranchBound($Cons$, x, χ, P1, $\underline{O}$, $\overline{O}$);

3.5.2 Discussion on the Computation Cost

Although the previous proposed algorithm can provide an effective solution to the considered optimization framework, it is worthy to discuss the efficiency of the algorithm since the MILP problem is NP-hard in general, and the time complexity is not polynomial unless NP is equal to P.

The computation cost mainly depends on the scale of the integer variables since they dominate the computation cost. In the residual part, we will discuss the availability of the algorithm in threefold. Firstly, to relax the integer constraint of the active subcarrier can greatly reduce the complexity, since half of the integer variables will be transferred to the linear ones. On the other hand, the impact to the performance is bounded, since the provided rate of each subcarrier is not large (i.e., 0.5Mbps) compared with the large number of subcarriers (i.e., 600), and the performance gap between the original result and relaxed one is bounded by $r_0 \cdot T \cdot N$.

Secondly, the number of REBSs in the disaster area is not the large. In general, the

radius of the coverage area of a macro BS is more than 5km (i.e., maximum of 20km in [55]), which means that for a certain range of disaster area, the actual number of macro base station is relative small.

Thirdly, the time span that optimization plan will deal with is much more larger than the computation time cost. In other word, the timeliness may not be the key concern for the problem so long as it can figure out the result within the acceptable time period. As mentioned in Chapter 1, the reconstruction might be finished for several days or even weeks, therefore we assume that a one-time execution is affordable.

Also, it is noted that for the length of each time slot, a smaller slot length may lead to a better system performance. The reason is, as the granularity of the time partition becomes finer, the adjustment toward the strategy for the REBSs will be more timely. However, on the other hand, the sampling frequencies of the energy and traffic in each time slot will rise accordingly. Because it is not possible to get the two profiles in arbitrary small granularity, and the performance improvement gained by the smaller granularity is limited. In addition, the computational complexity will be increased, since the scale of variables becomes larger. In this dissertation, the length of the time slot is set to be 1 hour, which is as in [5] and [29].

3.6 Performance Evaluation

In this section, the total system throughput of the proposed optimization framework is compared with the one of the Naive scheme through a computer-based simulations.

3.6.1 Settings of the Simulation

The parameters of the simulation are listed in table 3.1, and the parameters are set according to the previous analyses and the commercial products. As table 3.1 shows, we

Table 3.1: Experimental Parameters ©2014 IEEE.

Parameter	Value
The length of the time slot ($\|t_i\|$)	1 hour
The number of considered time slots (T)	10
Number of REBSs (N)	10
Number of Microgrids (M)	3
Bandwidth of the Backhaul link ($c_{n_j}^{n_k}$)	80Mbps to 300Mbps
Operating power consumption (e_0)	712.2W
Power consumption per each subcarrier (e_s)	1.06W
Number of subcarriers (S)	600
Battery capacity of REBS ($B_{n_j}^0$)	2000W
Battery capacity of Microgrid ($B_{m_k}^0$)	2000W
Amount of energy of REBS at t_1 ($B_{n_j}(t_1)$)	2000W
Amount of energy of Microgrid at t_1 ($B_{m_k}(t_1)$)	2000W
Rate of subcarriers (r_0)	0.5Mbps

assume that the length of each time slot t_i is 1 hour, and the number of considered time slot is 10 (i.e., $T = 10$), which means the optimization will cover a 10-hour period. There are 10 REBSs and 3 Microgrids in the network (i.e., $N = 10$ and $M = 3$). The REBSs will be interconnected with each other by microwave or long-distance Wifi. The bandwidth of the links that connects two neighbor REBSs are randomly chosen from 80Mbps to 300Mbps. Because we consider the macro base stations, the operating energy consumption is $712.2W$ (i.e., $e_0 = 712.2W$), the energy consumption of each active subcarrier is 1.06W (i.e., $e_s = 1.06$), and the upper bound of the active subcarrier is 600 (i.e., $S = 600$) according to the settings in [3]. In addition, the battery capacity is 2000W therefore $B_{n_j}^0 = 2000W$.

The considered topology is shown in Fig.3.2. The network backhaul is made up by bi-directional links and we use straight line to denote them. Microgrid a, b and c have 2, 3 and 1 associating REBS(s) respectively. In the experiment, we mainly investigate the performance of the total system throughput.

The Naive idea used in this section is same as the idea in section 2.5. The idea behind the Naive one is to activate the REBS so long as it has enough energy. Such energy

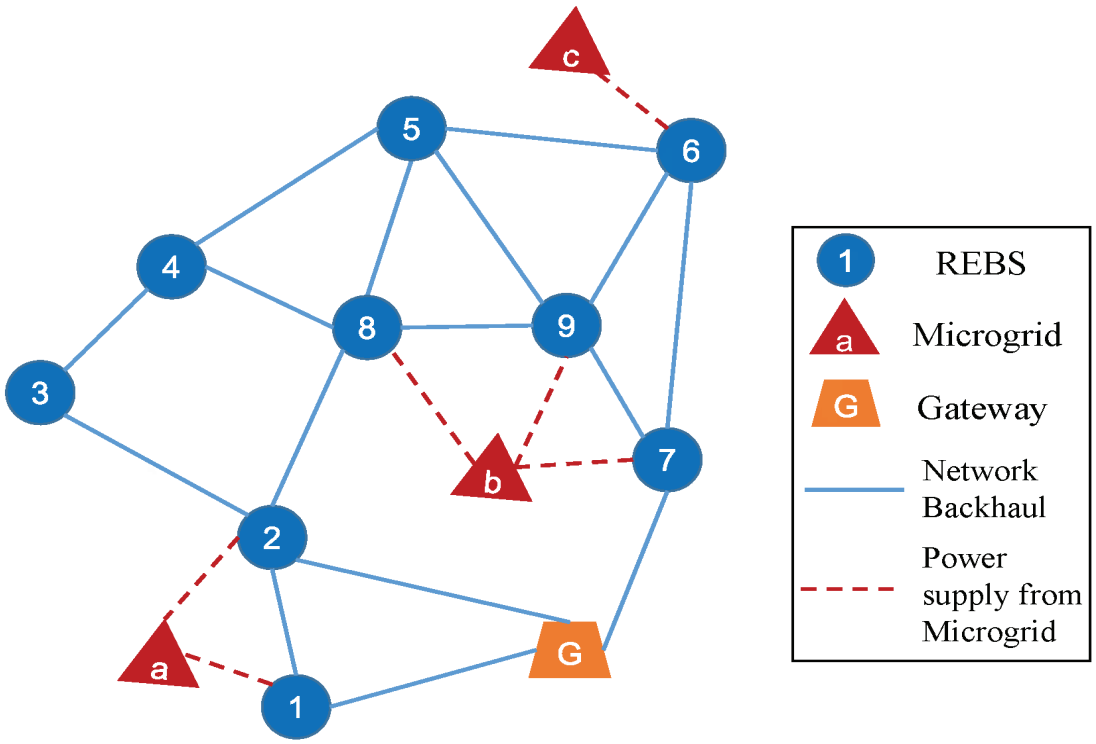

Figure 3.2: System topology used in the part of performance evaluation. ©2014 IEEE.

utilization strategy can be used in the non-disaster scenario. For the local data traffic demands, the Naive idea encourages the REBS support as much traffic as possible. If the traffic collection energy consumption (i.e., in Eq.3.14) can be fulfilled by the energy in the REBS's battery, then the associating amount of energy will be reduced in the battery. Otherwise the REBS will send the energy transmission request to the connecting Microgrid, after receiving all the energy transmission requests from the connecting REBSs, the Microgrid will firstly sort the requests in ascending order by the amount of energy required, and then such requests will be addressed orderly, until the energy inside the battery of Microgrid is insufficient for satisfying any of the residual REBS's demand. After Microgrid determines the transferred energy, we have the energy consumption strategies of REBSs. Finally, the max-flow algorithm is used to figure out the traffic distribution strategies of the REBSs.

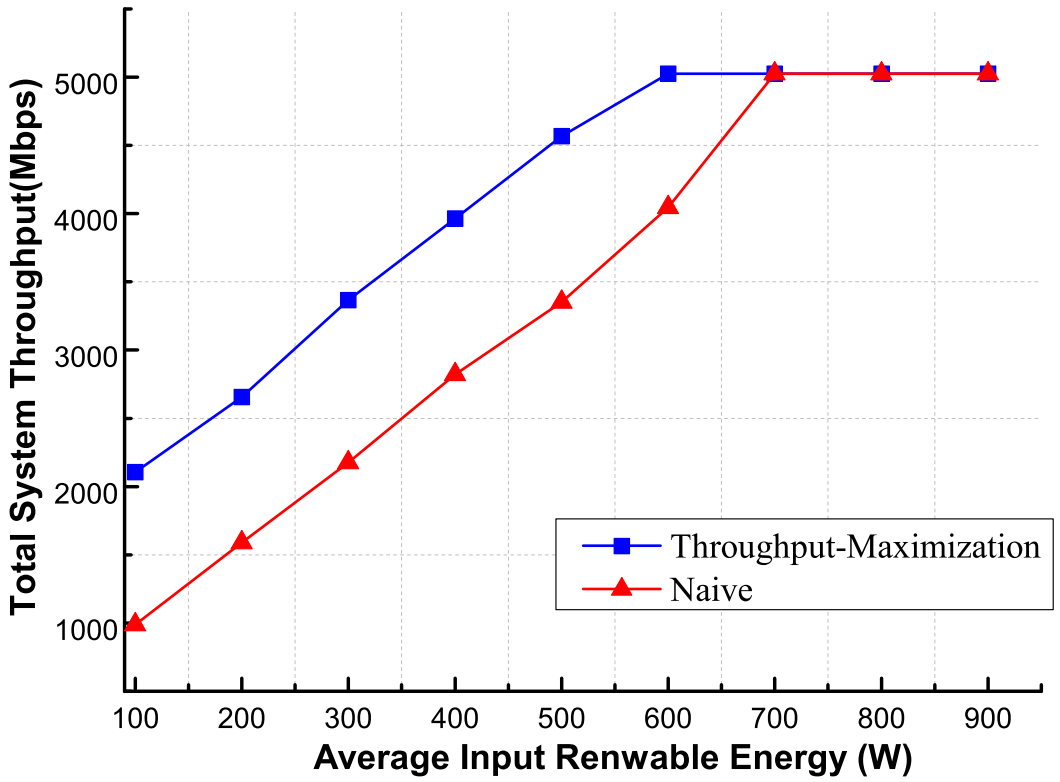

Figure 3.3: The effect of average input renewable energy on system throughput of the proposed scheme and naive scheme. ©2014 IEEE.

3.6.2 Impact of the Energy Input on Total System Throughput

At first, we analyze the relationship between the average input renewable energy of the REBSs and Microgrids, and the total system throughput. Therefore, we set the input renewable energy as the variables. The renewable energy input in each time slot (i.e., $l_{n_j}(t_i)$ and $h^{m_k}(t_i)$) is selected from the interval $[0.5 \cdot \text{x-axis value}, 1.5 \cdot \text{x-axis value}]$, and is i.i.d. At the same time, the data traffic demand of each REBS in each time slot is randomly and uniformly selected from $[40\text{Mbps}, 100\text{Mbps}]$ (i.e., $f_{n_j}(t_i) \in [40\text{Mbps}, 100\text{Mbps}]$). Other constant variables are set as the table 3.1 shows.

Fig. 3.3 demonstrates the relationship between the average input renewable energy of REBSs and Microgrids, and the total system throughput (i.e., U). As we can see from Fig. 3.3, there is a positive correlation between U and the renewable energy input. The reason is, as the green energy input increases, the longer active time and more subcarriers can be supported of each REBS. As a result, much more traffic will be transferred to the network gateway and U will be larger. In addition, it can be seen that the proposed joint energy and traffic throughput-maximization scheme has a better performance than the Naive scheme. The reason is, the Naive idea puts effort on the traffic issue, and ignores saving the energy for future use. Although the Naive idea can achieve the maximal system throughput in the first time slot, the energy may not be used optimally, therefore the performance may be unsatisfied in the upcoming time slots. It is worthwhile to note that, both of these schemes have an upper bound of the total system throughput (i.e., about 5000Mbps in this simulation). When the renewable energy input is sufficient, the only bottleneck of the network is the bandwidth, and the total system throughput is equal to the product of T and the network capacity for the traffic. In Fig. 3.3, when the green energy input is larger than 600W, the joint energy and traffic scheme reaches its upper bound while for the Naive idea, such upper bound cannot be reached until the energy input is larger than 700W.

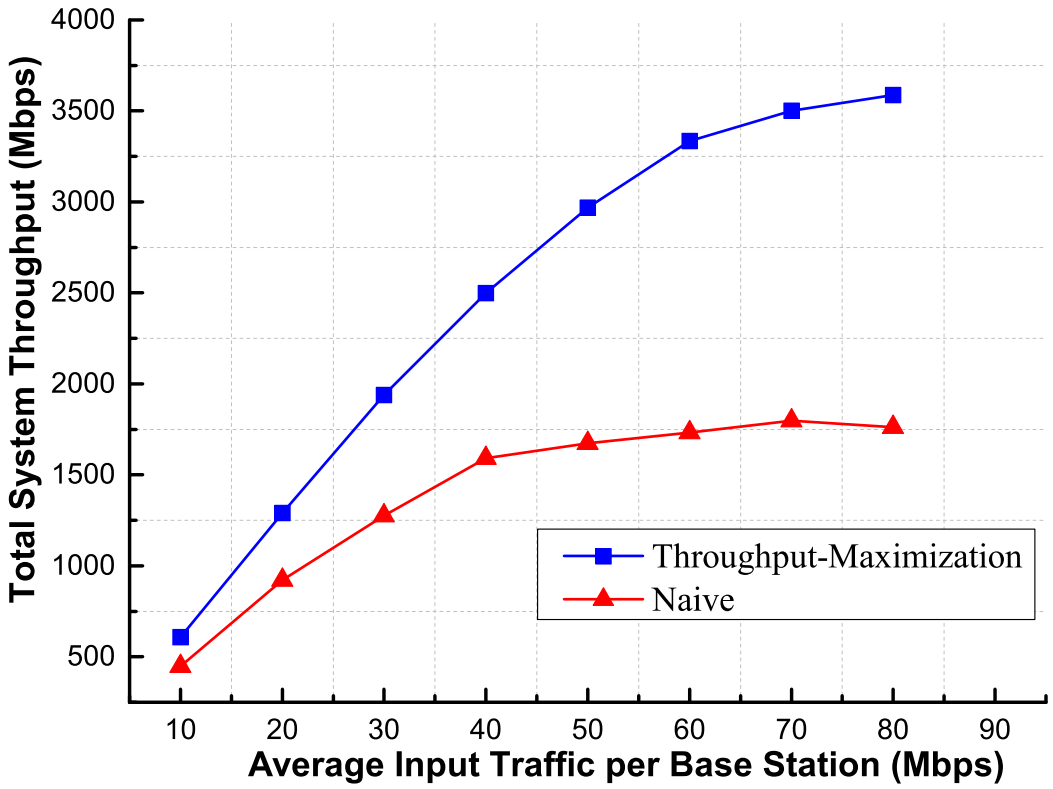

Figure 3.4: The effect of average input traffic per base station on total system throughput of the proposed scheme and naive scheme. ©2014 IEEE.

3.6.3 Impact of the Traffic Input on Total System Throughput

Secondly, we study the effect of the data traffic demand (traffic input) on the total system throughput. In this part, the data traffic demands of the REBSs (i.e., $f_{n_j}(t_i)$) are the variables, and the x-axis value denotes the expectation of such demands. The value of $f_{n_j}(t_i)$ is uniformly and randomly chosen from $[0.5 \cdot \text{x-axis value}, 1.5 \cdot \text{x-axis value}]$. The green energy inputs for REBSs and Microgrids are selected from $[100\text{W}, 300\text{W}]$ and are i.i.d.

Fig. 5.6 illustrate such relationship. From Fig. 5.6, it can be known that there is a clear performance gap between the proposed joint energy and traffic scheme, and the Naive idea. Along with the increase of the traffic input, the total system throughput will rise up accordingly, the result can be summarized as follows. As the input traffic becomes larger, the active REBSs can support more data traffic demand only with the cost of activating more subcarriers, the consumption of which is much more lower than activating more REBSs (i.e., $e_s = 1.06\text{W}$ while $e_0 = 712.2\text{W}$). When the traffic input is low, the total system throughput will be low as well, therefore the gap is not that large. As the traffic input becomes larger, the impact of the strategy on the performance is more obvious, therefore the gap becomes larger. Compared with the energy requirement (i.e., $e_0 = 712.2\text{W}$), the energy input is not enough (i.e., $l_{n_j}(t_i) \leq 300\text{W}$), therefore when the energy input is insufficient, the joint energy and traffic scheme may have a clear performance advantage when the data traffic input is high, which might be just the case in post-disaster scenario.

3.7 Summary

In this chapter, the throughput-maximization scheme is proposed. Firstly, we analyze the conditions in the post-disaster case, including the assumptions on the network structures, as well as the input profiles of energy and traffic. Secondly, we described the considered

scenario in a formalized manner, and then the network model, the energy related model and the traffic related model are demonstrated respectively. After that, the research objective is demonstrated using the aforementioned variables. In the fourth part, we prove that the considered problem is an MILP problem after the transformation of the constraints. The availability of the considered framework is analyzed in the next part. Finally, the numerical result is demonstrated.

Chapter 4

The Off-line Energy Efficient Scheduling and Load Distribution for REBS Mesh Networks

4.1 Introduction

Because the renewable energy is the only energy resource in the post-disaster area, the energy should be used in the best case. In addition, as mentioned in previous chapter, the considered time span is the estimated time duration for rehabilitating the network services in the daily manner. However, the reconstruction effort may not be controlled perfectly therefore the real time cost can be longer than the expectation. In that case, the designed scheme should use the energy efficiently. In this chapter, our proposal is twofold: the first is to maximize the total system throughput, and the second is to deal with the energy efficiency. We first define the energy efficiency, and then transform our goal into selecting the most energy efficient result from the strategies that with the maximal total system throughput. After that, we propose a two-stage optimization framework to achieve the Pareto-optimal result. Finally, we check our proposals via computer-based simulations. The numerical results demonstrate that besides achieving the maximal total

system throughput, the proposed two-stage optimization framework can provide higher energy efficiencies.

The major contributions of this chapter are summarized as follows:

- We analyze the potential drawbacks of the throughput maximization problem, and then propose a new objective considering the energy efficiency aspect.
- We demonstrate that the problem with the energy-efficiency objective is also the MILP problem.
- We propose a two-stage energy efficient throughput-maximization framework, and the proposed throughput-maximization scheme has better energy efficiency than the other strategies which also have the maximal total system throughput.
- We conduct the computer-based simulations, and show that the proposed two-stage optimization scheme achieves higher energy efficiency than the Naive idea and the original throughput maximization scheme.

4.2 System Model and Optimization Objective

In this section, we formulate the problem and describe the objective of this chapter. After that, the optimization objective is analyzed.

4.2.1 System Model

The considered scenarios and related variables are the same in Chapter 3, and we list them in Table 4.1 for convenience. As we mentioned, for the problem P1 in Eq. 3.23, there can be more than one solution. In this chapter, we consider the energy harvesting abilities of the REBSs and Microgrids are the available information. During $\mathcal{T}$, the total harvested energy of REBS n_j can be given by the following equation:

$$\sum_{t_i \in \mathcal{T}} l_{n_j}(t_i), \tag{4.1}$$

Table 4.1: Variable Summarization

Variable	Meaning
t_i	Index of time slot i.
T	Number of time slots.
$\mathcal{T} = \{t_1, t_2, ..., t_T\}$	Time span using time sample.
n_j	Index of REBS j.
N	Number of REBSs.
$\mathcal{N} = \{n_1, n_2, ..., n_N\}$	Set of REBSs.
(n_j, n_k)	Connection between n_j and n_k.
C	Number of links.
$\mathcal{C} = \{(n_{j_1}, n_{k_1}), ..., (n_{j_C}, n_{k_C})\}$	Set of the links.
$c_{n_j}^{n_k}$	Capacity of (n_j, n_k).
$G = (\mathcal{N}, \mathcal{C})$	Network topology.
$\rho_{n_j}(t_i)$	Operating status of n_j in t_i.
$c_(n_j, n_k)$	Link capacity of (n_j, n_k) in t_i.
F	Number of gateways.
g_f	Index of gateway f.
$\mathcal{G} = \{g_1, g_2, ..., g_F\}$	Set of gateways.
m_k	Index of Microgrid k.
M	Number of Microgrids.
$\mathcal{M} = \{m_1, m_2, ..., m_M\}$	Set of Microgrids.
$M^{(m_k)}$	Set of associating of REBSs of m_k.
$f_{n_j}(t_i)$	Supported traffic of n_j in t_i.
$d_{n_j}(t_i)$	Data traffic demand of n_j in t_i.
$l_{n_j}(t_i)$	Energy input of n_j in t_i.
$h^{m_k}(t_i)$	Energy input of m_k in t_i.
$h_{n_j}^{m_k}(t_i)$	Amount of energy sent to n_j by m_k in t_i.
$H_{n_j}(t_i)$	Energy input of n_j in t_i.
$P_{n_j}(t_i)$	Energy output of n_j in t_i.
$s_{n_j}(t_i)$	Number of active subcarriers of n_j in t_i.
e_0	Operating energy consumption.
e_s	Subcarrier energy consumption.
r_0	Rate of an active subcarrier.
S	Maximal number of active subcarriers.
$B_{n_j}(t_i)$	Battery level of n_j at the beginning of t_i.
$B_{n_j}^0$	Battery capacity of n_j.
$B_{n_j}(t_i)$	Battery level of m_k at the beginning of t_i.
$B_{m_k}^0$	Battery capacity of m_k.
$\mathcal{W}_{n_j}^B$	Weighted energy consumption of n_j.
$\mathcal{W}_{m_k}^M$	Weighted energy consumption of m_k.

and the total consumed local energy is as follows:

$$\sum_{t_i \in \mathcal{T}} \left\{ P_{n_j}(t_i) - \sum_{m_k \in \mathcal{M}} h_{n_j}^{m_k}(t_i) \right\}, \tag{4.2}$$

therefore for each REBS, its weighted consumed local energy $\mathcal{W}_{n_j}^B$, can be denoted as the following equation:

$$\mathcal{W}_{n_j}^B = \frac{\sum_{t_i \in \mathcal{T}} \left\{ P_{n_j}(t_i) - \sum_{m_k \in \mathcal{M}} h_{n_j}^{m_k}(t_i) \right\}}{\sum_{t_i \in \mathcal{T}} l_{n_j}(t_i)}. \tag{4.3}$$

Meanwhile, the total harvested energy of Microgrid m_k is denoted as follows:

$$\sum_{t_i \in \mathcal{T}} h^{m_k}(t_i), \tag{4.4}$$

and the total transmitted energy of m_k during the considered time span is as follows:

$$\sum_{t_i \in \mathcal{T}} \sum_{n_j \in \mathcal{M}^{(m_k)}} h_{n_j}^{m_k}(t_i). \tag{4.5}$$

Similarly, the weighted energy transmission of Microgrid m_k in $\mathcal{T}$ can be denoted as follows:

$$\mathcal{W}_{m_k}^M = \frac{\sum_{t_i \in \mathcal{T}} \sum_{n_j \in \mathcal{M}^{(m_k)}} h_{n_j}^{m_k}(t_i)}{\sum_{t_i \in \mathcal{T}} h^{m_k}(t_i)}. \tag{4.6}$$

4.2.2 Optimization Objective

Besides maximizing the total system throughput (i.e., P1), the objective in this chapter also contains figuring out the minimal summation of the weighted energy consumption of the REBSs and Microgrids:

$$\text{P2: } \mathbf{min} \left(\sum_{n_j \in \mathcal{N}} \mathcal{W}_{n_j}^B + \sum_{m_k \in \mathcal{M}} \mathcal{W}_{m_k}^M \right), \tag{4.7}$$

The problem P2 considers the combination of the energy harvesting abilities and the energy consumptions of the REBSs and Microgrids. It can be seen from Eq.4.2 and Eq.4.5 that the minimal energy consumption is taken into considerations in Eq.4.7. However, for different energy harvesting facilities, the amount of energy consumption may have different impacts on their operation. For example, if the local energy input for n_j is larger than $e_0 + S \cdot e_s$ in each time slot (i.e., $l_{n_j}(t_i)$ is sufficient for operation), then a large energy consumption will not impact its operation. In other words, for the REBSs or Microgrids with sufficient energy input, the objective will allow a larger energy consumption. Therefore, Eq.4.1 and Eq.4.5 are used as the dominators in Eq.4.3 and Eq.4.6.

The objective in this chapter is twofold: pursuing the minimal weighted energy consumption (i.e., P2), and figuring out the maximum total system throughput (i.e., P1). However, these two optimization goals may not be fulfilled simultaneously. Denote $\mathcal{D}$ as the possible solution set, and the element of which is with the maximal total system throughput. Therefore, we design the optimization goal as follows:

$$\text{P3: } \mathbf{min} \left(\sum_{n_j \in \mathcal{N}} \mathcal{W}^B_{n_j} + \sum_{m_k \in \mathcal{M}} \mathcal{W}^M_{m_k} \right),$$

where the definition domain is $\mathcal{D}$, and

$$\mathcal{D} = \left\{ \boldsymbol{a} \mid \mathcal{U}(\boldsymbol{a}) \geq \mathcal{U}(\boldsymbol{b}), \text{where } \boldsymbol{a} \neq \boldsymbol{b}, \text{ and } \boldsymbol{a}, \forall \ \boldsymbol{b} \in dom\ \mathcal{U}(\vec{\rho}, \vec{h}, \vec{f}, \vec{s}) \right\}. \tag{4.8}$$

The definition of $\mathcal{U}$ is same as the quadruple $\mathcal{U}$ in section 3.4. It can be seen that if the result of minimal weighted energy consumption happens to be the one with maximal total system throughput (i.e., the maximal total system throughput and minimal weighted energy consumption can be fulfilled simultaneously), then P3 can find the result as well.

On one hand, in section 3.5.1, we demonstrate that P1 is an MILP problem, and the constraints are the linear combination of the variables, therefore $dom\ \mathcal{U}(\vec{\rho}, \vec{h}, \vec{f}, \vec{s})$ satisfies the linear constraints. On the other hand, the denominator of Eq.4.7 is the combination

of constant values, while the numerator is the linear combination of variables, therefore Eq.4.7 is the linear objective function. As a result, it can be seen that problem P3 is also an MILP problem.

4.3 Proposed Two-stage Energy Efficiency Scheme

In order to figure out the result of problem P3, we design a two-stage energy efficiency scheme in this section. In general, the conceived optimization scheme contains two steps, and we will separately deal with the two objectives.

In the first step, we figure out the maximal total system throughput. Denote τ as the value of the maximal total system throughput, then τ is equal to:

$$\tau = \mathbf{max} \sum_{t_i \in \mathcal{T}} U(t_i) = \mathbf{max} \sum_{t_i \in \mathcal{T}} \sum_{n_j \in \mathcal{N}} f_{n_j}(t_i), \tag{4.9}$$

and τ subjects to constraints of problem P1. It can be seen that the calculated τ equals the value of $\boldsymbol{a}$ in Eq.4.8.

In the second step, τ is used as a constraint. We then put the weighted energy consumption as the minimized objective. The objective and the associating constraints can be given by the following equation:

$$\text{P4: } \mathbf{min} \sum_{n_j \in \mathcal{N}} \mathcal{W}^B_{n_j} + \sum_{m_k \in \mathcal{M}} \mathcal{W}^M_{m_k}, \tag{4.10}$$

subject to

$$\sum_{t_i \in \mathcal{T}} U(t_i) = \tau, \tag{4.11}$$

as well as the related constraints given by Eq. 3.1 to Eq. 3.22, Eq. 4.2 and Eq. 4.5. It is noted that problem P4 and P3 have the same results: on one hand, the equality in

Eq. 4.11 guarantees that the results of P4 has the maximal total system throughput, and therefore all the results of P4 satisfy Eq. 4.8; on the other hand, because the calculated strategies of P3 satisfy 4.8, then their total system throughput will be larger than the others', which is just the meaning of Eq. 4.11.

Algorithm 2: Two-stage Energy Efficient Scheme ©2014 IEEE.

Input: Network topology information: $\mathcal{N}, \mathcal{G}, \mathcal{M}, \mathcal{C}$.
Energy related information: e_s, e_0, $h_{n_j}^{m_k}(t_i)$, $h^{m_k}(t_i)$, $l_{n_k}(t_i)$.
Traffic related information: $d_{n_j}(t_i)$ r_0.
Output: $(\vec{\rho}, \vec{h}, \vec{f}, \vec{s})$ for problem P1.

1 Relax the integer constraints of $\vec{\rho}$ and $\vec{s}$ into linear ones, then the problem P1 is transformed into P1';
2 Solve the linear programming problem P1';
3 Let $\overline{O}$ record the result and $\boldsymbol{u}' = (\vec{\rho}', \vec{h}', \vec{f}', \vec{s}')$ is the associated variables;
4 **if** $\boldsymbol{u}'$ *satisfies integer constraints of P1* **then**
5 $\tau = \overline{O}$;
6 **else**
7 $\underline{O} = 0$;
8 $Cons$ = the constraints of P1;
9 Choose one relaxed constraint x that does not follow the constraints of P1. Let χ denote the value of x;
10 $(\tau, \overline{O})$= BranchBound($Cons$, x, χ, P1, $\underline{O}$, $\overline{O}$);
11 Relax the integer constraints of $\vec{\rho}$ and $\vec{s}$ into linear ones, then the problem P4 is transformed into the relaxed problem P4';
12 Solve the linear programming problem P4';
13 Let $\overline{O}$ record the result and $\boldsymbol{u} = (\vec{s}, \vec{\rho}, \vec{f}, \vec{h})$ is the associating variables;
14 **if** $\boldsymbol{u}$ *satisfies integer constraints of P4* **then**
15 **return** $\boldsymbol{u}$;
16 **else**
17 $\underline{O} = 0$;
18 $Cons$ = the constraints of P4;
19 Choose one relaxed constraint x that does not follow the constraints of P4. Let χ denote the value of x;
20 $(\underline{O}^*, \overline{O})$= BranchBound($Cons$, x, χ, P4, $\underline{O}$, $\overline{O}$);
21 **return** the strategy that achieves $\underline{O}^*$.

The major steps of the proposed two-stage energy efficient scheme are summarized in Algorithm 2. In Algorithm 2, there are two stages. Line 1 to line 10 denote the first stage, and the aim of which is to calculate τ. The Algorithm 2 will firstly use the relaxation technique to substitute the linear relaxations for the integer variables. After that, the

original MILP problem (P1) becomes the linear programming problem (P1'). Since there are a bunch of solutions for P1' (i.e., simplex method or interior point method), we omit the details of the procedure. If the solutions of P1' (i.e., $\boldsymbol{u}'(\vec{\rho'}, \vec{h'}, \vec{f'}, \vec{s'})$) happen to satisfy the constraints of P1, then $\tau = \overline{O}$, otherwise the *BranchBound* procedure is used to figure out the solutions of P1 based on $\boldsymbol{u}'$. the idea of *BranchBound* is to cut the solution set into several subsets, and gradually reduce the searching range by removing the unnecessary branches. We use τ to record the maximal value of P1. In the second step, we add 4.11 to the constraints list, and deal with problem P4. Similarly, the problem P4 will be relaxed, and we denote the objective in Eq.4.10 with the relaxed equalities and inequalities by P4'. After the solution of P4', $\boldsymbol{u}$, is figured out, we check whether $\boldsymbol{u}$ satisfies the constraints of P4 or not. If $\boldsymbol{u}$ can also be the result of P4, then we return $\boldsymbol{u}$, otherwise we will turn to *BranchBound* to find the strategy that has the least weighted energy consumption as well as satisfying the associating constraints of P4.

4.4 Performance Evaluation

In this section, we mainly study the features of the proposed two-stage scheme through the computer-based simulations. We mainly compare three schemes in this section: the scheme based on Naive idea (i.e., Naive), the throughput maximization scheme proposed in Chapter 3 (i.e., Throughput maximization), and the two-stage energy efficient scheme introduced in this chapter (i.e., Proposed two-stage).

4.4.1 Settings of the Simulation

Similar to Section 3.6, the considered network topology and experimental parameters are shown in Fig.4.1 and Table 4.2, respectively. As we can see from Fig. 4.1, we consider 10 REBSs, therefore $N = 10$, in which there is 1 gateway ($F = 1$). In the network, there are 3 Microgrids, and they respectively connect to 1, 2, and 3 REBSs. The bandwidth of each link is independently and randomly selected from the interval [80Mbps, 300Mbps].

Table 4.2: Experimental Parameters ©2014 IEEE.

Parameter	Value
The length of time slot ($\|t_i\|$)	1 hour
The number of considered time slots (T)	10
Number of REBSs (N)	10
Number of Microgrids (M)	3
Bandwidth of the Backhaul link ($c_{n_j}^{n_k}$)	80Mbps to 300Mbps
Operating power consumption (e_0)	712.2W
Power consumption per each subcarrier (e_s)	1.06W
Number of subcarriers (S)	600
Battery capacity of REBS ($B_{n_j}^0$)	2000W
Battery capacity of Microgrid ($B_{m_k}^0$)	2000W
Amount of energy of REBS at t_1 ($B_{n_j}(t_1)$)	2000W
Amount of energy of Microgrid at t_1 ($B_{m_k}(t_1)$)	2000W
Rate of subcarriers (r_0)	0.5Mbps

The length of the optimization period is a 10-hour long ($T_0 = 10$ hour), and each time sample represents 1 hour ($|t_i| = 1$ hour). Other parameters are shown in Table 4.2.

In this section, we set the performance metric as the consumed power per megabit, which can be denoted as the following equation:

$$\frac{\sum_{t_i \in \mathcal{T}} P_{n_j}(t_i)}{\tau}, \tag{4.12}$$

where τ is the variable defined in Eq. 4.9. It can be seen that Eq. 4.12 pursues the higher utilization of the energy, which is a more direct energy efficiency metric, without considering the factor of energy harvesting abilities.

4.4.2 Effect of Energy Input on Energy Efficiency

In this section, the energy input is set as the variable. The energy inputs of the REBSs and Microgrids in each time slot are the i.i.d. values and chosen from the interval $[0.5 \cdot \text{x-axis value}, 1.5 \cdot \text{x-axis value}]$. The amount of data traffic demand of each REBS is also uniformly and randomly selected from $[40\text{Mbps}, 100\text{Mbps}]$. Other parameters can be referred to Table 4.2. Fig. 4.2 illustrates the comparison of the consumed power per

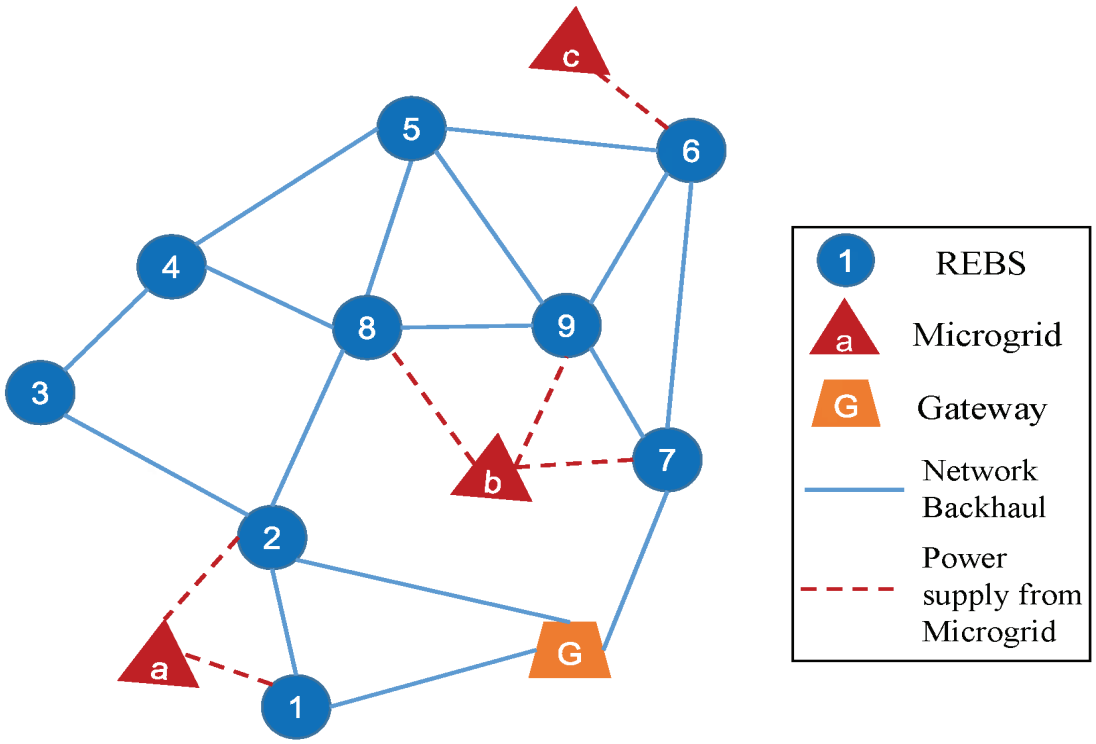

Figure 4.1: System topology used in the part of performance evaluation. ©2014 IEEE.

megabit of the three schemes. In this figure, we have the following observations. Firstly, the proposed two-stage scheme has the lowest consumed energy per megabit traffic, while the Naive scheme has the largest energy consumption per traffic unit. With considering the lower τ of the Naive scheme, the energy utilization of the Naive scheme is even worse. Secondly, there is a inversely proportional relationship between the considered energy efficiency metric, and the amount of input energy of the Naive scheme. This is due to the reason that as more renewable energy flowed into the battery of REBS, it can support more data traffic demands for each REBS, according to our observations in Section 3.6.2, the total system throughput will gradually be the same as the one of the proposed two-stage's. As a result, the performance gap of the Naive scheme and proposed two-stage scheme becomes smaller as the increase of the energy input.

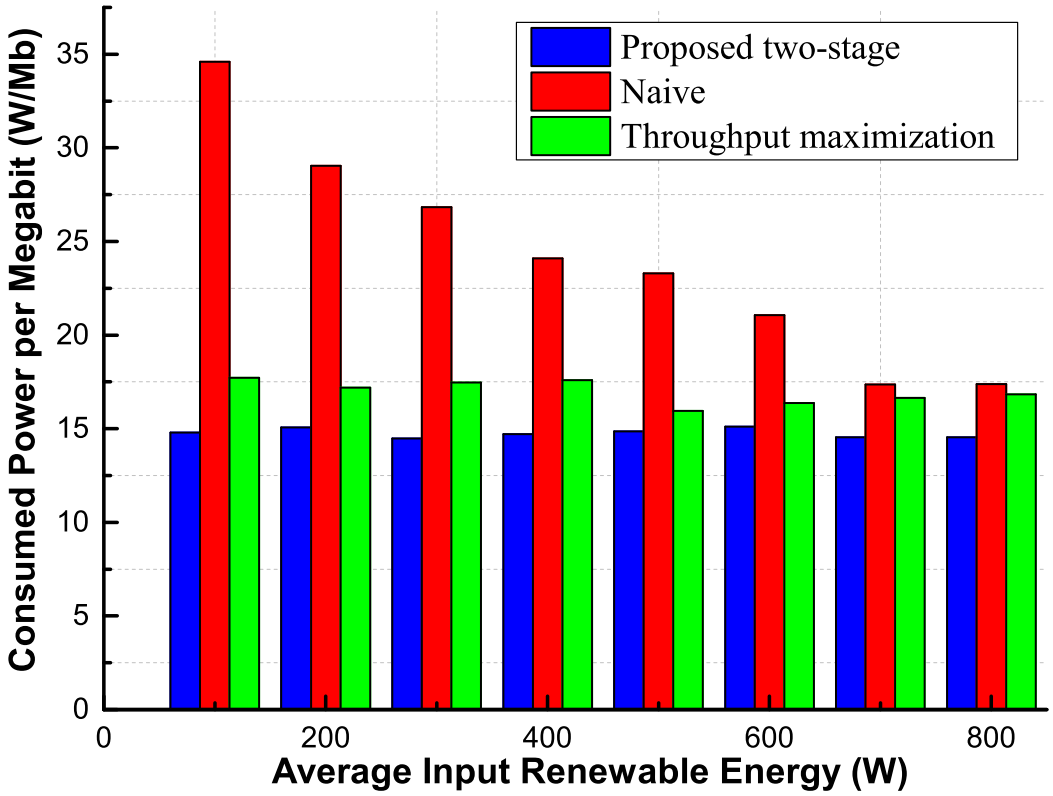

Figure 4.2: The effect of average input renewable energy on consumed power per megabit of the proposed scheme, naive scheme and throughput maximization scheme. ©2014 IEEE.

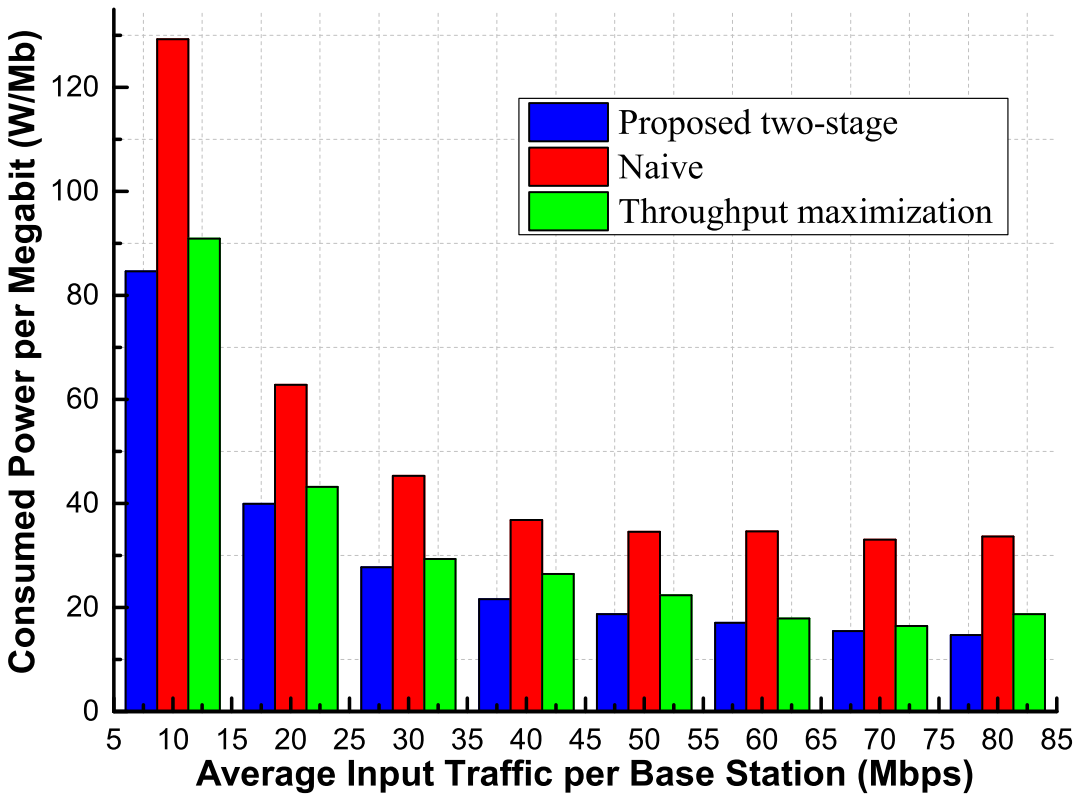

Figure 4.3: The effect of average input traffic per base station on consumed power per megabit of the proposed scheme, naive scheme and throughput maximization scheme. ©2014 IEEE.

4.4.3 Effect of Traffic Input on Energy Efficiency

In this section, the amount of the data traffic demand of each REBS in each time slot (i.e., $f_{n_j}(t_i)$) is set as the variable. We consider the i.i.d. $f_{n_j}(t_i)$ and $f_{n_j}(t_i)$ is chosen from the interval $[0.5 \cdot \text{x-axis value}, 1.5 \cdot \text{x-axis value}]$. And for the energy inputs of the energy harvesting facilities (i.e., $l_{n_j}(t_i)$ and $h^{m_k}(t_i)$), they are uniformly and randomly chosen from $[100\text{W}, 300\text{W}]$. The residual parameters can be referred to Table 4.2.

From Fig.4.3, it can be seen that the proposed two-stage scheme has the lowest consumed power per megabit among the three schemes, therefore the proposed two-stage scheme has the best performance, and the gap between the performance of the proposed two-stage and the Naive scheme is clear to see. Furthermore, it can be seen from Fig. 4.3 that as the average input traffic increases, the consumed energy per megabit will decrease. The rationale is twofold. Firstly, if the traffic input is larger, there will be more traffic distribution strategy candidates (i.e., the domain is larger), therefore the result will be at least equal or even larger. Secondly, for an active REBS, if there is still extra energy budget, therefore the total system throughput can be increased only with the energy cost of e_s. Therefore the τ can be improved if the input traffic increases.

4.5 Summary

In this chapter, we introduce a two stage energy efficient scheduling and load distribution scheme, which can strike the balance between the total system throughput and the associating energy consumption.

To this end, we firstly introduce the scenario that the proposed scheme will take effect. After that, the system model is formulated, and the optimization objective is analyzed, respectively. Thirdly, the two-stage energy efficiency optimization framework is demonstrated. In the last part, the energy efficiency of the proposed two-stage scheme is illustrated through the comparison with the throughput maximization only scheme and

the Naive scheme, under various energy inputs and data traffic demands.

Chapter 5

On the On-line Energy-Efficient of Throughput-Based Scheme for REBS Mesh Networks

5.1 Introduction

In Chapter 3 and Chapter 4, we consider that the data traffic demand profile is already known before conducting the optimization. In reality, the knowledge of such profile can be regarded as the expectation of the profile. Therefore, the schemes proposed in these two chapters can have good performance if the estimations of the data traffic demand profiles are precise (i.e., the estimations are just the real ones). However, the result for such precise estimation assumption may get the suboptimal result when such estimations are imprecise, owing to the fact that the data traffic demand profiles depend on the activities of the human beings, which are hard to predict in essence.

In this chapter, to deal with the problems of the off-line scheme (i.e., cannot adjust the strategy when operating, and have suboptimal result when it faces imprecise data

traffic demand), we propose an on-line scheme, and such scheme can dynamically adjust the old strategy, in order to achieve a better performance. At first, we revise the system model according to the new considered scenario. Secondly, we analyze the performance bound of the off-line scheme in term of the data demand estimation deviation. After that, an on-line dynamic adjusting scheme is envisioned and analyzed accordingly. At last, the advantages of the on-line scheme is demonstrated by the computer-based simulations.

The major contributions of this chapter are summarized as follows:

- The performance bound of the off-line scheme is theoretically analyzed, and the analysis demonstrates that when the estimation deviation is large, the result of the off-line scheme is unsatisfied.
- We propose an on-line dynamic adjusting scheme, which is based on the off-line optimization result, and can adjust the scheme according to the current precise data traffic demand profile.
- We demonstrate that the proposed on-line scheme can achieve better performance than the off-line scheme via the proof.
- Through the computer-based simulations, we show that the proposed on-line scheme is robust toward the imprecise data traffic, and the total system throughput of the on-line scheme is very close to the optimal scheme, which is the off-line scheme having the precise data traffic demand profile, in terms of the throughput and energy efficiency.

5.2 System Model

As mentioned in the introduction part, we consider the imprecise data traffic demand in this chapter. We assume that the real data traffic demand of the users under the coverage area of n_j in t_i is $d_{n_j}(t_i)$, and the expectation of $d_{n_j}(t_i)$ is denoted by $\overline{d}_{n_j}(t_i)$, therefore

their relationship can be given by the following equation:

$$d_{n_j}(t_i) = \overline{d}_{n_j}(t_i) + \epsilon_{n_j}(t_i), \tag{5.1}$$

where $\epsilon_{n_j}(t_i)$ denotes the estimation deviation of data traffic demand of the REBS n_j in time slot t_i. A large $\epsilon_{n_j}(t_i)$ means that the expectation of the data traffic demand $\overline{d}_{n_j}(t_i)$ is very different from the real data traffic demand profile $d_{n_j}(t_i)$.

In this chapter, we assume that before conducting the optimization, $\overline{d}_{n_j}(t_i)$ is the available information, since we can get such expectation by combining the population in the coverage area, the historical profile, the information of users' activities and so on (as we analyzed in Chapter 2). On the other hand, $d_{n_j}(t_i)$ can only be known at the beginning of t_i. For example, $d_{n_j}(t_{i+1})$ is the unknown information in t_i. Similar assumptions can be found in [44][51].

In our proposal, we only consider two kinds of traffic profile: the expectation and the instant precise one, and we do not consider additional features is available (i.e., the stochastic information such as the means and deviations in [47] and [56]). In addition, we only consider the imprecise for the traffic input estimation. On the contrary, for the energy estimation, we assume the precise information is available, since we can have a detailed knowledge of the environment, such as the weather information, the intensity of illumination and so on.

Other variables and parameters are same as the previous chapters. For convenience, we list them in Table 5.1.

5.3 Analysis on the Off-line Scheme

In this section, we conduct the analysis for the performance of the off-line scheme. We will give the upper bound and lower bound of the performance gap between the off-line

Table 5.1: Variable Summarization

Variable	Meaning
t_i	Index of time slot i.
T	Number of time slots.
$\mathcal{T} = \{t_1, t_2, ..., t_T\}$	Time span using time sample.
n_j	Index of REBS j.
N	Number of REBSs.
$\mathcal{N} = \{n_1, n_2, ..., n_N\}$	Set of REBSs.
(n_j, n_k)	Connection between n_j and n_k.
C	Number of links.
$\mathcal{C} = \{(n_{j_1}, n_{k_1}), ..., (n_{j_C}, n_{k_C})\}$	Set of the links.
$c_{n_j}^{n_k}$	Capacity of (n_j, n_k).
$G = (\mathcal{N}, \mathcal{C})$	Network topology.
$\rho_{n_j}(t_i)$	Operating status of n_j in t_i.
$c_(n_j, n_k)$	Link capacity of (n_j, n_k) in t_i.
F	Number of gateways.
g_f	Index of gateway f.
$\mathcal{G} = \{g_1, g_2, ..., g_F\}$	Set of gateways.
m_k	Index of Microgrid k.
M	Number of Microgrids.
$\mathcal{M} = \{m_1, m_2, ..., m_M\}$	Set of Microgrids.
$M^{(m_k)}$	Set of associating of REBSs of m_k.
$f_{n_j}(t_i)$	Supported traffic of n_j in t_i.
$d_{n_j}(t_i)$	Data traffic demand of n_j in t_i.
$\overline{d}_{n_j}(t_i)$	Estimated data traffic demand of n_j in t_i.
$\epsilon_{n_j}(t_i)$	Estimation deviation of $\overline{d}_{n_j}(t_i)$.
$l_{n_j}(t_i)$	Energy input of n_j in t_i.
$h^{m_k}(t_i)$	Energy input of m_k in t_i.
$h_{n_j}^{m_k}(t_i)$	Amount of energy sent to n_j by m_k in t_i.
$H_{n_j}(t_i)$	Energy input of n_j in t_i.
$P_{n_j}(t_i)$	Energy output of n_j in t_i.
$s_{n_j}(t_i)$	Number of active subcarriers of n_j in t_i.
e_0	Operating energy consumption.
e_s	Subcarrier energy consumption.
r_0	Rate of an active subcarrier.
S	Maximal number of active subcarriers.
$B_{n_j}(t_i)$	Battery level of n_j at the beginning of t_i.
$B_{n_j}^0$	Battery capacity of n_j.
$B_{n_j}(t_i)$	Battery level of m_k at the beginning of t_i.
$B_{m_k}^0$	Battery capacity of m_k.
$\mathcal{W}_{n_j}^B$	Weighted energy consumption of n_j.
$\mathcal{W}_{m_k}^M$	Weighted energy consumption of m_k.

scheme proposed in Chapter 3 with the expectation data traffic profile, and the off-line scheme with the perfect data traffic demand profile (i.e., the estimation is same as the real one, and the result is optimal).

As shown in Eq.5.1, there might be an estimation deviation $\epsilon_{n_j}(t_i)$ between the real data traffic demand $d_{n_j}(t_i)$ and its expectation $\overline{d}_{n_j}(t_i)$. Since $\overline{d}_{n_j}(t_i)$ can be either larger or smaller than $d_{n_j}(t_i)$, the available range of $\epsilon_{n_j}(t_i)$ is $\epsilon_{n_j}(t_i) \in (-\infty, +\infty)$. Denote $[\epsilon_{n_j}(t_i)]^+$ as the non-negative vector, and the value of which is equal to $\epsilon_{n_j}(t_i)$ if $\epsilon_{n_j}(t_i) > 0$, otherwise $[\epsilon_{n_j}(t_i)]^+ = 0$, then we have the following equation:

$$[\epsilon_{n_j}(t_i)]^+ = \mathbf{sup}\left\{\epsilon_{n_j}(t_i), 0\right\}. \tag{5.2}$$

Denote the quadruple $(\vec{\rho^*}, \vec{h^*}, \vec{f^*}, \vec{s^*})$ as the strategy figured out by the off-line scheme, and having the perfect data traffic demand profile (i.e., $d_{n_j}(t_i)$). Due to the optimality of the off-line scheme, $(\vec{\rho^*}, \vec{h^*}, \vec{f^*}, \vec{s^*})$ is the optimal result. On the other hand, let $(\vec{\rho'}, \vec{h'}, \vec{f'}, \vec{s'})$ be the strategy calculated by the off-line scheme using the data traffic demand expectation (i.e., $\overline{d}_{n_j}(t_i)$). Because the expectation is not always equal to the real one, therefore $(\vec{\rho'}, \vec{h'}, \vec{f'}, \vec{s'})$ might be sub-optimal. Theorem 5.3.2 analyzes the upper bound and lower bound of the performance gap between the off-line scheme using the perfect data traffic demand profile and the expectation.

We define a vector $\widetilde{\boldsymbol{d}}$, and the elements of $\widetilde{\boldsymbol{d}}$ are the smaller element of $\boldsymbol{d}$ and $\overline{\boldsymbol{d}}$ in the corresponding dimension, and the element of $\widetilde{\boldsymbol{d}}$, $\widetilde{d}_{n_j}(t_i)$, can be given by the following equation:

$$\widetilde{d}_{n_j}(t_i) = \mathbf{inf}\left\{d_{n_j}(t_i), \overline{d}_{n_j}(t_i)\right\}. \tag{5.3}$$

The following Lemma 5.3.1 reveals the relationship among the results with the different traffic input profiles:

Lemma 5.3.1 *Denote $\widetilde{\tau}$ as the maximal total system throughput given by the off-line*

scheme, and $\widetilde{\boldsymbol{d}}$ *is used as the traffic input profile. Then we have the following relationships among* τ^*, $\widetilde{\tau}$, *and* τ'*:*

$$\tau^* - \sum_{n_j \in \mathcal{N},\, t_i \in \mathcal{T}} \sum [\epsilon_{n_j}(t_i)]^+ \leq \widetilde{\tau} \leq \tau'. \tag{5.4}$$

Proof: Because the off-line scheme can always figure out the maximal total system throughput, $\widetilde{\tau}$ is the optimal result when the input data traffic demands are $\widetilde{\boldsymbol{d}}$. As a result, the total data traffic demands gap between $\widetilde{\boldsymbol{d}}$ and $\boldsymbol{d}$ can be given by the following equation:

$$\mathbf{1} \cdot \left(\boldsymbol{d} - \widetilde{\boldsymbol{d}} \right)^T = \sum_{n_j \in \mathcal{N},\, t_i \in \mathcal{T}} \sum [\epsilon_{n_j}(t_i)]^+. \tag{5.5}$$

Because the total system throughput gap will be no more than the total data traffic demands, the first inequality of Eq.5.4 holds. On the other hand, all the possible strategies calculated by the off-line scheme with the data traffic demand input $\widetilde{\boldsymbol{d}}$, can be found by the strategy set when the input traffic is $\overline{\boldsymbol{d}}$. In other words, the latter result is larger than or equal to the former one. Therefore, $\widetilde{\tau} \leq \tau'$ and the second inequality of Eq.5.4 holds.

■

Theorem 5.3.2 *Denote* τ^* *as the total system throughput of the strategy* $(\vec{\rho^*}, \vec{h^*}, \vec{f^*}, \vec{s^*})$*, and* τ' *as the total system throughput figured out by the strategy* $(\vec{\rho'}, \vec{h'}, \vec{f'}, \vec{s'})$*. When we use these two strategies, their associating result* τ^* *and* τ' *will satisfy the relationship given by the following inequalities:*

$$0 \leq \tau^* - \tau' \leq \boldsymbol{inf} \left\{ \sum_{n_j \in \mathcal{N}} \sum_{t_i \in \mathcal{T}} [\epsilon_{n_j}(t_i)]^+, \tau^* \right\}. \tag{5.6}$$

Proof: We will firstly prove the former inequality. As we mentioned above, the strategy $(\vec{\rho^*}, \vec{h^*}, \vec{f^*}, \vec{s^*})$ is established by the off-line scheme with the perfect data traffic demand information. Therefore τ^* is the optimal result since the off-line scheme will

return the optimal strategy. As a result, τ^* will be no smaller than τ'. Therefore the inequality $0 \leq \tau^* - \tau'$ holds.

Then we prove the latter inequality. According to Lemma 5.3.1, the gap between τ^* and τ' is less than the sum of each dimension of the estimation deviation. In addition, τ' is non-negative, hence the second inequality of Theorem 5.6 holds. ■

Theorem 5.6 demonstrates the performance bound of the off-line scheme. It can be seen that for the off-line scheme with the traffic input expectation, its performance depends on the precision of the traffic input estimation (i.e., the absolute value of $\epsilon_{n_j}(t_i)$), and a higher estimation deviation may cause a poorer performance. For example, when the energy input is very low and no REBS can operate, then both of τ^* and τ' will be 0 and the gap is 0 as well. When the energy input is adequate, then the total system throughput gap will be the upper bound, since the strategy figured out by the expectation cannot support a larger traffic demand.

5.4 Envisioned On-line Dynamic Adjusting Scheme

Theorem 5.3.2 reveals that as the traffic estimation deviation increases (i.e., the absolute value of $\epsilon_{n_j}(t_i)$ becomes larger), the performance of the off-line scheme might decrease accordingly. Therefore the off-line scheme might return an unsatisfied result if the estimation deviation is large. Aiming at such problem, we put forward an on-line dynamic adjusting scheme in this section. Such on-line strategy is based on the precise knowledge of the data traffic demand $d_{n_j}(t_i)$ at the beginning of t_i.

The on-line scheme makes use of the result of the off-line scheme. At first, we execute the off-line scheme once before the first time slot t_1. After getting the strategy of the off-line scheme, then the on-line dynamic adjusting scheme will be performed in every time slot in order to adjust the the future plans designed by the old plan. The old plan is

initialized by the off-line scheme, and stored by the three kinds of variables given by the following equations:

$$B_{n_j}^{Plan}(t_i) = B_{n_j}(t_i), \forall t_i \in \mathcal{T}, n_j \in \mathcal{N}, \tag{5.7}$$

$$B_{m_k}^{Plan}(t_i) = B_{m_k}(t_i), \forall t_i \in \mathcal{T}, m_k \in \mathcal{M}, \tag{5.8}$$

$$P_{n_j}^{Plan}(t_i) = P_{n_j}(t_i), \forall t_i \in \mathcal{T}, n_j \in \mathcal{N}. \tag{5.9}$$

In Eq.5.7, $B_{n_j}^{Plan}(t_i)$ is defined as the energy level of the battery of REBS n_j in t_i, in Eq.5.8, we denote $B_{m_k}^{Plan}(t_i)$ as the energy level of the battery of Microgrid m_k in t_i, and in Eq.5.9, the energy consumption of REBS n_j in t_i is denoted by $P_{n_j}^{Plan}(t_i)$. $B_{n_j}^{Plan}(t_i)$, $B_{m_k}^{Plan}(t_i)$ and $P_{n_j}^{Plan}(t_i)$ are established by the off-lines scheme before the time slot t_1. In each following time slot, we will use the on-line scheme to adjust the plan given by the off-line scheme and the on-line schemes in earlier time slots. For example, in t_i, we have the scheme which is given by the off-line scheme, and revised by the on-line schemes from t_1 to t_{i-1}, hence the on-line scheme aims at dealing with the such strategy, and returns the strategies from t_i to t_T. We use $\boldsymbol{B}_N^{Plan}$, $\boldsymbol{B}_M^{Plan}$ and $\boldsymbol{P}_N^{Plan}$ to represent the set of $B_{n_j}^{Plan}(t_i)$, $B_{m_k}^{Plan}(t_i)$ and $P_{n_j}^{Plan}(t_i)$, respectively.

Definition (*Maximum available spare energy*): The maximum available spare energy of the REBS n_j in t_i, $\mathcal{E}_{n_j}(t_i)$, is the minimum value of the planned energy level of n_j's battery $B_{n_j}^{Plan}$ from t_i to t_T:

$$\mathcal{E}_{n_j}(t_i) = \min_{t_i \le t \le t_T} B_{n_j}^{Plan}(t). \tag{5.10}$$

The $\mathcal{E}_{n_j}(t_i)$ is the maximum extra usable energy for n_j in time slot t_i, without impacting the strategy in the upcoming time slots. We will given the proof in the following

Theorem.

Theorem 5.4.1 *$\mathcal{E}_{n_j}(t_i)$ is the maximum available amount of energy can be used for REBS n_j in time slot t_i, and the consumption of such energy will not impact the future plans $\boldsymbol{P}_N^{Plan}$ from t_{i+1} to t_T.*

Proof: According to the battery evolution equation defined in Eq.3.9, the energy level of a certain REBS in the current time slot will be no less than the one in the next time slot (i.e., $B_{n_j}^{Plan}(t_i) \geq B_{n_j}^{Plan}(t_{i+1})$), if the renewable energy input is no less than the energy consumption in current time (i.e., $P_{n_j}^{Plan}(t_i) \geq H_{n_j}(t_i)$). Otherwise the energy level in the next time slot will be larger (i.e., $B_{n_j}^{Plan}(t_i) < B_{n_j}^{Plan}(t_{i+1})$). Not to affect the future strategies from t_{i+1} to t_T, for a certain REBS n_j, the following inequalities should be fulfilled accordingly:

$$\mathcal{E}_{n_j}(t_i) + P_{n_j}^{Plan}(t_{i+\alpha}) \leq H_{n_j}(t_{i+\alpha}) + B_{n_j}^{Plan}(t_{i+\alpha}), \tag{5.11}$$

where $\alpha \in \mathbb{Z}^+$ and $0 \leq \alpha \leq T - i$. In order to get the largest amount of $\mathcal{E}_{n_j}(t_i)$, more than one REBS should satisfy the equality constraint " = " in (5.11). Therefore $\mathcal{E}_{n_j}(t_i)$ is equal to the minimum value of $B_{n_j}^{Plan}(t)$, and Theorem 5.4.1 holds. ■

It is noted that the previous Definition 5.4 and Theorem 5.4.1 works for the battery of the REBSs, and it can be easily extended to the case of the Microgrids'. Due to lack of space, we omit such parts in this dissertation. From Theorem 5.4.1, it can be seen that $\mathcal{E}_{n_j}(t_i)$ is non-negative because of the constraint in Eq.3.9. As a result, the actual energy input for each REBS in each time slot of the on-line scheme will be no less than the one of the off-line scheme using the expectation traffic profile, and the total system throughput of the on-line scheme will be at least same as the one of the off-line scheme. Therefore the performance of the on-line scheme is guaranteed.

Since $\boldsymbol{d}(t_i)$ is available in t_i, an immediate idea is to use the off-line result to figure

out the optimal strategies from t_i to t_T. However, such consideration may not work due to the following reasons. Firstly, the off-line scheme is compute-intensive (i.e., NP-hard as described in Chapter 3), so it cannot be executed periodically in practice. Secondly, even if it is possible to use the off-line scheme in each time slot, the optimal result we get from the off-line scheme in t_i may modify the strategies in future time slots, and such effort may degrade the performance. This is because the current optimal result is based on the traffic information made up by the precise information ($\boldsymbol{d}(t_i)$) and the imprecise information (expectation in the following time slots), and such imprecise information will make the current optimal become sub-optimal in the future.

Let the vector $\boldsymbol{d}(t_i) = \{d_{n_1}(t_i), d_{n_2}(t_i), ..., d_{n_N}(t_i)\}$ represent the real data traffic demands of each REBSs in time slot t_i. For the energy input of the Microgrids and REBSs, we use $\boldsymbol{h}^{on}$ and $\boldsymbol{l}^{on}$ to denote them, respectively. The on-line dynamic adjusting scheme will be executed at the beginning of each time slot, and its procedure is denoted as Algorithm 3 shows. In Algorithm 3 and following descriptions, we omit the time label t_i because the on-line scheme will design the strategy only for the current time slot.

At first, the energy plan designed in earlier time $\boldsymbol{B}_N^{Plan}$, $\boldsymbol{B}_M^{Plan}$ and $\boldsymbol{P}_N^{Plan}$, the energy input information $\boldsymbol{h}^{on}$ and $\boldsymbol{l}^{on}$, the data traffic demand input $\boldsymbol{d}$, and the network topology information are established. After that, Algorithm 3 calculates the maximum available spare energy for each REBS (i.e., $\mathcal{E}_{n_j}(t_i)$) according to Eq. 5.4 based on $\boldsymbol{B}_N^{Plan}$, and the energy from the Microgrids is based on the previous plan $\boldsymbol{B}_M^{Plan}$, as line 1 to 3 shows. After we get the energy input, we then figure out the possible operating status $\rho_{n_j}^{on\_temp}$, and the maximum number of active subcarriers $s_{n_j}^{on\_temp}$, respectively:

$$\arg \max_{s_{n_j}^{on\_temp} \leq S, \rho_{n_j}^{on\_temp} \in \{0,1\}} \left\{ P'_{n_j} | P'_{n_j} \leq \mathcal{E}_{n_j} + P_{n_j}^{Plan} \right\}. \tag{5.12}$$

According to the definition, it can be seen that if $\mathcal{E}_{n_j} + P_{n_j}^{Plan}$ is no less than e_0, $\rho_{n_j}^{on\_temp}$ will be 1, and we use the set N_{avai} to store the REBSs that can support the operating

consumption (i.e., $\rho_{n_j}^{on\_temp} = 1$). It is noted that the strategy is not satisfied and energy-inefficient if we set all the REBSs in N_{avai} active (i.e., the active REBSs may not connect to any active REBS, hence it cannot carry any data traffic). We will make use of $\rho_{n_j}^{on\_temp}$ and $s_{n_j}^{on\_temp}$ to figure out the maximum total system throughput U^{on} in the current time slot, such procedure can be done by the linear programming techniques since the integer constraints are determined. After that, Algorithm 3 will find the maximum total system throughput in a iterative manner, and line 7 to 17 demonstrate such procedure. We first initialize the set cur_Node and ava_Node, and their initial values are equal to $\varnothing$ and N_{avai}, respectively. Secondly, the REBS in the set ava_Node will be moved to cur_Node if it has the most system throughput improvement, and Algorithm 3 will iteratively conduct such selection procedure until the current system throughput is equal to U^{on}. After cur_Node is decided, Algorithm 3 will then calculate the energy-efficient results $(\rho^{on}, h^{on}, f^{on}, s^{on})$ with the constraint of the maximum system throughput U^{on}. The future plan $\boldsymbol{B}_N^{Plan}$, $\boldsymbol{B}_M^{Plan}$ and $\boldsymbol{P}_N^{Plan}$ will be updated based on $(\rho^{on}, h^{on}, f^{on}, s^{on})$, and such results will be returned as the result of the on-line scheme.

5.5 Performance Evaluation

In this section, we check the performance of the proposed on-line dynamical adjusting scheme.

There are mainly four schemes compared in this part. The first one is the **off-line two stage energy efficient scheme** described in Chapter 4, which has the perfect data traffic demand information (Off-line with Perfect Information). Because the optimal feature of the off-line scheme, and the traffic input information is precise, therefore such scheme achieves the optimal performance in terms of the total system throughput and the energy efficiency. The second scheme is the **off-line two stage energy efficient scheme**, with the data traffic demand expectation (Off-line with Expected Information). As analyzed

Algorithm 3: On-line dynamic adjusting scheme ©2015 IEEE.

Input: Network topology information: $G(\mathcal{N}, \mathcal{C}), \mathcal{M}$.
Energy information: $\boldsymbol{B}_N^{Plan}$, $\boldsymbol{B}_M^{Plan}$, $\boldsymbol{P}_N^{Plan}$, $\boldsymbol{l}$, $\boldsymbol{h}$.
Traffic information: $\boldsymbol{d}$.
Output: $\boldsymbol{B}_N^{Plan}$, $\boldsymbol{B}_M^{Plan}$, $\boldsymbol{P}_N^{Plan}$, $(\rho^{on}, h^{on}, f^{on}, s^{on})$.

Figure out the maximal available spare energy $\mathcal{E}_{n_j}$ for each n_j according to equation 5.10;
For each m_k, **if** $n_j \in M^{(m_k)}$ **then**
    $\mathcal{E}_{n_j} = \mathcal{E}_{n_j} + \min_{t_T \geq t \geq t_i} \left\{ B_{m_k}^{Plan}(t_i) \right\} / |M^{(m_k)}|$;
For each n_j, set $\rho_{n_j}^{on\_temp}$ and $s_{n_j}^{on\_temp}$ by (3.6):
$\arg \max_{s_{n_j}^{on\_temp} \leq S, \rho_{n_j}^{on\_temp} \in \{0,1\}} \left\{ P'_{n_j} | P'_{n_j} \leq \mathcal{E}_{n_j} + P_{n_j}^{Plan} \right\}$;
Let $\mathcal{N}_{avai} = \{n | n \in \mathcal{N} \; and \; \rho_n^{on\_temp} == 1\}$;
Base on $\boldsymbol{d}$, $\rho_{n_j}^{on\_temp}$ and $s_{n_j}^{on\_temp}$, figure out the maximal system utility U^{on} in current time slot;
Initialize $cur\_Node = \{\mathcal{G}\}$, $ava\_Node = \mathcal{N}_{avai} - \{\mathcal{G}\}$;
Set $Utility = 0$;
while *True* **do**
    if $Utility == U^{on}$ **then**
        Set ρ^{on} according to cur_Node;
        Use ρ^{on}, $\boldsymbol{l}$, $\boldsymbol{h}$ and $\tau = U^{on}$, and assume in P4 in Eq. 4.10, s can be real value, to figure out P4. We will obtain s_{real}^{on}, f^{on}, h^{on};
        Let s^{on} be $\lceil s_{real}^{on} \rceil$;
        Use $\boldsymbol{P}_N^{Plan}$ to record the energy consumption plan, and update $\boldsymbol{B}_N^{Plan}$ and $\boldsymbol{B}_M^{Plan}$ for the left time slots according to $\boldsymbol{P}_N^{Plan}$;
        return $\boldsymbol{B}_N^{Plan}$, $\boldsymbol{B}_M^{Plan}$, $\boldsymbol{P}_N^{Plan}$, and $(\rho^{on}, h^{on}, f^{on}, s^{on})$;
    Choose $n_{max} \in ava\_Node$ that the system utility is maximized, with the assumptions that only REBSs in $\{n_{max}\} \cup cur\_Node$ are active, and the number of active subcarriers are given by $s_{n_j}^{on\_temp}$. Let U_{max} be the maximal system utility;
    $Utility = U_{max}$, $cur\_Node = cur\_Node \cup \{n_{max}\}$, $ava\_Node = ava\_Node \backslash \{n_{max}\}$;

Table 5.2: Experimental Parameters ©2015 IEEE.

Parameter	Value
The number of considered time slots (T)	5
The length of each time slot($\|t_i\|$)	1 hour
Number of REBSs (N)	10
Number of Microgrids (M)	3
Bandwidth of the Backhaul link ($c_{n_j}^{n_k}$)	80Mbps to 300Mbps
Operating power consumption (e_0)	712.2W
Power consumption per each subcarrier (e_s)	1.06W
Number of subcarriers (S)	600
Battery capacity of REBS ($B_{n_j}^0$)	2000W
Battery capacity of Microgrid ($B_{m_k}^0$)	2000W
Amount of energy of REBS at t_1 ($B_{n_j}(t_1)$)	2000W
Amount of energy of Microgrid at t_1 ($B_{m_k}(t_1)$)	2000W
Rate of subcarriers (r_0)	0.5Mbps

in the previous part, there might be the estimation deviation of the expectation, therefore it is the sub-optimal scheme. The third scheme is the **on-line scheme** proposed in this chapter, and it is used with the off-line scheme (Off-line Combined with On-line). Such scheme is the combination of the strategy of the on-line scheme and off-line scheme, it makes use of the expectation of the traffic input profile at the very beginning, and adjust the strategy in each time slot. The fourth scheme is the **Naive scheme**, and the details of which are similar to the one defined in Chapter 2: it addresses the total system throughput maximization issue as well as decreasing the energy consumption. In each time slot, the Microgrids will evenly distribute its energy to the connected REBSs, and then the REBSs will calculate the ρ and s according to the available energy. It can be seen that the Naive scheme is the myopic scheme, which will not consider the long-term impact caused by the strategy maximizing the current time slot. It can be used to examine the significance of the long-term optimization. Other related parameters are listed in Table 5.2.

From parameters shown in Table 5.2, we consider the optimization covering 5 hours (i.e., $T = 5$), and the length of each time slot is 1 hour (i.e., $|t_i| = 1$). The topology is shown in Fig.5.1. As we can see from Fig.5.1, there are 9 non-gateway REBSs and 2

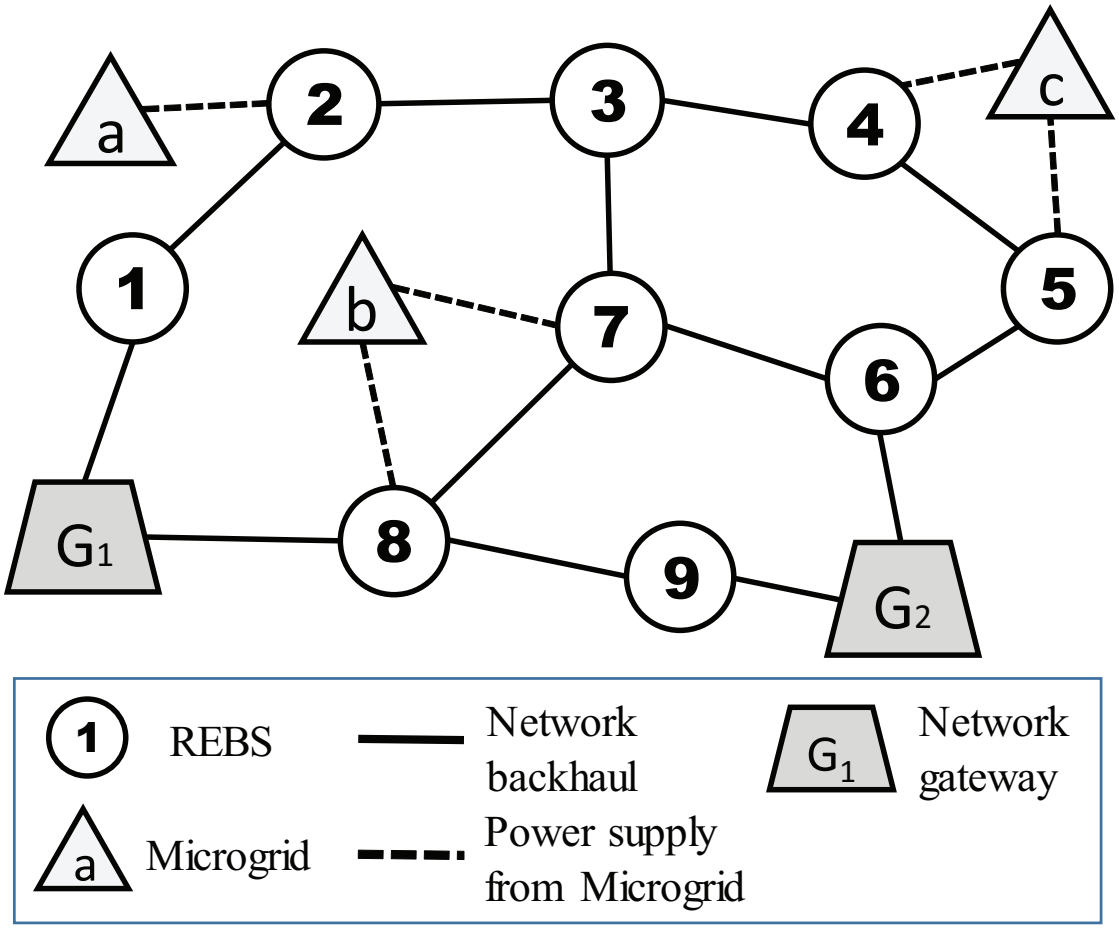

Figure 5.1: The topology used for the computer-based simulation. ©2015 IEEE.

network gateways in the considered area, therefore $N = 11$ and $F = 2$. The bandwidth of the interconnected links (i.e., microwave panel or long distance WiFi) between two neighboring REBSs are i.i.d. value selected from 80Mbps to 300Mbps. For Microgrid a, it only connects to n_2, and Microgrid b and c have the associating REBSs n_7, n_8 and n_4, n_5, respectively. It is noted that n_1, n_3, n_6 and n_9 do not have connections to any Microgrids. In this simulation, we also consider the macro base station as the previous chapters due to the economical concern (i.e., the CAPEX of the Microgrid connection and energy harvesting facilities), therefore the operating energy consumption (e_0), the per-subcarrier consumption (e_s), and the number of subcarriers (S) equals 712.2W, 1.06W, and 600, respectively based on the measurement in [5]. Both of the Microgrid and REBS have the battery with capacity of 2kW ($B^0_{n_j} = B^0_{m_k} = 2000W$). We consider the fully charged battery therefore the initial amount of energy of each battery for REBSs and Microgrids is $2000W$.

In this part, two kinds of performance metrics are considered, namely the total system throughput and the weighted energy consumption per traffic unit. The total system throughput is used to evaluate the amount of supported data traffic demands of the scheme, which is same as the definition in Eq.3.19, and the scheme having more total system throughput is considered to be better than the scheme with lower one. The second metric is the ratio of the weighted energy consumption (defined in Eq.4.7) to the total system throughput (defined in Eq.3.19). The scheme having the lower weighted energy consumption per traffic unit has better performance than the others, since it can use less energy to transfer the data.

5.5.1 Effect of Estimation Deviation of Data Traffic Demands on System Throughput and Energy Consumption

At first, we check the impact of the estimation deviation of the data traffic demand to the performances of the schemes. We use the "Off-line with Perfect Information" as the

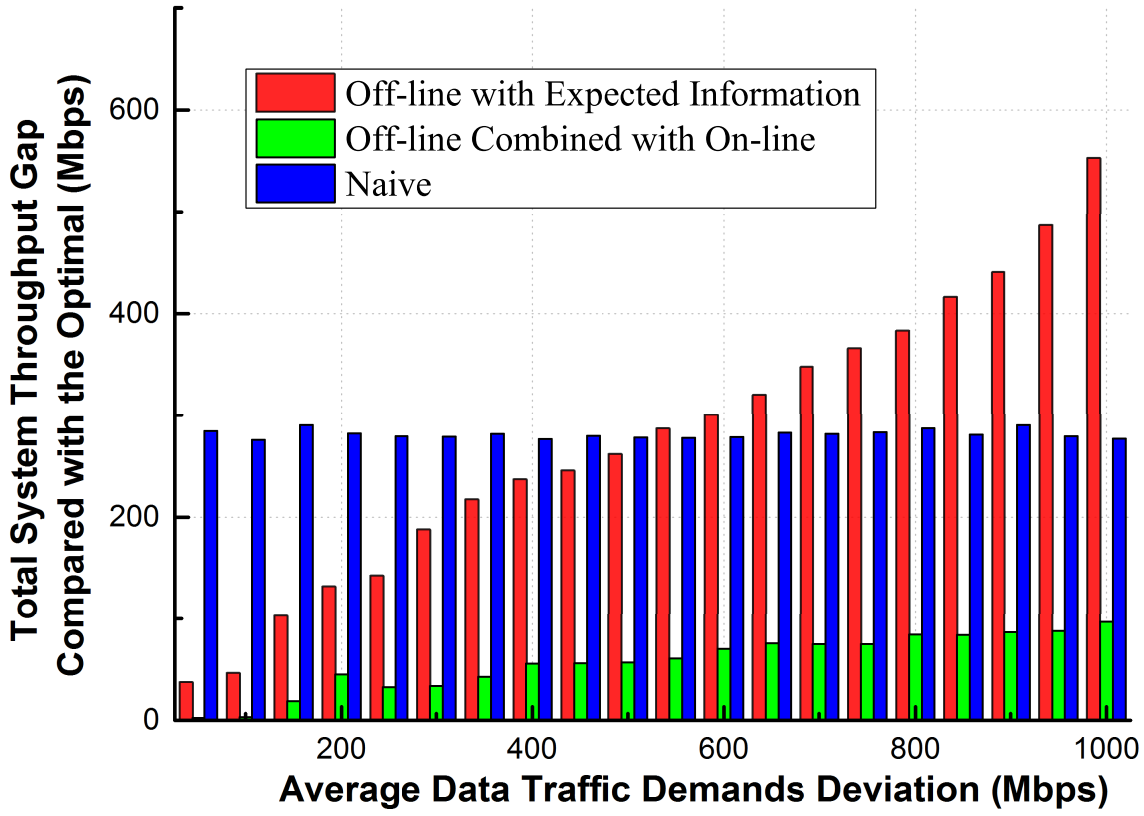

Figure 5.2: The effect of ϵ on system throughput of the off-line with expected information, off-line combined with on-line, and Naive scheme. ©2015 IEEE.

benchmark in this part, since it can achieve the optimal result. The energy inputs of the REBSs and Microgrids are independently and randomly chosen from the interval [100W, 300W]. The real data traffic demands of the REBSs are randomly chosen from the the interval [20Mbps, 50Mbps]. The Y-axis denotes the gap between the performance of the optimal scheme and the associating one, and the X-axis represents the the total amount of estimation deviation of the traffic input, and the value of x can be given by the following equation:

$$\sum [\epsilon]^{+} = \sum [\epsilon]^{-} = x, \tag{5.13}$$

which means that a large value of x will result in a large gap between the real traffic input and the expectation one. For the "Off-line with Expected Information", it will only use the expectation of the traffic input, and for the "Off-line Combined with On-line" scheme, both of the traffic input expectation and the precise value will be respectively utilized before t_1 and at the beginning of each time slot. Because the Naive idea does not consider the long-term result, it will collect the traffic input at the beginning of each time slot therefore only the precise traffic information will be used.

Fig.5.2 illustrates the total system throughput gap between the compared scheme (i.e., the scheme mentioned in the legend) and the optimal scheme (Off-line with Perfect Information), and several conclusions can be achieved from this figure.

Firstly, the Off-line combined with on-line scheme has the best performance since the gap is the lowest. Such scheme inherits the merits of using both of the traffic input expectation and the instant information: because of using the expectation (i.e., the long-term information) , the gap is small as a result. On the other hand, as the x value increases, the gap is still within a small value due to the timely adjusting based on the precise traffic input.

Secondly, the performance of the Off-line with expected information varies inversely to the average data traffic demand deviation, since the gap becomes larger as the increase of

x. Such phenomenon owes to the fact that a large amount of x means that the estimation of the traffic input is very imprecise, therefore the plan given by the off-line scheme is less trustable.

In addition, it is noted that when the deviation is less or equal than 450Mbps, the Off-line with expected information scheme performs better than the Naive one, but such relationship reverses when the deviation x is larger than 450Mbps. It means that the advantage of the long-term optimization will be compromised by the inaccurate traffic input information. Besides the aspects mentioned above, it can be seen from Fig.5.2 that the Naive scheme is free of the impact of traffic input estimation deviation. This is because the Naive idea will only utilize the precise traffic input at the beginning of each time slot.

Fig. 5.3 depicts the energy efficiency comparison of the Off-line with expected information scheme and the Off-line combined with on-line scheme. From the figure, several conclusions can be made, and we will discussion them accordingly.

Firstly, it can be seen that for the off-line with traffic expectation scheme, the energy efficiency is inversely proportional to the data traffic demand deviation of the input traffic. According to Fig.5.2, the total system throughput will decrease with the increase of x. Therefore, under the same energy budget (or same energy consumption), the supported traffic will decrease as the estimation deviation increases, and the energy efficiency will decrease as a result. On the other hand, the off-line combined with the on-line scheme has a relative stable relationship between the energy efficiency and average data traffic demand deviation, thanks to the timely adjust toward the designed plans based on the accurate traffic information. Therefore, the energy can be utilized in a more efficient manner.

Secondly, it is worthwhile to mention that when the estimation deviation is small, the declared energy efficiency of the Off-line with expected information scheme is better than the Off-line combine with on-line one. The reason behind such phenomenon is that

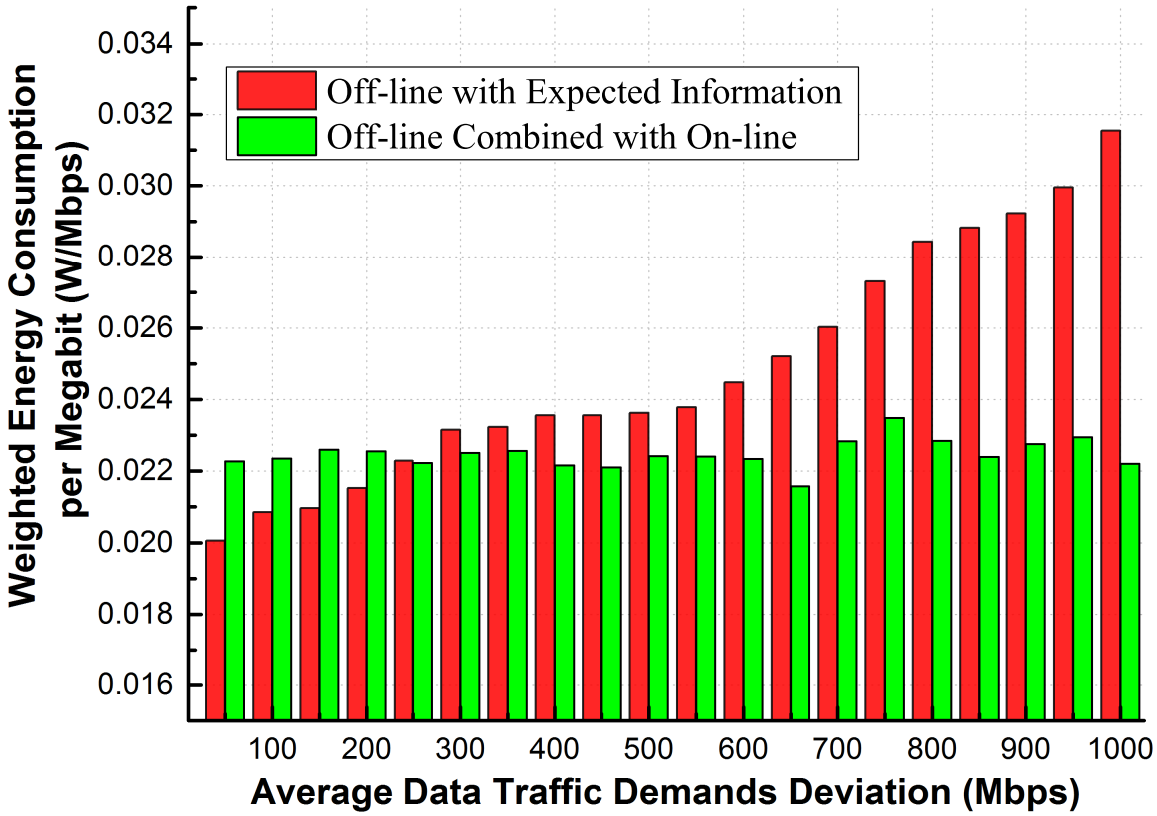

Figure 5.3: The effect of ϵ on energy efficiency of the off-line with expected information and off-line combined with on-line scheme. ©2015 IEEE.

we consider a Pareto-optimization, in which the object of total system throughput has a higher priority than the object of energy efficiency. Therefore when x is less than 250Mbps, achieving a higher total system throughput will consume a large amount of energy, which causes that the energy efficiency of the Off-line combine with on-line scheme worse than the Off-line with expected information scheme.

5.5.2 Effect of Total Available Energy on Total System Throughput and Energy Efficiency

Besides the estimation deviation, we would like to check the effect of other factors. This part contains the observations and associating analyses about the impact of energy input of the REBSs and Microgrids on the total system throughput and energy efficiency, respectively. The energy input of the REBSs and Microgrids are the i.i.d. variables, and selected from the interval $[0.5 \cdot \text{x-axis value}, 1.5 \cdot \text{x-axis value}]$. For the data traffic demand for the REBSs in the considered time span, it is also randomly and independently selected from $[20\text{Mbps}, 60\text{Mbps}]$. Finally, we set the estimation deviation value $\sum[\boldsymbol{\epsilon}]^+ = 200\text{Mbps}$ and $\sum[\boldsymbol{\epsilon}]^- = 200\text{Mbps}$, respectively. The rest parameters are the same as the ones in Table 5.2.

Fig.5.4 demonstrates the value of total system throughput of the four schemes, with the change of the renewable energy input of the REBSs and Microgrids. Several interesting conclusions can be made by Fig.5.4.

Firstly, the figure demonstrates an upward trend in the input of data traffic demand, therefore there is a proportional relationship between the amount of energy input and the total system throughput. As more energy is available for the REBS, the operating time can be prolonged and the number of active subcarriers can be increased, therefore the amount of supported traffic correspondingly becomes larger.

Secondly, it can be seen that the total system throughput of the Off-line combined with

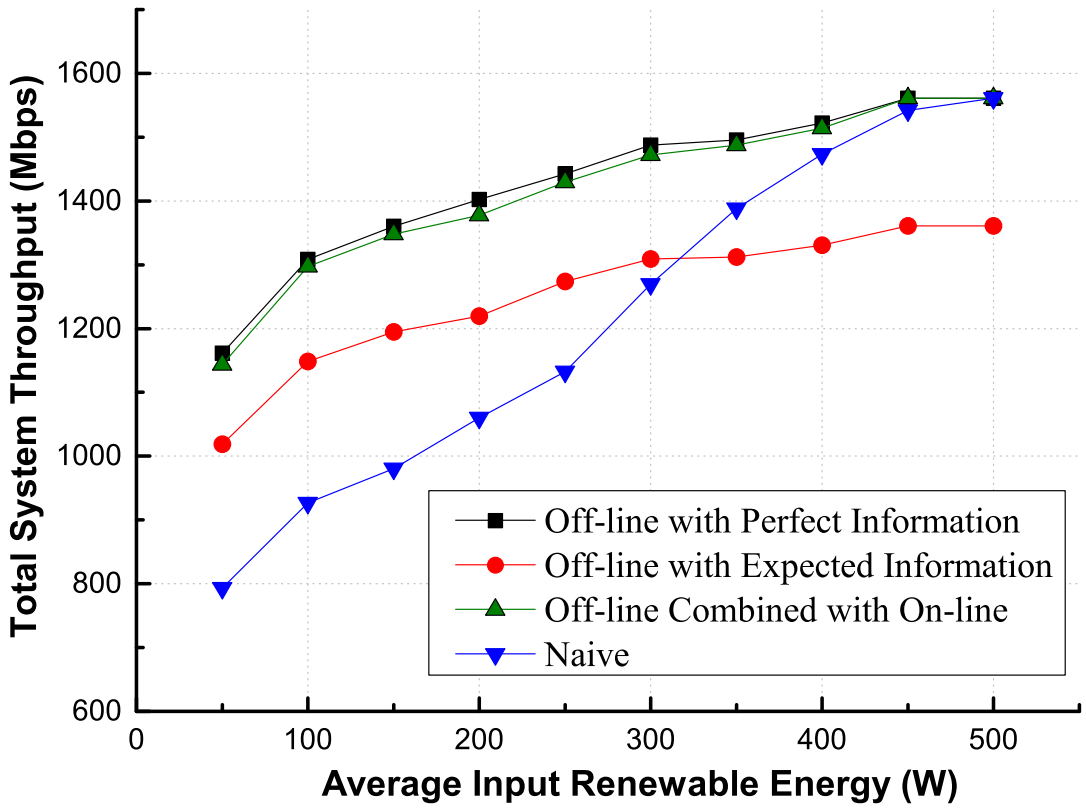

Figure 5.4: The effect of average input renewable energy on system throughput of the four schemes. ©2015 IEEE.

on-line scheme is very close to the one of the optimal scheme, which proves the effectiveness of the on-line scheme established in this chapter. This is because the combined scheme takes the long-term optimization as well as the instant traffic input information into consideration.

Thirdly, the traffic estimation deviation causes a noticeable performance gap between the Off-line with expected information and the optimal scheme. Even when the energy is enough for the operation (i.e., larger than 500W), the off-line only scheme still cannot achieve a desirable result, since its strategy is based on the traffic expectation, and the REBSs will not support larger traffic input due to the decision made before the time slot t_1.

Fourthly, the Naive scheme has the least total system throughput in the early stage. After the average renewable energy input is more than 300W, the result of the Naive scheme becomes better than the result of the off-line with expected information. This is because the Naive scheme will only take consideration of maximizing the system throughput in current time slot using the instant traffic input information, and it is greedy in essence. When the energy is enough, more operating time and subcarriers can be supported, and the optimal strategy will also become greedy, which is to strike the maximal system throughput in current slot, and therefore the Naive result will be closer to the optimal one.

In Fig.5.5, the energy efficiencies of the four schemes is illustrated. It can be seen that the energy efficiency is proportional to average energy input, since the lower y-axis value, the higher energy efficiency.

The major factor causes such phenomenon is, the energy consumed for the operating energy consumption will not directly support more data traffic demand. When the REBS is active, it is the subcarrier that carries the data traffic demand. Therefore, when the energy input is insufficient, a large ratio of the energy consumption will be used for

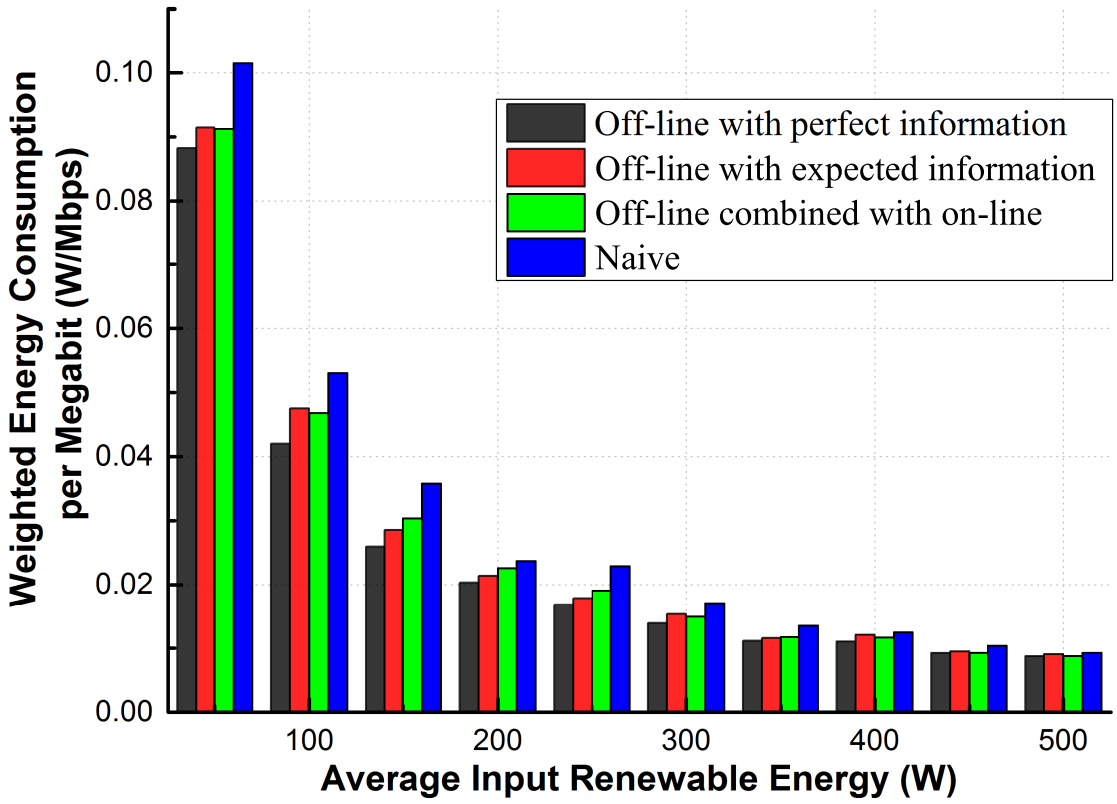

Figure 5.5: The effect of average input renewable energy on consumed power per megabit of the four schemes. ©2015 IEEE.

the operation, and as the amount of energy input becomes larger, the proportion of the subcarrier consumption will be larger as well. As a result, the energy efficiency will also increase. It can be seen that among the four schemes, Naive result has the least energy efficiency, given that the total system throughput of the Naive scheme is lower than the Off-line combined with on-line scheme, the actual performance of the Naive scheme is far behind than the one of Off-line combined with on-line scheme. This result underlines the importance of long-term optimization result.

5.5.3 Effect of Data Traffic Demands on Total System Throughput and Energy Efficiency

In order to check the effect of traffic input on the performance, we consider the data traffic demands of the REBSs as the variables in this part. The X-axis represents the average traffic input, and the real value for the REBSs in each time slot is randomly and independently selected from $[0.5 \cdot \text{x-axis value}, 1.5 \cdot \text{x-axis value}]$. On the other hand, the renewable energy input is also the i.i.d. value and chosen from the range [100W, 300W]. For the traffic estimation deviation, we set $\sum[\boldsymbol{\epsilon}]^+ = 200\text{Mbps}$ and $\sum[\boldsymbol{\epsilon}]^- = 200\text{Mbps}$. The rest parameters are set as Table 5.2.

Fig. 5.6 gives the comparison of the total system throughput of the four schemes. From this figure, it can be seen that there is a proportional relationship between the total system throughput and the traffic input, and such relationship is linear. This is because when the energy input budget is fixed, the amount of energy consumed for activating the subcarrier determines the final result, and if the energy input and network capacity are sufficient, the more traffic input, the more total system throughput. The Off-line combined with on-line scheme can get almost the same total system throughput as the one of the optimal scheme, and the Off-line with expected information scheme has a less total system throughput, since it will only make use of the traffic input expectation, and

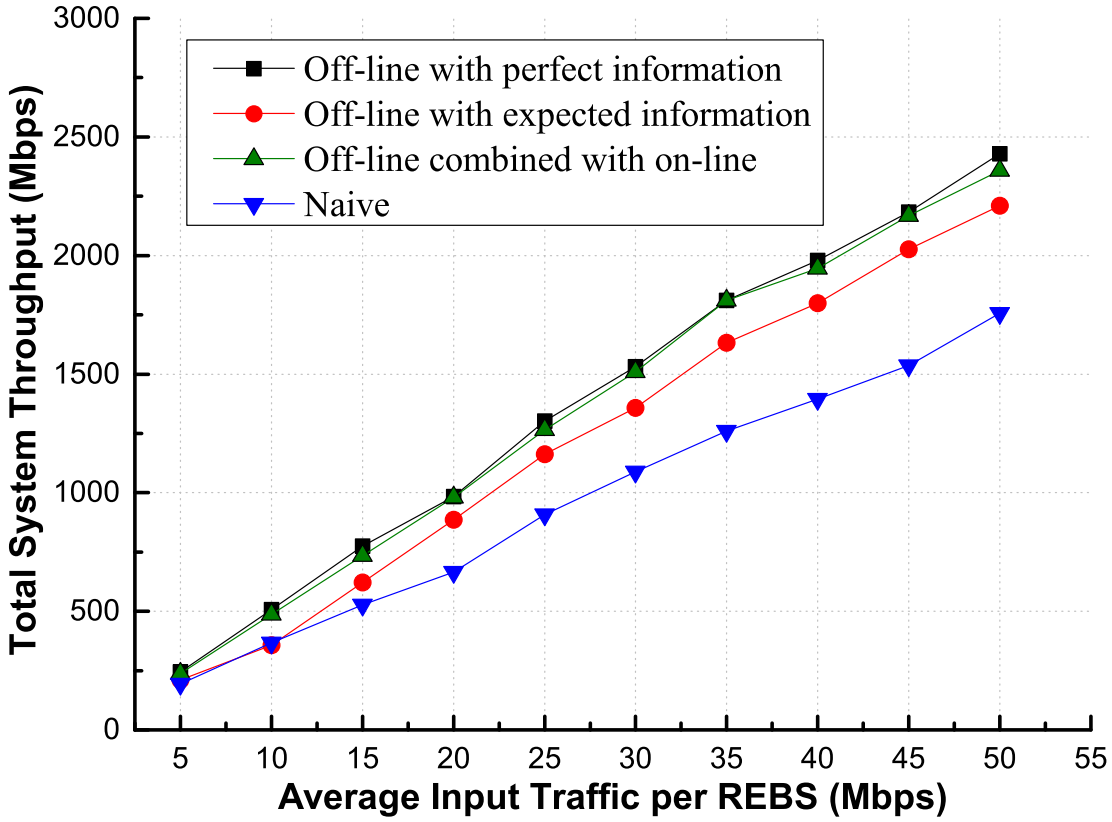

Figure 5.6: The effect of average input traffic per REBS on total system throughput of the four schemes. ©2015 IEEE.

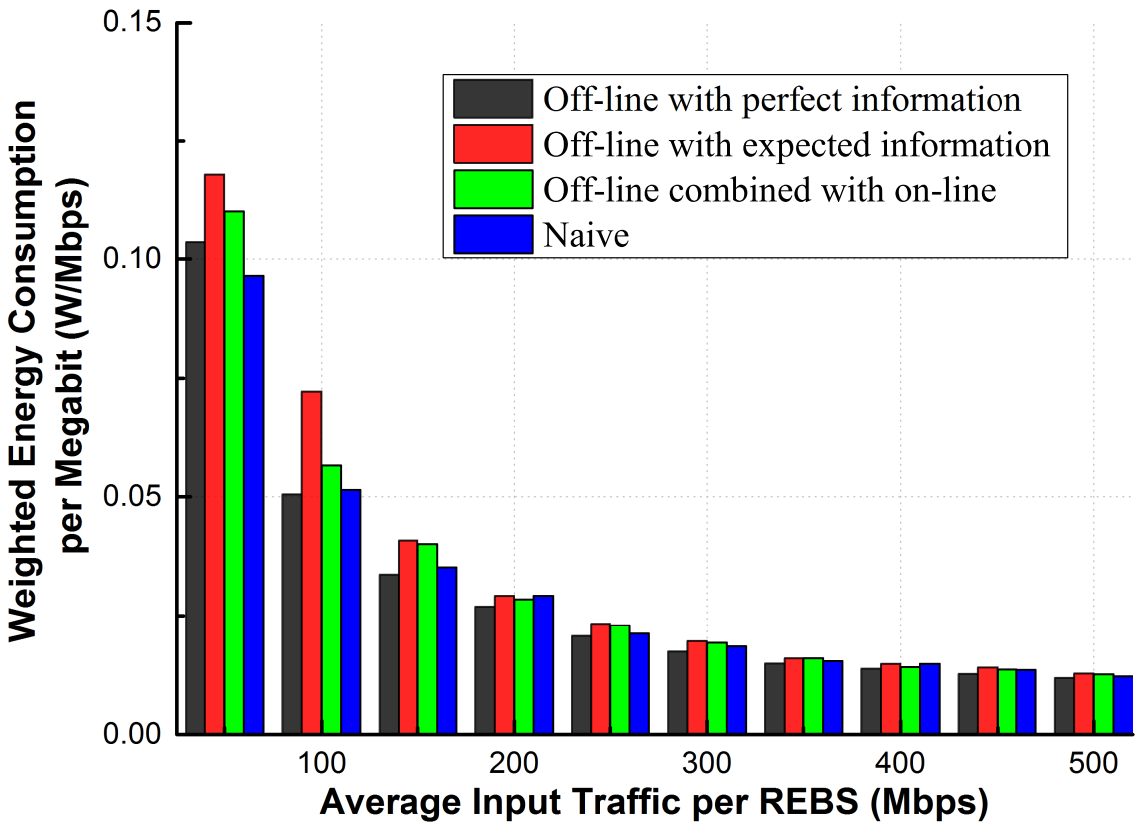

Figure 5.7: The effect of average input traffic per REBS on consumed power per megabit of the four schemes. ©2015 IEEE.

the estimation deviation results in such performance gap. The Naive scheme is with the worst total system throughput than the other three schemes. Moreover, it can be seen that there is an upward trend of the gap when the amount of traffic input increases. If the traffic input is in low level, the influence of the strategy will be small, since the total traffic input is small. As the traffic input increases, the influence of the strategy calculated by the scheme becomes more noticeable.

Fig.5.7 demonstrates the effects of the average traffic input of the REBSs on the energy efficiency of the four schemes. From Fig. 5.7, it can be seen that the energy efficiency is proportional to the traffic input. If the amount of traffic input is low, the operating energy consumption holds a high percentage in the total energy consumption, which means

that the REBS will use a large amount of energy to support a relative small amount of data. Therefore the associating energy efficiency is unsatisfied. As the traffic input becomes larger, the network can support more data traffic demand only at the cost of the subcarrier consumption, and the amount of which is far less than the operation energy consumption therefore the energy efficiency becomes higher.

5.6 Summary

In this chapter, we introduce an on-line dynamically adjusting scheme. Based on the plan of the off-line scheme using traffic input expectation, the envisioned on-line scheme will be executed at the beginning at each time slot and it utilizes the precise traffic in the current time slot, and such scheme can effectively avoid the impact of the inaccurate traffic demand estimation.

We firstly establish the system model by inducing the estimation deviation factor of the traffic input, then we analyze the performance bound of the off-line scheme in term of the estimation deviation factor. After that, we envision the on-line dynamic adjusting scheme. Such scheme makes use of the maximum available amount of energy, which will not affect the future plan, therefore the performance of the combined scheme (i.e., Off-line combined with on-line) is guaranteed. Finally, we illustrate and analyze the computer-based simulations. The numerical results reveal that the proposed Off-line combined with on-line scheme can return a satisfied result when the traffic estimation deviation is high, and it outperforms the off-line only scheme in different energy input levels and traffic input levels.

Chapter 6

Conclusion

6.1 Summary and Discussions

The emergence of renewable energy-enabled base station provides us an extra energy source to the cellular base stations. Due to the numerous recently happened disasters all over the world, network designer also need to take consideration of the energy consumption and traffic transmission strategies for the disaster case. In this thesis, we devote our efforts to the joint energy and traffic management in wireless mesh networks powered by renewable energy. The main contributions of this dissertation can be summarized in the following aspects.

- In Chapter 2, we introduced the REBS-based mesh networks and the associating settings in disaster area. We investigated the energy and traffic flows in the network. We pointed out that the energy input in a finite time horizon could be estimated with the information of weather forecast and the scale of the energy harvesting facilities. In addition, the data traffic demands profiles of the REBSs could also be evaluated by combining the information of the population, the ratio of active users, as well as the previous information. Then the literature review was conducted. We

also demonstrated the necessity of the joint optimization of energy and traffic via an example.

- In Chapter 3, we focused on promoting the REBS-based networks for emergency services powered by renewable energy. Firstly, we introduced the model for energy and traffic in detail, which included energy utilization, battery alternation and traffic transmission. After the literature review, we formulated the problem for the joint optimization of energy and traffic, and then an MILP optimization framework was proposed. At last, we verified the efficiency of our proposed optimization framework through the computer-based simulations. We demonstrated that the total system throughput of the joint optimization result was better than the myopic naive result.
- In Chapter 4, we extended our consideration, and proposed an energy-efficient throughput maximization scheme for the sake of energy efficiency. We defined the ratio of consumed energy to the harvested energy in the future as the energy efficiency of a certain REBS. The objective of the problem was the energy efficiency, and the maximal total system throughput was set as the constraint. Such problem was also an MILP problem and we proposed a two-stage optimization framework to deal with this problem. We justified that the proposed algorithm could achieve higher energy efficiency compared with the throughput-maximization-only scheme and the naive one. Therefore, through the new proposal, the renewable energy would be used efficiently.
- In Chapter 5, we proposed an on-line dynamically adjusting scheme based on the proposals in the previous two chapters. The old proposals made use of the expectation of the traffic profile, and the result would be suboptimal if such estimation was imprecise. To this end, we firstly analyzed the performance bound of the previous off-line result, and then an on-line energy-efficient of throughput-based scheme for the REBS-based mesh network was proposed. The on-line scheme firstly made use of the expectation of the traffic profile, and at the beginning of each time slot, the strategy would be changed accordingly, without affecting the old plan for futures. We developed a mathematical characterization for the on-line scheme, and

the computer-based simulations revealed that our proposed on-line scheme could significantly achieve better network performance compared with the off-line scheme and the naive scheme.

6.2 Future Directions

In this thesis, we proposed a throughput-maximization frameworks for the REBS-based mesh network and the associating algorithms. In addition, the energy efficiency as well as the estimation precision were taken into consideration. We list the possible extensions as the following aspects:

Firstly, it is noticed that we assume the perfect energy estimation profile in our considered model. In the causal case, such assumption may hold since the developed technology of the weather forecast and the sufficient statistical surveys of the historical profile. However, for some extreme cases (Such as the unexpected weather), there might also be deviation on the energy estimation profile. Therefore both of the energy and traffic estimation profiles are imprecise, and a deeper analysis of the relationship between the energy and traffic becomes necessary.

Secondly, in our consideration, the Microgrid acts only as the energy distributor. The recently academic publications study the availabilities for the deeper energy cooperation among the REBSs connected to the same Microgrid. The REBSs under the same Microgrid cluster can mutually transfer the energy inside the batteries. It would be interesting to consider the bi-directional energy transmission direction between the REBSs and the Microgrid.

Thirdly, for the model in the thesis, the limited number of the REBSs guarantees the availability for MILP problem solution in practice. We believe that along with the advance of weather forecast technique in the future, the granularity of the time slot will be

finer, and the length of time slot will be shrunk. Therefore an low complexity alternative is also needed if the scale of the problem becomes larger.

Bibliography

[1] T. Sakano, Z. Fadlullah, T. Ngo, H. Nishiyama, M. Nakazawa, F. Adachi, N. Kato, A. Takahara, T. Kumagai, H. Kasahara, and S. Kurihara, "Disaster-resilient networking: a new vision based on movable and deployable resource units," *Network, IEEE*, vol. 27, no. 4, pp. 40–46, July 2013.

[2] G. Auer, V. Giannini, I. Godor, P. Skillermark, M. Olsson, M. Imran, D. Sabella, M. Gonzalez, C. Desset, and O. Blume, "Cellular energy efficiency evaluation framework," in *Vehicular Technology Conference (VTC Spring), 2011 IEEE 73rd*, May 2011, pp. 1–6.

[3] O. Arnold, F. Richter, G. Fettweis, and O. Blume, "Power consumption modeling of different base station types in heterogeneous cellular networks," in *Future Network and Mobile Summit, 2010*, June 2010, pp. 1–8.

[4] K. Heimerl, K. Ali, J. Blumenstock, B. Gawalt, and E. Brewer, "Expanding rural cellular networks with virtual coverage," in *Presented as part of the 10th USENIX Symposium on Networked Systems Design and Implementation (NSDI 13)*. Lombard, IL: USENIX, 2013, pp. 283–296. [Online]. Available: https://www.usenix.org/conference/nsdi13/technical-sessions/presentation/heimurl

[5] G. Auer, V. Giannini, I. Godor, P. Skillermark, M. Olsson, M. Imran, D. Sabella, M. Gonzalez, C. Desset, and O. Blume, "Cellular energy efficiency evaluation framework," in *IEEE 73rd Vehicular Technology Conference (VTC Spring)*, May 2011, pp. 1–6.

[6] A. Kwasinski, V. Krishnamurthy, S. J., and R. Sharma, "Availability evaluation of micro-grids for resistant power supply during natural disasters," *IEEE Transactions on Smart Grid*, vol. 3, no. 4, pp. 2007–2018, Dec 2012.

[7] E. Daigneau, "Microgrids: A disaster-resistant power supply?" http://goo.gl/9wgdNS, Nov 2012, [Online; accessed 22-April-2014].

[8] A. Kwasinski and A. Kwasinski, "Architecture for green mobile network powered from renewable energy in microgrid configuration," in *Wireless Communications and Networking Conference (WCNC), 2013 IEEE*, April 2013, pp. 1273–1278.

[9] R. Anderson, A. Boulanger, W. Powell, and W. Scott, "Adaptive stochastic control for the smart grid," *Proceedings of the IEEE*, vol. 99, no. 6, pp. 1098–1115, June 2011.

[10] J. Leithon, S. Sun, and T. J. Lim, "Energy management strategies for base stations powered by the smart grid," in *Global Communications Conference (GLOBECOM), 2013 IEEE*, Dec 2013, pp. 2635–2640.

[11] J. Leithon, T. J. Lim, and S. Sun, "Online energy management strategies for base stations powered by the smart grid," in *Smart Grid Communications (SmartGridComm), 2013 IEEE International Conference on*, Oct 2013, pp. 199–204.

[12] X. Guan, Z. Xu, and Q.-S. Jia, "Energy-efficient buildings facilitated by microgrid," *Smart Grid, IEEE Transactions on*, vol. 1, no. 3, pp. 243–252, Dec 2010.

[13] S. Bu, F. Yu, and Y. Qian, "Energy-efficient cognitive heterogeneous networks powered by the smart grid," in *INFOCOM, 2013 Proceedings IEEE*, April 2013, pp. 980–988.

[14] S. Bu, F. Yu, and P. Liu, "Stochastic unit commitment in smart grid communications," in *Computer Communications Workshops (INFOCOM WKSHPS), 2011 IEEE Conference on*, April 2011, pp. 307–312.

[15] J. Xu, Y. Guo, and R. Zhang, "Comp meets energy harvesting: A new communication and energy cooperation paradigm," in *Global Communications Conference (GLOBECOM), 2013 IEEE*, Dec 2013, pp. 2508–2513.

[16] C. Wei, Z. Fadlullah, N. Kato, and A. Takeuchi, "Gt-cfs: A game theoretic coalition formulation strategy for reducing power loss in micro grids," *Parallel and Distributed Systems, IEEE Transactions on*, vol. 25, no. 9, pp. 2307–2317, Sept 2014.

[17] C. Wei, Z. Fadlullah, N. Kato, and I. Stojmenovic, "On optimally reducing power loss in micro-grids with power storage devices," *Selected Areas in Communications, IEEE Journal on*, vol. 32, no. 7, pp. 1361–1370, July 2014.

[18] J. Pan, R. Jain, and S. Paul, "A survey of energy efficiency in buildings and microgrids using networking technologies," *Communications Surveys Tutorials, IEEE*, vol. 16, no. 3, pp. 1709–1731, Third 2014.

[19] M. A. Marsan, L. Chiaraviglio, D. Ciullo, and M. Meo, "On the effectiveness of single and multiple base station sleep modes in cellular networks," *Computer Networks*, vol. 57, no. 17, pp. 3276 – 3290, 2013. [Online]. Available: http://www.sciencedirect.com/science/article/pii/S1389128613002429

[20] T. Han and N. Ansari, "Optimizing cell size for energy saving in cellular networks with hybrid energy supplies," in *Global Communications Conference (GLOBECOM), 2012 IEEE*, Dec 2012, pp. 5189–5193.

[21] M. Gatzianas, L. Georgiadis, and L. Tassiulas, "Control of wireless networks with rechargeable batteries," *IEEE Transactions on Wireless Communications*, vol. 9, no. 2, pp. 581–593, February 2010.

[22] W. Guo and T. O'Farrell, "Green cellular network: Deployment solutions, sensitivity and tradeoffs," in *Wireless Advanced (WiAd), 2011*, June 2011, pp. 42–47.

[23] G. Miao, N. Himayat, G. Li, and S. Talwar, "Low-complexity energy-efficient scheduling for uplink ofdma," *IEEE Transactions on Communications*, vol. 60, no. 1, pp. 112–120, January 2012.

[24] G. Auer, V. Giannini, C. Desset, I. Godor, P. Skillermark, M. Olsson, M. Imran, D. Sabella, M. Gonzalez, O. Blume, and A. Fehske, "How much energy is needed to run a wireless network?" *Wireless Communications, IEEE*, vol. 18, no. 5, pp. 40–49, October 2011.

[25] L. Chiaraviglio, M. Mellia, and F. Neri, "Reducing power consumption in backbone networks," in *Communications, 2009. ICC '09. IEEE International Conference on*, June 2009, pp. 1–6.

[26] W. Fisher, M. Suchara, and J. Rexford, "Greening backbone networks: Reducing energy consumption by shutting off cables in bundled links," in *Proceedings of the First ACM SIGCOMM Workshop on Green Networking*, ser. Green Networking '10. New York, NY, USA: ACM, 2010, pp. 29–34. [Online]. Available: http://doi.acm.org/10.1145/1851290.1851297

[27] Y. Li, H. Celebi, M. Daneshmand, C. Wang, and W. Zhao, "Energy-efficient femtocell networks: challenges and opportunities," *Wireless Communications, IEEE*, vol. 20, no. 6, pp. 99–105, December 2013.

[28] J. Piorno, C. Bergonzini, D. Atienza, and T. Rosing, "Prediction and management in energy harvested wireless sensor nodes," in *Wireless Communication, Vehicular Technology, Information Theory and Aerospace Electronic Systems Technology, 2009. Wireless VITAE 2009. 1st International Conference on*, May 2009, pp. 6–10.

[29] A. Fernandez, Y. Gala, and J. Dorronsoro, "Machine learning prediction of large area photovoltaic energy production," in *Second Workshop on Data Analytics for Renewable Energy Integration (DARE-14)*, Nancy, France, Sept 2014.

[30] J. Lu, S. Liu, Q. Wu, and Q. Qiu, "Accurate modeling and prediction of energy availability in energy harvesting real-time embedded systems," in *Green Computing Conference, 2010 International*, Aug 2010, pp. 469–476.

[31] S. He, J. Chen, F. Jiang, D. Yau, G. Xing, and Y. Sun, "Energy provisioning in wireless rechargeable sensor networks," in *INFOCOM, 2011 Proceedings IEEE*, April 2011, pp. 2006–2014.

[32] M. Marsan, G. Bucalo, A. Di Caro, M. Meo, and Y. Zhang, "Towards zero grid electricity networking: Powering bss with renewable energy sources," in *Communications Workshops (ICC), 2013 IEEE International Conference on*, June 2013, pp. 596–601.

[33] M. A. Marsan, L. Chiaraviglio, D. Ciullo, and M. Meo, "On the effectiveness of single and multiple base station sleep modes in cellular networks," *Computer Networks*, vol. 57, no. 17, pp. 3276 – 3290, 2013. [Online]. Available: http://www.sciencedirect.com/science/article/pii/S1389128613002429

[34] M. Zheleva, A. Paul, D. L. Johnson, and E. Belding, "Kwiizya: Local cellular network services in remote areas," in *Proceeding of the 11th Annual International Conference on Mobile Systems, Applications, and Services*, ser. MobiSys '13. New York, NY, USA: ACM, 2013, pp. 417–430. [Online]. Available: http://doi.acm.org/10.1145/2462456.2464458

[35] E. Oh and B. Krishnamachari, "Energy savings through dynamic base station switching in cellular wireless access networks," in *Global Telecommunications Conference (GLOBECOM 2010), 2010 IEEE*, Dec 2010, pp. 1–5.

[36] F. Han, Z. Safar, and K. Liu, "Energy-efficient base-station cooperative operation with guaranteed qos," *IEEE Transactions on Communications*, vol. 61, no. 8, pp. 3505–3517, August 2013.

[37] M. Marsan, L. Chiaraviglio, D. Ciullo, and M. Meo, "Optimal energy savings in cellular access networks," in *Communications Workshops, 2009. ICC Workshops 2009. IEEE International Conference on*, June 2009, pp. 1–5.

[38] S.-E. Elayoubi, L. Saker, and T. Chahed, "Optimal control for base station sleep mode in energy efficient radio access networks," in *INFOCOM, 2011 Proceedings IEEE*, April 2011, pp. 106–110.

[39] D. Willkomm, S. Machiraju, J. Bolot, and A. Wolisz, "Primary users in cellular networks: A large-scale measurement study," in *New Frontiers in Dynamic Spectrum Access Networks, 2008. DySPAN 2008. 3rd IEEE Symposium on*, Oct 2008, pp. 1–11.

[40] J. Yoon, S. Sen, J. Hare, and S. Banerjee, "Wiscape: A framework for measuring the performance of wide-area wireless networks," *Mobile Computing, IEEE Transactions on*, vol. 14, no. 8, pp. 1751–1764, Aug 2015.

[41] C. Peng, S.-B. Lee, S. Lu, H. Luo, and H. Li, "Traffic-driven power saving in operational 3g cellular networks," in *Proceedings of the 17th Annual International Conference on Mobile Computing and Networking*, ser. MobiCom '11. New York, NY, USA: ACM, 2011, pp. 121–132. [Online]. Available: http://doi.acm.org/10.1145/2030613.2030628

[42] K. Jacobson and W. Krzymien, "Cooperative vs multihop relaying in cellular systems," in *20th IEEE International Symposium on Personal, Indoor and Mobile Radio Communications*, Sept 2009, pp. 1853–1857.

[43] F. Mostafa, H. Nishiyama, R. Miura, and N. Kato, "On efficient traffic distribution for disaster area communication using wireless mesh networks," *Wireless Personal Communications*, vol. 74, no. 4, pp. 1311–1327, 2014. [Online]. Available: http://dx.doi.org/10.1007/s11277-013-1579-9

[44] S. Guo, L. T. Yang, G. Min, and X. Xie, "Green communication in energy renewable wireless mesh networks: Routing, rate control, and power allocation," *IEEE Transactions on Parallel and Distributed Systems*, vol. 99, no. PrePrints, p. 1, 2014.

[45] T. Ngo, H. Nishiyama, N. Kato, T. Sakano, and A. Takahara, "A spectrum-and energy-efficient scheme for improving the utilization of MDRU-based disaster resilient networks," *IEEE Transactions on Vehicular Technology - Special Section on Green Mobile Multimedia Communications*, vol. 63, no. 5, pp. 2027–2037, Jun. 2014.

[46] L. Xiang, X. Ge, C.-X. Wang, F. Y. Li, and F. Reichert, "Energy efficiency evaluation of cellular networks based on spatial distributions of traffic load and power consumption," *IEEE Transactions on Wireless Communications*, vol. 12, no. 3, pp. 961–973, March 2013.

[47] L. Cai, Y. Liu, T. Luan, X. Shen, J. Mark, and H. Poor, "Sustainability analysis and resource management for wireless mesh networks with renewable energy supplies," *IEEE Journal on Selected Areas in Communications*, vol. 32, no. 2, pp. 345–355, February 2014.

[48] J. Marašević, C. Stein, and G. Zussman, "Max-min fair rate allocation and routing in energy harvesting networks: Algorithmic analysis," in *Proceedings of the 15th ACM International Symposium on Mobile Ad Hoc Networking and Computing*, ser. MobiHoc '14. New York, NY, USA: ACM, 2014, pp. 367–376. [Online]. Available: http://doi.acm.org/10.1145/2632951.2632960

[49] Y. Guo, J. Xu, L. Duan, and R. Zhang, "Joint energy and spectrum cooperation for cellular communication systems," *Communications, IEEE Transactions on*, vol. 62, no. 10, pp. 3678–3691, Oct 2014.

[50] C. Ma, Z. Zhang, and Y. Yang, "Battery-aware router scheduling in wireless mesh networks," in *Parallel and Distributed Processing Symposium, 2006. IPDPS 2006. 20th International*, April 2006, pp. 10 pp.–.

[51] M. Cheng, X. Gong, L. Cai, and X. Jia, "Cross-layer throughput optimization with power control in sensor networks," *IEEE Transactions on Vehicular Technology*, vol. 60, no. 7, pp. 3300–3308, Sept 2011.

[52] M. Li, H. Nishiyama, N. Kato, Y. Owada, and K. Hamaguchi, "n the energy-efficient of throughput-based scheme using renewable energy for wireless mesh networks in disaster area," *Emerging Topics in Computing, IEEE Transactions on*, vol. 3, no. 3, pp. 420–431, Dec 2014.

[53] M. Li, H. Nishiyma, Y. Owada, and K. Hamaguchi, "On energy efficient scheduling and load distribution based on renewable energy for wireless mesh network in disaster area," in *The 13th IEEE International Conference on Trust, Security and Privacy in Computing and Communications (TrustCom-14)*, Sept 2014, pp. 465–472.

[54] J. Chen, X. Cao, P. Cheng, Y. Xiao, and Y. Sun, "Distributed collaborative control for industrial automation with wireless sensor and actuator networks," *IEEE Transactions on Industrial Electronics*, vol. 57, no. 12, pp. 4219–4230, Dec 2010.

[55] S. William, *Wireless Communications and Networks*, 2nd ed. Pearson Prentice Hall, 2005.

[56] X. Wang and L. Cai, "Stability region of opportunistic scheduling in wireless networks," *IEEE Transactions on Vehicular Technology*, vol. 63, no. 8, pp. 4017–4027, Oct 2014.

Publications

Journals

[1] Meng Li, Hiroki Nishiyama, Nei Kato, Yasunori Owada, and Kiyoshi Hamaguchi, "On the Energy-Efficient of Throughput-Based Scheme Using Renewable Energy for Wireless Mesh Networks in Disaster Area", *IEEE Transactions on emerging topics in computing*, Vol. 3, No. 3, pp. 420-431, Jan. 2015.

Refereed Conference Papers

[2] Meng Li, Hiroki Nishiyama, Yasunori Owada, and Kiyoshi Hamaguchi, "On Energy Efficient Scheduling and Load Distribution Based on Renewable Energy for Wireless Mesh Network in Disaster Area", *The 13th IEEE International Conference on Trust, Security and Privacy in Computing and Communications (IEEE TrustCom-14)*, Beijing, China, Sep. 2014.

[3] Meng Li, Hiroki Nishiyama, Nei Kato, Kimihiro Mizutani, Osamu Akashi, and Atsushi Takahara, "On the Fast-Convergence of Delay-Based Load Balancing over Multipaths for Dynamic Traffic Environments", *2013 International Conference on Wireless Communications and Signal Processing (WCSP 2013)*, Hangzhou, China, Oct. 2013.

Grants

Best paper award: Meng Li, Hiroki Nishiyama, Yasunori Owada, and Kiyoshi Hamaguchi, "On Energy Efficient Scheduling and Load Distribution Based on Renewable Energy for Wireless Mesh Network in Disaster Area", *The 13th IEEE International Conference on Trust, Security and Privacy in Computing and Communications (IEEE TrustCom-14)*, Beijing, China, Sep. 2014.

Appendix

Copyright Permissions

In this appendix we includes the permissions that were used to write this dissertation. The detail description of permissions are given in the following documents.

The permission grants from IEEE.

A Study on Joint Optimization of Traffic and Energy Management in Wireless Mesh Networks Powered by Renewable Energy

再生可能エネルギー駆動型無線メッシュネットワークにおける通信と電力効率の最適化に関する研究

A dissertation presented
by

Meng Li

submitted to
Tohoku University
in partial fulfillment of the requirements
for the degree of

Doctor of Philosophy

Supervisor: Professor Nei Kato

Department of Applied Information Sciences
Graduate School of Information Sciences
Tohoku University

January, 2016

To my family and my dear friends

Abstract

The recently happened natural disasters on a world scale tell us the importance of a well-considered emergency plan in the post-disaster treatment. The accommodation of network service is one important part, since a well-designed network provision will not only convey the rescue information to the outside, but also guarantee the communication demands of the people inside the disaster area. Nevertheless, a major obstacle to meet the communication demands in the post-disaster case is the unavailability of the crucial infrastructures (i.e., power transmission cables, Internet cables). The emergence of the Renewable Energy-enabled Base Station (REBS)-based mesh network is an emerging technique, which gives us a possible solution to deal with this issue. The REBS still has intermittent renewable energy supplies when the power from power plant is cut off, then with the help of vehicle-borne network gateway, such kind of network will keep operating after disaster.

The REBS-based mesh network is the network composed of interconnecting REBSs and Microgrids. All the REBSs and Microgrids have the energy harvesting facilities, which can get renewable energy from surrounding environment. The Microgrid can distribute the energy from its battery to the connected REBSs'. In the post-disaster case, the REBSs in the network run entirely on renewable energy sources and such energy could be the energy from local harvesting facilities or from the remote Microgrids'. Besides the energy aspect, REBSs will use the pre-equipped network facilities to connect their neighbors, send the data hop-by-hop, and finally rely on the vehicle-borne network gateway to transfer data to the Internet. However, in the post-disaster case, both of the energy and network bandwidth are limited. Therefore, such limited resources need to be arranged efficiently before the network get recovered.

This dissertation addresses the issue of designing the algorithms to accommodate the network service with the limited bandwidth and energy resource in the post-disaster case. Because the network has to deal with a large amount of data transfer demand, and need to fulfill such demand as much as possible, toward such a target, in this thesis, we study the joint energy and traffic management for throughput maximization in the post disaster scenario.

At first, we consider an off-line throughput-maximization scheme when we have the exact traffic and energy profile in the finite time horizon. To formulate the problem, we analyze and investigate the data and energy profile as well as network structure, and develop an optimization framework that considers limited input energy and link capacity in the considered time span. Then we formulate the considered scheme as a Mixed Integer Linear Programming (MILP) problem. The simulation results show that our proposal can achieve high total system throughput compared with the naive idea.

Secondly, we propose an energy efficient scheme based on the maximal throughput value. The energy efficiency is to minimize the weighted energy consumption, which equals the ratio of the consumed energy to the harvested energy. Such optimization framework is also the MILP problem. Through the extensive simulation results, we validate that our scheme could significantly improve network performance in energy efficiency, comparing with the naive scheme and throughput-maximization scheme.

Thirdly, we extend the off-line energy efficient throughput-maximization scheme into the on-line case. We consider the possible imprecise estimation of the data traffic demands, and analyze the effects of such imprecision on the performance. After that, an on-line dynamic adjusting scheme is proposed, in the proposed on-line scheme, REBSs will adjust the previous strategy according to the latest traffic information at the beginning of each time slot. The numerical results demonstrate that the proposed on-line scheme outperforms the off-line scheme and the naive one with regard to estimation error, energy efficiency and system throughput.

Acknowledgments

First and foremost, I would like to express my deepest gratitude to my advisor, Prof. Nei Kato, for his insightful guidance, continuous supportance and proving an excellent research atmosphere throughout my study in Tohoku University. I cannot have imagined having a better advisor and mentor for my study.

It is also my great honor to thank Prof. Suganuma, and Prof. Omachi for being my dissertation committee members and giving me constructive comments to this dissertation in its final form.

I would like to express my appreciation to Prof. Hiroki Nishiyama for his insightful guidance in my study. His high standards of the research have inspired me to keep challenging myself, and I have learned a lot from the discussions and comments from him. This dissertation cannot be finished without his help.

I would like to acknowledge the China Scholarship Council (CSC) Foundation, for offering the financial supportance during my study in Tohoku University, one of the most prestigious universities in Asia. I would also like to thank Ms. Motoko Shiraishi and Ms. Takako Kase for helping me with the enrollment process, and providing me with all the necessary administrative documents.

I am grateful to the unreserved helps from my friends during my stay in Japan in both of the academic and the daily life, especially Dr. Jiajia Liu, Dr. Chao Wei, Dr. Wei Zhao, Ngo Duc Thuan, Fomo Desmond, Ko Togashi, Kei Saito and Panu Avakul.

In addition, I would like to give my sincere thanks to members of the Kato-Nishiyama Laboratory for the joyful and unforgettable life in Japan: Prof. Zubair Md. Fadlullah, Prof. Mostafa Fouda, Mr. Kaoru Chiba, Ms. Kimi Nishimura, Dr. Wei Liu, Dr. Kaoru Ota, Dr. Zanjie Huang, Dr. Ahmed E.A.A. Abdulla, Yuichi Kawamoto, Katsuya Suto, Shucong Jia, Daisuke Takaishi, Kazuma Kanako, Monder Rehamnia, Bomin Mao, Fengxiao Tang, Kenta Suzuki, Takahiro Nozue, Atsushi Toshinari, Timonen Henri Lauri, Kazuma Yoshida, Asato Takahashi, Shintaro Arai, Masaya Ito, Kazuhiro Matsumoto, Kenta Ito, Shoki Oiyama, Shin Koseki, Yu Saito, Keisuke Sato ,Tota Nakajo, Keisuke Miyanabe, Rodrigo Bernardino Barros, Takanobu Endo, Takayuki Nakazawa, Masanori Horiuchi, Naoki Miyashita, Daiki Murayama, Naoto Yamada, Yunseong Lee, Tiago Gama Rodrigues, Ken Sasaki, Yuya Kasahara, Hideki Kuribayashi, Yoshiki Shino, Hiroaki Takagi, Shikhar, Michael R. Zielewski, Julian A. Rick, and Weiming Liao.

Finally, and most importantly, I would like to acknowledge the immeasurable and unwaving support given by my parents (Song Wang and Xianjun Li) and my girlfriend

(Li Qiang) during the years I have been working on this thesis. Words cannot describe my gratitude toward them.

My apologies if I have inadvertently omitted anyone to whom acknowledge is due.

Contents

Abstract **i**

Acknowledgments **iii**

1 Introduction **1**

1.1 Background 1
1.2 Challenging Issues with REBS-based Mesh Networks 6
1.3 Research Objectives 7
1.4 Thesis Outline 9
1.5 Contributions 10

2 Overview of REBS-based Mesh Networks and Its Associating Settings in Disaster Area **12**

2.1 Introduction to the REBS-based Mesh Networks 12
2.1.1 Energy Flows inside REBS 12
2.1.2 Traffic Flows in Network 14
2.2 Spatial and Temporal Diversities of the Traffic and Energy 15
2.3 Related Work 16
2.4 Our Research Target 19
2.5 The Advantage of Joint Optimization 21
2.6 Summary 22

3 The Off-line Scheduling and Load Distribution for REBS Mesh Networks **24**

3.1 Introduction 24
3.2 Preliminaries 25
3.2.1 The Way of Energy Cooperation 25
3.2.2 The Energy and Traffic Input Profiles 26
3.3 System Model 27
3.3.1 Network Model 27
3.3.2 Energy Related Model 28

3.3.3 Traffic Related Model . . . 31
3.4 Research Objective . . . 35
3.5 Problem Formulation . . . 36
3.5.1 The Equivalent Transformation of Constraints . . . 36
3.5.2 Discussion on the Computation Cost . . . 38
3.6 Performance Evaluation . . . 39
3.6.1 Settings of the Simulation . . . 39
3.6.2 Impact of the Energy Input on Total System Throughput . . . 43
3.6.3 Impact of the Traffic Input on Total System Throughput . . . 45
3.7 Summary . . . 45

4 The Off-line Energy Efficient Scheduling and Load Distribution for REBS Mesh Networks 47
4.1 Introduction . . . 47
4.2 System Model and Optimization Objective . . . 48
4.2.1 System Model . . . 48
4.2.2 Optimization Objective . . . 50
4.3 Proposed Two-stage Energy Efficiency Scheme . . . 52
4.4 Performance Evaluation . . . 54
4.4.1 Settings of the Simulation . . . 54
4.4.2 Effect of Energy Input on Energy Efficiency . . . 55
4.4.3 Effect of Traffic Input on Energy Efficiency . . . 59
4.5 Summary . . . 59

5 On the On-line Energy-Efficient of Throughput-Based Scheme for REBS Mesh Networks 61
5.1 Introduction . . . 61
5.2 System Model . . . 62
5.3 Analysis on the Off-line Scheme . . . 63
5.4 Envisioned On-line Dynamic Adjusting Scheme . . . 67
5.5 Performance Evaluation . . . 71
5.5.1 Effect of Estimation Deviation of Data Traffic Demands on System Throughput and Energy Consumption . . . 75
5.5.2 Effect of Total Available Energy on Total System Throughput and Energy Efficiency . . . 80
5.5.3 Effect of Data Traffic Demands on Total System Throughput and Energy Efficiency . . . 84
5.6 Summary . . . 87

6 Conclusion **88**
6.1 Summary and Discussions 88
6.2 Future Directions 90

Bibliography **92**

Publications **100**

Appendix **101**

List of Figures

1.1 The traditional power supply for base stations. 1
1.2 New power supply for cellular network with energy harvesting facilities and Microgrids. 3
1.3 The power supply for REBS in disaster. 4
1.4 The traffic transmission for REBS in disaster. 5

2.1 The energy and the traffic flows in the considered REBS-based mesh networks. ©2014 IEEE. 14
2.2 The cooperation of the data traffic transmission among the REBSs. 20
2.3 The system topology of the example, and the associating solutions of the Naive scheme and joint-optimization scheme, respectively. 23

3.1 Traffic flow between REBSs, and energy flow inside REBSs and Microgrids. ©2015 IEEE. 34
3.2 System topology used in the part of performance evaluation. ©2014 IEEE. 41
3.3 The effect of average input renewable energy on system throughput of the proposed scheme and naive scheme. ©2014 IEEE. 42
3.4 The effect of average input traffic per base station on total system throughput of the proposed scheme and naive scheme. ©2014 IEEE. 44

4.1 System topology used in the part of performance evaluation. ©2014 IEEE. 56
4.2 The effect of average input renewable energy on consumed power per megabit of the proposed scheme, naive scheme and throughput maximization scheme. ©2014 IEEE. 57
4.3 The effect of average input traffic per base station on consumed power per megabit of the proposed scheme, naive scheme and throughput maximization scheme. ©2014 IEEE. 58

5.1 The topology used for the computer-based simulation. ©2015 IEEE. . . . 74
5.2 The effect of ϵ on system throughput of the off-line with expected information, off-line combined with on-line, and Naive scheme. ©2015 IEEE. . . . 76

5.3 The effect of ϵ on energy efficiency of the off-line with expected information and off-line combined with on-line scheme. ©2015 IEEE. 79
5.4 The effect of average input renewable energy on system throughput of the four schemes. ©2015 IEEE. 81
5.5 The effect of average input renewable energy on consumed power per megabit of the four schemes. ©2015 IEEE. 83
5.6 The effect of average input traffic per REBS on total system throughput of the four schemes. ©2015 IEEE. 85
5.7 The effect of average input traffic per REBS on consumed power per megabit of the four schemes. ©2015 IEEE. 86

List of Tables

3.1 Experimental Parameters ©2014 IEEE. 40

4.1 Variable Summarization 49
4.2 Experimental Parameters ©2014 IEEE. 55

5.1 Variable Summarization 64
5.2 Experimental Parameters ©2015 IEEE. 73

List of Acronyms

BS Base Station
CAPEX CAPital EXpenditure
COW Cell On Wheel
MILP Mixed Integer and Linear Programming
OPEX OPerating EXpense
PVT Poisson-Voronoi Tessellation
REBS Renewable Energy-enabled Base Station
SMS Short Message Service
SPOF Single Point Of Failure
VOIP Voice Over Internet Protocol
WSAN Wireless Sensor and Actuator Networks

Chapter 1

Introduction

1.1 Background

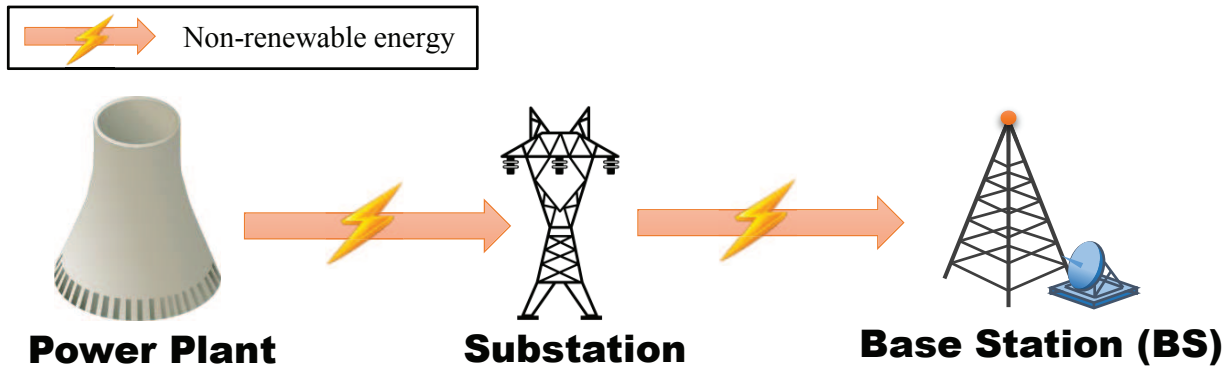

Figure 1.1: The traditional power supply for base stations.

The time of electricity usage of the human beings can be date back to hundreds of years ago. Thanks to the widespread usage of electricity and the fast development of the communication technology in recent years, the related energy supply and communication techniques have been drawing much attention. The traditional power supply for cellular networks is the non-renewable energy from power plant, its voltage will be transformed from high to low by electricity substation, and then the Base Station (BS) is powered by such low-voltage non-renewable energy (Fig. 1.1). However, this energy source and transmission approach have several shortcomings as follows:

- The traditional power plants use non-renewable energy resources (i.e., fossil fuels and nuclear fuel) to generate electricity. Such kind of energy resources aggravate environmental pollution (i.e, green house gases, radioactive waste).
- The CAPital EXpenditure (CAPEX) and OPerating EXpense (OPEX) of the plants are high. In other words, not all the places can afford to establish the power plant or connect to the power grid. Therefore, people outside the power plant's coverage area cannot use the electricity.
- There is a Single Point Of Failure (SPOF) problem for such architecture. The Base Stations (BSs) solely use the energy from power plants. Therefore, if the energy supply is cut off, or the power transmission cable is damaged, the BSs cannot operate due to the lack of energy.

The appearance of the Microgrids and Renewable Energy-enabled Base Station (REBS) offers a solution to deal with the above-mentioned shortcomings. These new type of power grids and cellular BSs can harvest the renewable energy (i.e., solar energy, wind energy) from ambient environments via energy harvesting facilities (i.e., solar panel, wind turbine) (Fig. 1.2).

Therefore, on a daily basis, the REBS will have extra cost-free energy input besides the expensive non-renewable energy supply, by using energy harvesting facilities. The introduced renewable energy input can effectively reduce the consumption of non-renewable energy. The non-renewable energy from power plant will be firstly transmitted to the Microgrid's place, then the Microgrid will deliver such non-renewable energy as well as its harvested renewable energy to the connected REBSs. For the REBS, it will combine such energy input with the energy from its local energy harvesting facilities as its operating energy sources. Additionally, because the REBS itself still has energy supply even the energy from power plant is cut off, such feature enables us to explore its availability in the case of zero grid energy input, such as the post-disaster communication case (Fig. 1.3).

The REBS - based mesh network is a mesh network composed by Microgrids and associating REBSs, which is designed for the provision of network service in disaster area.

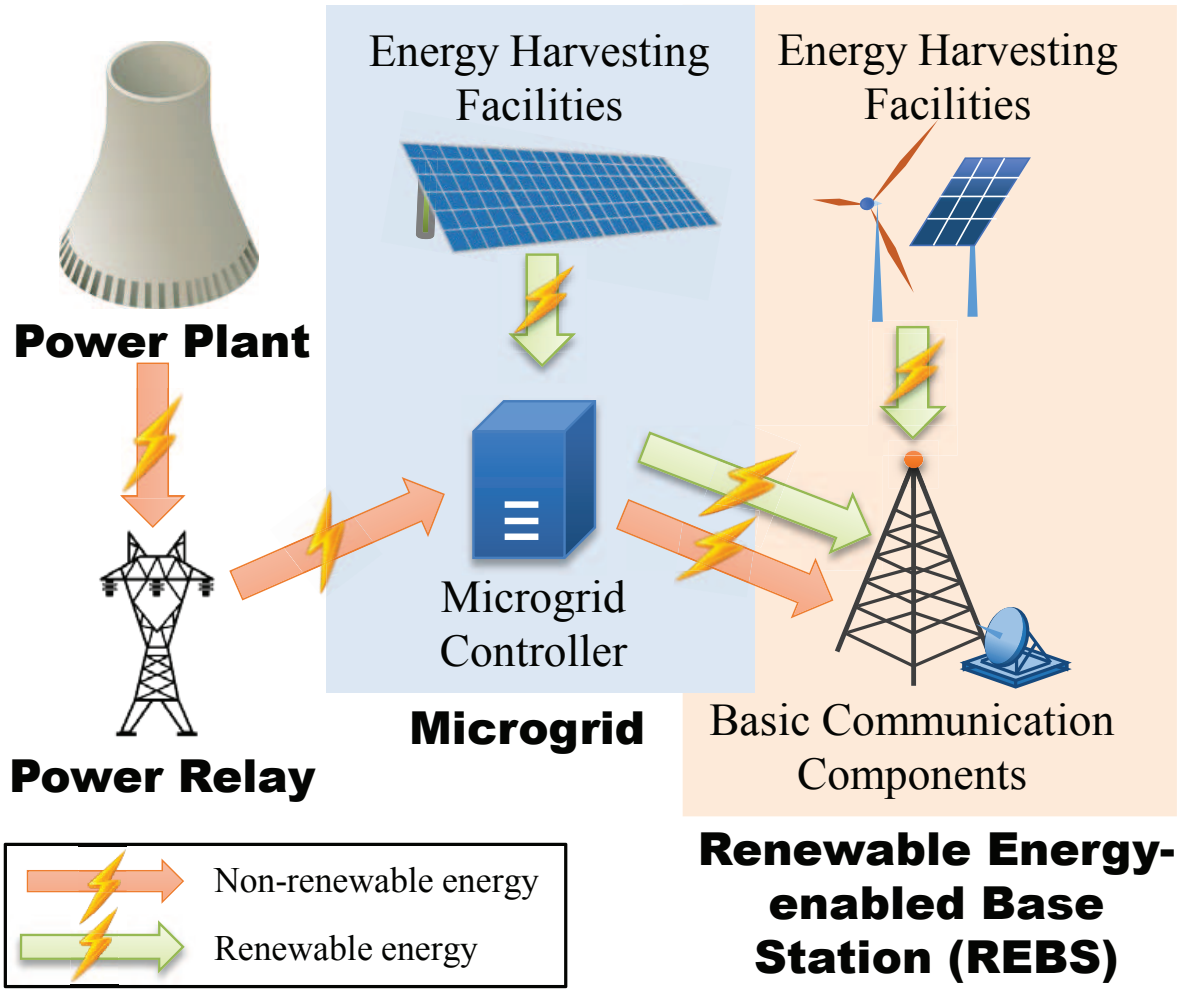

Figure 1.2: New power supply for cellular network with energy harvesting facilities and Microgrids.

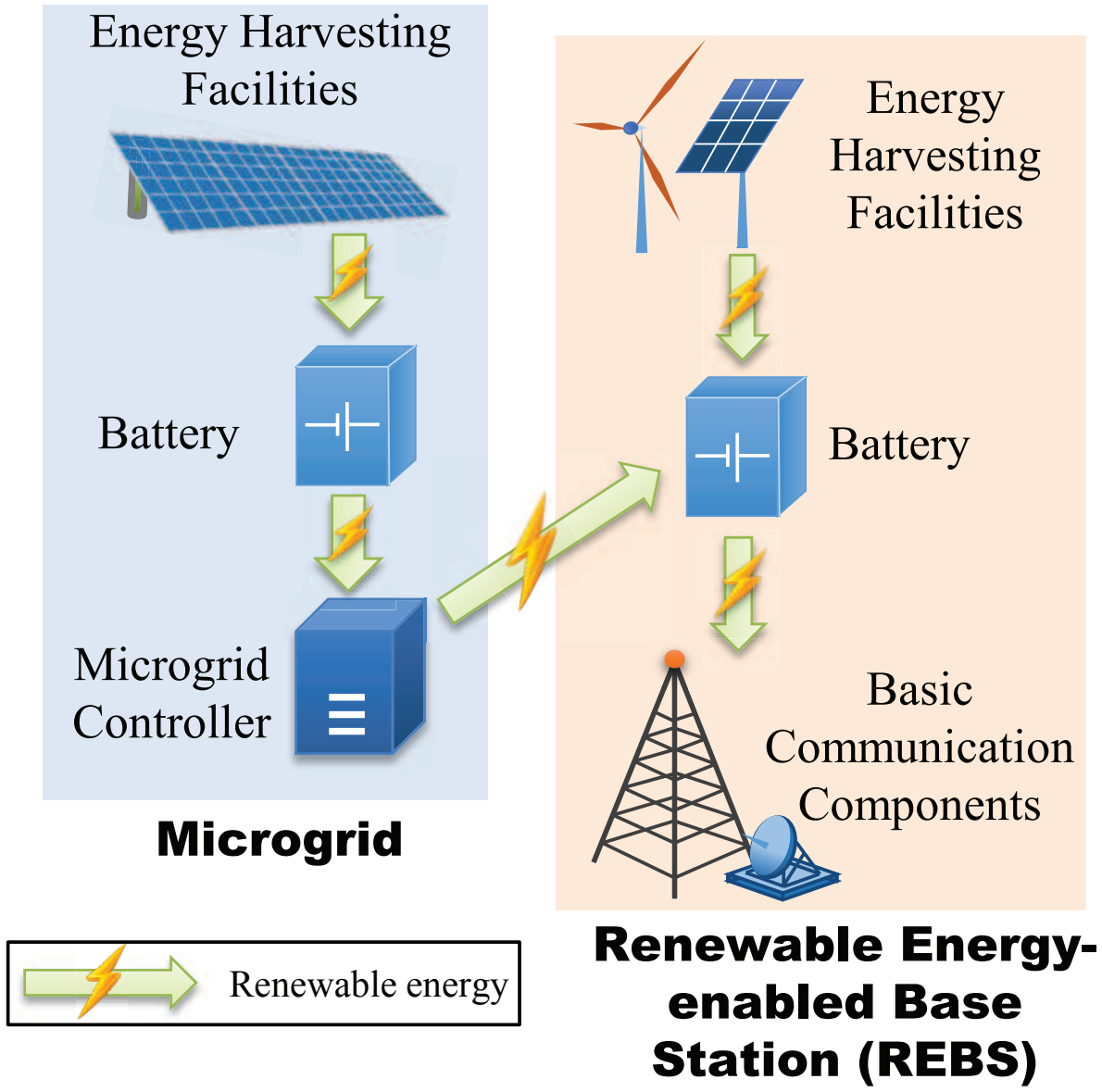

Figure 1.3: The power supply for REBS in disaster.

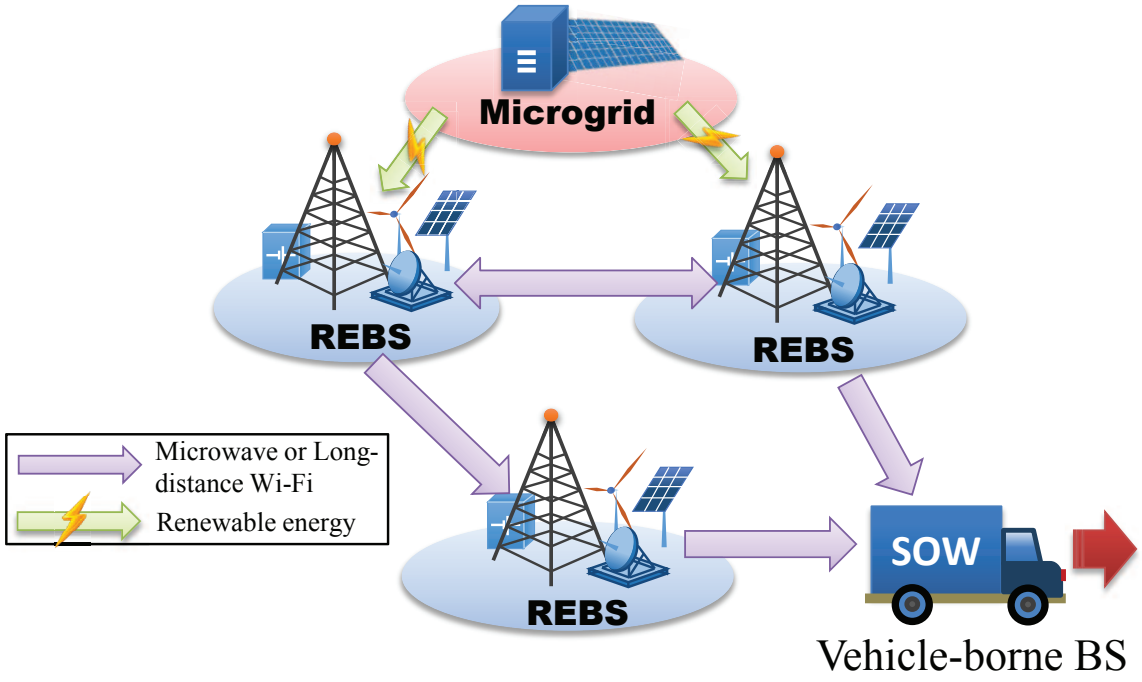

Figure 1.4: The traffic transmission for REBS in disaster.

It has one or multiple network gateway, which can provide network access to the outside Internet. The REBSs are interconnected by microwave plate or long-distance Wi-Fi. The data of the users inside the area is firstly collected by the local REBS, and such data will be transferred to the gateway hop-by-hop (Fig. 1.4). The network gateways are in charge of collecting the data traffic demands and transferring to the outside area. In the post-disaster case, the gateway should be easy-deployed and can accommodate network services in a rapid manner. Therefore, the vehicle-borne cellular is a relative reasonable choice, such as Movable and Deployable Resource Unit (MDRU) [1], or Cell On Wheel (COW).

A large number of research efforts have been devoted motivated by the above advantages of REBS - based mesh network. The utmost concern for such kind of network structure is the shortage of energy and network bandwidth. For the energy resources, because of the destruction of the disaster, the REBSs of the network are solely relying on the renewable energy. However, the input renewable energy may not always meet the operating demands. For example, the solar panel cannot harvest energy at night hence

input energy for REBS will be zero then. On the other hand, for the communication resources, the network connection may also be affected by the disaster. Although the vehicle-borne BSs (i.e., Switch On Wheel, SOW) resolve the concern of providing the network gateway in the emergency case, the destruction to the original network connections calls for a consideration toward the scarce network bandwidth. Furthermore, the rebuild effort for the affected area may last several days or even weeks. Therefore, an algorithm need to be proposed so as to effectively utilize the limited energy and communication resources. Additionally, the algorithm should deal with the finite time horizon and fulfill the data transmission demand as much as possible, because the applications such as Voice Over Internet Protocol (VOIP) or Short Message Service (SMS) will increase sharply after disaster, and then network throughput will be the major concern.

1.2 Challenging Issues with REBS-based Mesh Networks

In the last section, we discuss various features of the REBS-based mesh networks. Although the above-mentioned network components and structures satisfy the preconditions of accommodating network services in the post-disaster case, there are still several challenging issues yet to be solved. In order to design the scheme for the algorithm in post-disaster scenario, the following issues should be addressed accordingly.

Firstly, the energy inputs of the REBSs and Microgrids are instable and unbalanced. This is due to the different weather conditions and deployment places, respectively. As a result, for a certain energy harvesting facility, the input energy changes with time, and different energy harvesting facilities may have different energy inputs at the same time. Therefore, the algorithm will consider the spatial and temporal diversities of the renewable energy input.

Secondly, the data traffic demands of the users inside the affected area are also changing

with time and different from place to place. For example, the population densities for different REBS coverage areas are not the same, and for a certain REBS, the activities of the people inside the area are changing as time elapsed. Hence such features of the data traffic demand should also be considered.

Thirdly, as mentioned in the last section, the data traffic for a certain REBS will be relayed by the neighbor REBSs, and finally transferred to the network gateway in a hop-by-hop manner, therefore it is a multi-hop transmission. Moreover, there could be more than one transmission path for the data traffic demands of REBS, because the data traffic can be delivered to the network gateway by different neighbor REBSs.

Last but not least, the algorithm should aim at serving the data traffic demand as much as possible, and such provision should cover the finite time horizon and be energy-efficient. The reasons are threefold. The first reason is the sharp increase of data traffic demands after disaster. Therefore, the amount of data traffic transmission becomes the major concern. Secondly, because the REBSs operate solely on the renewable energy, the algorithm should address energy efficiency. For the rebuilt effort, it cannot be done at once, and the long-term optimization should be taken into consideration as well.

1.3 Research Objectives

The provision of network services is one important requirement for the post-disaster scenario. Because an efficient scheme can not only help the emergency relief by delivering the usable information to rescuers, but also satisfy the requirement for communication of the people in the affected place. The energy for the network is insufficient, and the REBSs in the disaster area cannot operate when the renewable energy is not enough. Therefore, the operation period of the REBSs in the network is limited. At the same time, the REBS will neither serve the users nor relay the data traffic demand of the other REBSs' if it is switched off. Therefore, the usage and transmission of the energy of REBSs and

Microgrids, and the transmission of the traffic among the REBSs should be considered jointly.

In this dissertation, we mainly focus on the occasions for the operating status of the REBSs (i.e., switch on, switch off), and the associating data traffic transmission policies for each REBSs. We will propose the optimization frameworks and algorithms for achieving different objectives. In addition, we validate our new proposals via theoretical analyses. Moreover, we will compare our proposals with other existing methodologies in terms of total system throughput and energy efficiency.

At first, we would like to propose a joint energy and traffic throughput-maximization algorithm for the REBS-based mesh network in the post-disaster scenario. The proposed scheme will determine the the energy distribution policy of the Microgrid, the time for switching on the REBSs, the number of collected data traffic demands for REBSs, and the data transmission policies including the local collected data traffic demands as well as the relayed ones.

Secondly, we will extend the previous model, and address the energy efficiency issue. Besides achieving maximized system throughput, the new model considers the total weighted renewable energy consumption of the REBSs as well. The result will have a less weighted energy consumption than the other strategies that have the maximal system throughput.

It is noticed that the previous proposed schemes are designed only for the idealized off-line case in which the energy and traffic estimation profiles are just the real ones. However, the solution for such assumption may not work when the data traffic demand is not estimated precisely. Therefore, we assume the traffic profile is inexact, and then we propose a dynamically adjusting scheme, in order to deal with the imprecise traffic estimation. Such scheme will be executed in each time slot to revise the old strategy. Compared with the off-line scheme, the on-line scheme can achieve higher performances even without precise traffic estimation profile.

1.4 Thesis Outline

The remainder of this thesis is outlined as follows:

Chapter 2 Overview of REBS-based Mesh Network and Its Associating Settings in Disaster Area. We introduce the REBS-based mesh networks in this chapter. At first, we analyze the factors cause energy alternation, as well as the way of traffic transmission inside this network. Then we analyze the reasons of the spatial and temporal diversities of the energy and traffic profiles. In addition, we analyze the availabilities of the traffic and energy profile estimation. After that, we retrospect the recently representative literatures. At last, we use an example to demonstrate the importance of the joint optimization of the energy and traffic.

Chapter 3: The Off-line Scheduling and Load Distribution for REBS Mesh Networks. In this chapter, an algorithm is proposed for maximizing the total system throughput for the considered scenario demonstrated in Chapter 2. Firstly, we model the operating behaviors of REBS, and the associating energy distribution between Microgrid and traffic transmission among REBSs, respectively. Secondly, we demonstrate the related work and discuss the problems that we would like to consider. Thirdly, we formulate the throughput-maximization problem for the joint optimization of energy and traffic. Fourthly, we demonstrate that the problem is a Mixed Integer Linear Programming (MILP). At the end of the chapter, we demonstrate that the optimized scheme has better performance than the existed methodology.

Chapter 4: The Off-line Energy Efficient Scheduling and Load Distribution for REBS Mesh Networks. In this chapter, we extend our consideration. Based on the maximized throughput, we proposed an energy efficient scheme. The energy efficiency is defined as the ratio of the consumed energy to the harvested energy. We define the energy efficiency as the optimization objective in the model, and the maximized throughput is regarded as the constraint. Because the harvested energy is the constant value (i.e., the profile of energy input is known), therefore such added constraints will not affect the

MILP feature of the considered problem. After that, we propose a two-stage algorithm in which the weighted energy consumption as well as the total system throughput are addressed. At last, we validate the energy efficiencies of the considered algorithms via numerical simulations.

Chapter 5. On the On-line Energy-Efficient of Throughput-Based Scheme for REBS Mesh Networks. In this chapter, we extend the previous research. The proposed models in Chapter 3 and 4 consider the energy and traffic profiles in a certain time span, which can be regarded as the expectations for such profiles. In previous consideration, we assume the expectations are always the real ones (i.e., the variance is zero). However, the result for such off-line assumption may not get the best result when facing the imprecise profile estimation. Therefore, an on-line dynamically adjusting scheme is proposed in this chapter. Firstly, we prove the performance bound of the off-line scheme in the previous chapter, and then an on-line energy-efficient of throughput-based scheme for REBS-based networks is introduced. This scheme is based on the result of the off-line scheme, and in each execution time, the on-line scheme will adjust the old plan based on the current-available information. The adjustment will not affect the future optimization strategy of the old plan, therefore it will have a better performance than the off-line one. We demonstrate that the proposed on-line scheme outperforms than the off-line one and naive scheme in term of the system throughput.

The summaries of thesis and the related discussions of the future works are demonstrated in the last chapter.

1.5 Contributions

In this dissertation, we studies the joint optimization of traffic and energy management in wireless mesh networks powered by renewable energy. The main contributions of the dissertation are summarized as follows:

1. We combine the energy and traffic management, and formulate a joint-optimization framework. After that, we propose a throughput-maximization algorithm in order to assist the distribution of the traffic and energy consumption of the REBSs in the network. In addition, we check the optimality of the proposal with regard to the total system throughput.

2. On the basis of our first throughput-maximization proposal, we develop an energy-efficient algorithm in order to reduce the energy consumption. Therefore, the new scheme has better sustainability in contrast with our first proposal. At last, we demonstrate that our proposal has better energy efficiency compare with the previous proposal as well as the naive idea.

3. We propose an on-line dynamically adjusting scheme handling the imprecise estimation traffic profile. We prove the performance bound of the off-line scheme, which is determined by the precision of the traffic estimation. Then an on-line scheme is proposed, which will adjust the old strategy without affecting the future plan. We finally conduct various simulations in order to justify the efficiency of our on-line proposal in relation to total system throughput and energy efficiency.

Chapter 2

Overview of REBS-based Mesh Networks and Its Associating Settings in Disaster Area

2.1 Introduction to the REBS-based Mesh Networks

In the disaster situation, both of the energy and network resources are limited. Therefore the distribution of the energy and traffic becomes our major concern. This chapter begins with the introduction of the network components, and we categorize such components by demonstrating the energy flows and traffic flows.

2.1.1 Energy Flows inside REBS

As we discussed in the last chapter, after disaster, it is assumed that the REBSs in the disaster area will solely rely on the renewable energy. The input energy for each REBS can be divided into two categories. The first one is from the connected Microgrids, which is the green energy harvested by the energy harvesting facilities of the Microgrids'. The

second one is from the REBS's local energy harvesting facilities. In the residual part of this dissertation, these two kinds of energies will be denoted by remote energy input and local energy input, respectively. Both of these two kinds of energy inputs will be then directed to the battery of the REBS.

The Battery of the REBS is used to store the input energy, and such kind of energy might be used at once, or stored in the battery for future use. For the energy usage of each REBS, there are mainly two factors. The first factor is the static energy consumption, which is the certain amount of energy consumed so long as the REBS is activated. Such static energy consumption is induced by air conditioning consumption, the AC/DC converter waste, and so on. The exact energy consumption depends on the scale of the base station: the larger the size, the more the energy consumption it will cause. For example, the static energy consumption of the macro base station is 712W per hour (from the EARTH project in [2]), while for the LTE micro base station with one sector and one power amplifier, the hourly cost will be about 120W [3]. The other factor is the dynamic energy consumption. which is proportional to the number of activated subcarriers. Each subcarrier will cause a fixed amount of energy consumption, and will carry a certain amount of data traffic demands from the users'. Therefore on one hand, the number of activated subcarrier determines the upper bound of the collected uplink traffic, and on the other hand, it is also proportional to the dynamic consumed energy. Besides these two factors, there are also other energy consumptions, such as the energy used by the point-to-point data traffic transmission between two REBSs. However, such kind of energy usage is not significant, for instance, the point-to-point data traffic transmission is about 50W, which is far less than the static consumption 712.2W of the macro base station. Therefore, in the rest of this dissertation, such kind of consumption is neglected. The details of the energy flows inside an REBS is as the left part of Figure 2.1 shows. It is noted that the energy consumption only happens when the REBS is active (i.e., is switched on), otherwise, there will be no energy output.

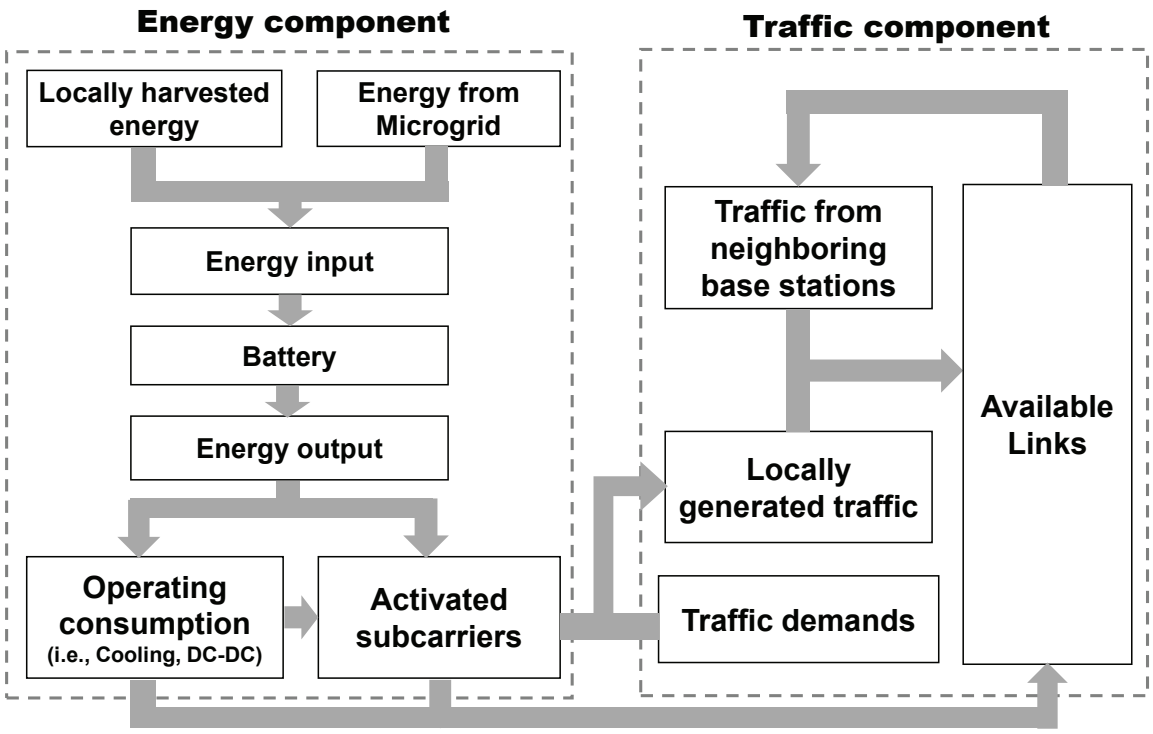

Figure 2.1: The energy and the traffic flows in the considered REBS-based mesh networks. ©2014 IEEE.

2.1.2 Traffic Flows in Network

As mentioned in the last chapter, the damages caused by the disaster will make the original network infrastructure (such as the connections to the MTSO, PSTN or others) unavailable. Therefore the REBS-based mesh network becomes our major concern. Because of the mesh feature, for each REBS, it has to not only deal with the local data traffic demand, but also help the neighbors' traffic reach the network gateway.

For a certain REBS, we denote the local data traffic demand as the one generated by the users in its coverage area. However, due to the limitation of the energy budget and bandwidth, such demands might not be fulfilled all the time. When the REBS is switched on, it can serve the local data traffic demand, and the amount of served data is limited by the number of activated subcarriers. We denote the amount of such to-be-served local

data traffic demand as local data traffic input. On the other hand, the REBS may receive the data traffic demand from activated neighbor REBSs, and that is the remote data traffic input.

Each REBS needs to deal with both of the local and remote data traffic input. There are two possible exits for the traffic: the first exit is the connected active REBSs, the connected active REBSs can act as a relay to transfer the traffic. If the REBS has a direct connection to the gateway, then it can directly send the traffic to the gateway. It is noted that the amount of the transferred traffic of each point-to-point link should be less than the bandwidth. For example, the Microwave panel such as MDR-8000 can afford about 300Mbps, while the typical bandwidth of the current long-distance WiFi such as NanoBridge can provide 80Mbps [4]. The traffic flows in the network is as the right part of Figure 2.1 shows.

According to the experimental result in [1], the state-of-the-art vehicle-borne cellular gateway has sufficient capabilities to transfer the traffics inside the network to the outside, therefore we assume that all the traffic sent to the network gateway can be dealt by the network gateways.

2.2 Spatial and Temporal Diversities of the Traffic and Energy

Due to the zero-grid energy input feature of the post-disaster case, the green energy generated from the energy harvesting facility is the only energy source. However, the energy input of such facility are not constant as the elapse of time. For example, the input energy of solar panel depends on the illumination intensity, and it is not hard to derive that the energy input at night would be zero, since there is no available sunlight in the evening. Similarly, the wind power also changes with time, therefore the wind turbine cannot have a stable energy input. For the REBSs in different places, the energy input

are not the same as well. Therefore the energy input of REBSs are different from time to time and from place to place.

On the other hand, the REBSs in the network also experience the spatial and temporal diversities of the data traffic demands. People inside the post-disaster area are likely to assemble in big shelters such as the stadium or auditorium. According to [5], one can estimate the data traffic demand by summarizing the details of the population in the coverage area as well as the ratio of active users. For each REBSs, the number of active users inside the coverage area causes the spatial diversity of the data traffic demand, while the changes of people's behaviors give the evidence in support for the temporal diversity of the data traffic demand.

2.3 Related Work

For the importance of the the considered structures and the associating schemes, a large number of research efforts have been devoted.

In [6] [7] [8], it is shown that in the post-disaster case, the Microgrid could play an important role in the energy distribution. Before disaster, the Microgrid is the energy distributer: it is used for handing off the energy received from power plant, to the connected BSs. When the disaster cause the disconnection of power plant to Microgrid, the Microgrid will then act in "Island Mode", which means the Microgrid will be apart from power grid, and it will use the solar panel or wind turbine to harvest the energy from ambient environment, such energy can be either stored in the local battery or sent to the connected REBSs. In [9], the control strategies of the Microgrid are studied, and in [10] [11] the energy management strategies are explored in order to reduce the non-renewable energy consumption from power grid with considering battery capacities, energy losses and so on. By inducing the Microgrid, it is demonstrated in [12] that the energy consumption cost can be significantly reduced by designing the schedule over a finite time

horizon. The similar Microgrid-assisted energy-efficient researches can be found in [13] [14] [15] [16] [17] and [18].

Besides the research on the assistance of the Microgrids in the post-disaster case, several studies are conducted so as to better utilize the energy of the REBSs. [3] [5] [19] deal with the non-renewable powered cellular systems. As the extensions, [20] [21] [22] [23] consider the hybrid energy input for the base stations, which includes the renewable energy from energy harvesting facilities, as well as the non-renewable energy from power plant.

Because the energy is sufficient in the above cases, these references are mainly address the issue of reducing the non-renewable energy consumption (or cost). The first aspect is to reduce the non-renewable energy consumption while fulfilling the users' requests. For the importance of the REBSs in reducing the OPEX, the second aspect is to reduce the associating costs for the non-renewable energy consumption. It is noted that these two kinds of objective are both for the energy efficiencies of the networks. [5] [3] [24] [25] and [26] investigate the energy consumptions of the base stations in the cellular network. The different energy-efficiency strategies for various scenarios are reviewed in [27].

As the only energy supply in the post-disaster case, the input renewable energy are analyzed in several literatures. According to the conclusion of [28] [29] [30] [31] and [32], one can get the expectation of the energy input profile by combining the information of the history input profile, the energy harvesting facilities (i.e., the size of solar panel, the type of wind turbine), the climate of the local area (i.e., the sunlight intensity and wind power). In [33] [34] [35] [36] [37] and [38], switching off the REBSs in the off-peak time of data traffic demand is demonstrated to be an efficient solution for saving the energy. When the base station is deactivated, the associating energy consumption would be zero, and the energy input would be zero at that time.

As another important aspect in the post-disaster case, in [39] and [40], the large-scale dataset of data traffic in cellular networks is studied. In [41], it is exhibited the high

fluctuation of data traffic demand of cellular network in both of time and space.

The flow control and load distribution schemes without considering the consumed energy are extensively studied. For example, for the transmission paths, [42] put the efforts on the trade off between the multiple one-hop paths and multiple hops in cellular networks. For the last-hop to the network gateway, [43] studies the load-balancing schemes for the gateway side, the proposed method can transfer some of the connections to the congested gateways, to the other light traffic gateways. However, in the post-disaster case, the bottleneck of the network performance caused by the limited energy has to be considered. Although the above-mentioned works cannot be directly employed, they shed lights on the latter studies on the joint optimization. Because of the diversities in spatial and temporal for both of the energy and traffic, the joint optimization scheme should be considered in the post-disaster case. Based on the assumptions, the existing studies for such studies can be categorized into three aspects. The first aspect is the optimization for a snapshot of the traffic and energy status. For example, in [44], the combination of routing, rate control as well as energy allocation are taken into consideration. In [45], the spectrum and energy efficiencies are addressed, the k-shortest path are employed to transfer the data traffic. Although both of the energy and traffic are covered in the solutions, the battery issues are not included, which may result in suboptimal result in the long run, in the condition of that energy or/and traffic profile are varying as the time elapse. [46] considers the spatial diversity of the traffic and energy consumption for Poisson-Voronoi tessellation (PVT) cellular networks, and explores the proposed energy-efficiency model. The second kind of studies assumes that the link capacities between two connected neighbor REBSs are always ample. For example, in [47], the energy input is supposed to follow G/G/1 process while the data input follows Poisson process respectively, and the way of transmitting the collected data traffic to the destinations is not in the scope of the consideration. Similarly, [48] considers various fairness routing strategies for the energy harvesting network with limited battery capacity, on the other hand, the routing are only supposed to be unsplittable routing or routing tree. In [49], the cooperations between the

neighboring REBSs in terms of spectrum and energy are explored, while the study is not based on the disaster case therefore the way of transmitting the data traffic is beyond the scope of this study. The study of [50] aims at extending the batteries' lives by carefully controlling the charging and discharging time. Thirdly, several works are conducted under the assumption that the energy is enough for sensor or BSs. In [51], a throughput maximization scheme is proposed, which can improve the network throughput and reduce the energy consumption.

It is noted that almost all of the above-mentioned solutions are solely relying on the local renewable energy supplies, and at our best knowledge, we are the pioneers that employing the remote energy input from the Microgrid in the REBS-based mesh networks, with considering the temporal-spatial diversities of energy input as well as the data traffic demands [52] [53].

2.4 Our Research Target

The target of this dissertation is to design the optimization frameworks, which aims at supporting the users' data traffic transmission demands as many as possible, and it also gives the best effort to reduce the energy consumption.

To realize such goal, the battery plays a crucial role, because the limited energy input should be used in the best time. Therefore, for the REBSs, the occasion for switching on or off, and the number of activated subcarriers when is switching on should be the controlled variables in order to save the current available energy for the future use. As a result, the topology of the REBS-based mesh network changes periodically because of the on and off status of the REBSs. It is noted that the operating status may not only affect the local supported data traffic, but also have the impact on the neighbors'. For example, as Figure 2.2 shows, in a certain time, REBS a wants to transfer its local supported data traffic. Because a does not have direct connection to the gateway, therefore, it has

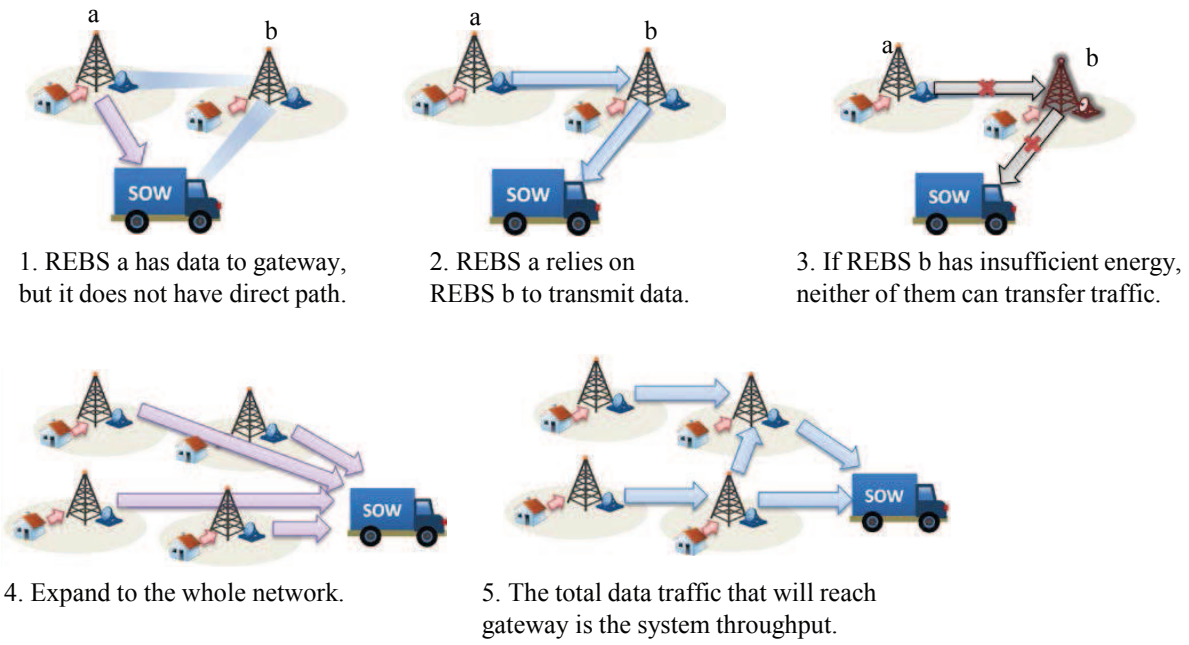

Figure 2.2: The cooperation of the data traffic transmission among the REBSs.

to rely on REBS b to relay the data. However, if b is switched off, then REBS a cannot transfer its data, because there is no available path to the gateway. For a certain time, the activated REBSs will carry the collected data traffic demand to the network gateway, and the collected data traffic demands is based on the temporally and spatially varying data traffic demands. The amount of collected traffic and the traffic delivering strategy are also the controlled variables. By combining the traffic and energy scheduling strategies, the scheme for improving the amount of supported data traffic demands of the users' within a certain time span can be derived. In the previous example, if we expand the single time slot condition to the whole network, then it will be the simplest case of our considered problem, and the total data traffic that reaches the network gateway is the total system throughput, which will be one of our goals in the thesis. In addition, in this thesis, we will also deal with the energy efficiencies, as well as the imprecise of the traffic profile.

2.5 The Advantage of Joint Optimization

As we mentioned, this dissertation will consider the joint optimization of the energy and traffic for the considered scenario. In order to address the necessity of the joint optimization, an example is introduced in this section. In the example, the Naive idea is used as the control algorithm: the major policy behind the Naive idea is to switch on the REBS so long it has enough energy.

The considered topology contains 7 REBSs and 1 network gateway. For simplicity, each REBS has 3.0 units of data traffic demand. The operating consumption equals 3.3 unit, and REBS 1, 2, 3, 4, 6 have initial energy of 6.6 unit while REBS 5 and 7 have 5.0 unit energy, in other words, these two categories of REBSs can operate for 2 and 1 time slot, respectively. The wireless connections and the capacity of each link are shown in Fig. 2.3. We consider the optimization for two time units, and the total system throughput is the sum of the system throughput within the considered time span. The topology and associating strategies of the two schemes are shown in Figure 2.3.

It can be seen that the energy and traffic strategies of the Naive scheme are not jointly considered (i.e., to get the maximum system throughput in current time, not the long-term optimization), and in the first time unit, all the REBSs can operate because of the sufficient energy, and the system throughput is 21.0 unit. In the second time, REBS 5 and 7 cannot be switched on due to lack of energy, and the system throughput is 8.0 then. The total system throughput is 29.0.

The strategy when considering the joint optimization is somehow different: REBS 5 is turned off in the first time unit even though it has enough energy, and the system throughput is 17.0, which is less than the one of Naive scheme. However, in the second time unit, REBS 5 has enough energy to operate, and is switched on. The system throughput is 17.0 then and the total system throughput is 34.0.

It can be seen that with the joint optimization scheme, the performance can be im-

proved.

2.6 Summary

In this chapter, we introduce the features of the REBS-based mesh network in disaster condition. Firstly, the rough graphs of the energy evolution and traffic transmission are demonstrated. After that, in the post-disaster scenario, the energy and traffic are various, and such varieties embody in space and time. We clarify the reasons that cause the diversities. In addition, the literature review is given by categories. Aiming at the drawbacks of the existed studies, we set the research goals in this dissertation, and the importance of joint optimization is addressed via an example.

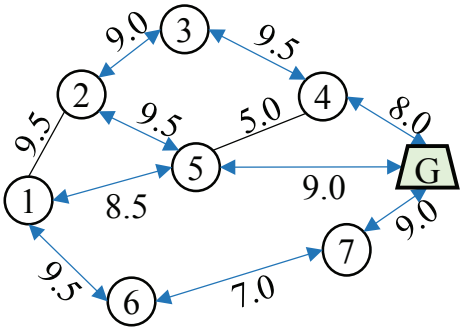

1. Network topology

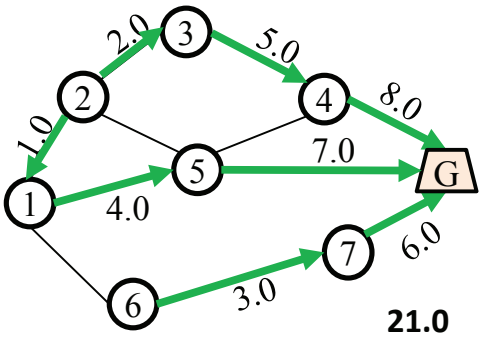

2. The system throughput in the first time unit is 21.0

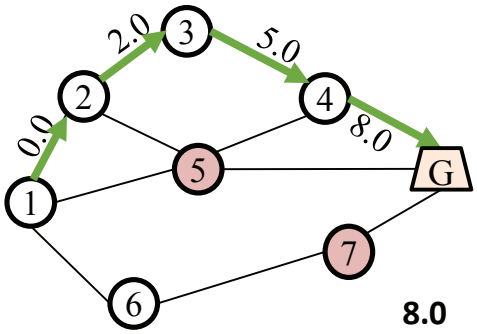

3. The system throughput in the second time unit is 8.0

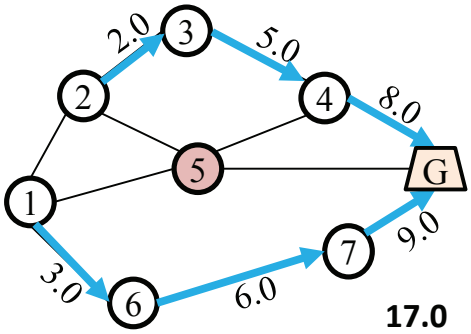

4. The system throughput in the first time unit is 17.0

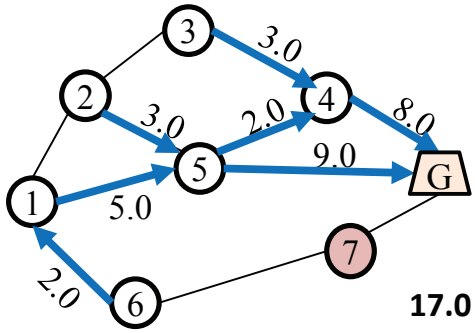

5. The system throughput in the second time unit is 17.0

Figure 2.3: The system topology of the example, and the associating solutions of the Naive scheme and joint-optimization scheme, respectively.

Chapter 3

The Off-line Scheduling and Load Distribution for REBS Mesh Networks

3.1 Introduction

In recent decades, the disasters happened all over the world demonstrate the importance of post-disaster treatment for the disaster area. The REBS-based mesh network is regarded as an effective solution for accommodating network services for such scenario, and we will subject the study to this network. However, as mentioned in the example in last chapter, the energy allocation strategy should be designed with the traffic distribution strategy in order to achieve good performance. In this chapter, we focus on maximizing the total system throughput, in other words, the users' data traffic demands are tried to be satisfied as mush as possible. To this end, we first investigate the characteristics in the post-disaster case. After that, we formulate the problem and propose the optimization framework. At the end of this chapter, we demonstrate the computer-based simulations. From the results, it can be seen that the proposed throughput optimization framework

can provide much higher total system throughput than the Naive idea.

The contributions of this chapter are summarized as follows:

- We analyze the scenario for the post-disaster case, and then give the reasonable assumptions for such scenario.
- We formulate the problem of maximizing the total system throughput with the assumption that the full-knowledge of the energy input profile as well as the traffic demand profile are available.
- Based on the formulated problem, we demonstrate its MILP-problem feature, and then an optimization framework is established for achieving the maximized total system throughput.
- We numerically demonstrate that the joint-optimization framework will yield performance improvement compared with the Naive solution in term of the total system throughput under various conditions.

3.2 Preliminaries

3.2.1 The Way of Energy Cooperation

As mentioned in previous chapter, the mission of the Microgrid in island mode is to deliver its local harvested energy to the connected REBSs. Therefore, the input energy for each REBS is the combination of the local energy harvesting facility, as well as the remote Microgrid. Due to such infrastructure limitations, the local energy input of REBS can only be used locally.

3.2.2 The Energy and Traffic Input Profiles

In order to design a long-term strategy, the knowledge of the energy input as well as the traffic demand of each REBS during this period is needed.

As analyzed in Chapter 2, the diversities of the energy input embody in time and space dimension. Therefore, for a certain REBS, the energy input changes with time. According to the analyses in [29][30][31], the energy input prediction can be derived by summarizing the information of weather condition (i.e., the wind strength is proportional to the energy input of wind turbine) and the historical energy provisions (i.e., the energy input changes periodically). Since the hourly energy input prediction can be achieved relative precisely with the modern techniques, we assume energy harvesting profiles of REBSs and Microgrids are the available information in the dissertation. It is noted that such technique is often used with the collaborative control with Wireless Sensor and Actuator Networks (WSANs) [54], in order to improve the harvesting efficiencies.

On the other hand, in the post-disaster area, the damages to the residential places will force the people to be gathered in the temporary shelters, such as the gymnasium and parks covered by the REBSs. Although in the causal case, it is relative hard to predict the data traffic demand due to the unpredictable people's activities, the data traffic demand after the disaster is much more simple, because the people inside the shelters will not move frequently. As a result, based on the previous researches such as [5], the data traffic demands can be estimated more precisely by the combination of the population, the ratio of active users as time elapse, the trend of the data traffic demand, and the previous profiles.

3.3 System Model

In this section, the system model is presented. As Fig. 1.3 and Fig. 1.4 shows, the energy flows and traffic flows are simultaneously existed in the considered network structure. Therefore, in the following subsections, we will respectively describe these two kinds of models. In addition, as the junction of the energy and traffic, the model that representing the network topology will be shown at first.

3.3.1 Network Model

The network topology can be denoted as an undirected graph $G = (\mathcal{N}, \mathcal{C})$, where $\mathcal{N}$ and $\mathcal{C}$ denote the set of REBSs in the disaster area and the connected links between two neighbor REBSs, respectively. Let n_i denote the ith REBS and therefore $\mathcal{N}$ equals $\{n_1, n_2, \ldots, n_N\}$, and N is the cardinal number of $\mathcal{N}$. For the two neighbor REBSs n_j and n_k, if there is a wired or wireless connection (n_j, n_k), then $(n_j, n_k) \in \mathcal{C}$, and the weight of (n_j, n_k), $c_{n_j}^{n_k}$, denotes its capacity.

When the input energy is sufficient, all the REBSs can be switched on and the aforementioned G can be used to denote the network topology during the considered time. However, in the post-disaster case, the REBSs may not be switched on all the time, since the energy input is not enough. When the REBS is inactive, the associated connections cannot be utilized, therefore the network topology will change with time due to the on-off status of the REBSs. Let $c_{(n_j,n_k)}(t_i)$ and $\rho_{n_j}(t_i)$ be the link capacity of (n_j, n_k) and the operating status of n_j in t_i, respectively, then $c_{(n_j,n_k)}(t_i)$ can be defined according to the following equations:

$$0 \leq c_{(n_j,n_k)}(t_i) \leq c_{n_j}^{n_k} \cdot \rho_{n_j}(t_i), \tag{3.1}$$

$$0 \leq c_{(n_j,n_k)}(t_i) \leq c_{n_j}^{n_k} \cdot \rho_{n_k}(t_i), \tag{3.2}$$

where $\rho_{n_j}(t_i)$ is a boolean variable and it can be given by

$$\rho_{n_j}(t_i) = \begin{cases} 1 & \text{if } n_j \text{ is active in } t_i, \\ 0 & \text{otherwise.} \end{cases} \tag{3.3}$$

From Eq.3.1 and 3.2, it can be seen that the operating status of a certain REBS determines the availabilities of the links: the link can be used if and only if the REBSs at the both ends are switched on.

We consider multiple network gateways in the scenario. We denote $\mathcal{G} = \{g_1, g_2, \ldots, g_F\}$ as the set of gateways. The cardinal number of $\mathcal{G}$ is F, and $\mathcal{G} \subset \mathcal{N}$. For the Microgrids, let $\mathcal{M}(\mathcal{M} = \{m_1, m_2, \ldots, m_M\})$ be the set of Microgrids, and $|\mathcal{M}| = M$. After disaster, several connections between Microgrids and REBSs are still available, we denote the set of the associating REBSs of m_k by $M^{(m_k)} = \{n_1^{m_k}, n_2^{m_k}, \ldots\}(n_i^{m_k} \in \mathcal{N})$. For some REBSs, because of the destruction to the connections, it will not have any energy input from Microgrids, therefore the union of $M^{(m_k)}$ $(m_k \in \mathcal{M})$ may not be equal to $\mathcal{N}$ for all instances.

3.3.2 Energy Related Model

As mentioned in Fig.2.1, the input energy of each REBS generally falls into two categories: the one is the local input energy from its own energy harvesting facilities, and the other one is the energy from Microgrid.

For the local energy input, it can only be used in the local place, this is due to the single energy transmission direction of the link between Microgrid and the REBSs. Let $l_{n_j}(t_i)$ be the local energy input of n_j in t_i. For a certain REBS, if it has the connection to the Microgrids, then the remote energy input is available. Suppose for Microgrid m_k, the amount of green energy it can receive in time t_i is $h^{m_k}(t_i)$, and the amount of energy that is sent to n_j is $h_{n_j}^{m_k}(t_i)$. It is noted that $h_{n_j}^{m_k}(t_i)$ also depends on the existence of the connection, and $h_{n_j}^{m_k}(t_i)$ is equal to 0 if there is no connection. The relationship between

$h_{n_j}^{m_k}(t_i)$ and $h^{m_k}(t_i)$ is given by the following equation:

$$0 \leq \sum_{n_j \in \mathcal{M}^{(m_k)}} h_{n_j}^{m_k}(t_i) \leq h^{m_k}(t_i) + B_{m_k}(t_i), \tag{3.4}$$

where $B_{m_k}(t_i)$ denotes the left energy of Microgrid m_k at the beginning of time t_i, the related formulation of the batteries will be demonstrated later. Eq.3.4 defines the constraint that the total amount of transferred energy in t_i should be less than the total available green energy of m_k.

Therefore, the total energy input of the REBS n_j in t_i can be defined according to the following equations:

$$H_{n_j}(t_i) = l_{n_j}(t_i) + \sum_{m_k \in \mathcal{M}} h_{n_j}^{m_k}(t_i). \tag{3.5}$$

It is noted that not all the REBSs have the remote energy input, this is because the damages of the disaster may cause the disconnection of the energy transmission links between the certain REBSs and Microgrids. Hence these REBSs will only have the local energy input.

So far the energy input of the REBSs is defined. The energy consumption aspect will be defined in the residual part of this section. After disaster, the REBSs will solely depend on the green energy to accommodate the network services. The total energy consumption of n_j in t_i is denoted by $P_{n_j}(t_i)$. As described in Fig. 2.1, $P_{n_j}(t_i)$ is the sum of the operating energy consumption and the subcarrier energy consumption. The subcarrier energy consumption is proportional to the number of active subcarriers [5], and let $s_{n_j}(t_i)$ ($s_{n_j}(t_i) \in \mathbb{Z}^+$) denote the number of active subcarriers of n_j in t_i, and we use e_s to represent the amount of consumed energy per active subcarrier. Moreover, we use e_0 to represent the static operating energy consumption. Therefore, for REBS n_j, the

energy consumption in t_i can be calculated by the following equations:

$$P_{n_j}(t_i) = [(s_{n_j}(t_i) \cdot e_s) + e_0] \cdot \rho_{n_j}(t_i), \tag{3.6}$$

From Eq.3.6, it can be seen that $P_{n_j}(t_i)$ is not zero only if $\rho_{n_j}(t_i)$ is 1. When $\rho_{n_j}(t_i) = 1$, the subcarrier can be activated, and the maximal number of active subcarriers is limited by S. Such relationship can be defined by the following equations:

$$0 \leq s_{n_j}(t_i) \leq S, \tag{3.7}$$

and

$$s_{n_j}(t_i) \leq S \cdot \rho_{n_j}(t_i). \tag{3.8}$$

It is noted that in the energy consumption model, the data transmission energy consumption is not taken into consideration, since such amount is not significant compared with these two major factors based on our analysis in Chapter 2.

The battery with finite capacity is equipped for each REBS and Microgrid, so as to stock the local or remote green energy input. The battery is with finite capacity, and let $B_{n_j}(t_i)$ denote the volume of residual energy in the battery of n_j at the beginning of t_i. Therefore, the energy evolution of the battery can be denoted as follows:

$$B_{n_j}(t_{i+1}) = B_{n_j}(t_i) + H_{n_j}(t_i) - P_{n_j}(t_i). \tag{3.9}$$

From Eq.3.9, the residual energy volume of a certain battery is determined by the original energy level $B_{n_j}(t_i)$, the total energy input $H_{n_j}(t_i)$, as well as the energy consumption during the current time $P_{n_j}(t_i)$. Moreover, the energy level of REBS n_j in t_i should be limited by its battery capacity $B^0_{n_j}$. Therefore, $B_{n_j}(t_i)$ can be denoted as the following constraint:

$$0 \leq B_{n_j}(t_i) \leq B^0_{n_j}. \tag{3.10}$$

As shown in Fig.1.3, the battery of the Microgrid also plays a crucial role in the disaster. The evolution of the battery of the Microgrid is similar to the REBS's. Denote $B^0_{m_k}$ as the battery capacity of the Microgrid, then the battery level of m_k in t_i should firstly satisfy the capacity constraint:

$$0 \leq B_{m_k}(t_i) \leq B^0_{m_k}, \tag{3.11}$$

Different from REBS, there will be no remote energy input for the Microgrids. For m_k, the energy output will be the energy transmitted to the connected REBSs. Then the energy evolution of m_k in t_i should then satisfy the evolution constraint:

$$B_{m_k}(t_{i+1}) = B_{m_k}(t_i) + h^{m_k}(t_i) - \sum_{n_j \in \mathcal{M}^{(m_k)}} h^{m_k}_{n_j}(t_i), \tag{3.12}$$

where $h^{m_k}(t_i)$ is the energy input of m_k in t_i, and $\sum_{n_j \in \mathcal{M}^{(m_k)}} h^{m_k}_{n_j}(t_i)$ represents the amount of energy that transmitted to the connected REBSs. The $B_{m_k}(t_i)$ is the residual energy level of m_k at the beginning of t_i.

3.3.3 Traffic Related Model

As demonstrated in 2.1, there might be two kinds of traffic inputs for a certain REBS. The first one is the locally generated traffic, and the second one is the traffic from neighboring REBSs.

The locally generated traffic is the traffic collected from the users in the coverage area of the REBS, and we use the data traffic demand to denote the such traffic. Denote $d_{n_j}(t_i)$ as the amount data traffic demand of n_j in t_i. In the post-disaster case, the input energy is insufficient, which will cause that the data traffic demand can be only partially satisfied. Let $f_{n_j}(t_i)$ be the real supported data traffic demand of n_j in t_i, therefore the

actual supported data traffic demand is limited by the data traffic demand:

$$0 \leq f_{n_j}(t_i) \leq d_{n_j}(t_i). \tag{3.13}$$

In t_i, the data traffic demand can be satisfied if and only if n_j is active. In other words, $f_{n_j}(t_i)$ is larger than 0 only if $\rho_{n_j}(t_i)$ is 1. On the other hand, the number of active subcarrier is also proportional to the actual supported traffic demand $f_{n_j}(t_i)$:

$$f_{n_j}(t_i) \leq \rho_{n_j}(t_i) \cdot s_{n_j}(t_i) \cdot r_0, \tag{3.14}$$

where $s_{n_j}(t_i)$ is the number of active subcarrier in t_i, and r_0 is the rate can be provided by an active subcarrier. It can be seen from Eq. 3.1, 3.2, 3.6 and 3.14 that there are the junctions between the energy and traffic scheduling strategy: when the REBSs as well as associating subcarriers are active, there might be more energy that will be consumed, but at the same time, the more traffic can be collected and transmitted.

Besides the local data traffic demand, the REBSs in the network also assume the responsibilities for relaying the neighbors' to the network gateways. The traffic sent from neighbors is denoted as the remote data traffic demands. We will present the traffic transmission from the point of view of flow: let $f_{n_l}^{(n_j,n_k)}(t_i)$ be the amount of actual supported data traffic demand of REBS n_l, and sent from n_j to n_k in t_i. Moreover, denote $f^{(n_j,n_k)}(t_i)$ as the total traffic that sent from n_j to n_k in t_i, then $f^{(n_j,n_k)}(t_i)$ and $f_{n_l}^{(n_j,n_k)}(t_i)$ have the following relationship:

$$f^{(n_j,n_k)}(t_i) = \sum_{n_l \in \mathcal{N}} f_{n_l}^{(n_j,n_k)}(t_i) \leq c_{(n_j,n_k)}(t_i). \tag{3.15}$$

It is noted that in Eq. 3.15, n_l and n_j can be the same REBS. Because the REBS n_j has

to deal with the local actual supported traffic demand $f_{n_j}(t_i)$, therefore

$$f_{n_j}(t_i) = \sum_{u \in \mathcal{N} \setminus \{n_j\}} f_{n_j}^{(n_j,u)}(t_i), \forall n_j \in \mathcal{N}. \tag{3.16}$$

The non-gateway REBSs are acting as relays when transferring the neighbors' traffic. As a result, for the non-gateway REBS n_j, it aims at sending the local traffic demand as well as the remote traffic demand to the network gateways. Therefore, the REBSs should follow the constraints below:

$$f_{n_j}^{(u,v)}(t_i) = -f_{n_j}^{(v,u)}(t_i), \forall u, v, n_j \in \mathcal{N}, \tag{3.17}$$

$$\sum_{v \in \mathcal{N}} f_{n_j}^{(u,v)}(t_i) = 0, \forall u \in \mathcal{N} \setminus (\{n_j\} \cup \mathcal{G}), n_j \in \mathcal{N}, \tag{3.18}$$

where the sign in Eq.3.17 represents the direction of the flow. The zero in Eq. 3.18 denotes that as the relay, n_j need to send all the relayed traffic.

We use an example to particularize the aforementioned models. Fig. 3.1 demonstrate the snapshot of network structure and the Microgrid connections of the example, and the time label is ignored. As shown in this figure, there are 5 REBSs, in which g_1 is the network gateway. In this figure, n_2 is inactive, and it can neither collect the local data traffic demand (i.e., Eq. 3.14) nor transfer the local and remote traffic input (i.e., Eq. 3.1, 3.2). On the other hand, n_4 connects to g_1, n_1 and n_3 and n_4 is active, therefore n_4 can collect and send the traffic. Because all the neighbors of n_4 are active, the amount of traffic sent to each REBS can be denoted as $f^{(n_4,n_1)}$, $f^{(n_4,n_3)}$ and $f^{(n_4,g_1)}$, respectively, and the sum of them is equal to f_{n_4} according to Eq. 3.16 and 3.18. In addition, the links in Fig. 3.1 are bi-directional hence the REBSs at the both side of the link can mutually transfer the data to each other.

In the energy layer, there are 2 Microgrids, hence $|M| = 2$. Since there is no connection

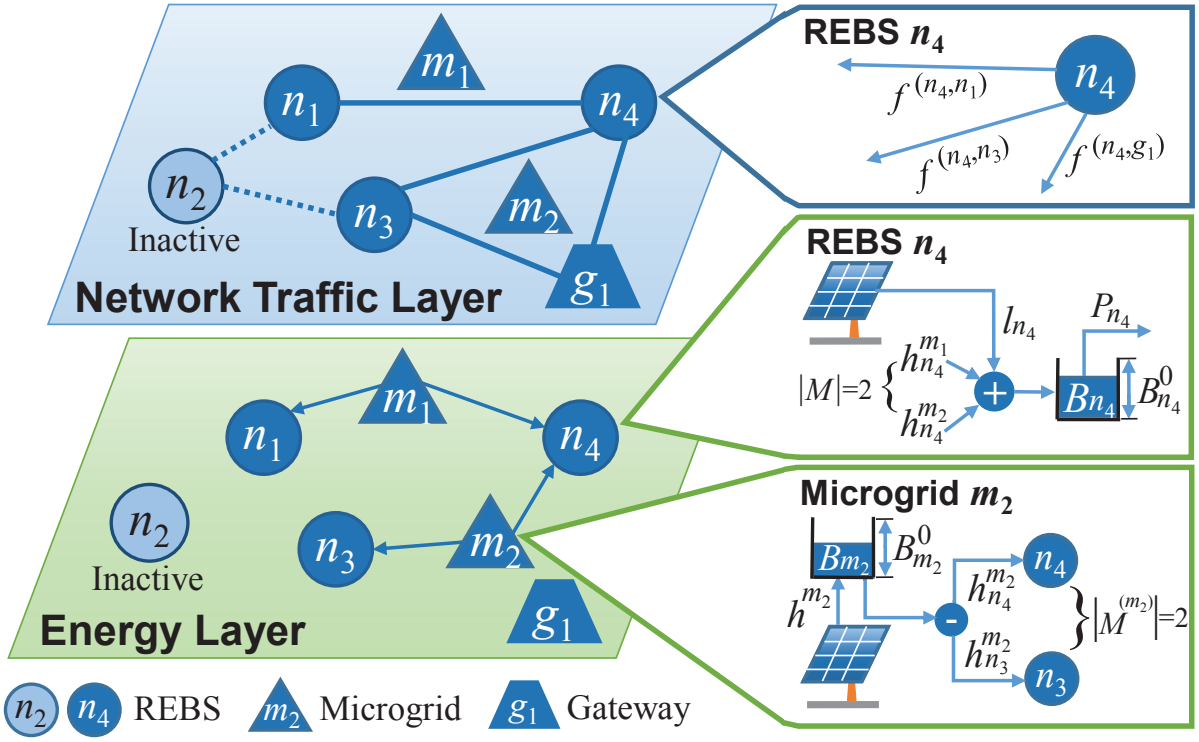

Figure 3.1: Traffic flow between REBSs, and energy flow inside REBSs and Microgrids. ©2015 IEEE.

to the Microgrids, n_2 does not have remote energy input. On the other hand, n_4 and n_1 have connection to Microgrid m_1 therefore they can receive the energy from m_1. In addition, n_4 can also get the remote energy from m_2, and according to Eq. 3.5, the amount of received remote energy is $h_{n_4}^{m_1} + h_{n_4}^{m_2}$, while the local energy input is l_{n_4}, and the total energy input of n_4 is $H_{n_4} = h_{n_4}^{m_1} + h_{n_4}^{m_2} + l_{n_4}$. The energy input will first reach the place of the battery as Fig. 1.3 shows, and then be used to activate the REBS and associating subcarriers (i.e., Eq.3.9 and Eq.3.6). From the viewpoint of the Microgrid, it will harvest the green energy and deliver to the connected REBSs. Take m_2 for the example, it will receive the h^{m_2} unit of local energy input, and send $h_{n_4}^{m_2}$ and $h_{n_3}^{m_2}$ to REBS n_4 and n_3, respectively. Note that the energy will also be sent to the battery of m_2 at first.

3.4 Research Objective

Let $[0, T_0)$ denote the considering time span, in which T_0 is used to denote the time that the network will be reconstructed. The time-slotted system is used in our consideration, which means that interval $[0, T_0)$ will be divided into equal samples. If T is the number of time slots, and the length of each sample is denoted by t_0, then $[0, T_0)$ can be denoted as the set $\mathcal{T} = \{t_1, t_2, ..., t_T\}$, where t_i $(0 \leq i \leq T)$ is the index of time slot i. We assume that the energy input and data traffic demand of each REBS and Microgrid will not change within each time sample.

The optimization objective in this chapter is to maximize the total system throughput. The total system throughput is the sum of system throughput in the considering time span:

$$U = \sum_{t_i \in \mathcal{T}} U(t_i), \tag{3.19}$$

where U and $U(t_i)$ denote the total system throughput and system throughput in t_i, respectively.

The system throughput in t_i, $U(t_i)$, is the sum of the data traffic sent to the network gateways:

$$U(t_i) = \sum_{g_k \in \mathcal{G}} \sum_{n_j \in \mathcal{N}} f^{(n_j, g_k)}(t_i). \tag{3.20}$$

According to Eq. 3.16, Eq. 3.17 and Eq. 3.18, the amount of data traffic which is sent to the network gateway is equal to the sum of the actual supported traffic demand of the REBSs. Therefore, the system throughput in t_i can be given by the following equation:

$$U(t_i) = \sum_{n_j \in \mathcal{N}} f_{n_j}(t_i), \tag{3.21}$$

and

$$U = \sum_{t_i \in \mathcal{T}} \sum_{n_j \in \mathcal{N}} f_{n_j}(t_i). \tag{3.22}$$

Our objective in this chapter is to maximize the total system throughput for the considered time span:

$$\text{P1: } \mathbf{max}\ U = \mathbf{max} \sum_{t_i \in \mathcal{T}} \sum_{n_j \in \mathcal{N}} f_{n_j}(t_i). \tag{3.23}$$

According the equations from Eq. 3.1 to Eq. 3.22, the variables that will affect the result of U are fourfold: the operating status of the REBS in each time slot (i.e., $\rho_{n_j}(t_i)$), the amount of energy distribution of each Microgrid in each time slot (i.e., $h_{n_j}^{m_k}(t_i)$), the amount of flow sent to each neighbor for each REBS in each time slot (i.e., $f_{n_l}^{(n_j,n_k)}(t_i)$), and the number of active subcarriers of each REBS in each time slot (i.e., $s_{n_j}(t_i)$). We use a quadruple $\mathcal{U}(\vec{\rho}, \vec{h}, \vec{f}, \vec{s})$ to represent the designed strategy, where $\vec{\rho}$, $\vec{h}$, $\vec{f}$ and $\vec{s}$ denote the strategy of the above-mentioned operating status, energy distribution, flow distribution, and number of active subcarrier, respectively.

3.5 Problem Formulation

3.5.1 The Equivalent Transformation of Constraints

Based on the aforementioned analysis, the maximized total system throughput can be calculated by a decent choice of the quadruple $\mathcal{U}$.

Eq. 3.6 can be transferred as the following equations:

$$P_{n_j}(t_i) = s_{n_j}(t_i) \cdot e_s \cdot \rho_{n_j}(t_i) + e_0 \cdot \rho_{n_j}(t_i), \tag{3.24}$$

and it can be seen that such constraint includes the non-linear variable combinations (Eq.3.14 is non-linear as well), therefore the optimization problem defined in Eq.3.23 is non-linear. However, the problem has special structure, and the non-linear constraint can

be transformed by the following procedures. Let us introduce a new extra variable $\delta_{n_j}(t_i)$, which is equal to:

$$\delta_{n_j}(t_i) = e_s \cdot \rho_{n_j}(t_i). \tag{3.25}$$

Moreover, we have the following relationship:

$$\delta_{n_j}(t_i) = e_s \cdot \rho_{n_j}(t_i) \leq S \cdot (\rho_{n_j}(t_i))^2 = S \cdot \rho_{n_j}(t_i). \tag{3.26}$$

Therefore Eq.3.23 and Eq.3.14 can be given as follows:

$$P_{n_j}(t_i) = s_{n_j}(t_i) \cdot \delta_{n_j}(t_i) + e_0 \cdot \rho_{n_j}(t_i), \tag{3.27}$$

and

$$f_{n_j}(t_i) \leq \delta_{n_j}(t_i) \cdot r_0. \tag{3.28}$$

It can be seen that the objective funtion in Eq.3.23 (P1) is the linear combination of $\mathcal{U}$. On the other hand, the equations that contain $\vec{s}$ and $\vec{\rho}$ are the linear combinations of integer variables, since $\rho_{n_j}(t_i)$ can only be 1 or 0, and the number of active subcarriers can only be the integers from 0 to S. Moreover, the residual equalities and inequalities from Eq.3.1 to Eq. 3.18 are linear. Therefore the problem with the combination of linear and integer constraint of the variable can be described as the MILP problem.

The MILP problem can be efficiently attacked by many of existing approaches such as branch and bound or cutting plane, In Algorithm 1, we demonstrate the algorithm of the branch and bound, and the detail steps of the procedure of branch and bound is in the appendix of [53].

Algorithm 1: Off-line Total System Throughput Maximization Scheme

Input: Network topology information: $\mathcal{N}, \mathcal{G}, \mathcal{M}, \mathcal{C}$.
Energy related information: e_s, e_0, $h_{n_j}^{m_k}(t_i)$, $h^{m_k}(t_i)$, $l_{n_k}(t_i)$.
Traffic related information: $d_{n_j}(t_i)$ r_0.
Output: $(\vec{\rho}, \vec{h}, \vec{f}, \vec{s})$ for problem P1.

Relax the integer constraints of $\vec{\rho}$ and $\vec{s}$ into linear ones, then the problem P1 is transformed into P1';
Solve the linear programming problem P1';
Let $\overline{O}$ record the result and $\boldsymbol{u}' = (\vec{\rho}', \vec{h}', \vec{f}', \vec{s}')$ is the associated variables;
if $\boldsymbol{u}'$ *satisfies integer constraints of P1* **then**
    $\underline{O}^* = \overline{O}$;
else
    $\underline{O} = 0$;
    $Cons$ = the constraints of P1;
    Choose one relaxed constraint x that does not follow the constraints of P1. Let χ denote the value of x;
    $(\underline{O}^*, \overline{O})$= BranchBound($Cons$, x, χ, P1, $\underline{O}$, $\overline{O}$);

3.5.2 Discussion on the Computation Cost

Although the previous proposed algorithm can provide an effective solution to the considered optimization framework, it is worthy to discuss the efficiency of the algorithm since the MILP problem is NP-hard in general, and the time complexity is not polynomial unless NP is equal to P.

The computation cost mainly depends on the scale of the integer variables since they dominate the computation cost. In the residual part, we will discuss the availability of the algorithm in threefold. Firstly, to relax the integer constraint of the active subcarrier can greatly reduce the complexity, since half of the integer variables will be transferred to the linear ones. On the other hand, the impact to the performance is bounded, since the provided rate of each subcarrier is not large (i.e., 0.5Mbps) compared with the large number of subcarriers (i.e., 600), and the performance gap between the original result and relaxed one is bounded by $r_0 \cdot T \cdot N$.

Secondly, the number of REBSs in the disaster area is not the large. In general, the

radius of the coverage area of a macro BS is more than 5km (i.e., maximum of 20km in [55]), which means that for a certain range of disaster area, the actual number of macro base station is relative small.

Thirdly, the time span that optimization plan will deal with is much more larger than the computation time cost. In other word, the timeliness may not be the key concern for the problem so long as it can figure out the result within the acceptable time period. As mentioned in Chapter 1, the reconstruction might be finished for several days or even weeks, therefore we assume that a one-time execution is affordable.

Also, it is noted that for the length of each time slot, a smaller slot length may lead to a better system performance. The reason is, as the granularity of the time partition becomes finer, the adjustment toward the strategy for the REBSs will be more timely. However, on the other hand, the sampling frequencies of the energy and traffic in each time slot will rise accordingly. Because it is not possible to get the two profiles in arbitrary small granularity, and the performance improvement gained by the smaller granularity is limited. In addition, the computational complexity will be increased, since the scale of variables becomes larger. In this dissertation, the length of the time slot is set to be 1 hour, which is as in [5] and [29].

3.6 Performance Evaluation

In this section, the total system throughput of the proposed optimization framework is compared with the one of the Naive scheme through a computer-based simulations.

3.6.1 Settings of the Simulation

The parameters of the simulation are listed in table 3.1, and the parameters are set according to the previous analyses and the commercial products. As table 3.1 shows, we

Table 3.1: Experimental Parameters ©2014 IEEE.

Parameter	Value
The length of the time slot ($\|t_i\|$)	1 hour
The number of considered time slots (T)	10
Number of REBSs (N)	10
Number of Microgrids (M)	3
Bandwidth of the Backhaul link ($c_{n_j}^{n_k}$)	80Mbps to 300Mbps
Operating power consumption (e_0)	712.2W
Power consumption per each subcarrier (e_s)	1.06W
Number of subcarriers (S)	600
Battery capacity of REBS ($B_{n_j}^0$)	2000W
Battery capacity of Microgrid ($B_{m_k}^0$)	2000W
Amount of energy of REBS at t_1 ($B_{n_j}(t_1)$)	2000W
Amount of energy of Microgrid at t_1 ($B_{m_k}(t_1)$)	2000W
Rate of subcarriers (r_0)	0.5Mbps

assume that the length of each time slot t_i is 1 hour, and the number of considered time slot is 10 (i.e., $T = 10$), which means the optimization will cover a 10-hour period. There are 10 REBSs and 3 Microgrids in the network (i.e., $N = 10$ and $M = 3$). The REBSs will be interconnected with each other by microwave or long-distance Wifi. The bandwidth of the links that connects two neighbor REBSs are randomly chosen from 80Mbps to 300Mbps. Because we consider the macro base stations, the operating energy consumption is $712.2W$ (i.e., $e_0 = 712.2W$), the energy consumption of each active subcarrier is 1.06W (i.e., $e_s = 1.06$), and the upper bound of the active subcarrier is 600 (i.e., $S = 600$) according to the settings in [3]. In addition, the battery capacity is 2000W therefore $B_{n_j}^0 = 2000W$.

The considered topology is shown in Fig.3.2. The network backhaul is made up by bi-directional links and we use straight line to denote them. Microgrid a, b and c have 2, 3 and 1 associating REBS(s) respectively. In the experiment, we mainly investigate the performance of the total system throughput.

The Naive idea used in this section is same as the idea in section 2.5. The idea behind the Naive one is to activate the REBS so long as it has enough energy. Such energy

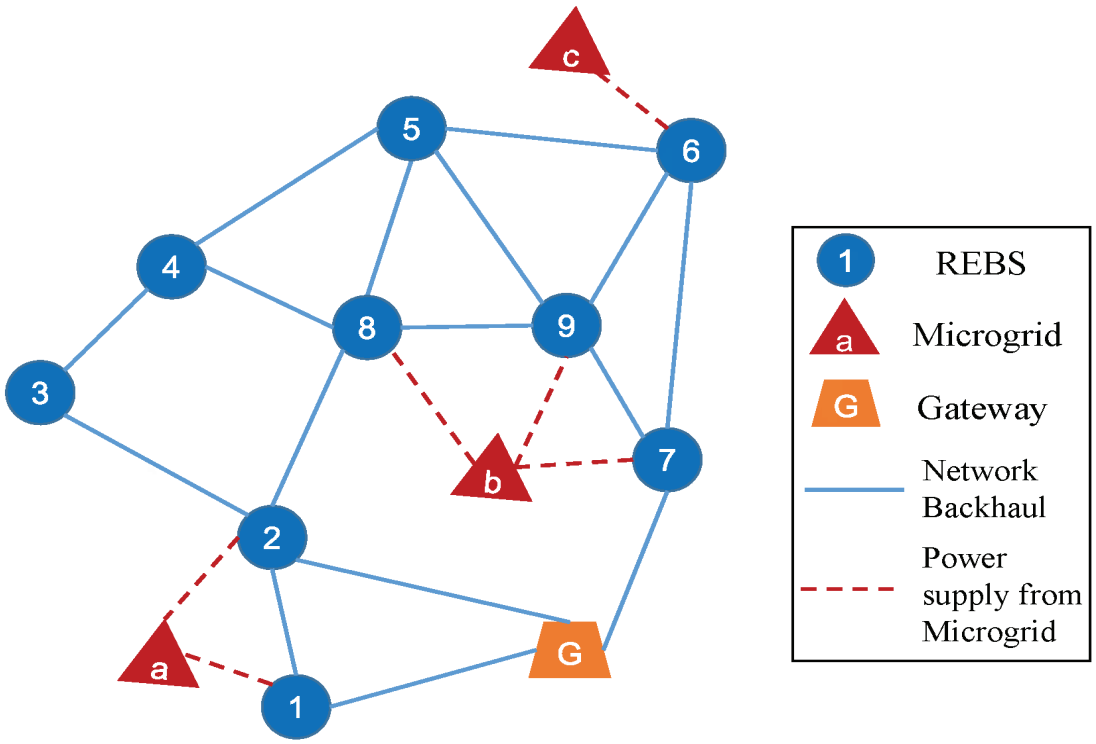

Figure 3.2: System topology used in the part of performance evaluation. ©2014 IEEE.

utilization strategy can be used in the non-disaster scenario. For the local data traffic demands, the Naive idea encourages the REBS support as much traffic as possible. If the traffic collection energy consumption (i.e., in Eq.3.14) can be fulfilled by the energy in the REBS's battery, then the associating amount of energy will be reduced in the battery. Otherwise the REBS will send the energy transmission request to the connecting Microgrid, after receiving all the energy transmission requests from the connecting REBSs, the Microgrid will firstly sort the requests in ascending order by the amount of energy required, and then such requests will be addressed orderly, until the energy inside the battery of Microgrid is insufficient for satisfying any of the residual REBS's demand. After Microgrid determines the transferred energy, we have the energy consumption strategies of REBSs. Finally, the max-flow algorithm is used to figure out the traffic distribution strategies of the REBSs.

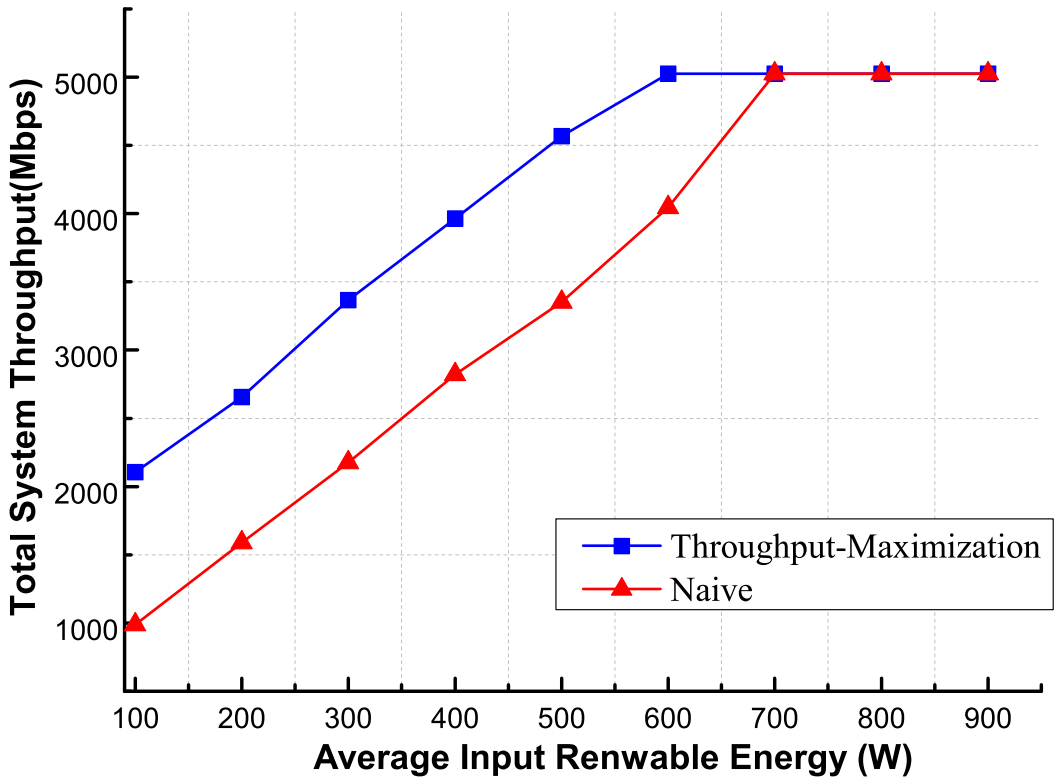

Figure 3.3: The effect of average input renewable energy on system throughput of the proposed scheme and naive scheme. ©2014 IEEE.

3.6.2 Impact of the Energy Input on Total System Throughput

At first, we analyze the relationship between the average input renewable energy of the REBSs and Microgrids, and the total system throughput. Therefore, we set the input renewable energy as the variables. The renewable energy input in each time slot (i.e., $l_{n_j}(t_i)$ and $h^{m_k}(t_i)$) is selected from the interval $[0.5 \cdot \text{x-axis value}, 1.5 \cdot \text{x-axis value}]$, and is i.i.d. At the same time, the data traffic demand of each REBS in each time slot is randomly and uniformly selected from $[40\text{Mbps}, 100\text{Mbps}]$ (i.e., $f_{n_j}(t_i) \in [40\text{Mbps}, 100\text{Mbps}]$). Other constant variables are set as the table 3.1 shows.

Fig. 3.3 demonstrates the relationship between the average input renewable energy of REBSs and Microgrids, and the total system throughput (i.e., U). As we can see from Fig. 3.3, there is a positive correlation between U and the renewable energy input. The reason is, as the green energy input increases, the longer active time and more subcarriers can be supported of each REBS. As a result, much more traffic will be transferred to the network gateway and U will be larger. In addition, it can be seen that the proposed joint energy and traffic throughput-maximization scheme has a better performance than the Naive scheme. The reason is, the Naive idea puts effort on the traffic issue, and ignores saving the energy for future use. Although the Naive idea can achieve the maximal system throughput in the first time slot, the energy may not be used optimally, therefore the performance may be unsatisfied in the upcoming time slots. It is worthwhile to note that, both of these schemes have an upper bound of the total system throughput (i.e., about 5000Mbps in this simulation). When the renewable energy input is sufficient, the only bottleneck of the network is the bandwidth, and the total system throughput is equal to the product of T and the network capacity for the traffic. In Fig. 3.3, when the green energy input is larger than 600W, the joint energy and traffic scheme reaches its upper bound while for the Naive idea, such upper bound cannot be reached until the energy input is larger than 700W.

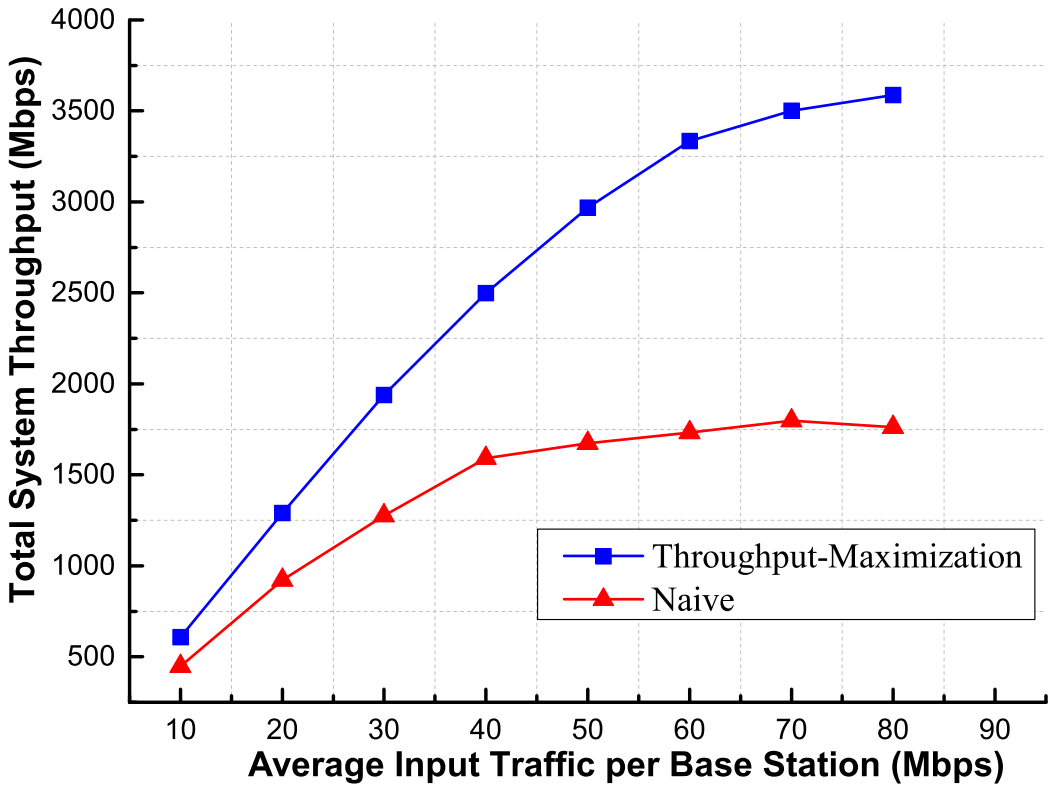

Figure 3.4: The effect of average input traffic per base station on total system throughput of the proposed scheme and naive scheme. ©2014 IEEE.

3.6.3 Impact of the Traffic Input on Total System Throughput

Secondly, we study the effect of the data traffic demand (traffic input) on the total system throughput. In this part, the data traffic demands of the REBSs (i.e., $f_{n_j}(t_i)$) are the variables, and the x-axis value denotes the expectation of such demands. The value of $f_{n_j}(t_i)$ is uniformly and randomly chosen from $[0.5 \cdot \text{x-axis value}, 1.5 \cdot \text{x-axis value}]$. The green energy inputs for REBSs and Microgrids are selected from $[100\text{W}, 300\text{W}]$ and are i.i.d.

Fig. 5.6 illustrate such relationship. From Fig. 5.6, it can be known that there is a clear performance gap between the proposed joint energy and traffic scheme, and the Naive idea. Along with the increase of the traffic input, the total system throughput will rise up accordingly, the result can be summarized as follows. As the input traffic becomes larger, the active REBSs can support more data traffic demand only with the cost of activating more subcarriers, the consumption of which is much more lower than activating more REBSs (i.e., $e_s = 1.06\text{W}$ while $e_0 = 712.2\text{W}$). When the traffic input is low, the total system throughput will be low as well, therefore the gap is not that large. As the traffic input becomes larger, the impact of the strategy on the performance is more obvious, therefore the gap becomes larger. Compared with the energy requirement (i.e., $e_0 = 712.2\text{W}$), the energy input is not enough (i.e., $l_{n_j}(t_i) \leq 300\text{W}$), therefore when the energy input is insufficient, the joint energy and traffic scheme may have a clear performance advantage when the data traffic input is high, which might be just the case in post-disaster scenario.

3.7 Summary

In this chapter, the throughput-maximization scheme is proposed. Firstly, we analyze the conditions in the post-disaster case, including the assumptions on the network structures, as well as the input profiles of energy and traffic. Secondly, we described the considered

scenario in a formalized manner, and then the network model, the energy related model and the traffic related model are demonstrated respectively. After that, the research objective is demonstrated using the aforementioned variables. In the fourth part, we prove that the considered problem is an MILP problem after the transformation of the constraints. The availability of the considered framework is analyzed in the next part. Finally, the numerical result is demonstrated.

Chapter 4

The Off-line Energy Efficient Scheduling and Load Distribution for REBS Mesh Networks

4.1 Introduction

Because the renewable energy is the only energy resource in the post-disaster area, the energy should be used in the best case. In addition, as mentioned in previous chapter, the considered time span is the estimated time duration for rehabilitating the network services in the daily manner. However, the reconstruction effort may not be controlled perfectly therefore the real time cost can be longer than the expectation. In that case, the designed scheme should use the energy efficiently. In this chapter, our proposal is twofold: the first is to maximize the total system throughput, and the second is to deal with the energy efficiency. We first define the energy efficiency, and then transform our goal into selecting the most energy efficient result from the strategies that with the maximal total system throughput. After that, we propose a two-stage optimization framework to achieve the Pareto-optimal result. Finally, we check our proposals via computer-based simulations. The numerical results demonstrate that besides achieving the maximal total

system throughput, the proposed two-stage optimization framework can provide higher energy efficiencies.

The major contributions of this chapter are summarized as follows:

- We analyze the potential drawbacks of the throughput maximization problem, and then propose a new objective considering the energy efficiency aspect.
- We demonstrate that the problem with the energy-efficiency objective is also the MILP problem.
- We propose a two-stage energy efficient throughput-maximization framework, and the proposed throughput-maximization scheme has better energy efficiency than the other strategies which also have the maximal total system throughput.
- We conduct the computer-based simulations, and show that the proposed two-stage optimization scheme achieves higher energy efficiency than the Naive idea and the original throughput maximization scheme.

4.2 System Model and Optimization Objective

In this section, we formulate the problem and describe the objective of this chapter. After that, the optimization objective is analyzed.

4.2.1 System Model

The considered scenarios and related variables are the same in Chapter 3, and we list them in Table 4.1 for convenience. As we mentioned, for the problem P1 in Eq. 3.23, there can be more than one solution. In this chapter, we consider the energy harvesting abilities of the REBSs and Microgrids are the available information. During $\mathcal{T}$, the total harvested energy of REBS n_j can be given by the following equation:

$$\sum_{t_i \in \mathcal{T}} l_{n_j}(t_i), \tag{4.1}$$

Table 4.1: Variable Summarization

Variable	Meaning
t_i	Index of time slot i.
T	Number of time slots.
$\mathcal{T} = \{t_1, t_2, ..., t_T\}$	Time span using time sample.
n_j	Index of REBS j.
N	Number of REBSs.
$\mathcal{N} = \{n_1, n_2, ..., n_N\}$	Set of REBSs.
(n_j, n_k)	Connection between n_j and n_k.
C	Number of links.
$\mathcal{C} = \{(n_{j_1}, n_{k_1}), ..., (n_{j_C}, n_{k_C})\}$	Set of the links.
$c_{n_j}^{n_k}$	Capacity of (n_j, n_k).
$G = (\mathcal{N}, \mathcal{C})$	Network topology.
$\rho_{n_j}(t_i)$	Operating status of n_j in t_i.
$c_(n_j, n_k)$	Link capacity of (n_j, n_k) in t_i.
F	Number of gateways.
g_f	Index of gateway f.
$\mathcal{G} = \{g_1, g_2, ..., g_F\}$	Set of gateways.
m_k	Index of Microgrid k.
M	Number of Microgrids.
$\mathcal{M} = \{m_1, m_2, ..., m_M\}$	Set of Microgrids.
$M^{(m_k)}$	Set of associating of REBSs of m_k.
$f_{n_j}(t_i)$	Supported traffic of n_j in t_i.
$d_{n_j}(t_i)$	Data traffic demand of n_j in t_i.
$l_{n_j}(t_i)$	Energy input of n_j in t_i.
$h^{m_k}(t_i)$	Energy input of m_k in t_i.
$h_{n_j}^{m_k}(t_i)$	Amount of energy sent to n_j by m_k in t_i.
$H_{n_j}(t_i)$	Energy input of n_j in t_i.
$P_{n_j}(t_i)$	Energy output of n_j in t_i.
$s_{n_j}(t_i)$	Number of active subcarriers of n_j in t_i.
e_0	Operating energy consumption.
e_s	Subcarrier energy consumption.
r_0	Rate of an active subcarrier.
S	Maximal number of active subcarriers.
$B_{n_j}(t_i)$	Battery level of n_j at the beginning of t_i.
$B_{n_j}^0$	Battery capacity of n_j.
$B_{n_j}(t_i)$	Battery level of m_k at the beginning of t_i.
$B_{m_k}^0$	Battery capacity of m_k.
$\mathcal{W}_{n_j}^B$	Weighted energy consumption of n_j.
$\mathcal{W}_{m_k}^M$	Weighted energy consumption of m_k.

and the total consumed local energy is as follows:

$$\sum_{t_i \in \mathcal{T}} \left\{ P_{n_j}(t_i) - \sum_{m_k \in \mathcal{M}} h_{n_j}^{m_k}(t_i) \right\}, \tag{4.2}$$

therefore for each REBS, its weighted consumed local energy $\mathcal{W}_{n_j}^B$, can be denoted as the following equation:

$$\mathcal{W}_{n_j}^B = \frac{\sum_{t_i \in \mathcal{T}} \left\{ P_{n_j}(t_i) - \sum_{m_k \in \mathcal{M}} h_{n_j}^{m_k}(t_i) \right\}}{\sum_{t_i \in \mathcal{T}} l_{n_j}(t_i)}. \tag{4.3}$$

Meanwhile, the total harvested energy of Microgrid m_k is denoted as follows:

$$\sum_{t_i \in \mathcal{T}} h^{m_k}(t_i), \tag{4.4}$$

and the total transmitted energy of m_k during the considered time span is as follows:

$$\sum_{t_i \in \mathcal{T}} \sum_{n_j \in \mathcal{M}^{(m_k)}} h_{n_j}^{m_k}(t_i). \tag{4.5}$$

Similarly, the weighted energy transmission of Microgrid m_k in $\mathcal{T}$ can be denoted as follows:

$$\mathcal{W}_{m_k}^M = \frac{\sum_{t_i \in \mathcal{T}} \sum_{n_j \in \mathcal{M}^{(m_k)}} h_{n_j}^{m_k}(t_i)}{\sum_{t_i \in \mathcal{T}} h^{m_k}(t_i)}. \tag{4.6}$$

4.2.2 Optimization Objective

Besides maximizing the total system throughput (i.e., P1), the objective in this chapter also contains figuring out the minimal summation of the weighted energy consumption of the REBSs and Microgrids:

$$\text{P2: } \mathbf{min} \left(\sum_{n_j \in \mathcal{N}} \mathcal{W}_{n_j}^B + \sum_{m_k \in \mathcal{M}} \mathcal{W}_{m_k}^M \right), \tag{4.7}$$

The problem P2 considers the combination of the energy harvesting abilities and the energy consumptions of the REBSs and Microgrids. It can be seen from Eq.4.2 and Eq.4.5 that the minimal energy consumption is taken into considerations in Eq.4.7. However, for different energy harvesting facilities, the amount of energy consumption may have different impacts on their operation. For example, if the local energy input for n_j is larger than $e_0 + S \cdot e_s$ in each time slot (i.e., $l_{n_j}(t_i)$ is sufficient for operation), then a large energy consumption will not impact its operation. In other words, for the REBSs or Microgrids with sufficient energy input, the objective will allow a larger energy consumption. Therefore, Eq.4.1 and Eq.4.5 are used as the dominators in Eq.4.3 and Eq.4.6.

The objective in this chapter is twofold: pursuing the minimal weighted energy consumption (i.e., P2), and figuring out the maximum total system throughput (i.e., P1). However, these two optimization goals may not be fulfilled simultaneously. Denote $\mathcal{D}$ as the possible solution set, and the element of which is with the maximal total system throughput. Therefore, we design the optimization goal as follows:

$$\text{P3: } \mathbf{min} \left(\sum_{n_j \in \mathcal{N}} \mathcal{W}^B_{n_j} + \sum_{m_k \in \mathcal{M}} \mathcal{W}^M_{m_k} \right),$$

where the definition domain is $\mathcal{D}$, and

$$\mathcal{D} = \left\{ \boldsymbol{a} \mid \mathcal{U}(\boldsymbol{a}) \geq \mathcal{U}(\boldsymbol{b}), \text{where } \boldsymbol{a} \neq \boldsymbol{b}, \text{ and } \boldsymbol{a}, \forall \ \boldsymbol{b} \in dom\ \mathcal{U}(\vec{\rho}, \vec{h}, \vec{f}, \vec{s}) \right\}. \tag{4.8}$$

The definition of $\mathcal{U}$ is same as the quadruple $\mathcal{U}$ in section 3.4. It can be seen that if the result of minimal weighted energy consumption happens to be the one with maximal total system throughput (i.e., the maximal total system throughput and minimal weighted energy consumption can be fulfilled simultaneously), then P3 can find the result as well.

On one hand, in section 3.5.1, we demonstrate that P1 is an MILP problem, and the constraints are the linear combination of the variables, therefore $dom\ \mathcal{U}(\vec{\rho}, \vec{h}, \vec{f}, \vec{s})$ satisfies the linear constraints. On the other hand, the denominator of Eq.4.7 is the combination

of constant values, while the numerator is the linear combination of variables, therefore Eq.4.7 is the linear objective function. As a result, it can be seen that problem P3 is also an MILP problem.

4.3 Proposed Two-stage Energy Efficiency Scheme

In order to figure out the result of problem P3, we design a two-stage energy efficiency scheme in this section. In general, the conceived optimization scheme contains two steps, and we will separately deal with the two objectives.

In the first step, we figure out the maximal total system throughput. Denote τ as the value of the maximal total system throughput, then τ is equal to:

$$\tau = \mathbf{max} \sum_{t_i \in \mathcal{T}} U(t_i) = \mathbf{max} \sum_{t_i \in \mathcal{T}} \sum_{n_j \in \mathcal{N}} f_{n_j}(t_i), \tag{4.9}$$

and τ subjects to constraints of problem P1. It can be seen that the calculated τ equals the value of $\boldsymbol{a}$ in Eq.4.8.

In the second step, τ is used as a constraint. We then put the weighted energy consumption as the minimized objective. The objective and the associating constraints can be given by the following equation:

$$\text{P4: } \mathbf{min} \sum_{n_j \in \mathcal{N}} \mathcal{W}^B_{n_j} + \sum_{m_k \in \mathcal{M}} \mathcal{W}^M_{m_k}, \tag{4.10}$$

subject to

$$\sum_{t_i \in \mathcal{T}} U(t_i) = \tau, \tag{4.11}$$

as well as the related constraints given by Eq. 3.1 to Eq. 3.22, Eq. 4.2 and Eq. 4.5. It is noted that problem P4 and P3 have the same results: on one hand, the equality in

Eq. 4.11 guarantees that the results of P4 has the maximal total system throughput, and therefore all the results of P4 satisfy Eq. 4.8; on the other hand, because the calculated strategies of P3 satisfy 4.8, then their total system throughput will be larger than the others', which is just the meaning of Eq. 4.11.

Algorithm 2: Two-stage Energy Efficient Scheme ©2014 IEEE.

Input: Network topology information: $\mathcal{N}, \mathcal{G}, \mathcal{M}, \mathcal{C}$.
Energy related information: e_s, e_0, $h_{n_j}^{m_k}(t_i)$, $h^{m_k}(t_i)$, $l_{n_k}(t_i)$.
Traffic related information: $d_{n_j}(t_i)$ r_0.
Output: $(\vec{\rho}, \vec{h}, \vec{f}, \vec{s})$ for problem P1.

1 Relax the integer constraints of $\vec{\rho}$ and $\vec{s}$ into linear ones, then the problem P1 is transformed into P1';
2 Solve the linear programming problem P1';
3 Let $\overline{O}$ record the result and $\boldsymbol{u}' = (\vec{\rho}', \vec{h}', \vec{f}', \vec{s}')$ is the associated variables;
4 **if** $\boldsymbol{u}'$ *satisfies integer constraints of P1* **then**
5 $\tau = \overline{O}$;
6 **else**
7 $\underline{O} = 0$;
8 $Cons$ = the constraints of P1;
9 Choose one relaxed constraint x that does not follow the constraints of P1. Let χ denote the value of x;
10 $(\tau, \overline{O})$= BranchBound($Cons$, x, χ, P1, $\underline{O}$, $\overline{O}$);
11 Relax the integer constraints of $\vec{\rho}$ and $\vec{s}$ into linear ones, then the problem P4 is transformed into the relaxed problem P4';
12 Solve the linear programming problem P4';
13 Let $\overline{O}$ record the result and $\boldsymbol{u} = (\vec{s}, \vec{\rho}, \vec{f}, \vec{h})$ is the associating variables;
14 **if** $\boldsymbol{u}$ *satisfies integer constraints of P4* **then**
15 **return** $\boldsymbol{u}$;
16 **else**
17 $\underline{O} = 0$;
18 $Cons$ = the constraints of P4;
19 Choose one relaxed constraint x that does not follow the constraints of P4. Let χ denote the value of x;
20 $(\underline{O}^*, \overline{O})$= BranchBound($Cons$, x, χ, P4, $\underline{O}$, $\overline{O}$);
21 **return** the strategy that achieves $\underline{O}^*$.

The major steps of the proposed two-stage energy efficient scheme are summarized in Algorithm 2. In Algorithm 2, there are two stages. Line 1 to line 10 denote the first stage, and the aim of which is to calculate τ. The Algorithm 2 will firstly use the relaxation technique to substitute the linear relaxations for the integer variables. After that, the

original MILP problem (P1) becomes the linear programming problem (P1'). Since there are a bunch of solutions for P1' (i.e., simplex method or interior point method), we omit the details of the procedure. If the solutions of P1' (i.e., $\boldsymbol{u}'(\vec{\rho'}, \vec{h'}, \vec{f'}, \vec{s'})$) happen to satisfy the constraints of P1, then $\tau = \overline{O}$, otherwise the *BranchBound* procedure is used to figure out the solutions of P1 based on $\boldsymbol{u}'$. the idea of *BranchBound* is to cut the solution set into several subsets, and gradually reduce the searching range by removing the unnecessary branches. We use τ to record the maximal value of P1. In the second step, we add 4.11 to the constraints list, and deal with problem P4. Similarly, the problem P4 will be relaxed, and we denote the objective in Eq.4.10 with the relaxed equalities and inequalities by P4'. After the solution of P4', $\boldsymbol{u}$, is figured out, we check whether $\boldsymbol{u}$ satisfies the constraints of P4 or not. If $\boldsymbol{u}$ can also be the result of P4, then we return $\boldsymbol{u}$, otherwise we will turn to *BranchBound* to find the strategy that has the least weighted energy consumption as well as satisfying the associating constraints of P4.

4.4 Performance Evaluation

In this section, we mainly study the features of the proposed two-stage scheme through the computer-based simulations. We mainly compare three schemes in this section: the scheme based on Naive idea (i.e., Naive), the throughput maximization scheme proposed in Chapter 3 (i.e., Throughput maximization), and the two-stage energy efficient scheme introduced in this chapter (i.e., Proposed two-stage).

4.4.1 Settings of the Simulation

Similar to Section 3.6, the considered network topology and experimental parameters are shown in Fig.4.1 and Table 4.2, respectively. As we can see from Fig. 4.1, we consider 10 REBSs, therefore $N = 10$, in which there is 1 gateway ($F = 1$). In the network, there are 3 Microgrids, and they respectively connect to 1, 2, and 3 REBSs. The bandwidth of each link is independently and randomly selected from the interval [80Mbps, 300Mbps].

Table 4.2: Experimental Parameters ©2014 IEEE.

Parameter	Value
The length of time slot ($\|t_i\|$)	1 hour
The number of considered time slots (T)	10
Number of REBSs (N)	10
Number of Microgrids (M)	3
Bandwidth of the Backhaul link ($c_{n_j}^{n_k}$)	80Mbps to 300Mbps
Operating power consumption (e_0)	712.2W
Power consumption per each subcarrier (e_s)	1.06W
Number of subcarriers (S)	600
Battery capacity of REBS ($B_{n_j}^0$)	2000W
Battery capacity of Microgrid ($B_{m_k}^0$)	2000W
Amount of energy of REBS at t_1 ($B_{n_j}(t_1)$)	2000W
Amount of energy of Microgrid at t_1 ($B_{m_k}(t_1)$)	2000W
Rate of subcarriers (r_0)	0.5Mbps

The length of the optimization period is a 10-hour long ($T_0 = 10$ hour), and each time sample represents 1 hour ($|t_i| = 1$ hour). Other parameters are shown in Table 4.2.

In this section, we set the performance metric as the consumed power per megabit, which can be denoted as the following equation:

$$\frac{\sum_{t_i \in \mathcal{T}} P_{n_j}(t_i)}{\tau}, \tag{4.12}$$

where τ is the variable defined in Eq. 4.9. It can be seen that Eq. 4.12 pursues the higher utilization of the energy, which is a more direct energy efficiency metric, without considering the factor of energy harvesting abilities.

4.4.2 Effect of Energy Input on Energy Efficiency

In this section, the energy input is set as the variable. The energy inputs of the REBSs and Microgrids in each time slot are the i.i.d. values and chosen from the interval $[0.5 \cdot \text{x-axis value}, 1.5 \cdot \text{x-axis value}]$. The amount of data traffic demand of each REBS is also uniformly and randomly selected from $[40\text{Mbps}, 100\text{Mbps}]$. Other parameters can be referred to Table 4.2. Fig. 4.2 illustrates the comparison of the consumed power per

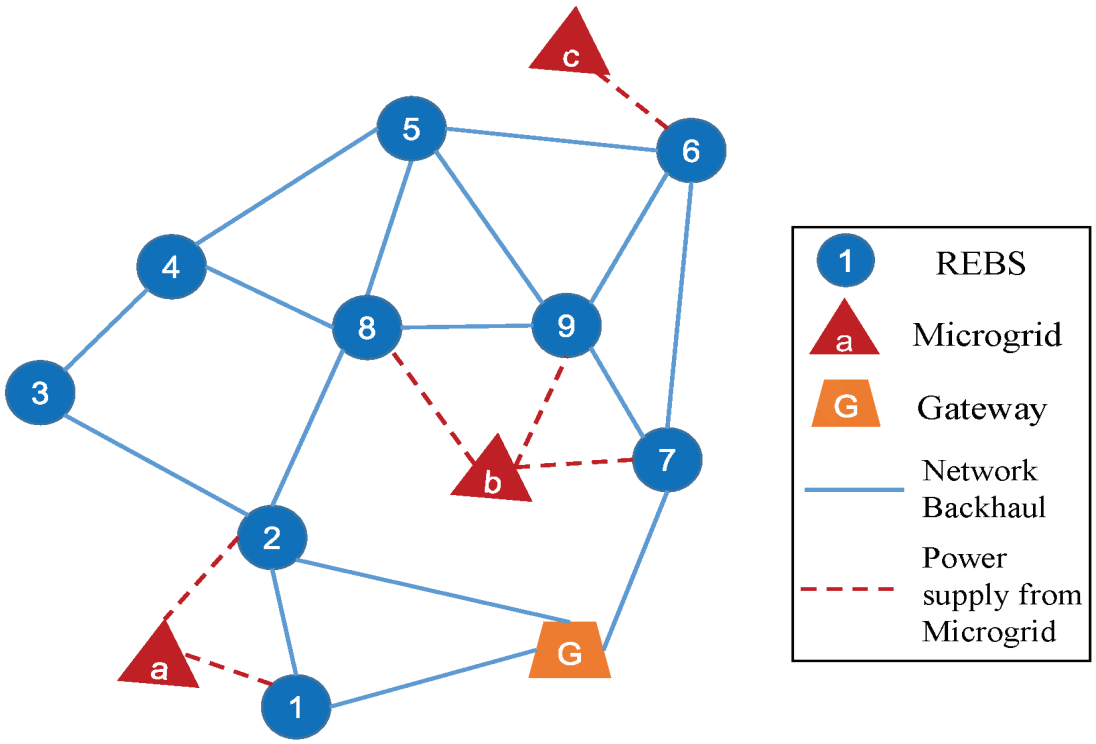

Figure 4.1: System topology used in the part of performance evaluation. ©2014 IEEE.

megabit of the three schemes. In this figure, we have the following observations. Firstly, the proposed two-stage scheme has the lowest consumed energy per megabit traffic, while the Naive scheme has the largest energy consumption per traffic unit. With considering the lower τ of the Naive scheme, the energy utilization of the Naive scheme is even worse. Secondly, there is a inversely proportional relationship between the considered energy efficiency metric, and the amount of input energy of the Naive scheme. This is due to the reason that as more renewable energy flowed into the battery of REBS, it can support more data traffic demands for each REBS, according to our observations in Section 3.6.2, the total system throughput will gradually be the same as the one of the proposed two-stage's. As a result, the performance gap of the Naive scheme and proposed two-stage scheme becomes smaller as the increase of the energy input.

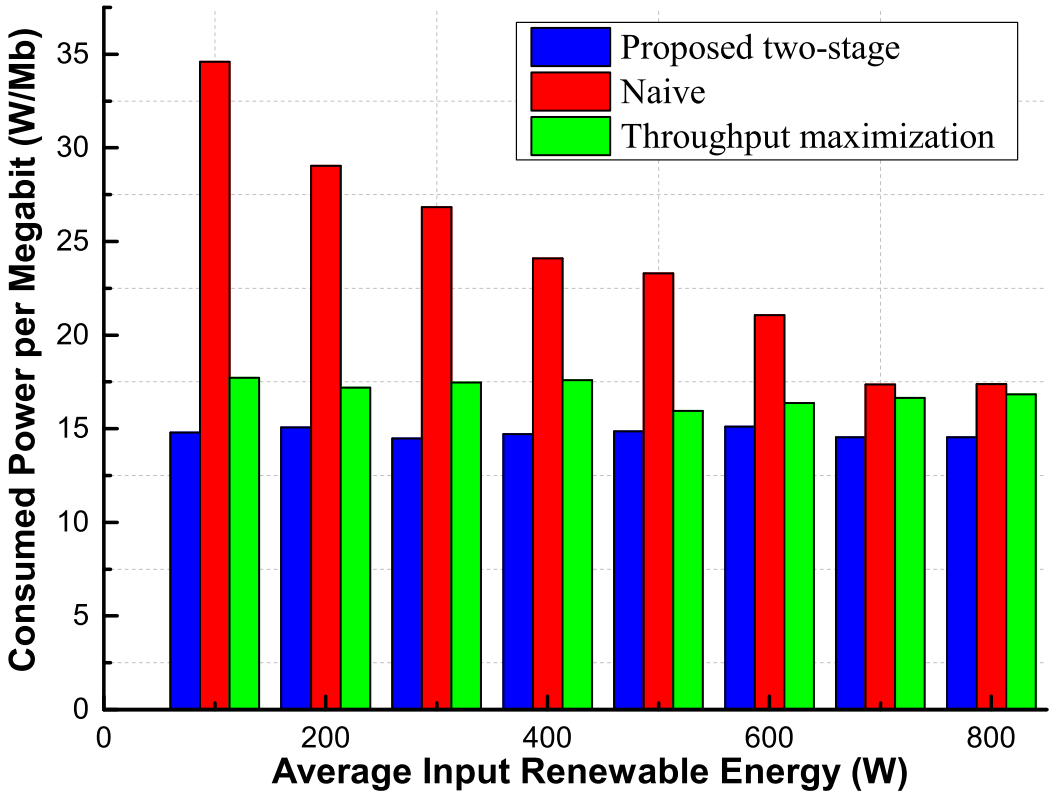

Figure 4.2: The effect of average input renewable energy on consumed power per megabit of the proposed scheme, naive scheme and throughput maximization scheme. ©2014 IEEE.

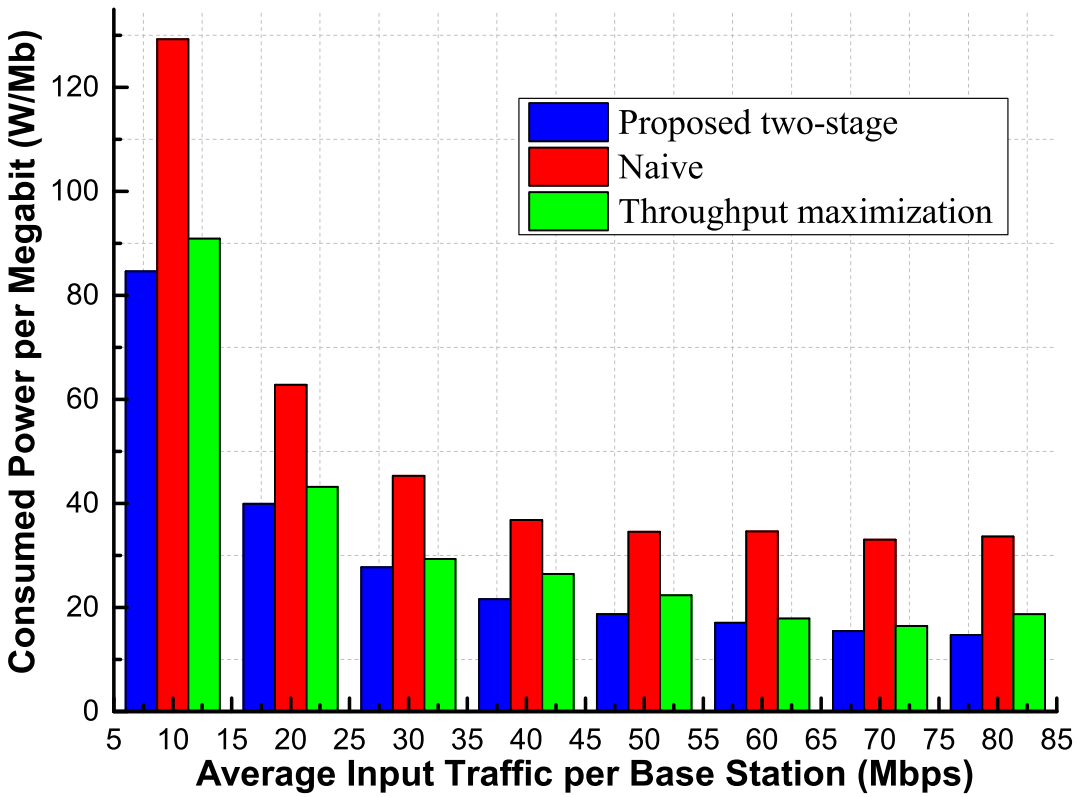

Figure 4.3: The effect of average input traffic per base station on consumed power per megabit of the proposed scheme, naive scheme and throughput maximization scheme. ©2014 IEEE.

4.4.3 Effect of Traffic Input on Energy Efficiency

In this section, the amount of the data traffic demand of each REBS in each time slot (i.e., $f_{n_j}(t_i)$) is set as the variable. We consider the i.i.d. $f_{n_j}(t_i)$ and $f_{n_j}(t_i)$ is chosen from the interval $[0.5 \cdot \text{x-axis value}, 1.5 \cdot \text{x-axis value}]$. And for the energy inputs of the energy harvesting facilities (i.e., $l_{n_j}(t_i)$ and $h^{m_k}(t_i)$), they are uniformly and randomly chosen from $[100\text{W}, 300\text{W}]$. The residual parameters can be referred to Table 4.2.

From Fig.4.3, it can be seen that the proposed two-stage scheme has the lowest consumed power per megabit among the three schemes, therefore the proposed two-stage scheme has the best performance, and the gap between the performance of the proposed two-stage and the Naive scheme is clear to see. Furthermore, it can be seen from Fig. 4.3 that as the average input traffic increases, the consumed energy per megabit will decrease. The rationale is twofold. Firstly, if the traffic input is larger, there will be more traffic distribution strategy candidates (i.e., the domain is larger), therefore the result will be at least equal or even larger. Secondly, for an active REBS, if there is still extra energy budget, therefore the total system throughput can be increased only with the energy cost of e_s. Therefore the τ can be improved if the input traffic increases.

4.5 Summary

In this chapter, we introduce a two stage energy efficient scheduling and load distribution scheme, which can strike the balance between the total system throughput and the associating energy consumption.

To this end, we firstly introduce the scenario that the proposed scheme will take effect. After that, the system model is formulated, and the optimization objective is analyzed, respectively. Thirdly, the two-stage energy efficiency optimization framework is demonstrated. In the last part, the energy efficiency of the proposed two-stage scheme is illustrated through the comparison with the throughput maximization only scheme and

the Naive scheme, under various energy inputs and data traffic demands.

Chapter 5

On the On-line Energy-Efficient of Throughput-Based Scheme for REBS Mesh Networks

5.1 Introduction

In Chapter 3 and Chapter 4, we consider that the data traffic demand profile is already known before conducting the optimization. In reality, the knowledge of such profile can be regarded as the expectation of the profile. Therefore, the schemes proposed in these two chapters can have good performance if the estimations of the data traffic demand profiles are precise (i.e., the estimations are just the real ones). However, the result for such precise estimation assumption may get the suboptimal result when such estimations are imprecise, owing to the fact that the data traffic demand profiles depend on the activities of the human beings, which are hard to predict in essence.

In this chapter, to deal with the problems of the off-line scheme (i.e., cannot adjust the strategy when operating, and have suboptimal result when it faces imprecise data

traffic demand), we propose an on-line scheme, and such scheme can dynamically adjust the old strategy, in order to achieve a better performance. At first, we revise the system model according to the new considered scenario. Secondly, we analyze the performance bound of the off-line scheme in term of the data demand estimation deviation. After that, an on-line dynamic adjusting scheme is envisioned and analyzed accordingly. At last, the advantages of the on-line scheme is demonstrated by the computer-based simulations.

The major contributions of this chapter are summarized as follows:

- The performance bound of the off-line scheme is theoretically analyzed, and the analysis demonstrates that when the estimation deviation is large, the result of the off-line scheme is unsatisfied.
- We propose an on-line dynamic adjusting scheme, which is based on the off-line optimization result, and can adjust the scheme according to the current precise data traffic demand profile.
- We demonstrate that the proposed on-line scheme can achieve better performance than the off-line scheme via the proof.
- Through the computer-based simulations, we show that the proposed on-line scheme is robust toward the imprecise data traffic, and the total system throughput of the on-line scheme is very close to the optimal scheme, which is the off-line scheme having the precise data traffic demand profile, in terms of the throughput and energy efficiency.

5.2 System Model

As mentioned in the introduction part, we consider the imprecise data traffic demand in this chapter. We assume that the real data traffic demand of the users under the coverage area of n_j in t_i is $d_{n_j}(t_i)$, and the expectation of $d_{n_j}(t_i)$ is denoted by $\overline{d}_{n_j}(t_i)$, therefore

their relationship can be given by the following equation:

$$d_{n_j}(t_i) = \overline{d}_{n_j}(t_i) + \epsilon_{n_j}(t_i), \tag{5.1}$$

where $\epsilon_{n_j}(t_i)$ denotes the estimation deviation of data traffic demand of the REBS n_j in time slot t_i. A large $\epsilon_{n_j}(t_i)$ means that the expectation of the data traffic demand $\overline{d}_{n_j}(t_i)$ is very different from the real data traffic demand profile $d_{n_j}(t_i)$.

In this chapter, we assume that before conducting the optimization, $\overline{d}_{n_j}(t_i)$ is the available information, since we can get such expectation by combining the population in the coverage area, the historical profile, the information of users' activities and so on (as we analyzed in Chapter 2). On the other hand, $d_{n_j}(t_i)$ can only be known at the beginning of t_i. For example, $d_{n_j}(t_{i+1})$ is the unknown information in t_i. Similar assumptions can be found in [44][51].

In our proposal, we only consider two kinds of traffic profile: the expectation and the instant precise one, and we do not consider additional features is available (i.e., the stochastic information such as the means and deviations in [47] and [56]). In addition, we only consider the imprecise for the traffic input estimation. On the contrary, for the energy estimation, we assume the precise information is available, since we can have a detailed knowledge of the environment, such as the weather information, the intensity of illumination and so on.

Other variables and parameters are same as the previous chapters. For convenience, we list them in Table 5.1.

5.3 Analysis on the Off-line Scheme

In this section, we conduct the analysis for the performance of the off-line scheme. We will give the upper bound and lower bound of the performance gap between the off-line

Table 5.1: Variable Summarization

Variable	Meaning
t_i	Index of time slot i.
T	Number of time slots.
$\mathcal{T} = \{t_1, t_2, ..., t_T\}$	Time span using time sample.
n_j	Index of REBS j.
N	Number of REBSs.
$\mathcal{N} = \{n_1, n_2, ..., n_N\}$	Set of REBSs.
(n_j, n_k)	Connection between n_j and n_k.
C	Number of links.
$\mathcal{C} = \{(n_{j_1}, n_{k_1}), ..., (n_{j_C}, n_{k_C})\}$	Set of the links.
$c_{n_j}^{n_k}$	Capacity of (n_j, n_k).
$G = (\mathcal{N}, \mathcal{C})$	Network topology.
$\rho_{n_j}(t_i)$	Operating status of n_j in t_i.
$c_(n_j, n_k)$	Link capacity of (n_j, n_k) in t_i.
F	Number of gateways.
g_f	Index of gateway f.
$\mathcal{G} = \{g_1, g_2, ..., g_F\}$	Set of gateways.
m_k	Index of Microgrid k.
M	Number of Microgrids.
$\mathcal{M} = \{m_1, m_2, ..., m_M\}$	Set of Microgrids.
$M^{(m_k)}$	Set of associating of REBSs of m_k.
$f_{n_j}(t_i)$	Supported traffic of n_j in t_i.
$d_{n_j}(t_i)$	Data traffic demand of n_j in t_i.
$\overline{d}_{n_j}(t_i)$	Estimated data traffic demand of n_j in t_i.
$\epsilon_{n_j}(t_i)$	Estimation deviation of $\overline{d}_{n_j}(t_i)$.
$l_{n_j}(t_i)$	Energy input of n_j in t_i.
$h^{m_k}(t_i)$	Energy input of m_k in t_i.
$h_{n_j}^{m_k}(t_i)$	Amount of energy sent to n_j by m_k in t_i.
$H_{n_j}(t_i)$	Energy input of n_j in t_i.
$P_{n_j}(t_i)$	Energy output of n_j in t_i.
$s_{n_j}(t_i)$	Number of active subcarriers of n_j in t_i.
e_0	Operating energy consumption.
e_s	Subcarrier energy consumption.
r_0	Rate of an active subcarrier.
S	Maximal number of active subcarriers.
$B_{n_j}(t_i)$	Battery level of n_j at the beginning of t_i.
$B_{n_j}^0$	Battery capacity of n_j.
$B_{n_j}(t_i)$	Battery level of m_k at the beginning of t_i.
$B_{m_k}^0$	Battery capacity of m_k.
$\mathcal{W}_{n_j}^B$	Weighted energy consumption of n_j.
$\mathcal{W}_{m_k}^M$	Weighted energy consumption of m_k.

scheme proposed in Chapter 3 with the expectation data traffic profile, and the off-line scheme with the perfect data traffic demand profile (i.e., the estimation is same as the real one, and the result is optimal).

As shown in Eq.5.1, there might be an estimation deviation $\epsilon_{n_j}(t_i)$ between the real data traffic demand $d_{n_j}(t_i)$ and its expectation $\overline{d}_{n_j}(t_i)$. Since $\overline{d}_{n_j}(t_i)$ can be either larger or smaller than $d_{n_j}(t_i)$, the available range of $\epsilon_{n_j}(t_i)$ is $\epsilon_{n_j}(t_i) \in (-\infty, +\infty)$. Denote $[\epsilon_{n_j}(t_i)]^+$ as the non-negative vector, and the value of which is equal to $\epsilon_{n_j}(t_i)$ if $\epsilon_{n_j}(t_i) > 0$, otherwise $[\epsilon_{n_j}(t_i)]^+ = 0$, then we have the following equation:

$$[\epsilon_{n_j}(t_i)]^+ = \mathbf{sup}\left\{\epsilon_{n_j}(t_i), 0\right\}. \tag{5.2}$$

Denote the quadruple $(\vec{\rho^*}, \vec{h^*}, \vec{f^*}, \vec{s^*})$ as the strategy figured out by the off-line scheme, and having the perfect data traffic demand profile (i.e., $d_{n_j}(t_i)$). Due to the optimality of the off-line scheme, $(\vec{\rho^*}, \vec{h^*}, \vec{f^*}, \vec{s^*})$ is the optimal result. On the other hand, let $(\vec{\rho'}, \vec{h'}, \vec{f'}, \vec{s'})$ be the strategy calculated by the off-line scheme using the data traffic demand expectation (i.e., $\overline{d}_{n_j}(t_i)$). Because the expectation is not always equal to the real one, therefore $(\vec{\rho'}, \vec{h'}, \vec{f'}, \vec{s'})$ might be sub-optimal. Theorem 5.3.2 analyzes the upper bound and lower bound of the performance gap between the off-line scheme using the perfect data traffic demand profile and the expectation.

We define a vector $\widetilde{\boldsymbol{d}}$, and the elements of $\widetilde{\boldsymbol{d}}$ are the smaller element of $\boldsymbol{d}$ and $\overline{\boldsymbol{d}}$ in the corresponding dimension, and the element of $\widetilde{\boldsymbol{d}}$, $\widetilde{d}_{n_j}(t_i)$, can be given by the following equation:

$$\widetilde{d}_{n_j}(t_i) = \mathbf{inf}\left\{d_{n_j}(t_i), \overline{d}_{n_j}(t_i)\right\}. \tag{5.3}$$

The following Lemma 5.3.1 reveals the relationship among the results with the different traffic input profiles:

Lemma 5.3.1 *Denote $\widetilde{\tau}$ as the maximal total system throughput given by the off-line*

scheme, and $\widetilde{\boldsymbol{d}}$ *is used as the traffic input profile. Then we have the following relationships among* τ^*, $\widetilde{\tau}$, *and* τ'*:*

$$\tau^* - \sum_{n_j \in \mathcal{N},\, t_i \in \mathcal{T}} \sum [\epsilon_{n_j}(t_i)]^+ \leq \widetilde{\tau} \leq \tau'. \tag{5.4}$$

Proof: Because the off-line scheme can always figure out the maximal total system throughput, $\widetilde{\tau}$ is the optimal result when the input data traffic demands are $\widetilde{\boldsymbol{d}}$. As a result, the total data traffic demands gap between $\widetilde{\boldsymbol{d}}$ and $\boldsymbol{d}$ can be given by the following equation:

$$\mathbf{1} \cdot \left(\boldsymbol{d} - \widetilde{\boldsymbol{d}} \right)^T = \sum_{n_j \in \mathcal{N},\, t_i \in \mathcal{T}} \sum [\epsilon_{n_j}(t_i)]^+. \tag{5.5}$$

Because the total system throughput gap will be no more than the total data traffic demands, the first inequality of Eq.5.4 holds. On the other hand, all the possible strategies calculated by the off-line scheme with the data traffic demand input $\widetilde{\boldsymbol{d}}$, can be found by the strategy set when the input traffic is $\overline{\boldsymbol{d}}$. In other words, the latter result is larger than or equal to the former one. Therefore, $\widetilde{\tau} \leq \tau'$ and the second inequality of Eq.5.4 holds.

■

Theorem 5.3.2 *Denote* τ^* *as the total system throughput of the strategy* $(\vec{\rho^*}, \vec{h^*}, \vec{f^*}, \vec{s^*})$*, and* τ' *as the total system throughput figured out by the strategy* $(\vec{\rho'}, \vec{h'}, \vec{f'}, \vec{s'})$*. When we use these two strategies, their associating result* τ^* *and* τ' *will satisfy the relationship given by the following inequalities:*

$$0 \leq \tau^* - \tau' \leq \boldsymbol{inf} \left\{ \sum_{n_j \in \mathcal{N}} \sum_{t_i \in \mathcal{T}} [\epsilon_{n_j}(t_i)]^+, \tau^* \right\}. \tag{5.6}$$

Proof: We will firstly prove the former inequality. As we mentioned above, the strategy $(\vec{\rho^*}, \vec{h^*}, \vec{f^*}, \vec{s^*})$ is established by the off-line scheme with the perfect data traffic demand information. Therefore τ^* is the optimal result since the off-line scheme will

return the optimal strategy. As a result, τ^* will be no smaller than τ'. Therefore the inequality $0 \leq \tau^* - \tau'$ holds.

Then we prove the latter inequality. According to Lemma 5.3.1, the gap between τ^* and τ' is less than the sum of each dimension of the estimation deviation. In addition, τ' is non-negative, hence the second inequality of Theorem 5.6 holds. ■

Theorem 5.6 demonstrates the performance bound of the off-line scheme. It can be seen that for the off-line scheme with the traffic input expectation, its performance depends on the precision of the traffic input estimation (i.e., the absolute value of $\epsilon_{n_j}(t_i)$), and a higher estimation deviation may cause a poorer performance. For example, when the energy input is very low and no REBS can operate, then both of τ^* and τ' will be 0 and the gap is 0 as well. When the energy input is adequate, then the total system throughput gap will be the upper bound, since the strategy figured out by the expectation cannot support a larger traffic demand.

5.4 Envisioned On-line Dynamic Adjusting Scheme

Theorem 5.3.2 reveals that as the traffic estimation deviation increases (i.e., the absolute value of $\epsilon_{n_j}(t_i)$ becomes larger), the performance of the off-line scheme might decrease accordingly. Therefore the off-line scheme might return an unsatisfied result if the estimation deviation is large. Aiming at such problem, we put forward an on-line dynamic adjusting scheme in this section. Such on-line strategy is based on the precise knowledge of the data traffic demand $d_{n_j}(t_i)$ at the beginning of t_i.

The on-line scheme makes use of the result of the off-line scheme. At first, we execute the off-line scheme once before the first time slot t_1. After getting the strategy of the off-line scheme, then the on-line dynamic adjusting scheme will be performed in every time slot in order to adjust the the future plans designed by the old plan. The old plan is

initialized by the off-line scheme, and stored by the three kinds of variables given by the following equations:

$$B_{n_j}^{Plan}(t_i) = B_{n_j}(t_i), \forall t_i \in \mathcal{T}, n_j \in \mathcal{N}, \tag{5.7}$$

$$B_{m_k}^{Plan}(t_i) = B_{m_k}(t_i), \forall t_i \in \mathcal{T}, m_k \in \mathcal{M}, \tag{5.8}$$

$$P_{n_j}^{Plan}(t_i) = P_{n_j}(t_i), \forall t_i \in \mathcal{T}, n_j \in \mathcal{N}. \tag{5.9}$$

In Eq.5.7, $B_{n_j}^{Plan}(t_i)$ is defined as the energy level of the battery of REBS n_j in t_i, in Eq.5.8, we denote $B_{m_k}^{Plan}(t_i)$ as the energy level of the battery of Microgrid m_k in t_i, and in Eq.5.9, the energy consumption of REBS n_j in t_i is denoted by $P_{n_j}^{Plan}(t_i)$. $B_{n_j}^{Plan}(t_i)$, $B_{m_k}^{Plan}(t_i)$ and $P_{n_j}^{Plan}(t_i)$ are established by the off-lines scheme before the time slot t_1. In each following time slot, we will use the on-line scheme to adjust the plan given by the off-line scheme and the on-line schemes in earlier time slots. For example, in t_i, we have the scheme which is given by the off-line scheme, and revised by the on-line schemes from t_1 to t_{i-1}, hence the on-line scheme aims at dealing with the such strategy, and returns the strategies from t_i to t_T. We use $\boldsymbol{B}_N^{Plan}$, $\boldsymbol{B}_M^{Plan}$ and $\boldsymbol{P}_N^{Plan}$ to represent the set of $B_{n_j}^{Plan}(t_i)$, $B_{m_k}^{Plan}(t_i)$ and $P_{n_j}^{Plan}(t_i)$, respectively.

Definition (*Maximum available spare energy*): The maximum available spare energy of the REBS n_j in t_i, $\mathcal{E}_{n_j}(t_i)$, is the minimum value of the planned energy level of n_j's battery $B_{n_j}^{Plan}$ from t_i to t_T:

$$\mathcal{E}_{n_j}(t_i) = \min_{t_i \le t \le t_T} B_{n_j}^{Plan}(t). \tag{5.10}$$

The $\mathcal{E}_{n_j}(t_i)$ is the maximum extra usable energy for n_j in time slot t_i, without impacting the strategy in the upcoming time slots. We will given the proof in the following

Theorem.

Theorem 5.4.1 *$\mathcal{E}_{n_j}(t_i)$ is the maximum available amount of energy can be used for REBS n_j in time slot t_i, and the consumption of such energy will not impact the future plans $\boldsymbol{P}_N^{Plan}$ from t_{i+1} to t_T.*

Proof: According to the battery evolution equation defined in Eq.3.9, the energy level of a certain REBS in the current time slot will be no less than the one in the next time slot (i.e., $B_{n_j}^{Plan}(t_i) \geq B_{n_j}^{Plan}(t_{i+1})$), if the renewable energy input is no less than the energy consumption in current time (i.e., $P_{n_j}^{Plan}(t_i) \geq H_{n_j}(t_i)$). Otherwise the energy level in the next time slot will be larger (i.e., $B_{n_j}^{Plan}(t_i) < B_{n_j}^{Plan}(t_{i+1})$). Not to affect the future strategies from t_{i+1} to t_T, for a certain REBS n_j, the following inequalities should be fulfilled accordingly:

$$\mathcal{E}_{n_j}(t_i) + P_{n_j}^{Plan}(t_{i+\alpha}) \leq H_{n_j}(t_{i+\alpha}) + B_{n_j}^{Plan}(t_{i+\alpha}), \tag{5.11}$$

where $\alpha \in \mathbb{Z}^+$ and $0 \leq \alpha \leq T - i$. In order to get the largest amount of $\mathcal{E}_{n_j}(t_i)$, more than one REBS should satisfy the equality constraint " = " in (5.11). Therefore $\mathcal{E}_{n_j}(t_i)$ is equal to the minimum value of $B_{n_j}^{Plan}(t)$, and Theorem 5.4.1 holds. ■

It is noted that the previous Definition 5.4 and Theorem 5.4.1 works for the battery of the REBSs, and it can be easily extended to the case of the Microgrids'. Due to lack of space, we omit such parts in this dissertation. From Theorem 5.4.1, it can be seen that $\mathcal{E}_{n_j}(t_i)$ is non-negative because of the constraint in Eq.3.9. As a result, the actual energy input for each REBS in each time slot of the on-line scheme will be no less than the one of the off-line scheme using the expectation traffic profile, and the total system throughput of the on-line scheme will be at least same as the one of the off-line scheme. Therefore the performance of the on-line scheme is guaranteed.

Since $\boldsymbol{d}(t_i)$ is available in t_i, an immediate idea is to use the off-line result to figure

out the optimal strategies from t_i to t_T. However, such consideration may not work due to the following reasons. Firstly, the off-line scheme is compute-intensive (i.e., NP-hard as described in Chapter 3), so it cannot be executed periodically in practice. Secondly, even if it is possible to use the off-line scheme in each time slot, the optimal result we get from the off-line scheme in t_i may modify the strategies in future time slots, and such effort may degrade the performance. This is because the current optimal result is based on the traffic information made up by the precise information ($\boldsymbol{d}(t_i)$) and the imprecise information (expectation in the following time slots), and such imprecise information will make the current optimal become sub-optimal in the future.

Let the vector $\boldsymbol{d}(t_i) = \{d_{n_1}(t_i), d_{n_2}(t_i), ..., d_{n_N}(t_i)\}$ represent the real data traffic demands of each REBSs in time slot t_i. For the energy input of the Microgrids and REBSs, we use $\boldsymbol{h}^{on}$ and $\boldsymbol{l}^{on}$ to denote them, respectively. The on-line dynamic adjusting scheme will be executed at the beginning of each time slot, and its procedure is denoted as Algorithm 3 shows. In Algorithm 3 and following descriptions, we omit the time label t_i because the on-line scheme will design the strategy only for the current time slot.

At first, the energy plan designed in earlier time $\boldsymbol{B}_N^{Plan}$, $\boldsymbol{B}_M^{Plan}$ and $\boldsymbol{P}_N^{Plan}$, the energy input information $\boldsymbol{h}^{on}$ and $\boldsymbol{l}^{on}$, the data traffic demand input $\boldsymbol{d}$, and the network topology information are established. After that, Algorithm 3 calculates the maximum available spare energy for each REBS (i.e., $\mathcal{E}_{n_j}(t_i)$) according to Eq. 5.4 based on $\boldsymbol{B}_N^{Plan}$, and the energy from the Microgrids is based on the previous plan $\boldsymbol{B}_M^{Plan}$, as line 1 to 3 shows. After we get the energy input, we then figure out the possible operating status $\rho_{n_j}^{on\_temp}$, and the maximum number of active subcarriers $s_{n_j}^{on\_temp}$, respectively:

$$\arg \max_{s_{n_j}^{on\_temp} \leq S, \rho_{n_j}^{on\_temp} \in \{0,1\}} \left\{ P'_{n_j} | P'_{n_j} \leq \mathcal{E}_{n_j} + P_{n_j}^{Plan} \right\}. \tag{5.12}$$

According to the definition, it can be seen that if $\mathcal{E}_{n_j} + P_{n_j}^{Plan}$ is no less than e_0, $\rho_{n_j}^{on\_temp}$ will be 1, and we use the set N_{avai} to store the REBSs that can support the operating

consumption (i.e., $\rho_{n_j}^{on\_temp} = 1$). It is noted that the strategy is not satisfied and energy-inefficient if we set all the REBSs in N_{avai} active (i.e., the active REBSs may not connect to any active REBS, hence it cannot carry any data traffic). We will make use of $\rho_{n_j}^{on\_temp}$ and $s_{n_j}^{on\_temp}$ to figure out the maximum total system throughput U^{on} in the current time slot, such procedure can be done by the linear programming techniques since the integer constraints are determined. After that, Algorithm 3 will find the maximum total system throughput in a iterative manner, and line 7 to 17 demonstrate such procedure. We first initialize the set cur_Node and ava_Node, and their initial values are equal to $\varnothing$ and N_{avai}, respectively. Secondly, the REBS in the set ava_Node will be moved to cur_Node if it has the most system throughput improvement, and Algorithm 3 will iteratively conduct such selection procedure until the current system throughput is equal to U^{on}. After cur_Node is decided, Algorithm 3 will then calculate the energy-efficient results $(\rho^{on}, h^{on}, f^{on}, s^{on})$ with the constraint of the maximum system throughput U^{on}. The future plan $\boldsymbol{B}_N^{Plan}$, $\boldsymbol{B}_M^{Plan}$ and $\boldsymbol{P}_N^{Plan}$ will be updated based on $(\rho^{on}, h^{on}, f^{on}, s^{on})$, and such results will be returned as the result of the on-line scheme.

5.5 Performance Evaluation

In this section, we check the performance of the proposed on-line dynamical adjusting scheme.

There are mainly four schemes compared in this part. The first one is the **off-line two stage energy efficient scheme** described in Chapter 4, which has the perfect data traffic demand information (Off-line with Perfect Information). Because the optimal feature of the off-line scheme, and the traffic input information is precise, therefore such scheme achieves the optimal performance in terms of the total system throughput and the energy efficiency. The second scheme is the **off-line two stage energy efficient scheme**, with the data traffic demand expectation (Off-line with Expected Information). As analyzed

Algorithm 3: On-line dynamic adjusting scheme ©2015 IEEE.

Input: Network topology information: $G(\mathcal{N}, \mathcal{C}), \mathcal{M}$.
Energy information: $\boldsymbol{B}_N^{Plan}$, $\boldsymbol{B}_M^{Plan}$, $\boldsymbol{P}_N^{Plan}$, $\boldsymbol{l}$, $\boldsymbol{h}$.
Traffic information: $\boldsymbol{d}$.
Output: $\boldsymbol{B}_N^{Plan}$, $\boldsymbol{B}_M^{Plan}$, $\boldsymbol{P}_N^{Plan}$, $(\rho^{on}, h^{on}, f^{on}, s^{on})$.

Figure out the maximal available spare energy $\mathcal{E}_{n_j}$ for each n_j according to equation 5.10;
For each m_k, **if** $n_j \in M^{(m_k)}$ **then**
    $\mathcal{E}_{n_j} = \mathcal{E}_{n_j} + \min_{t_T \geq t \geq t_i} \left\{ B_{m_k}^{Plan}(t_i) \right\} / |M^{(m_k)}|$;
For each n_j, set $\rho_{n_j}^{on\_temp}$ and $s_{n_j}^{on\_temp}$ by (3.6):
$\arg \max_{s_{n_j}^{on\_temp} \leq S, \rho_{n_j}^{on\_temp} \in \{0,1\}} \left\{ P'_{n_j} | P'_{n_j} \leq \mathcal{E}_{n_j} + P_{n_j}^{Plan} \right\}$;
Let $\mathcal{N}_{avai} = \{n | n \in \mathcal{N} \; and \; \rho_n^{on\_temp} == 1\}$;
Base on $\boldsymbol{d}$, $\rho_{n_j}^{on\_temp}$ and $s_{n_j}^{on\_temp}$, figure out the maximal system utility U^{on} in current time slot;
Initialize $cur\_Node = \{\mathcal{G}\}$, $ava\_Node = \mathcal{N}_{avai} - \{\mathcal{G}\}$;
Set $Utility = 0$;
while *True* **do**
    if $Utility == U^{on}$ **then**
        Set ρ^{on} according to cur_Node;
        Use ρ^{on}, $\boldsymbol{l}$, $\boldsymbol{h}$ and $\tau = U^{on}$, and assume in P4 in Eq. 4.10, s can be real value, to figure out P4. We will obtain s_{real}^{on}, f^{on}, h^{on};
        Let s^{on} be $\lceil s_{real}^{on} \rceil$;
        Use $\boldsymbol{P}_N^{Plan}$ to record the energy consumption plan, and update $\boldsymbol{B}_N^{Plan}$ and $\boldsymbol{B}_M^{Plan}$ for the left time slots according to $\boldsymbol{P}_N^{Plan}$;
        return $\boldsymbol{B}_N^{Plan}$, $\boldsymbol{B}_M^{Plan}$, $\boldsymbol{P}_N^{Plan}$, and $(\rho^{on}, h^{on}, f^{on}, s^{on})$;
    Choose $n_{max} \in ava\_Node$ that the system utility is maximized, with the assumptions that only REBSs in $\{n_{max}\} \cup cur\_Node$ are active, and the number of active subcarriers are given by $s_{n_j}^{on\_temp}$. Let U_{max} be the maximal system utility;
    $Utility = U_{max}$, $cur\_Node = cur\_Node \cup \{n_{max}\}$, $ava\_Node = ava\_Node \backslash \{n_{max}\}$;

Table 5.2: Experimental Parameters ©2015 IEEE.

Parameter	Value
The number of considered time slots (T)	5
The length of each time slot($\|t_i\|$)	1 hour
Number of REBSs (N)	10
Number of Microgrids (M)	3
Bandwidth of the Backhaul link ($c_{n_j}^{n_k}$)	80Mbps to 300Mbps
Operating power consumption (e_0)	712.2W
Power consumption per each subcarrier (e_s)	1.06W
Number of subcarriers (S)	600
Battery capacity of REBS ($B_{n_j}^0$)	2000W
Battery capacity of Microgrid ($B_{m_k}^0$)	2000W
Amount of energy of REBS at t_1 ($B_{n_j}(t_1)$)	2000W
Amount of energy of Microgrid at t_1 ($B_{m_k}(t_1)$)	2000W
Rate of subcarriers (r_0)	0.5Mbps

in the previous part, there might be the estimation deviation of the expectation, therefore it is the sub-optimal scheme. The third scheme is the **on-line scheme** proposed in this chapter, and it is used with the off-line scheme (Off-line Combined with On-line). Such scheme is the combination of the strategy of the on-line scheme and off-line scheme, it makes use of the expectation of the traffic input profile at the very beginning, and adjust the strategy in each time slot. The fourth scheme is the **Naive scheme**, and the details of which are similar to the one defined in Chapter 2: it addresses the total system throughput maximization issue as well as decreasing the energy consumption. In each time slot, the Microgrids will evenly distribute its energy to the connected REBSs, and then the REBSs will calculate the ρ and s according to the available energy. It can be seen that the Naive scheme is the myopic scheme, which will not consider the long-term impact caused by the strategy maximizing the current time slot. It can be used to examine the significance of the long-term optimization. Other related parameters are listed in Table 5.2.

From parameters shown in Table 5.2, we consider the optimization covering 5 hours (i.e., $T = 5$), and the length of each time slot is 1 hour (i.e., $|t_i| = 1$). The topology is shown in Fig.5.1. As we can see from Fig.5.1, there are 9 non-gateway REBSs and 2

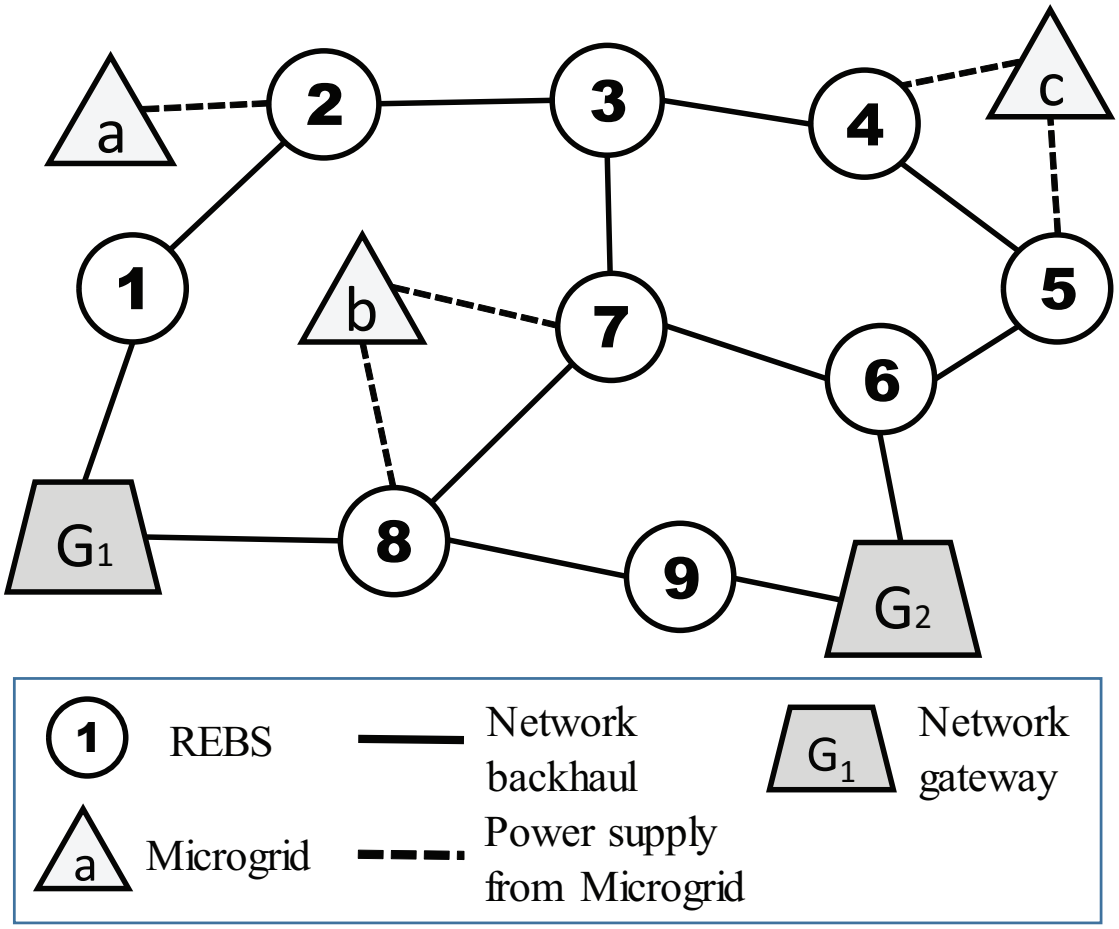

Figure 5.1: The topology used for the computer-based simulation. ©2015 IEEE.

network gateways in the considered area, therefore $N = 11$ and $F = 2$. The bandwidth of the interconnected links (i.e., microwave panel or long distance WiFi) between two neighboring REBSs are i.i.d. value selected from 80Mbps to 300Mbps. For Microgrid a, it only connects to n_2, and Microgrid b and c have the associating REBSs n_7, n_8 and n_4, n_5, respectively. It is noted that n_1, n_3, n_6 and n_9 do not have connections to any Microgrids. In this simulation, we also consider the macro base station as the previous chapters due to the economical concern (i.e., the CAPEX of the Microgrid connection and energy harvesting facilities), therefore the operating energy consumption (e_0), the per-subcarrier consumption (e_s), and the number of subcarriers (S) equals 712.2W, 1.06W, and 600, respectively based on the measurement in [5]. Both of the Microgrid and REBS have the battery with capacity of 2kW ($B^0_{n_j} = B^0_{m_k} = 2000W$). We consider the fully charged battery therefore the initial amount of energy of each battery for REBSs and Microgrids is $2000W$.

In this part, two kinds of performance metrics are considered, namely the total system throughput and the weighted energy consumption per traffic unit. The total system throughput is used to evaluate the amount of supported data traffic demands of the scheme, which is same as the definition in Eq.3.19, and the scheme having more total system throughput is considered to be better than the scheme with lower one. The second metric is the ratio of the weighted energy consumption (defined in Eq.4.7) to the total system throughput (defined in Eq.3.19). The scheme having the lower weighted energy consumption per traffic unit has better performance than the others, since it can use less energy to transfer the data.

5.5.1 Effect of Estimation Deviation of Data Traffic Demands on System Throughput and Energy Consumption

At first, we check the impact of the estimation deviation of the data traffic demand to the performances of the schemes. We use the "Off-line with Perfect Information" as the

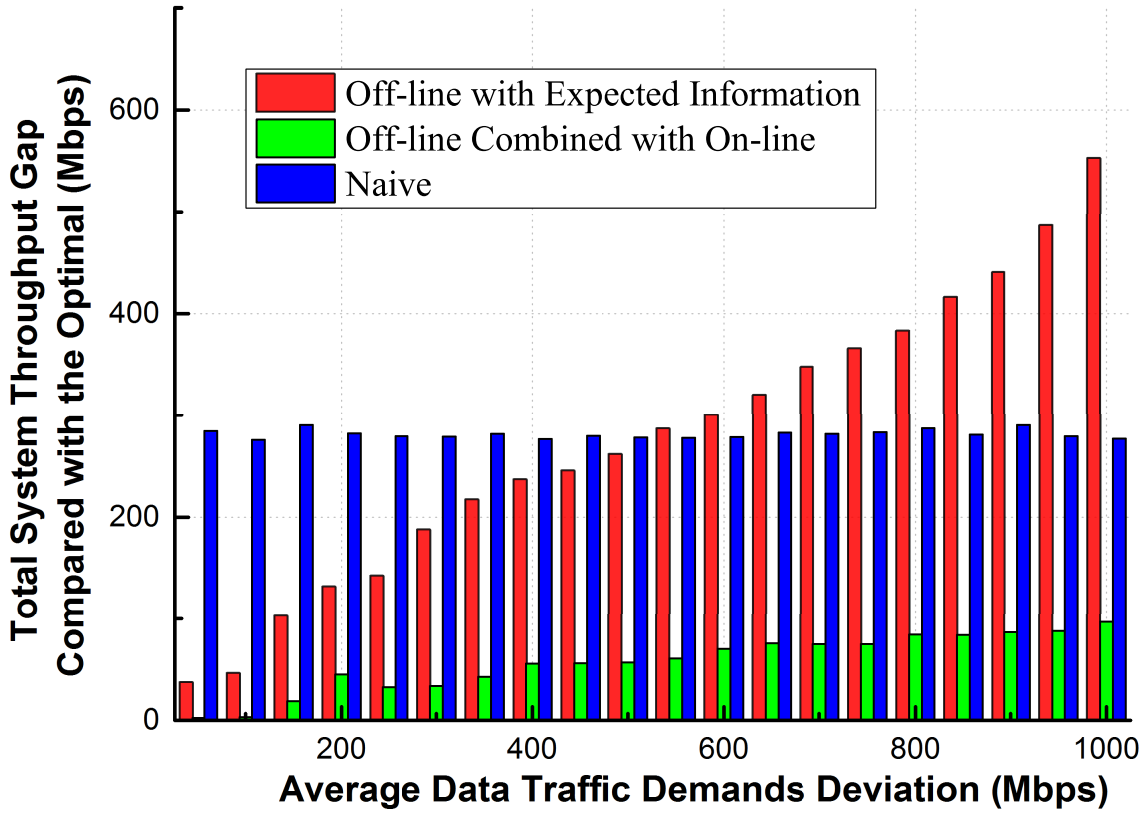

Figure 5.2: The effect of ϵ on system throughput of the off-line with expected information, off-line combined with on-line, and Naive scheme. ©2015 IEEE.

benchmark in this part, since it can achieve the optimal result. The energy inputs of the REBSs and Microgrids are independently and randomly chosen from the interval [100W, 300W]. The real data traffic demands of the REBSs are randomly chosen from the the interval [20Mbps, 50Mbps]. The Y-axis denotes the gap between the performance of the optimal scheme and the associating one, and the X-axis represents the the total amount of estimation deviation of the traffic input, and the value of x can be given by the following equation:

$$\sum [\epsilon]^{+} = \sum [\epsilon]^{-} = x, \tag{5.13}$$

which means that a large value of x will result in a large gap between the real traffic input and the expectation one. For the "Off-line with Expected Information", it will only use the expectation of the traffic input, and for the "Off-line Combined with On-line" scheme, both of the traffic input expectation and the precise value will be respectively utilized before t_1 and at the beginning of each time slot. Because the Naive idea does not consider the long-term result, it will collect the traffic input at the beginning of each time slot therefore only the precise traffic information will be used.

Fig.5.2 illustrates the total system throughput gap between the compared scheme (i.e., the scheme mentioned in the legend) and the optimal scheme (Off-line with Perfect Information), and several conclusions can be achieved from this figure.

Firstly, the Off-line combined with on-line scheme has the best performance since the gap is the lowest. Such scheme inherits the merits of using both of the traffic input expectation and the instant information: because of using the expectation (i.e., the long-term information) , the gap is small as a result. On the other hand, as the x value increases, the gap is still within a small value due to the timely adjusting based on the precise traffic input.

Secondly, the performance of the Off-line with expected information varies inversely to the average data traffic demand deviation, since the gap becomes larger as the increase of

x. Such phenomenon owes to the fact that a large amount of x means that the estimation of the traffic input is very imprecise, therefore the plan given by the off-line scheme is less trustable.

In addition, it is noted that when the deviation is less or equal than 450Mbps, the Off-line with expected information scheme performs better than the Naive one, but such relationship reverses when the deviation x is larger than 450Mbps. It means that the advantage of the long-term optimization will be compromised by the inaccurate traffic input information. Besides the aspects mentioned above, it can be seen from Fig.5.2 that the Naive scheme is free of the impact of traffic input estimation deviation. This is because the Naive idea will only utilize the precise traffic input at the beginning of each time slot.

Fig. 5.3 depicts the energy efficiency comparison of the Off-line with expected information scheme and the Off-line combined with on-line scheme. From the figure, several conclusions can be made, and we will discussion them accordingly.

Firstly, it can be seen that for the off-line with traffic expectation scheme, the energy efficiency is inversely proportional to the data traffic demand deviation of the input traffic. According to Fig.5.2, the total system throughput will decrease with the increase of x. Therefore, under the same energy budget (or same energy consumption), the supported traffic will decrease as the estimation deviation increases, and the energy efficiency will decrease as a result. On the other hand, the off-line combined with the on-line scheme has a relative stable relationship between the energy efficiency and average data traffic demand deviation, thanks to the timely adjust toward the designed plans based on the accurate traffic information. Therefore, the energy can be utilized in a more efficient manner.

Secondly, it is worthwhile to mention that when the estimation deviation is small, the declared energy efficiency of the Off-line with expected information scheme is better than the Off-line combine with on-line one. The reason behind such phenomenon is that

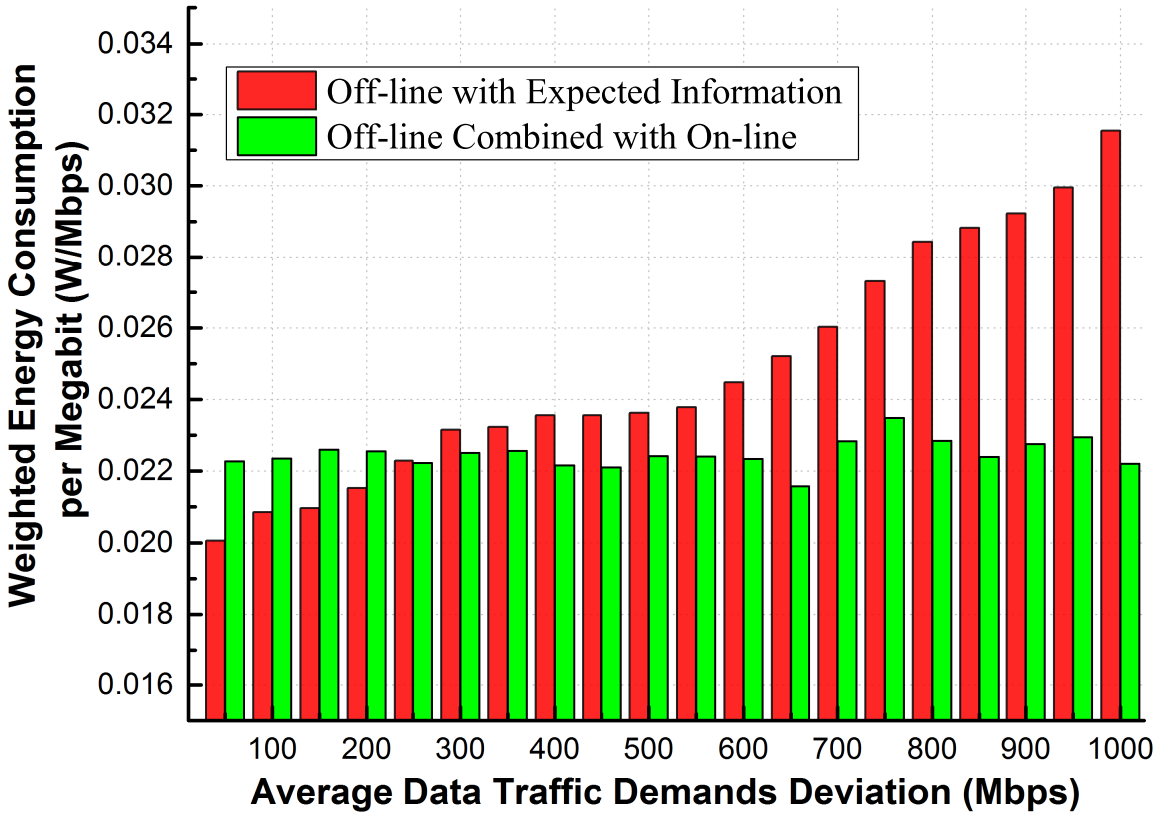

Figure 5.3: The effect of ϵ on energy efficiency of the off-line with expected information and off-line combined with on-line scheme. ©2015 IEEE.

we consider a Pareto-optimization, in which the object of total system throughput has a higher priority than the object of energy efficiency. Therefore when x is less than 250Mbps, achieving a higher total system throughput will consume a large amount of energy, which causes that the energy efficiency of the Off-line combine with on-line scheme worse than the Off-line with expected information scheme.

5.5.2 Effect of Total Available Energy on Total System Throughput and Energy Efficiency

Besides the estimation deviation, we would like to check the effect of other factors. This part contains the observations and associating analyses about the impact of energy input of the REBSs and Microgrids on the total system throughput and energy efficiency, respectively. The energy input of the REBSs and Microgrids are the i.i.d. variables, and selected from the interval $[0.5 \cdot \text{x-axis value}, 1.5 \cdot \text{x-axis value}]$. For the data traffic demand for the REBSs in the considered time span, it is also randomly and independently selected from $[20\text{Mbps}, 60\text{Mbps}]$. Finally, we set the estimation deviation value $\sum[\boldsymbol{\epsilon}]^+ = 200\text{Mbps}$ and $\sum[\boldsymbol{\epsilon}]^- = 200\text{Mbps}$, respectively. The rest parameters are the same as the ones in Table 5.2.

Fig.5.4 demonstrates the value of total system throughput of the four schemes, with the change of the renewable energy input of the REBSs and Microgrids. Several interesting conclusions can be made by Fig.5.4.

Firstly, the figure demonstrates an upward trend in the input of data traffic demand, therefore there is a proportional relationship between the amount of energy input and the total system throughput. As more energy is available for the REBS, the operating time can be prolonged and the number of active subcarriers can be increased, therefore the amount of supported traffic correspondingly becomes larger.

Secondly, it can be seen that the total system throughput of the Off-line combined with

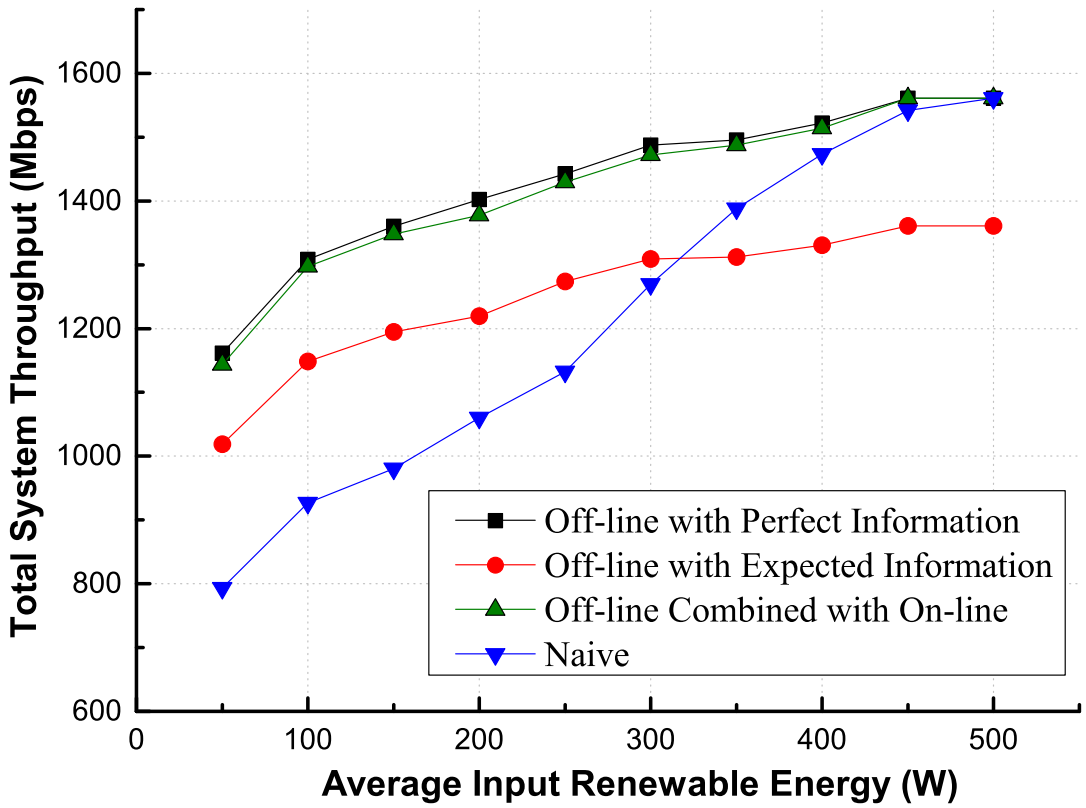

Figure 5.4: The effect of average input renewable energy on system throughput of the four schemes. ©2015 IEEE.

on-line scheme is very close to the one of the optimal scheme, which proves the effectiveness of the on-line scheme established in this chapter. This is because the combined scheme takes the long-term optimization as well as the instant traffic input information into consideration.

Thirdly, the traffic estimation deviation causes a noticeable performance gap between the Off-line with expected information and the optimal scheme. Even when the energy is enough for the operation (i.e., larger than 500W), the off-line only scheme still cannot achieve a desirable result, since its strategy is based on the traffic expectation, and the REBSs will not support larger traffic input due to the decision made before the time slot t_1.

Fourthly, the Naive scheme has the least total system throughput in the early stage. After the average renewable energy input is more than 300W, the result of the Naive scheme becomes better than the result of the off-line with expected information. This is because the Naive scheme will only take consideration of maximizing the system throughput in current time slot using the instant traffic input information, and it is greedy in essence. When the energy is enough, more operating time and subcarriers can be supported, and the optimal strategy will also become greedy, which is to strike the maximal system throughput in current slot, and therefore the Naive result will be closer to the optimal one.

In Fig.5.5, the energy efficiencies of the four schemes is illustrated. It can be seen that the energy efficiency is proportional to average energy input, since the lower y-axis value, the higher energy efficiency.

The major factor causes such phenomenon is, the energy consumed for the operating energy consumption will not directly support more data traffic demand. When the REBS is active, it is the subcarrier that carries the data traffic demand. Therefore, when the energy input is insufficient, a large ratio of the energy consumption will be used for

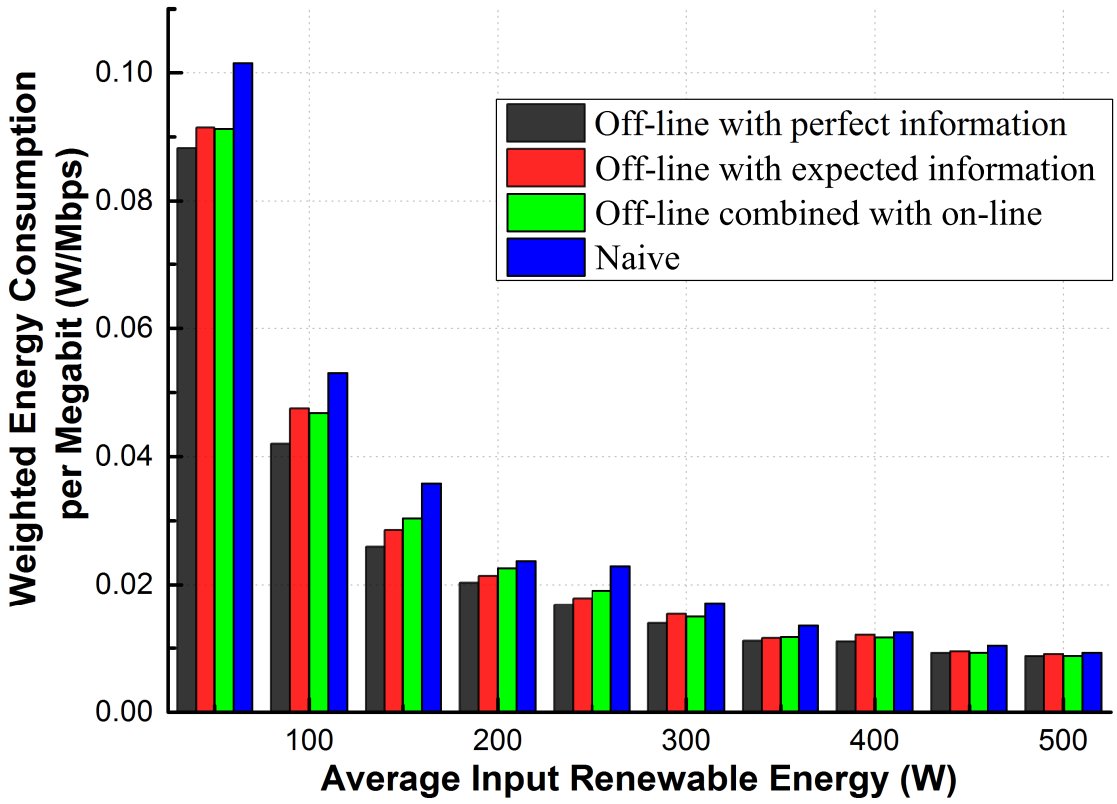

Figure 5.5: The effect of average input renewable energy on consumed power per megabit of the four schemes. ©2015 IEEE.

the operation, and as the amount of energy input becomes larger, the proportion of the subcarrier consumption will be larger as well. As a result, the energy efficiency will also increase. It can be seen that among the four schemes, Naive result has the least energy efficiency, given that the total system throughput of the Naive scheme is lower than the Off-line combined with on-line scheme, the actual performance of the Naive scheme is far behind than the one of Off-line combined with on-line scheme. This result underlines the importance of long-term optimization result.

5.5.3 Effect of Data Traffic Demands on Total System Throughput and Energy Efficiency

In order to check the effect of traffic input on the performance, we consider the data traffic demands of the REBSs as the variables in this part. The X-axis represents the average traffic input, and the real value for the REBSs in each time slot is randomly and independently selected from $[0.5 \cdot \text{x-axis value}, 1.5 \cdot \text{x-axis value}]$. On the other hand, the renewable energy input is also the i.i.d. value and chosen from the range [100W, 300W]. For the traffic estimation deviation, we set $\sum[\boldsymbol{\epsilon}]^+ = 200\text{Mbps}$ and $\sum[\boldsymbol{\epsilon}]^- = 200\text{Mbps}$. The rest parameters are set as Table 5.2.

Fig. 5.6 gives the comparison of the total system throughput of the four schemes. From this figure, it can be seen that there is a proportional relationship between the total system throughput and the traffic input, and such relationship is linear. This is because when the energy input budget is fixed, the amount of energy consumed for activating the subcarrier determines the final result, and if the energy input and network capacity are sufficient, the more traffic input, the more total system throughput. The Off-line combined with on-line scheme can get almost the same total system throughput as the one of the optimal scheme, and the Off-line with expected information scheme has a less total system throughput, since it will only make use of the traffic input expectation, and

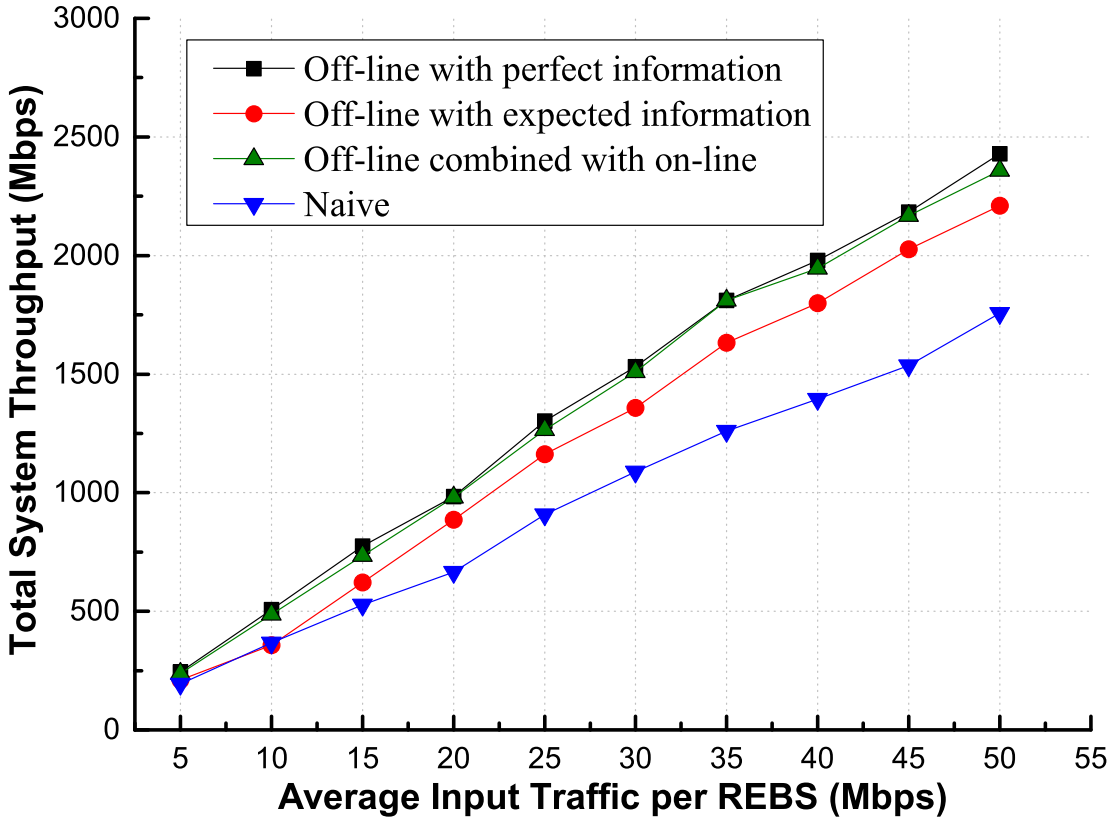

Figure 5.6: The effect of average input traffic per REBS on total system throughput of the four schemes. ©2015 IEEE.

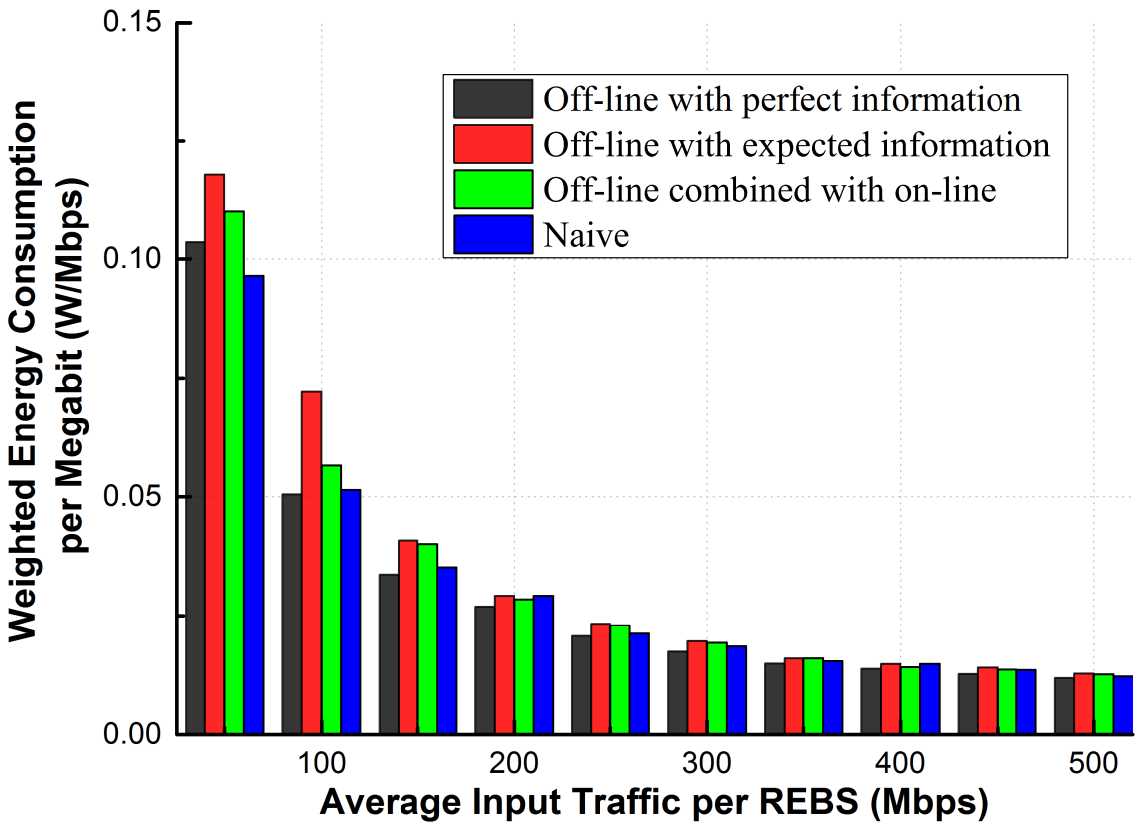

Figure 5.7: The effect of average input traffic per REBS on consumed power per megabit of the four schemes. ©2015 IEEE.

the estimation deviation results in such performance gap. The Naive scheme is with the worst total system throughput than the other three schemes. Moreover, it can be seen that there is an upward trend of the gap when the amount of traffic input increases. If the traffic input is in low level, the influence of the strategy will be small, since the total traffic input is small. As the traffic input increases, the influence of the strategy calculated by the scheme becomes more noticeable.

Fig.5.7 demonstrates the effects of the average traffic input of the REBSs on the energy efficiency of the four schemes. From Fig. 5.7, it can be seen that the energy efficiency is proportional to the traffic input. If the amount of traffic input is low, the operating energy consumption holds a high percentage in the total energy consumption, which means

that the REBS will use a large amount of energy to support a relative small amount of data. Therefore the associating energy efficiency is unsatisfied. As the traffic input becomes larger, the network can support more data traffic demand only at the cost of the subcarrier consumption, and the amount of which is far less than the operation energy consumption therefore the energy efficiency becomes higher.

5.6 Summary

In this chapter, we introduce an on-line dynamically adjusting scheme. Based on the plan of the off-line scheme using traffic input expectation, the envisioned on-line scheme will be executed at the beginning at each time slot and it utilizes the precise traffic in the current time slot, and such scheme can effectively avoid the impact of the inaccurate traffic demand estimation.

We firstly establish the system model by inducing the estimation deviation factor of the traffic input, then we analyze the performance bound of the off-line scheme in term of the estimation deviation factor. After that, we envision the on-line dynamic adjusting scheme. Such scheme makes use of the maximum available amount of energy, which will not affect the future plan, therefore the performance of the combined scheme (i.e., Off-line combined with on-line) is guaranteed. Finally, we illustrate and analyze the computer-based simulations. The numerical results reveal that the proposed Off-line combined with on-line scheme can return a satisfied result when the traffic estimation deviation is high, and it outperforms the off-line only scheme in different energy input levels and traffic input levels.

Chapter 6

Conclusion

6.1 Summary and Discussions

The emergence of renewable energy-enabled base station provides us an extra energy source to the cellular base stations. Due to the numerous recently happened disasters all over the world, network designer also need to take consideration of the energy consumption and traffic transmission strategies for the disaster case. In this thesis, we devote our efforts to the joint energy and traffic management in wireless mesh networks powered by renewable energy. The main contributions of this dissertation can be summarized in the following aspects.

- In Chapter 2, we introduced the REBS-based mesh networks and the associating settings in disaster area. We investigated the energy and traffic flows in the network. We pointed out that the energy input in a finite time horizon could be estimated with the information of weather forecast and the scale of the energy harvesting facilities. In addition, the data traffic demands profiles of the REBSs could also be evaluated by combining the information of the population, the ratio of active users, as well as the previous information. Then the literature review was conducted. We

also demonstrated the necessity of the joint optimization of energy and traffic via an example.

- In Chapter 3, we focused on promoting the REBS-based networks for emergency services powered by renewable energy. Firstly, we introduced the model for energy and traffic in detail, which included energy utilization, battery alternation and traffic transmission. After the literature review, we formulated the problem for the joint optimization of energy and traffic, and then an MILP optimization framework was proposed. At last, we verified the efficiency of our proposed optimization framework through the computer-based simulations. We demonstrated that the total system throughput of the joint optimization result was better than the myopic naive result.
- In Chapter 4, we extended our consideration, and proposed an energy-efficient throughput maximization scheme for the sake of energy efficiency. We defined the ratio of consumed energy to the harvested energy in the future as the energy efficiency of a certain REBS. The objective of the problem was the energy efficiency, and the maximal total system throughput was set as the constraint. Such problem was also an MILP problem and we proposed a two-stage optimization framework to deal with this problem. We justified that the proposed algorithm could achieve higher energy efficiency compared with the throughput-maximization-only scheme and the naive one. Therefore, through the new proposal, the renewable energy would be used efficiently.
- In Chapter 5, we proposed an on-line dynamically adjusting scheme based on the proposals in the previous two chapters. The old proposals made use of the expectation of the traffic profile, and the result would be suboptimal if such estimation was imprecise. To this end, we firstly analyzed the performance bound of the previous off-line result, and then an on-line energy-efficient of throughput-based scheme for the REBS-based mesh network was proposed. The on-line scheme firstly made use of the expectation of the traffic profile, and at the beginning of each time slot, the strategy would be changed accordingly, without affecting the old plan for futures. We developed a mathematical characterization for the on-line scheme, and

the computer-based simulations revealed that our proposed on-line scheme could significantly achieve better network performance compared with the off-line scheme and the naive scheme.

6.2 Future Directions

In this thesis, we proposed a throughput-maximization frameworks for the REBS-based mesh network and the associating algorithms. In addition, the energy efficiency as well as the estimation precision were taken into consideration. We list the possible extensions as the following aspects:

Firstly, it is noticed that we assume the perfect energy estimation profile in our considered model. In the causal case, such assumption may hold since the developed technology of the weather forecast and the sufficient statistical surveys of the historical profile. However, for some extreme cases (Such as the unexpected weather), there might also be deviation on the energy estimation profile. Therefore both of the energy and traffic estimation profiles are imprecise, and a deeper analysis of the relationship between the energy and traffic becomes necessary.

Secondly, in our consideration, the Microgrid acts only as the energy distributor. The recently academic publications study the availabilities for the deeper energy cooperation among the REBSs connected to the same Microgrid. The REBSs under the same Microgrid cluster can mutually transfer the energy inside the batteries. It would be interesting to consider the bi-directional energy transmission direction between the REBSs and the Microgrid.

Thirdly, for the model in the thesis, the limited number of the REBSs guarantees the availability for MILP problem solution in practice. We believe that along with the advance of weather forecast technique in the future, the granularity of the time slot will be

finer, and the length of time slot will be shrunk. Therefore an low complexity alternative is also needed if the scale of the problem becomes larger.

Bibliography

[1] T. Sakano, Z. Fadlullah, T. Ngo, H. Nishiyama, M. Nakazawa, F. Adachi, N. Kato, A. Takahara, T. Kumagai, H. Kasahara, and S. Kurihara, "Disaster-resilient networking: a new vision based on movable and deployable resource units," *Network, IEEE*, vol. 27, no. 4, pp. 40–46, July 2013.

[2] G. Auer, V. Giannini, I. Godor, P. Skillermark, M. Olsson, M. Imran, D. Sabella, M. Gonzalez, C. Desset, and O. Blume, "Cellular energy efficiency evaluation framework," in *Vehicular Technology Conference (VTC Spring), 2011 IEEE 73rd*, May 2011, pp. 1–6.

[3] O. Arnold, F. Richter, G. Fettweis, and O. Blume, "Power consumption modeling of different base station types in heterogeneous cellular networks," in *Future Network and Mobile Summit, 2010*, June 2010, pp. 1–8.

[4] K. Heimerl, K. Ali, J. Blumenstock, B. Gawalt, and E. Brewer, "Expanding rural cellular networks with virtual coverage," in *Presented as part of the 10th USENIX Symposium on Networked Systems Design and Implementation (NSDI 13)*. Lombard, IL: USENIX, 2013, pp. 283–296. [Online]. Available: https://www.usenix.org/conference/nsdi13/technical-sessions/presentation/heimurl

[5] G. Auer, V. Giannini, I. Godor, P. Skillermark, M. Olsson, M. Imran, D. Sabella, M. Gonzalez, C. Desset, and O. Blume, "Cellular energy efficiency evaluation framework," in *IEEE 73rd Vehicular Technology Conference (VTC Spring)*, May 2011, pp. 1–6.

[6] A. Kwasinski, V. Krishnamurthy, S. J., and R. Sharma, "Availability evaluation of micro-grids for resistant power supply during natural disasters," *IEEE Transactions on Smart Grid*, vol. 3, no. 4, pp. 2007–2018, Dec 2012.

[7] E. Daigneau, "Microgrids: A disaster-resistant power supply?" http://goo.gl/9wgdNS, Nov 2012, [Online; accessed 22-April-2014].

[8] A. Kwasinski and A. Kwasinski, "Architecture for green mobile network powered from renewable energy in microgrid configuration," in *Wireless Communications and Networking Conference (WCNC), 2013 IEEE*, April 2013, pp. 1273–1278.

[9] R. Anderson, A. Boulanger, W. Powell, and W. Scott, "Adaptive stochastic control for the smart grid," *Proceedings of the IEEE*, vol. 99, no. 6, pp. 1098–1115, June 2011.

[10] J. Leithon, S. Sun, and T. J. Lim, "Energy management strategies for base stations powered by the smart grid," in *Global Communications Conference (GLOBECOM), 2013 IEEE*, Dec 2013, pp. 2635–2640.

[11] J. Leithon, T. J. Lim, and S. Sun, "Online energy management strategies for base stations powered by the smart grid," in *Smart Grid Communications (SmartGridComm), 2013 IEEE International Conference on*, Oct 2013, pp. 199–204.

[12] X. Guan, Z. Xu, and Q.-S. Jia, "Energy-efficient buildings facilitated by microgrid," *Smart Grid, IEEE Transactions on*, vol. 1, no. 3, pp. 243–252, Dec 2010.

[13] S. Bu, F. Yu, and Y. Qian, "Energy-efficient cognitive heterogeneous networks powered by the smart grid," in *INFOCOM, 2013 Proceedings IEEE*, April 2013, pp. 980–988.

[14] S. Bu, F. Yu, and P. Liu, "Stochastic unit commitment in smart grid communications," in *Computer Communications Workshops (INFOCOM WKSHPS), 2011 IEEE Conference on*, April 2011, pp. 307–312.

[15] J. Xu, Y. Guo, and R. Zhang, "Comp meets energy harvesting: A new communication and energy cooperation paradigm," in *Global Communications Conference (GLOBECOM), 2013 IEEE*, Dec 2013, pp. 2508–2513.

[16] C. Wei, Z. Fadlullah, N. Kato, and A. Takeuchi, "Gt-cfs: A game theoretic coalition formulation strategy for reducing power loss in micro grids," *Parallel and Distributed Systems, IEEE Transactions on*, vol. 25, no. 9, pp. 2307–2317, Sept 2014.

[17] C. Wei, Z. Fadlullah, N. Kato, and I. Stojmenovic, "On optimally reducing power loss in micro-grids with power storage devices," *Selected Areas in Communications, IEEE Journal on*, vol. 32, no. 7, pp. 1361–1370, July 2014.

[18] J. Pan, R. Jain, and S. Paul, "A survey of energy efficiency in buildings and microgrids using networking technologies," *Communications Surveys Tutorials, IEEE*, vol. 16, no. 3, pp. 1709–1731, Third 2014.

[19] M. A. Marsan, L. Chiaraviglio, D. Ciullo, and M. Meo, "On the effectiveness of single and multiple base station sleep modes in cellular networks," *Computer Networks*, vol. 57, no. 17, pp. 3276 – 3290, 2013. [Online]. Available: http://www.sciencedirect.com/science/article/pii/S1389128613002429

[20] T. Han and N. Ansari, "Optimizing cell size for energy saving in cellular networks with hybrid energy supplies," in *Global Communications Conference (GLOBECOM), 2012 IEEE*, Dec 2012, pp. 5189–5193.

[21] M. Gatzianas, L. Georgiadis, and L. Tassiulas, "Control of wireless networks with rechargeable batteries," *IEEE Transactions on Wireless Communications*, vol. 9, no. 2, pp. 581–593, February 2010.

[22] W. Guo and T. O'Farrell, "Green cellular network: Deployment solutions, sensitivity and tradeoffs," in *Wireless Advanced (WiAd), 2011*, June 2011, pp. 42–47.

[23] G. Miao, N. Himayat, G. Li, and S. Talwar, "Low-complexity energy-efficient scheduling for uplink ofdma," *IEEE Transactions on Communications*, vol. 60, no. 1, pp. 112–120, January 2012.

[24] G. Auer, V. Giannini, C. Desset, I. Godor, P. Skillermark, M. Olsson, M. Imran, D. Sabella, M. Gonzalez, O. Blume, and A. Fehske, "How much energy is needed to run a wireless network?" *Wireless Communications, IEEE*, vol. 18, no. 5, pp. 40–49, October 2011.

[25] L. Chiaraviglio, M. Mellia, and F. Neri, "Reducing power consumption in backbone networks," in *Communications, 2009. ICC '09. IEEE International Conference on*, June 2009, pp. 1–6.

[26] W. Fisher, M. Suchara, and J. Rexford, "Greening backbone networks: Reducing energy consumption by shutting off cables in bundled links," in *Proceedings of the First ACM SIGCOMM Workshop on Green Networking*, ser. Green Networking '10. New York, NY, USA: ACM, 2010, pp. 29–34. [Online]. Available: http://doi.acm.org/10.1145/1851290.1851297

[27] Y. Li, H. Celebi, M. Daneshmand, C. Wang, and W. Zhao, "Energy-efficient femtocell networks: challenges and opportunities," *Wireless Communications, IEEE*, vol. 20, no. 6, pp. 99–105, December 2013.

[28] J. Piorno, C. Bergonzini, D. Atienza, and T. Rosing, "Prediction and management in energy harvested wireless sensor nodes," in *Wireless Communication, Vehicular Technology, Information Theory and Aerospace Electronic Systems Technology, 2009. Wireless VITAE 2009. 1st International Conference on*, May 2009, pp. 6–10.

[29] A. Fernandez, Y. Gala, and J. Dorronsoro, "Machine learning prediction of large area photovoltaic energy production," in *Second Workshop on Data Analytics for Renewable Energy Integration (DARE-14)*, Nancy, France, Sept 2014.

[30] J. Lu, S. Liu, Q. Wu, and Q. Qiu, "Accurate modeling and prediction of energy availability in energy harvesting real-time embedded systems," in *Green Computing Conference, 2010 International*, Aug 2010, pp. 469–476.

[31] S. He, J. Chen, F. Jiang, D. Yau, G. Xing, and Y. Sun, "Energy provisioning in wireless rechargeable sensor networks," in *INFOCOM, 2011 Proceedings IEEE*, April 2011, pp. 2006–2014.

[32] M. Marsan, G. Bucalo, A. Di Caro, M. Meo, and Y. Zhang, "Towards zero grid electricity networking: Powering bss with renewable energy sources," in *Communications Workshops (ICC), 2013 IEEE International Conference on*, June 2013, pp. 596–601.

[33] M. A. Marsan, L. Chiaraviglio, D. Ciullo, and M. Meo, "On the effectiveness of single and multiple base station sleep modes in cellular networks," *Computer Networks*, vol. 57, no. 17, pp. 3276 – 3290, 2013. [Online]. Available: http://www.sciencedirect.com/science/article/pii/S1389128613002429

[34] M. Zheleva, A. Paul, D. L. Johnson, and E. Belding, "Kwiizya: Local cellular network services in remote areas," in *Proceeding of the 11th Annual International Conference on Mobile Systems, Applications, and Services*, ser. MobiSys '13. New York, NY, USA: ACM, 2013, pp. 417–430. [Online]. Available: http://doi.acm.org/10.1145/2462456.2464458

[35] E. Oh and B. Krishnamachari, "Energy savings through dynamic base station switching in cellular wireless access networks," in *Global Telecommunications Conference (GLOBECOM 2010), 2010 IEEE*, Dec 2010, pp. 1–5.

[36] F. Han, Z. Safar, and K. Liu, "Energy-efficient base-station cooperative operation with guaranteed qos," *IEEE Transactions on Communications*, vol. 61, no. 8, pp. 3505–3517, August 2013.

[37] M. Marsan, L. Chiaraviglio, D. Ciullo, and M. Meo, "Optimal energy savings in cellular access networks," in *Communications Workshops, 2009. ICC Workshops 2009. IEEE International Conference on*, June 2009, pp. 1–5.

[38] S.-E. Elayoubi, L. Saker, and T. Chahed, "Optimal control for base station sleep mode in energy efficient radio access networks," in *INFOCOM, 2011 Proceedings IEEE*, April 2011, pp. 106–110.

[39] D. Willkomm, S. Machiraju, J. Bolot, and A. Wolisz, "Primary users in cellular networks: A large-scale measurement study," in *New Frontiers in Dynamic Spectrum Access Networks, 2008. DySPAN 2008. 3rd IEEE Symposium on*, Oct 2008, pp. 1–11.

[40] J. Yoon, S. Sen, J. Hare, and S. Banerjee, "Wiscape: A framework for measuring the performance of wide-area wireless networks," *Mobile Computing, IEEE Transactions on*, vol. 14, no. 8, pp. 1751–1764, Aug 2015.

[41] C. Peng, S.-B. Lee, S. Lu, H. Luo, and H. Li, "Traffic-driven power saving in operational 3g cellular networks," in *Proceedings of the 17th Annual International Conference on Mobile Computing and Networking*, ser. MobiCom '11. New York, NY, USA: ACM, 2011, pp. 121–132. [Online]. Available: http://doi.acm.org/10.1145/2030613.2030628

[42] K. Jacobson and W. Krzymien, "Cooperative vs multihop relaying in cellular systems," in *20th IEEE International Symposium on Personal, Indoor and Mobile Radio Communications*, Sept 2009, pp. 1853–1857.

[43] F. Mostafa, H. Nishiyama, R. Miura, and N. Kato, "On efficient traffic distribution for disaster area communication using wireless mesh networks," *Wireless Personal Communications*, vol. 74, no. 4, pp. 1311–1327, 2014. [Online]. Available: http://dx.doi.org/10.1007/s11277-013-1579-9

[44] S. Guo, L. T. Yang, G. Min, and X. Xie, "Green communication in energy renewable wireless mesh networks: Routing, rate control, and power allocation," *IEEE Transactions on Parallel and Distributed Systems*, vol. 99, no. PrePrints, p. 1, 2014.

[45] T. Ngo, H. Nishiyama, N. Kato, T. Sakano, and A. Takahara, "A spectrum-and energy-efficient scheme for improving the utilization of MDRU-based disaster resilient networks," *IEEE Transactions on Vehicular Technology - Special Section on Green Mobile Multimedia Communications*, vol. 63, no. 5, pp. 2027–2037, Jun. 2014.

[46] L. Xiang, X. Ge, C.-X. Wang, F. Y. Li, and F. Reichert, "Energy efficiency evaluation of cellular networks based on spatial distributions of traffic load and power consumption," *IEEE Transactions on Wireless Communications*, vol. 12, no. 3, pp. 961–973, March 2013.

[47] L. Cai, Y. Liu, T. Luan, X. Shen, J. Mark, and H. Poor, "Sustainability analysis and resource management for wireless mesh networks with renewable energy supplies," *IEEE Journal on Selected Areas in Communications*, vol. 32, no. 2, pp. 345–355, February 2014.

[48] J. Marašević, C. Stein, and G. Zussman, "Max-min fair rate allocation and routing in energy harvesting networks: Algorithmic analysis," in *Proceedings of the 15th ACM International Symposium on Mobile Ad Hoc Networking and Computing*, ser. MobiHoc '14. New York, NY, USA: ACM, 2014, pp. 367–376. [Online]. Available: http://doi.acm.org/10.1145/2632951.2632960

[49] Y. Guo, J. Xu, L. Duan, and R. Zhang, "Joint energy and spectrum cooperation for cellular communication systems," *Communications, IEEE Transactions on*, vol. 62, no. 10, pp. 3678–3691, Oct 2014.

[50] C. Ma, Z. Zhang, and Y. Yang, "Battery-aware router scheduling in wireless mesh networks," in *Parallel and Distributed Processing Symposium, 2006. IPDPS 2006. 20th International*, April 2006, pp. 10 pp.–.

[51] M. Cheng, X. Gong, L. Cai, and X. Jia, "Cross-layer throughput optimization with power control in sensor networks," *IEEE Transactions on Vehicular Technology*, vol. 60, no. 7, pp. 3300–3308, Sept 2011.

[52] M. Li, H. Nishiyama, N. Kato, Y. Owada, and K. Hamaguchi, "n the energy-efficient of throughput-based scheme using renewable energy for wireless mesh networks in disaster area," *Emerging Topics in Computing, IEEE Transactions on*, vol. 3, no. 3, pp. 420–431, Dec 2014.

[53] M. Li, H. Nishiyma, Y. Owada, and K. Hamaguchi, "On energy efficient scheduling and load distribution based on renewable energy for wireless mesh network in disaster area," in *The 13th IEEE International Conference on Trust, Security and Privacy in Computing and Communications (TrustCom-14)*, Sept 2014, pp. 465–472.

[54] J. Chen, X. Cao, P. Cheng, Y. Xiao, and Y. Sun, "Distributed collaborative control for industrial automation with wireless sensor and actuator networks," *IEEE Transactions on Industrial Electronics*, vol. 57, no. 12, pp. 4219–4230, Dec 2010.

[55] S. William, *Wireless Communications and Networks*, 2nd ed. Pearson Prentice Hall, 2005.

[56] X. Wang and L. Cai, "Stability region of opportunistic scheduling in wireless networks," *IEEE Transactions on Vehicular Technology*, vol. 63, no. 8, pp. 4017–4027, Oct 2014.

Publications

Journals

[1] Meng Li, Hiroki Nishiyama, Nei Kato, Yasunori Owada, and Kiyoshi Hamaguchi, "On the Energy-Efficient of Throughput-Based Scheme Using Renewable Energy for Wireless Mesh Networks in Disaster Area", *IEEE Transactions on emerging topics in computing*, Vol. 3, No. 3, pp. 420-431, Sept. 2015.

Refereed Conference Papers

[2] Meng Li, Hiroki Nishiyama, Yasunori Owada, and Kiyoshi Hamaguchi, "On Energy Efficient Scheduling and Load Distribution Based on Renewable Energy for Wireless Mesh Network in Disaster Area", *The 13th IEEE International Conference on Trust, Security and Privacy in Computing and Communications (IEEE TrustCom-14)*, Beijing, China, Sept. 2014.

[3] Meng Li, Hiroki Nishiyama, Nei Kato, Kimihiro Mizutani, Osamu Akashi, and Atsushi Takahara, "On the Fast-Convergence of Delay-Based Load Balancing over Multipaths for Dynamic Traffic Environments", *2013 International Conference on Wireless Communications and Signal Processing (WCSP 2013)*, Hangzhou, China, Oct. 2013.

Grants

Best paper award: Meng Li, Hiroki Nishiyama, Yasunori Owada, and Kiyoshi Hamaguchi, "On Energy Efficient Scheduling and Load Distribution Based on Renewable Energy for Wireless Mesh Network in Disaster Area", *The 13th IEEE International Conference on Trust, Security and Privacy in Computing and Communications (IEEE TrustCom-14)*, Beijing, China, Sep. 2014.

Appendix

Copyright Permissions

In this appendix we includes the permissions that were used to write this dissertation. The detail description of permissions are given in the following documents.

The permission grants from IEEE.

Title:	On Energy Efficient Scheduling and Load Distribution Based on Renewable Energy for Wireless Mesh Network in Disaster Area
Conference Proceedings:	Trust, Security and Privacy in Computing and Communications (TrustCom), 2014 IEEE 13th International Conference on
Author:	Meng Li; Nishiyama, H.; Owada, Y.; Hamaguchi, K.
Publisher:	IEEE
Date:	24-26 Sept. 2014

Thesis / Dissertation Reuse

The IEEE does not require individuals working on a thesis to obtain a formal reuse license, however, you may print out this statement to be used as a permission grant:

Requirements to be followed when using any portion (e.g., figure, graph, table, or textual material) of an IEEE copyrighted paper in a thesis:

1) In the case of textual material (e.g., using short quotes or referring to the work within these papers) users must give full credit to the original source (author, paper, publication) followed by the IEEE copyright line © 2011 IEEE.
2) In the case of illustrations or tabular material, we require that the copyright line © [Year of original publication] IEEE appear prominently with each reprinted figure and/or table.
3) If a substantial portion of the original paper is to be used, and if you are not the senior author, also obtain the senior author's approval.

Requirements to be followed when using an entire IEEE copyrighted paper in a thesis:

1) The following IEEE copyright/ credit notice should be placed prominently in the references: © [year of original publication] IEEE. Reprinted, with permission, from [author names, paper title, IEEE publication title, and month/year of publication]
2) Only the accepted version of an IEEE copyrighted paper can be used when posting the paper or your thesis on-line.
3) In placing the thesis on the author's university website, please display the following message in a prominent place on the website: In reference to IEEE copyrighted material which is used with permission in this thesis, the IEEE does not endorse any of [university/educational entity's name goes here]'s products or services. Internal or personal use of this material is permitted. If interested in reprinting/republishing IEEE copyrighted material for advertising or promotional purposes or for creating new collective works for resale or redistribution, please go to http://www.ieee.org/publications_standards/publications/rights/rights_link.html to learn how to obtain a License from RightsLink.

If applicable, University Microfilms and/or ProQuest Library, or the Archives of Canada may supply single copies of the dissertation.